BULLETIN
OF THE AMERICAN PHYSICAL SOCIETY

Program of the 51st Annual Gaseous Electronics Conference and the 4th International Conference on Reactive Plasmas

October 19–22, 1998
Maui, Hawaii

October 1998
Volume 43, No. 5

BULLETIN
OF THE AMERICAN PHYSICAL SOCIETY

Coden BAPSA6 ISSN: 0003-0503
Series II, Vol. 43, No. 5 **October 1998**

APS COUNCIL 1998

Editor: Barrett H. Ripin
Meeting Publications Coordinator: Danita Boonchaisri

APS MEETINGS DEPARTMENT
One Physics Ellipse
College Park, MD 20740-3844
Telephone: (301) 209-3200
FAX: (301) 209-0866
Donna Baudrau, *Meetings Manager*
Terri Adorjan, *Assistant Meetings Manager*
Karen MacFarland, *Assistant to the Meetings Manager*
Don Wise, *Registrar*

Staff Representatives
Barrett Ripin, *Associate Executive Officer*; Irving Lerch, *Director of International Affairs*; Robert L. Park, *Director, Public Information*; Michael Lubell, *Director, Public Affairs*; Stanley Brown, *Administrative Editor*; Reid Terwilliger, *Director of Editorial Office Services*; Michael Stephens, *Controller and Assistant Treasurer*

The *Bulletin of The American Physical Society* is published 10X in 1998, March, April, May, July, October (2X), November (3X), and December, by The American Physical Society, through the American Institute of Physics. It contains advance information about meetings of the Society, including abstracts of papers to be presented, as well as transactions of past meetings. Reprints of papers can be obtained only by writing directly to the authors.

The *Bulletin* is delivered, on subscription, by Periodicals mail. Complete volumes are also available on microfilm. **APS Members** may subscribe to individual issues, or for the entire year. **Nonmembers** may subscribe to the Bulletin at the following rates: Domestic $440; Foreign Surface $460; Air Freight $485. Information on prices, as well as subscription orders, renewals, and address changes, should be addressed as follows: **For APS Members**—Membership Department, The American Physical Society, One Physics Ellipse, College Park, MD 20740-3844. **For Nonmembers**—Circulation and Fulfillment Division, The American Institute of Physics, 500 Sunnyside Blvd., Woodbury, NY 11797. Allow at least 6 weeks advance notice. For address changes, please send both the old and new addresses, and, if possible, include a mailing label from a recent issue. Requests from subscribers for missing issues will be honored without charge only if received within 6 months of the issue's actual date of publication.

The *Bulletin of The American Physical Society* (ISSN: 0003-0503) is published ten times a year for The American Physical Society by the American Institute of Physics. 1998 subscription rate is $440 for domestic nonmembers. Postmaster: Send address changes to *Bulletin of The American Physical Society*, AIP, 500 Sunnyside Boulevard, Woodbury, NY 11797-2999. Periodicals postage paid at Woodbury, NY, and additional mailing offices.

On the Cover: The Aston Wailea Resort on the Pacific Ocean in Wailea, Maui, Hawaii.

BULLETIN
OF THE AMERICAN PHYSICAL SOCIETY

Vol. 43, No. 5, October 1998

51st Annual Gaseous Electronics Conference and
4th International Conference on Reactive Plasmas

TABLE OF CONTENTS

General Information iii
GEC Executive Committee iii
ICRP Organizing Committee iii
Sessions iii
GEC Student Award for Excellence iv
Guest Programs iv
Tuesday, October 20th iv
Wednesday, October 21st iv
E-mail and Other Business Services vi
Registration iv
Audio-Visual Equipment v
Conference Banquet v
Call for Nominations for GEC General and Executive Committees v
Conference Secretary v
Maui High Performance Computing Center v
A. Short Course vi
B. Tours vi
Please Note vi
Epitome vii
Main Text 1407
Monday 1407

Tuesday 1441
Wednesday 1472
Thursday 1499
Author Index 1513
Maps and Floor Plans . . . . . **At End of Issue**
Condensed Epitome . . . . . **Back Covers**

51st Annual Gaseous Electronics Conference and 4th International Conference on Reactive Plasmas

October 19–22, 1998; Maui, Hawaii

GENERAL INFORMATION

Welcome to the joint meeting of the Gaseous Electronics Conference (GEC) and the International Conference on Reactive Plasmas (ICRP). This is the 51st meeting of the GEC, a topical conference of the American Physical Society, and the fourth meeting of the ICRP. This year's conference will be highlighted by the Allis Prize lecture by Ray Flannery, the ICRP Distinguished Lecture by Hideo Sugai, and a GEC Foundation Talk by Robert Crompton. Other sessions include topics in plasma processing of materials, collisions, diagnostics, and innovative plasma sources. There will be both oral and poster sessions, with a post-deadline oral session included on the program for the first time this year. This year's conference will also feature the GEC Student Award for Excellence. Following the conference, on Friday, 23 October, there will be a short course on parallel computing at the Maui High Performance Computing Center.

GEC EXECUTIVE COMMITTEE

M. J. Kushner, Chair, University of Illinois
G. N. Hays, Chair-Elect, Sandia National Labs.
C. B. Fleddermann, Secretary, U.of New Mexico
L. Vuscovic, Secy.-Elect, Old Dominion Univ.
T. Walker, Past-Secretary, Univ. of Wisconsin
G. A. Hebner, Treas., Sandia National Labs.
T. Gay, Univ. of Nebraska
G. Kroesen, Eindhoven Univ. Technol.
P. Loewenhardt, Applied Materials, Inc.
T. J. Sommerer, General Electric R & D Center
K. Tachibana, Kyoto University

ICRP ORGANIZING COMMITTEE

T. Makabe, Chair, Keio Univeristy
S. Miyake, Co-chair, Osaka University
A. Kono, Secretary, Nagoya Univeristy
H. Fujiyama, Nagasaki University
K. Nanbu, Tohuku University
Y. Sakai, Hokkaido University
S. Samukawa, NEC Corporation
M. Sekine, Toshiba Corporation
T. Shinoda, Fujitsu Ltd.
H. Sugai, Nagoya University
H. Tanaka, Sophia University
K. Tsujimoto, Hitachi Ltd.

SESSIONS

Plenary sessions will include presentations by:

Ray Flannery, Georgia Tech, Allis Prize Lecture, *Three-Body Recombination at Thermal and Ultra-Low Energies.*

Robert Crompton, Australian National University, GEC Foundation Talk, *Electron Swarms.*

Hideo Sugai, Nagoya University, ICRP Distinguished Lecturer, *High-Density Plasma Sources and Technology for the Next Generation.*

Arranged sessions include:

- Electron-atom collisions
- RF plasmas
- Oxide etch
- Electron transport
- Pulsed rf plasmas
- Electron-molecule collision
- Surface reactions
- Environmental plasmas
- Electron and ion transport
- Laser diagnostics
- ICP discharges
- Dust in silane plasmas
- Plasma jets
- Plasma deposition
- Magnetized plasmas
- Collisions in plasmas

- Plasma diagnostics
- Thermal plasmas
- Lamps and displays
- Pulsed microwave discharges
- Laser and excimer sources
- Etch and deposition simulation
- Negative ions in pulsed discharges

For the first time, this year there will also be a session containing post-deadline papers.

GEC STUDENT AWARD FOR EXCELLENCE

In order to recognize and encourage the outstanding contributions students make to the Gaseous Electronics Conference, the GEC will continue to present an award for the best paper presented by a student. The award winner will be chosen by a subcommittee of the GEC executive committee. Students competing for the $500 award are:

Ion C. Abraham, University of Wisconsin- Madison, [Session FT2] *Absolute Line Integrated Densities of CF, CF2, and CF3 in a GEC Reference Cell.*

Heidi Anderson, University of Wisconsin- Madison, [Session IT2] *Radiometric Efficiency of Barium Discharge Plasmas.*

Pascal Chabert, Lab. PRIAM, Unite Mixte de Recherche CNRS-ONERA, [Session DM3] *Negative Ion Detection Using Electrostatic Probes.*

Erik Edelberg, University of California- Santa Barbara, [Session BM3] *Measurements and Simulations of the Energy Distributions of Ions Bombarding Radio-Frequency Biased Electrodes in an Inductively Coupled Plasma Reactor.*

Ronald Kinder, University of Illinois, [Session NW1] *Consequences of Mode Structure on Ion Fluxes in ECR Sources for Materials Processing.*

Kazuo Takahashi, Kyoto University, [Session NW3] *Two- Dimensional Melting in a Coulomb Crystal of Dusty Plasmas.*

GUEST PROGRAMS

The Aston Wailea Resort offers a variety of off-site activities including horseback riding, helicopter tours, snorkeling, and a sunset dinner cruise. Days have been set aside for GEC/ICRP attendees and their guests to participate in some of these activities together; please see the bulletin board at the conference registration desk for further information. Alternatively, independent arrangements for these activities can be made through the hotel. On-site activities may also be arranged through the hotel activities desk.

The hotel has arranged the following activities for conference attendees:

TUESDAY, OCTOBER 20TH
Afternoon Snorkel Cruise on the Pride of Maui

The afternoon snorkel cruise includes sodas, a barbecued lunch, snorkel equipment, boogie boards, floatation devices, and optical masks. SCUBA, SNUBA, and underwater cameras are available for an extra charge. The vessel includes hot water shower, glassbottom viewing port, upper sunning deck, a spacious protected cabin area, modern heads, and fishing.

Time: 1:15 p.m. – 5:45 p.m.

Price: $42.00 - adults, $24.00 - children (3–17)

WEDNESDAY, OCTOBER 21ST
Maui, Above and Below

Experience a narrated tour with emphasis on Maui's natural wonders. It unfolds from the slopes of a dormant Hawaiian volcano, on to the unveiling of the secrets of a native rain forest and concludes with visiting the sea creatures in Hawaii's most spectacular tropical aquarium. Includes all entrance fees to Haleakala National Park, Hawaii Nature Center, and the Maui Ocean Center.

Time: 7:30 – 3:00 p.m.

Price: $78.00 - adults, $70.00 children (4–12)

E-MAIL AND OTHER BUSINESS SERVICES

E-mail access is available to GEC/ICRP participants at the Aloha Business Center in the lobby of the conference hotel. E-mail access will be at a conference rate of $16/half hour, $24/hour, with a $8 minimum. FAX services and office supplies are also available at the center.

REGISTRATION

The conference registration booth will be in the breezeway outside the conference center. Registration

hours will be 5:00 p.m. to 8:00 p.m. on Sunday, October 18, and 7:00 a.m. to 3:00 p.m., October 19–22.

AUDIO-VISUAL EQUIPMENT

Each room will be equipped with overhead projector and slide projector. If additional equipment is required, please contact the conference secretary or the registration booth.

CONFERENCE BANQUET

There will be a banquet held on the evening of Wednesday, 21 October for conference attendees and their guests. The banquet will be preceded by a reception starting at 18:00 (6:00 p.m.).

CALL FOR NOMINATIONS FOR GEC GENERAL AND EXECUTIVE COMMITTEES

The GEC Executive Committee (ExComm) is the governing body of the GEC. It is the responsibility of ExComm to oversee the ''cradle-to-grave'' operation of the conference. This includes selection of meeting sites, budgetary decisions, selection of special topics and invited speakers, accepting/rejecting abstracts and arranging of the program. The ExComm formally meets three times a year: the General Committee and ExComm meetings during the GEC, and the Summer ExComm Meeting where the program of the next GEC is arranged. There are numerous communications between members of the ExComm (usually e-mail) during the year to see to the successful completion of their duties. We have been fortunate over the years to have a dedicated group of volunteers who have been willing to take on these very necessary roles.

The by-laws of the Gaseous Electronics Conference describe the process whereby members of the ExComm are elected. At the GEC Business Meeting (to be held on Tuesday, October 20, 11:30 a.m.) nominations are accepted for members of the GEC General Committee (GenComm). The GenComm consists of the ExComm and six at-large members elected at the Business Meeting. The eligible voting membership of the GEC (defined as those attending the Business Meeting) elect these six at-large members. The GenComm then meets to fulfill its only duty: to elect new members of ExComm.

The ExComm membership consists of the Chair, Treasurer, Past-Secretary, Secretary, Secretary-elect, past or incoming Chair and four at-large members. The Chair is a 4-year term (1-year incoming, 2-years chair, 1-year past-chair), the secretary is a 3-year term (1-year incoming, 1-year secretary, 1-year past- secretary), and all other ExComm members serve 2 years. (The secretary is the person who manages the local arrangements for the meeting and is usually ''recruited'' and appointed to the ExComm.)

The ExComm welcomes nominations, including self- nominations, for both the GenComm and ExComm. Becoming a GenComm and/or ExComm member provides a unique opportunity to see both how the GEC is run and to influence its future direction by helping to define the programs and choose future sites. Please submit your nominations to the GEC Chair or any member of the ExComm (listed earlier in this announcement). The ExComm also welcomes inquiries on hosting the GEC.

CONFERENCE SECRETARY

Further information on the conference may be obtained from the conference secretary at the following address:

Prof. Charles Fleddermann
Dept. of Electrical and Comp. Eng.
EECE Building
University of New Mexico
Albuquerque, NM 87131
(505) 277-5628 (Voice)
(505) 277-1439 (FAX)
Email: cbf@eece.unm.edu

MAUI HIGH PERFORMANCE COMPUTING CENTER

The Maui High Performance Computing Center (MHPCC) is located a short distance from the conference hotel. The MHPCC will be offering GEC/

ICRP attendees a short course and Center tours.

A. Short Course

The MHPCC will offer a short course, *Introduction to Parallel Programming*, on Friday morning,

October 23 from 8:30 to 12:30 p.m.

Cost for the course will be $25.

Further information can be obtained from Kelly Suzuki at the MHPCC. She may be contacted via email at: workshop@mhpcc.edu or by FAX at (808) 879-5018.

B. Tours

The MHPCC will also offer GEC/ICRP attendees tours which will include an overview of the MHPCC and some demonstrations. The demonstrations might include Wildfire Modeling, a wildfire behavior model using an actual fire that occurred in Yosemite National Park in August 1996; a Remote Radiation Therapy Treatment Planning model; a VRML model of the Lanai Aquifer System; and perhaps an AMOS demo depicting image reconstruction of data collected by the Air Force Maui Optical Station on Haleakala. Tours will take 1-1/2 to 2 hours and will be limited to 20 - 25 people at a time. Tours will begin on Tuesday, 20 October and will be offered on additional days if there is sufficient demand. Sign-up for tours must be at least one day before the actual tour.

PLEASE NOTE

The APS has made every effort to provide accurate and complete information in this *Bulletin*. However, changes or corrections may occasionally be necessary and may be made without notice after the date of publication. To ensure that you receive the most up-to-date information, please check the meeting Corrigenda distributed with this *Bulletin*.

Epitome of the 1998 GEC/ICRP Meeting

7:30 MONDAY MORNING 19 OCTOBER 1998

AM1 **Electron-Atom Scattering**
Teubner, Vuskovic
Plumeria/Jade Room, Aston Wailea

AM2 **RF Glows**
Nakano.
Maile Room, Aston Wailea

AM3 **Oxide Etch**
Tachibana, Nakagawa
South Pacific Ballroom, Aston Wailea

10:00 MONDAY MORNING 19 OCTOBER 1998

BM1 **Electron Transport**
Olthoff, Nakamura, Morris
Plumeria/Jade Room, Aston Wailea

BM2 **RF & Pulsed Plasmas**
Braithwaite, Economou
Maile Room, Aston Wailea

BM3 **Energy Distribution Diagnostics**
Donnelly
South Pacific Ballroom, Aston Wailea

13:30 MONDAY AFTERNOON 19 OCTOBER 1998

CM1 **Foundations of Gaseous Electronics**
Crompton
Plumeria/Jade/Maile Room, Aston Wailea

14:45 MONDAY AFTERNOON 19 OCTOBER 1998

DM1 **Lamps and Displays**
Kroesen, Shinoda
Plumeria/Jade Room, Aston Wailea

DM2 **Pulsed & Microwave Glows**
Boswell, Hebner
Maile Room, Aston Wailea

DM3 **Innovative Plasma Sources: Diagnostics and Applications**
Kuzumoto
South Pacific Ballroom, Aston Wailea

17:15 MONDAY AFTERNOON 19 OCTOBER 1998

EMP1 **Dusty Plasmas**
Haku/Pikake Room, Aston Wailea

EMP2 **Charged Particle Diagnostics**
Haku/Pikake Room, Aston Wailea

EMP3 **Coronas/Breakdown**
Haku/Pikake Room, Aston Wailea

EMP4 **Deposition**
Haku/Pikake Room, Aston Wailea

EMP5 **Plasma-Surface Interaction and Sheaths**
Haku/Pikake Room, Aston Wailea

EMP6 **Inductively Coupled Plasmas**
Haku/Pikake Room, Aston Wailea

EMP7 **Heavy Particle Collisions**
Haku/Pikake Room, Aston Wailea

EMP8 **Helicon Plasmas**
Haku/Pikake Room, Aston Wailea

7:30 TUESDAY MORNING 20 OCTOBER 1998

FT1 **Electron / Ion Transport**
Setser
Plumeria/Jade Room, Aston Wailea

FT2 **Laser Diagnostics**
Uchino, Kono
Maile Room, Aston Wailea

FT3 **Inductively Coupled Plasmas I**
Caughman
South Pacific Ballroom, Aston Wailea

10:00 TUESDAY MORNING 20 OCTOBER 1998

GT1 **Post-Deadline Session**
Plumeria/Jade Room, Aston Wailea

GT2 **Nucleation and Growth of Dust Particles**
Shiratani, Fujiyama
Maile Room, Aston Wailea

GT3 **Inductively Coupled Plasmas II**
Hayashi
South Pacific Ballroom, Aston Wailea

13:30 TUESDAY AFTERNOON 20 OCTOBER 1998

HT1 **ICRP Distinguished Lecturer**
Sugai
Plumeria/Jade/Maile Room, Aston Wailea

14:45 TUESDAY AFTERNOON 20 OCTOBER 1998

IT1 **Heavy-Particle Interactions**
Feagin, Wiese, Schultz
Plumeria/Jade Room, Aston Wailea

IT2 **Lamps**
Piejak, Ishigami, Ukegawa
Maile Room, Aston Wailea

IT3 **Etching and Deposition Simulation**
Kinoshita
South Pacific Ballroom, Aston Wailea

17:15 TUESDAY AFTERNOON 20 OCTOBER 1998

JTP1 **Optical Diagnostics: Active Species**
Haku/Pikake Room, Aston Wailea

JTP2 **Optical Diagnostics**
Haku/Pikake Room, Aston Wailea

JTP3 **Plasma Jets**
Haku/Pikake Room, Aston Wailea

JTP4 **Magnetron Plasmas**
Haku/Pikake Room, Aston Wailea

JTP5 **Etch**
Haku/Pikake Room, Aston Wailea

JTP6 **Glows**
Haku/Pikake Room, Aston Wailea

JTP7 **Electron / Ion Transport and Chemistry**
Haku/Pikake Room, Aston Wailea

7:30 WEDNESDAY MORNING 21 OCTOBER 1998

KW1 **Electron-Molecule Scattering**
Brunger, McKoy
Plumeria/Jade Room, Aston Wailea

KW2 **Surface Reactions**
Ohiwa, Hikosaka
Maile Room, Aston Wailea

KW3 **Environmental Applications**
Sawin, Morrow
South Pacific Ballroom, Aston Wailea

10:15 WEDNESDAY MORNING 21 OCTOBER 1998

LW1 **Allis Prize Lecture**
Flannery
Plumeria/Jade/Maile Room, Aston Wailea

11:15 WEDNESDAY MORNING 21 OCTOBER 1998

MW1 **GEC Business Meeting**
Plumeria/Jade/Maile Room, Aston Wailea

13:15 WEDNESDAY AFTERNOON 21 OCTOBER 1998

NW1 **DC and Microwave Glows**
Ganguly
Plumeria/Jade Room, Aston Wailea

NW2 **Lasers and Excimer Sources**
Piper, Sakai
Maile Room, Aston Wailea

NW3 **Transient Discharges and Collective Effects in Dusty Plasmas**
South Pacific Ballroom, Aston Wailea

15:15 WEDNESDAY AFTERNOON 21 OCTOBER 1998

OWP1 **ECR Plasmas**
Haku/Pikake Room, Aston Wailea

OWP2 **Displays, Lamps, and Lasers**
Haku/Pikake Room, Aston Wailea

OWP3 **Positive and Negative Ions in Plasmas**
Haku/Pikake Room, Aston Wailea

OWP4 **Innovative Plasma Applications**
Haku/Pikake Room, Aston Wailea

OWP5 **RF Glows**
Haku/Pikake Room, Aston Wailea

OWP6 **Lepton Collisions with Molecules**
Haku/Pikake Room, Aston Wailea

OWP7 **Electron-Atom Collisions**
Haku/Pikake Room, Aston Wailea

18:00 WEDNESDAY AFTERNOON 21 OCTOBER 1998

PW1 **Reception and Banquet**
Aulani Ballroom, Aston Wailea

7:30 THURSDAY MORNING 22 OCTOBER 1998

QR1 **Plasma Jets**
Krier, Moss
Plumeria/Jade Room, Aston Wailea

QR2 **Deposition**
Takai, Shimogaki
Maile Room, Aston Wailea

QR3 **Magnetized Plasmas**
South Pacific Ballroom, Aston Wailea

10:00 THURSDAY MORNING 22 OCTOBER 1998

RR1 **Collisional Processes in Plasmas**
Tanaka, Morgan
Plumeria/Jade Room, Aston Wailea

RR2 **Plasma Diagnostics**
Loewenhardt
Maile Room, Aston Wailea

RR3 **Magnetized Plasmas and Thermal Plasmas**
Serikov
South Pacific Ballroom, Aston Wailea

13:45 THURSDAY AFTERNOON 22 OCTOBER 1998

SR1 **Advanced Plasma Processing**
Watanabe, Tetsu, Samukawa, Horiike
Plumeria/Jade Room, Aston Wailea

SR2 **Plasma Surface Interactions**
Aydil
Maile Room, Aston Wailea

SESSION AM1: ELECTRON-ATOM SCATTERING

Monday morning, 19 October 1998; Plumeria/Jade Room, Aston Wailea at 7:30
Chuck Noren, Jet Propulsion Laboratory, presiding

Invited Papers

7:30
AM1 1 Electron Scattering from Alkali Atoms.
P.J.O. TEUBNER, *Department of Physics, The Flinders University of South Australia, GPO Box 2100, Adelaide, South Australia, Australia 5001*

A series of scattering experiments of electrons from laser excited lithium and potassium atoms has been performed. Orientation and alignment parameters have been measured at several incident energies over a very wide angular range. These parameters provide very sensitive tests of the theory of electron scattering from atoms. The experiments will be described and the results compared with the predictions of several theories. In the case of electron scattering from lithium we find excellent agreement with the predictions of the convergent close coupling calculation. The agreement between experiment and theory is not as good in the case of electron scattering from potassium.

8:00
AM1 2 Absolute Cross Sections of Low-Energy Electron Collisions with Excited Atoms.
LEPOSAVA VUSKOVIC, *Old Dominion University*

Electrons in the energy range 1-30 eV present the dominant charged particle group in most low-temperature plasmas. Experimental work on collisions between the electrons in this energy range and excited atoms is still relatively rare, because of practical difficulties. Such experiments are not only important because of their fundamental interest, but also because they provide data relevant to practical problems. Mechanisms underlying many phenomena in weakly ionized gas are based, in part, on the low-energy electron collisions with atoms and molecules. Ionization balance in partially ionized gas is maintained by a combination of excitation and ionization processes involving electrons. In addition, the momentum transfer from low-energy electrons to neutral particles is a significant mechanism in the heating of heavy particles. On the other hand, it is well known that excited states, especially metastables, are the intermediate states in the multi-step ionization processes from ground-state atoms and molecules. Further, collisions between electrons and excited states are the dominant mechanism for ionization at higher gas pressures, usually competing with the energy pooling processes involving two excited states. A review will be given of the absolute differential cross section measurements, with the emphasis on the recoil atom measurements. The advantages and limitations of this technique will be discussed with respect to the measured absolute differential cross section for elastic, inelastic, and superelastic electron scattering. The total ionization cross section of excited sodium has been determined in the energy range from threshold to 30 eV by measurements of collisionally produced ions as a function of electron energy.

Contributed Papers

8:30
AM1 3 Polarized Electron Impact Excitation of Krypton* T.J. GAY, H.M. AL-KHATEEB, B.G. BIRDSEY, T.C. BOWEN, M.L. JOHNSTON, *University of Nebraska, Lincoln, NE 68588-0111* We have studied the impact excitation of Kr by transversely-polarized electrons, measuring the integrated Stokes parameters of light emitted when the excited $4p^5 5p$ manifold decays to the $4p^5 5s$ configuration. Such measurements are particularly sensitive to spin-orbit effects in the excitation process. Our data will be compared with the most recent close-coupling and perturbative calculations. Potential sources of systematic experimental error will be discussed, including the effects of the electron-beam energy width.

*Supported by NSF Grant PHY-9732258

8:45
AM1 4 Position Sensitive, Recoil Atom Spectroscopy: A New Technique for the Measurement of Low Energy Electron Scattering Cross Sections K.W. TRANTHAM#, S.J. BUCKMAN, *Australian National University* We have developed a highly efficient technique for the measurement of near threshold inelastic electron scattering. Metastable atoms, produced by electron impact, are detected as a function of their recoil position with a two dimensional position sensitive detector (PSD). By using a supersonic atomic beam, a pulsed electron beam and time-of-flight gating of the PSD, recoil atom patterns with intensities which are directly proportional to the electron scattering cross section can be measured. The gain in efficiency over conventional techniques using scattered electron detection are substantial. Examples of the technique and possible applications will be presented. #Permanent address: Arkansas Technical University, Russellville, Arkansas.

9:00
AM1 5 Simultaneous Electron-Impact Ionization–Excitation of Helium KLAUS BARTSCHAT, *Drake University** The gen-

eral R-matrix code for electron-impact ionization [1] has been modified (i) to allow for high incident electron energies within the Plane-Wave Born Approximation (PWBA) and (ii) to improve upon the description of both the target ground state and the interaction of the ejected electron with the residual ion via an R-matrix with pseudo-states (RMPS) approach [2,3]. Results for cross sections (total, single-, double-, and triple-differential) as well as parameters measured in electron–photon coincidence experiments [4] for electron impact ionization–excitation to the $He^+(2p)$ excited ionic state will be presented and compared with recent experimental data and predictions from other theoretical approaches. 1. K. Bartschat, Comp. Phys. Commun. **75**, 219 (1993) 2. K. Bartschat *et al.*, J. Phys. B **29**, 115 (1996) 3. P.J. Marchalant and K. Bartschat, Phys. Rev. A **56** (1997), R1697 4. M. Dogan *et al.*, J. Phys. B **31**, 1611 (1998)

*This work is supported by the National Science Foundation under grant PHY-9605124.

9:15

AM1 6 Temporary Negative Ion Resonances in Electron Scattering by Group II Metals J.P. SULLIVAN, D.S. NEWMAN, R.P. MCEACHRAN, S.J. BUCKMAN, *Australian National University* P.D. BURROW, J.A. MICHEJDA, *University of Nebraska* K BARTSCHAT, *Drake University* A range of different experimental (electron transmission, elastic electron scattering, decay photon detection) and theoretical (Breit-Pauli R-matrix, phaseshift analysis) techniques have been used to study the formation and decay of transient negative ions (resonances) in low-energy electron scattering from the Group II metals Mg, Zn, Cd and Hg. Some remarkable similarities are observed in the spectra. The various techniques enable refinements to be made to previous classifications of some of the observed resonances. Several new classifications are also proposed. This work is supported in part by the NSF under grant PHY-9605124.

SESSION AM2: RF GLOWS

Monday morning, 19 October 1998
Maile Room, Aston Wailea at 7:30
J. Johannes, Sandia National Labs, presiding

Contributed Papers

7:30

AM2 1 Hybrid Monte Carlo-fluid model for an rf Ar glow discharge, and comparison with a dc glow discharge. ANNEMIE BOGAERTS, RENAAT GIJBELS, *University of Antwerp, Belgium.* WIM GOEDHEER, *FOM-Institute for Plasmaphysics "Rijnhuizen", The Netherlands.* A two-dimensional hybrid model has been developed for an rf discharge in argon, based on a Monte Carlo model for electrons, and a fluid model for electrons and argon ions. Collision processes taken into account in the Monte Carlo model comprise elastic collisions with argon atoms, electron impact excitation and ionization from the argon ground state, and electron-electron Coulomb scattering. The fluid model consists of the continuity equations for electrons and argon ions, and the transport equations based on diffusion and migration. Moreover, an energy balance equation is included for the electrons. These equations are coupled to Poisson equation to obtain a self-consistent electric field distribution. Typical results of the model include the densities and fluxes of argon ions and electrons, the electron energy distribution function, the potential and electric field distribution, information about collision processes in the plasma, etc., all as a function of position in the plasma and time in the rf-cycle.

7:45

AM2 2 Stress Reduction in Silicon Dioxide Layers by Pulsing an Oxygen/Silane Helicon Diffusion Plasma C. CHARLES, R.W. BOSWELL, *Plasma Research Lab, Australian National University* A low pressure, high density helicon reactor used to deposit silicon dioxide (SiO_2) from a mixture of oxygen/silane has been pulsed with a constant "on" time of 500 μsec and a duty cycle varying from 10% to 100%. Over this range, the deposition rate changes by only a factor of 2.5 implying that deposition is continuing in the post discharge with a time constant of 1 ms. For duty cycles of 30% and above, the films show good characteristics but the 10% duty cycle has a somewhat higher "p-etch" implying some porosity. The pulsing reduces the compressive stress by at least a factor of two. This is correlated with the reduction in the measured plasma potential and density implying that for the present conditions, the stress is determined by the energy and number of ions striking the growing film. For the low ion energies considered here ($\leqslant$ 50 eV) a simple model using a temporal evolution of the ion energies and fluxes measured in an argon plasma suggests that the compressive stress would decrease in the post-discharge with a time constant of about 80 μsec, assuming that the total stress is the integral of the stress over the "on" period and the "off" period. The experimental results in oxygen/silane plasmas show that this is probably an upper limit and the actual decay time may be considerably less.

8:00

AM2 3 B-Spline Based Sampling Techniques for Particle Simulations in Plasmas T. YAMAGUCHI, *Showa Electric Wire & Cable Co. Ltd.* Y. OHMORI, *Sapporo Univ.* P.L.G. VENTZEK, *Motorola Inc.* K. KITAMORI, *Hokkaido Inst. of Technology* One of the reasons for the "slowness" of particle simulations of plasmas derives from the large number of particles required to gather reasonable statistics. We have developed a simulation scheme that treats both electrons and ions as particles and solves for their motion with Poisson's equation in a self consistently for a 1D parallel plate capacitively coupled discharge. At the end of each time-step we employ a Legendre Polynomial Weighted Sampling (LPWS) technique to sample the space, velocity and energy distribution functions of the particles. Then, new Monte Carlo particles are launched using a B-Spline method with information from the LPWS distributions to define the positions and velocities of the new particles. Advantages are that the B-Spline is that the electric field can be determined analytically and that this allows for a calculation of the electric field with a constant and minimum of particles throughout the simulation. This will be illustrated using argon and will include a dc self bias on the powered electrode.

8:15

AM2 4 Optimization of Plasma Uniformity Using Hollow-Cathode Structures in RF Discharges* DA ZHANG, MARK J. KUSHNER, *University of Illinois, Urbana, IL 61801 USA* Obtaining high plasma densities with uniform fluxes to the substrate in radio frequency (rf) capacitively coupled discharges is often difficult due to electric field enhancement at the edges of the electrodes. Nonplanar or segmented electrodes have been proposed to leverage electric field nonuniformites to produce uniform fluxes. Sugawara recently demonstrated a concentric hollow-cathode electrode with which uniform ion fluxes were produced.[1] In this paper, we report on a computational investigation of the concentric

hollow-cathode electrode in low pressure rf discharges operating in Ar and Ar/Cl_2 mixtures using the the 2-dimensional Hybrid Plasma Equipment Model (HPEM).[2] We found that the radial distribution of plasma density could be controlled by the spacing and depth of the hollow cathode segments. When operating at critical p-d the depth of the gap of the concentric electrodes determined the intensity of the resulting local hollow cathode plasma and, to some degree, the local electron temperature. A parametric study and comparisons to experiments are used to investigate the limits of this technique.

*Work was supported by SRC and NSF.

[1]M. Sugawara and T. Asami, Surf. Coatings Technol., v.73, 1 (1995).
[2]S. Rauf and M. J. Kushner, J. Appl. Phys. v.83, 5087 (1998).

8:30

AM2 5 Two-dimensional Simulation of RF CF_4 Discharge Using the Particle-in-Cell/Monte Carlo Method K. DENPOH, *Central Research Laboratory, Tokyo Electron Ltd.* K. NANBU, *Institute of Fluid Science, Tohoku University, Japan* Two-dimensional structure of rf CF_4 plasma is investigated using the Particle-in-Cell/Monte Carlo method. The charged species considered are the electron, five positive ions(CF_3^+, CF_2^+, CF^+, C^+, F^+), and two negative ions(F^-, CF_3^-). The collisions taken into account are the electron-CF_4, positive-negative ion recombination, and electron-CF_3^+ recombination. We also implemented the ion-CF_4 collision using our collision model which includes not only the elastic collision but also endothermic reactions such as dissociation and electron detachment from negative ions. A self-bias at the powered electrode is determined by balancing fluxes of positive and negative charges coming to the powered electrode so as to make the dc component of the current null. The discharge structure is characterized by both an asymmetric electric field in the axial direction due to the self-bias at the powered electrode and an enhanced electric field around the edge of the powered electrode. We found, for example, that a double-layer appears in the radial component of the electric field near the edge of the sheath along the cylindrical reactor wall. Of course the double-layer in the axial component of the electric field is observed as in one-dimensional simulations.

Invited Papers

8:45

AM2 6 Modeling of two-frequency capacitively-coupled plasmas.
NOBUHIKO NAKANO, *Keio University*

Useful modeling for plasma process is highly required to save the time and cost of the reactor and process development. Several type of plasma etching reactor (2f-CCP, UHF, ICP, NLD, ECR etc.) are developed for future critical dimension. Especially the two-frequency capacitively coupled plasma(2f-CCP) using HF or VHF(13.56 ~ 100 MHz) for the plasma production and LF(~1MHz) for the bias has the remarkable performance that realize contact hole of 0.1μm ϕ in diameter and 10 in aspect ratio by Ar and fluorocarbon gas mixture. SiO_2 etching is a one of difficult process to control for the tradeoff between etching rate and etch selectivity. Therefore the macroscopic and microscopic understanding of the plasma physics and chemistry is necessary. In this work, dual-frequency plasma in Ar and Ar/CF_4 gas mixture are modeled by two-dimensional relaxation continuum(RCT) model, considering the radical transport including the reaction in the gas phase and on the surface. The results are compared with the time dependent two dimensional(2D-t) image of optical emission spectroscopy. The effects of driving and bias frequency and the self bias for the plasma structures are discussed with comparison between pure Ar and Ar 95%/CF4 mixture. The effects on etching are also discussed for the ion flux and energy, and the radical transports considering surface material and area.

Contributed Papers

9:15

AM2 7 Dependence of driving frequency on capacitively coupled plasma in CF_4 S. SEGAWA, *Tokyo Electron Limited* M. KURIHARA, N. NAKANO, T. MAKABE, *Keio University, Japan* A radio-frequency CF_4 plasma in reactive-ion etcher with parallel plate geometry is investigated in one dimensional relaxation continuum model. Electrons play the leading role in non-equilibrium reactions in CF_4 rf discharges. One of the most important characteristics in reactive plasmas for etching is the degree of the electronegativity, defined as the ratio of the number density of the negative ion to the positive. The electronegativity and the transport of negative ions have a large effect on the plasma structure and processing. The effect of external driving frequency is numerically studied between 13.56 MHz and 200 MHz for 50 mTorr and 200 mTorr. In these studies the plasma density is kept constant ~ 10^{11} cm^{-3} as changing the applied voltage from 50 V to 680 V, considering the charged species CF_3^+, CF_2^+, CF^+, C^+, F^+, F^-, and electron. The amount of negative ion strongly depends on the pressure and the driving frequency. We also discuss the ion mean energy onto the substrate as a function of the driving frequency.

9:30

AM2 8 Monte Carlo Simulations of Collisionless Heating in RF Plasma Sheaths GEORGE GOZADINOS, DAVID VENDER, MILES TURNER, *PRL, DCU** Collisionless heating of electrons in rf sheaths is important in low pressure capacitive discharges, but it is difficult to separate the power loss in this process from other loss mechanisms experimentally. Theoretical models are thus best compared to simulations. A Monte Carlo simulation is used to examine the details of the electron-sheath interaction and the resulting power loss is compared to theoretical estimates derived from the 'hard wall' model, in which single electrons are assumed to collide elastically with a moving sheath edge. The theory is sensitive to the form of the incident electron velocity distribution and expected to apply only when the electron thermal velocity greatly exceeds the velocity of the moving sheath edge. Both self-consistent electric fields derived from PIC simulations and model fields are used for comparison. The Monte Carlo simulations highlight the importance of a small field which exists between the plasma and the position of the moving sheath edge. Scaling with both applied rf voltage and frequency is examined.

*This work is supported by Association EURATOM DCU Contract ERB 50004 CT960011

SESSION AM3: OXIDE ETCH

Monday morning, 19 October 1998; South Pacific Ballroom, Aston Wailea at 7:30; M. Itoh, Nagoya University, presiding

Invited Paper

7:30

AM3 1 Gas Phase and Surface Diagnostics in Fluorocarbon Plasmas for SiO_2 Etching.
KUNIHIDE TACHIBANA, *Department of Electronic Science and Engineering, Kyoto University*

Etching selectivity and its reproducibility are key issues in the etching of SiO_2 over Si in ULSI processing. In various plasma sources, especially in high density sources such as ICP, ECR, etc., the controlling method of F atom density relative to CF_x radical density has become an essential problem. Surface conditions of the substrate and chamber walls, however, are reflected in the gas phase reactions ineviably, so that *in situ* diagnostics of both gas phase species and surface bonding states are required for understanding the overall chemistry in SiO_2 etching. For the gas phase diagnostics we have developed two new techniques, i.e., VUV laser absorption spectroscopy (VUV-LAS) using a tunable laser around 95.5 nm region for the detection of F atoms and electron attachment mass spectrometry (EAMS) for the detection of polymerized species. VUV-LAS has an advantage over previously developed methods in the determination of absolute density with higher accuracy, and EAMS is suited for detecting big clusterized molecules or radicals with less fragmentation. For the *in situ* surface diagnostics Fourier-transform infrared phase-modulated spectroscopic ellipsometry (FT-IR PMSE) has been developed to diagnose surface bonds on Si and SiO_2 substrates formed by exposing to plasmas. Chemical bonds such as $-CF_x$, $-CH_xF_y$, $-SiF_x$ as well as Si-C and C-C have been detected successfuly by this method. Systematic measurements of radical densities have been carried out in various source gases such as CF_4, CHF_3, C_2F_6 and C_4F_8, and the effects of dilution gases such as H_2 and O_2 have also been investigated. For understanding the production and loss processes of those radicals, the rise and fall characteristics of the densities have been measured by pulsing the discharge. At the same time the changes in the surface chemical bonds have been monitored by FT-IR PMSE and their dependence on the discharge conditions and substrate bias conditions have been investigated. Those data are combined together with other data obtained by laser induced fluorescence measurements of CF and CF_2 radicals in the gas phase and XPS analyses of substrates, and the reaction chemistry in the etching of SiO_2 will be argued for realizing better selectivity and reproducibility.

Contributed Papers

8:00

AM3 2 Loss Processes of F atoms in High-Density CF_4–H_2 Plasmas K. SASAKI, K. USUI, C. SUZUKI, K. KADOTA, *Department of Electronics, Nagoya University, Nagoya 464-8603, Japan* The addition of H_2 into CF_4 plasmas is widely employed to enhance the etching selectivity of SiO_2 over Si in contact hole processing. The high etching selectivity of SiO_2 is attributed to the low F atom density in CF_4–H_2 plasmas. Generally, it is considered that a gas-phase reaction $F + H_2 \rightarrow HF + H$ plays an important role in the reduction of the F atom density. In the present work, we have measured the absolute F atom density in high-density CF_4–H_2 plasmas by vacuum ultraviolet absorption spectroscopy. The decay time constant of the F atom density in the afterglow has also been measured to clearly the loss processes of F atoms. Helicon-wave CF_4–H_2 plasmas having a high electron density ($\simeq 1 \times 10^{12}$ cm^{-3}) were produced in a linear machine with a uniform magnetic field of 1 kG. The rf power applied to the plasma was 1 kW at 13.56 MHz. The pressure of CF_4 was fixed at 5 mTorr with a flow rate of 4.4 ccm. The pressure of H_2 was varied from 0 to 5 mTorr by changing the flow rate. Both the density and the lifetime of F atoms decreased with the H_2 partial pressure. However, the density and lifetime were not determined uniquely by the H_2 partial pressure; they were strongly affected by the conditions of the chamber surface. This means that the reduction of the F atom density in CF_4–H_2 plasmas is governed by surface chemistry as well as the gas-phase reaction $F + H_2 \rightarrow HF + H$.

8:15

AM3 3 Mechanism Investigation of F atom Scavenge by Si-top-electrode in Fluorocarbon Plasma M. OKIGAWA, H. HAYASHI, S. MORISHITA, M. INOUE, M. SEKINE, *Association of Super-Advanced Electronics Technologies (ASET)* We investigated the changes in $CF_{x(x=1,2,3)}$, Si, and F radical-densities which resulted from ion-bombardment onto the Si-top-electrode in C_4F_8/Ar or CF_4/Ar plasma. The energy of ion-bombardment was controlled by a 13.56 MHz rf bias applied to the top electrode where 500 MHz power was also supplied for ECR plasma excitation. A typical result was when top biasing voltage increases, F radical-density gradually decreases in the C_4F_8/Ar plasma and Si density increases. In order to clarify how F atoms are reduced, we also evaluated CF_4/Ar plasma. We found that the change in F density due to the ion- bombardment in the C_4F_8/Ar plasma is much larger than that in the CF_4/Ar plasma though the F densities without biasing are almost the same in both cases. Furthermore, we discovered that the ratio of CF_2 to F in C_4F_8/Ar does not change when the top biasing increases, nevertheless, the ratio in CF_4/Ar decreases with a rise in biasing. Taking into account that an F radical is produced from a CF_2 radical in a C_4F_8/Ar gas system[1], these results indicate that the reduction of F density in a C_4F_8/Ar gas system with electrode biasing is due to the decline in CF_2 density. Also the differences in the results for C_4F_8 and CF_4 could not be explained by the hypothesis that Si in the plasma directly reacts with F to scavenge F atoms. In the meeting we will discuss fluorocarbon film composition and etching characteristics as well. This work was supported by NEDO.

[1]Hayashi et.al., Plasma Processing Symp., Hamamatsu Japan, 1998 p. 577.

8:30
AM3 4 Diode Laser Measurements in High Density Fluorocarbon Plasmas HAROLD ANDERSON, *University of New Mexico* LEE PERRY, *University of New Mexico* Inductively coupled, high-density plasma reactors are expected to play a key role in next generation 0.25 μm semiconductor manufacturing. This work focuses on diode laser diagnostics of two such reactors: a non-commercial GEC Cell inductively coupled plasma and a commercial AMAT 5300 HDP oxide etcher. In this study, we employ diode lasers in the mid-IR regime (3-11 μm) to detect radicals important to oxide etching. The experiments in this study focused on radical concentrations found in the reactor under typical high-density plasma etching conditions. Gas phase measurements of etchant species (CF and CF_2) formed from dissociation of a C_2F_6 plasma, and etch-product species formed from plasma surface interactions are described. The technique is crucial to plasma model development since it is one of the few techniques that can reliably measure the absolute density of ground state radical species formed by electron impact dissociation in the discharge. A database of neutral radical species concentrations at various reactor power, bias and pressure settings is presented. This database is essential for theoretical plasma model calibration and validation.[1]

[1]This work has been supported by SEMATECH

8:45
AM3 5 Effects of Gas Flow Structures on Radical- and Product-density Distributions on Wafers in Low-pressure Plasma Etching Reactors M. IKEGAWA, *Hitachi* J. KOBAYASHI, *Hitachi* R. FUKUYAMA, *Hitachi* Gas flows in recent high-etching-rate reactors are becoming an increasing concern because they must be accurately controlled to get better uniformities of etching rate, selectivity, and profile on large wafers. For low-pressure etching reactors, such as a magneto-microwave plasma reactor, gas flows are characterized as a rarefied gas flow. These gas flows in etching reactors were calculated using a direct simulation Monte Carlo program[1]. The uniformity of radical- and etching-product concentration distributions on the wafer, which influence the etching rate distribution, was improved by using a cylindrical ring around the wafer or an improved gas-supply structure.

[1]M. Ikegawa & J. Kobayashi, JSME International Journal Series II, 33, No.3 (1990) p.463.

Invited Paper

9:00
AM3 6 Diagnostics and etch characteristics in UHF plasmas.*
YUKITO NAKAGAWA, TSUTOMU TSUKADA, *ANELVA Corp, Japan* .
SEIJI SAMUKAWA, *NEC Corp, Japan*†

Plasma properties, etch characteristics and advantages of a new plasma source where a UHF power is used to ignite the plasma are reported. Plasma was produced using two different antennas and data obtained are discussed comparatively. First, a spokewise antenna consisted of 12 spokes arranged similar to the spokes in a wheel was studied. Though, the UHF power was applied to two rods in the same line, the UHF power radiates uniformly from antenna to the plasma. Secondly, a multi window antenna, constructed with a re-entrant type cavity resonator having 6 quartz windows on the bottom plate was used. Here, the UHF power confines in the cavity and radiates through the quartz windows to the plasma. The dimensions of both antennas were selected to be resonated at 500 MHz. The pressure range of a stable plasmas and the electron temperature observed with both antenna are found to be the same, while the plasma production efficiency and radial uniformity of the plasma are improved with the multi-window antenna. The radial uniformity of plasma over ϕ300mm area is $< \pm 5\%$ at the plasma density of $10^{11}cm^{-3}$. The electron temperature is observed to be < 3 eV for both antennas even in the plasma production region. A chlorine plasma produced by the spokewise antenna was used to etch poly-Si with 0.1μm patterns. The plasma yields good etching characteristics without notching or CD loss and produces the selectivity to under-layer SiO_2 over 100. Further, the etching characteristics are found to be the same regardless of poly-Si is doped or non-doped, or the type of doping. Since the multi-window antenna produces a higher density plasma, it was used for SiO_2 etching with C_4F_8 gases. This chemistry etches ϕ 0.12μm contact holes satisfying all the requirements. Accordingly, UHF plasma source meets fine and critical etching requirements those are demanded by the future semiconductor industry.

*This work is promoted as a joint research of ANELVA Corp., NEC Corp. and NIHON KOSHUHA Co., Ltd.
†The author thanks Dr. Tsukada, ANELVA and Dr. Samukawa, NEC.

Contributed Paper

9:30
AM3 7 New Radical-Injection Method for SiO_2 Plasma Etching with Non-Perfluorocompound Gas Chemistries SEIJI SAMUKAWA, KEN-ICHIRO TSUDA, *NEC Corporation, Japan* To control the generation of radicals used for the etching of silicon dioxide, we developed a radical-injection method that uses the iodofluorocarbon chemistry (environmentally alternatives to perfluorocarbon chemistry) in an ultra-high-frequency (UHF: 500MHz) plasma. In the UHF plasma, the mean electron energy is about 2 eV and electrons with an energy of more than 5 eV are drastically reduced i.e., the electron energy distribution function is non-maxwellian. The C-I bonds (2.0 eV) of an iodofluorocarbon gases (such as, CF_3I, CF_2I_2, and C_2F_5I) are therefore selectively dissociated in the UHF plasma, whereas the C-F bonds (4.9 eV) are not. As a result, the plasma completely suppresses the generation of F atoms, which causes low selectivity of SiO_2 to

underlying-Si,and contains a higher concentration (more than 10^{13} cm^{-3}) of CF_3 and CF_2 radicals. Moreover, the concentration of CF_2 and CF_3 radicals can be controlled precisely by adjusting the gas flow and the mixture ratio of these gases. It is very important in high-performance SiO_2 etching to have a high concentration of these radicals and to control the density ratio between them because the CF_3 produces the CF_3^+ ions which are the main etchant of SiO_2 and because CF_2 radicals are the main precursors for polymerization on the underlying Si.

SESSION BM1: ELECTRON TRANSPORT

Monday morning, 19 October 1998; Plumeria/Jade Room, Aston Wailea at 10:00; Peter Ventzek, Motorola, Inc., presiding

Invited Papers

10:00

BM1 1 Review of Electron Interaction Data for Plasma Processing Gases.

JAMES OLTHOFF, *NIST**

To assess the behavior of gases in their uses in manufacturing semiconductor devices and other applications, and to promote the modeling of these processes, it is necessary to have accurate information on the fundamental interactions of low energy ($<$ 100 eV) electrons with process gases. In support of this effort, we have undertaken the assessment and evaluation of the available information on cross sections and rate coefficients for collisional interactions of electrons with three groups of gases: those used in etching, deposition, or cleaning (e.g., CF_4, CHF_3, C_2F_6, C_3F_8, Cl_2, SF_6, NF_3 and HBr), those used as buffer gases (e.g., Ar, He), and those that are present in practical systems as impurities (e.g., O_2, N_2, H_2O). In this talk we summarize our assessed data on cross sections and rate coefficients for the gases whose review is completed: CF_4 , CHF_3, C_2F_6 , C_3F_8, and Cl_2. We also indicate specific electron-interaction data needs for these gases. In this regard, knowledge is lacking on two important basic processes, namely, dissociation into neutral fragments by electron impact and electron interactions with vibrationally and electronically excited species. In addition, with the sole exception of the electron-impact ionization of radicals from CF_4, there are few published data on the interactions of slow electrons with the radicals of these plasma processing gases. The recommended data for the reviewed gases and CCl_2F_2 are available via the World Wide Web at http://www.eeel.nist.gov/811/refdata.

*Work performed with Loucas Christophorou

10:30

BM1 2 Swarm Derived Cross Section Sets for Molecules Relevant to Plasma Processing.

Y. NAKAMURA, *Keio University*

During last several years, we have been engaged in determining sets of electron collision cross sections for molecules, such as SiH_4, Si_2H_6, GeH_4, CH_4, C_2H_6, CO_2, O_2, and CF_4. Works on C_2F_6 and C_3F_8 are also at their final stage. Our general scheme used in the study is, first, to measure the electron drift velocity and longitudinal diffusion coefficient in dilute molecular gas-rare gas (mainly argon) mixtures, typically of 1 to 10%, and in the pure molecular gas and, if possible, to measure the ionization and attachment coefficients in these gases. The E/N dependence of the drift velocity and the longitudinal diffusion coefficient of electrons in the dilute mixtures indicates the energy dependence of the vibrational excitation cross sections of the molecule. On the other hand, because of its small concentration, the elastic momentum cross section of the molecule has effectively negligible contribution to the swarm parameters in the mixture. It is, therefore, possible to determine the vibrational cross sections from them. We actually were able to see the resonance structures of the vibrational cross sections of SiH_4 for the first time (SiH_4: Kurachi and Nakamura, J. Phys. D 21, 602, 1988, ibid. 22, 107, 1989, IEEE Trans. Plasma Sci. 19, 262, 1991; GeH_4: Soejima and Nakamura, J. Vac. Sci. Technolo. A11, 1161, 1993; Si_2H_6: Nakamura, manuscript in preparation). Once these inelastic cross sections were known, the following measurement and analysis of the swarm parameters in the pure molecular gas are carried out to determine its elastic momentum transfer cross section in low energy region. So far we had applied our complete procedure to CO_2, C_2H_6 and CF_4 (CO_2: Nakamura, Aust. J. Phys. 48, 357, 1995; C_2H_6: Shishikura, Asano and Nakamura, J. Phys. D 30, 1610, 1997; CF_4: manuscript in preparation). We have just completed the measurements on C_2F_6 and C_3F_8, and preliminary results on their vibrational cross sections were obtained (ICAMDATA 1997) and we are now working on the elastic momentum cross section for these molecules. Also we might find an evidence of temporally negative-ion state of the C_3F_8 molecule (unpublished).

11:00

BM1 3 Reactivity of Air Plasma Ions with Aromatic Hydrocarbons.

ROBERT A. MORRIS, *Air Force Research Laboratory*

Rate constants and product distributions have been measured for reactions of the atmospheric primary cations O^+, O_2^+, N^+, N_2^+, and NO^+ with a selection of aromatic hydrocarbons using a Selected Ion Flow Tube (SIFT) instrument.

Aromatics studied included benzene and toluene, and all of the reactions were found to be fast. Benzene reacted mainly or exclusively by non-dissociative charge transfer with all the above ions except for N_2^+, for which dissociative charge transfer was the major channel. Toluene reacted mainly by non-dissociative charge transfer in all cases, with minor dissociative pathways found for O^+, N^+, and N_2^+. Since N_2^+ cleaves the benzene aromatic ring, these results may be relevant to plasma processing schemes for destroying volatile organic compounds (VOC's). The results are also being used in modeling studies of the effects of plasma ions on hydrocarbon combustion and ignition.

Contributed Papers

11:30

BM1 4 Electron transport in time varying fields Z.M. RASPOPOVIĆ, S. SAKADŽIĆ, S. BZENIĆ, Z.LJ. PETROVIĆ, *Institute of Physics, University of Belgrade, Belgrade, Yugoslavia.** Monte Carlo simulation was applied to study the electron transport in ramp model gas for high frequency crossed electric and magnetic fields. The frequencies between 1 MHz and 1 GHz were covered for E/N between 1 Td and 100 Td. The addition of a constant magnetic field to a sinusoidal electric field reduces the effect of anomalous diffusion[1]. If both fields are sinusoidal the perpendicular component of the drift velocity is modulated by 2ω, as expected. However, it is asymmetric in respect to the zero level and at high values of B/N time dependence becomes complex. Anomalous longitudinal diffusion develops for two components of the diffusion tensor. Hall diffusion has a complicated non-sinusoidal time profile. The calculations were extended to argon including a non-conservative process of ionization.

*Supported by MNTRS 01E03 project.

[1]K.Maeda, T.Makabe, N.Nakano, S.Bzenić and Z.Lj.Petrović, Phys. Rev. E **55** (1997) 5901

11:45

BM1 5 A Calculation Technique for Transverse Evolution of Electron Swarms in Gases* HIROTAKE SUGAWARA, YOSUKE SAKAI, *Hokkaido University, Japan* A simulation technique for observing the time-dependent electron swarm evolution in transverse direction was developed based on a propagator method[1]. Under an electric field applied in x direction, the temporal variation of the nth-order spatial moments of electrons with respect to y direction, $m_{y,n}(\boldsymbol{v},t) = \int_{\boldsymbol{r}} y^n f(\boldsymbol{r},\boldsymbol{v},t)\mathrm{d}\boldsymbol{r}$ $(n \geq 0)$, were calculated in order to derive the higher order transverse diffusion coefficients D_T, D_{T4}, D_{T6}, $\cdots$. The calculations were performed using a series of moment equations described in velocity space; $(\partial/\partial t)m_{y,n} = -a_x(\partial/\partial v_x)m_{y,n} + nv_y m_{y,n-1} + (\partial/\partial t)_{\mathrm{coll}} m_{y,n}$, in which $m_{y,n}$ can be expanded as $m_{y,n}(v,\theta,\phi,t) = \Sigma_{k=0}^{n} w_{n,k}(v,\theta,t)\cos^k\phi$. When the spatial and velocity distributions of initial electrons are azimuthally symmetric around x and v_x axes respectively, $w_{n,k} = 0$ for n and k with different parities, thus, D_{Tn} can be derived from a simultaneous calculation of $w_{0,0}$, $w_{1,1}$, $w_{2,0}$, $w_{2,2}$, $w_{3,1}$, $w_{3,3}$, $\cdots$, $w_{n,n}$. The calculation result of D_{Tn} in SF_6 and CCl_2F_2 agreed well with that by a Monte Carlo simulation.

*Work in part supported by Grant-in-Aid No.10750201 by the Ministry of Education, Science, Sports and Culture, Japan.

[1]H.Sugawara *et al.* 1998 *J.Phys.D: Appl.Phys.* **31** 319-27

SESSION BM2: RF & PULSED PLASMAS
Monday morning, 19 October 1998
Maile Room, Aston Wailea at 10:00
A. Brockhaus, University of Wuppertal, Germany, presiding

Contributed Papers

10:00

BM2 1 Energy Control of Ions from a Capacitive Coupled Plasma using an RF Resonance Method N. GOTO, *Central Research Institute of Electric Power Industry* The high plasma density features in an RF resonance method have been investigated. The RF resonance method has been studied for developing an efficient ion extraction technique for isotope separation. The RF resonance method can induce a strong electric field even in bulk. Simulation results obtained by using the XPDP1 code show that the induced electric field produces a high plasma density of about $10^{11} cm^{-3}$ at a pressure of 1mTorr. The RF resonance method is described as a sheath-plasma resonance, and is dependent on applied frequency, magnetic flux density, its direction, gap distance between electrodes, sheath thickness and plasma density. It is demonstrated that the applied magnetic flux density and voltage can control the plasma density at a constant gas pressure and frequency. Sheath thickness differs for different applied magnetic flux densities, because sheath thickness is one of the parameters which determines the resonance. The ion energy fed into the electrodes is related to the sheath thickness. As a result, the applied magnetic flux density and voltage can control the plasma density and the ion energy. Different ion density distributions at an electrode at a constant plasma density with different applied magnetic flux densities and voltages are calculated.

10:15

BM2 2 Large Area VHF-PECVD using a Ladder-Shaped Electrode H. YAMAKOSHI, K. YAMAGUCHI, S. MORITA, M. MURATA, *Mitsubishi Heavy Industries, Ltd.* M. YOSHIOKA, Y. KAWAI, *Interdisciplinary Graduate School of Engineering Sciences, Kyushu U.* VHF silane plasmas have shown to deposit high quality amorphous and microcrystalline films at high rates. However, nonuniformity of plasma density, due to voltage distribution in a large area electrode caused by standing wave and stray impedance becomes nontrivial in this frequency range. A ladder-shaped electrode has proven to provide a high deposition-rate and high deposition-uniformity with conventional 13.56 MHz excitation. In this paper, we applied the electrode to the VHF plasma excitation. The plasma density generated at the VHF frequency; using said electrode, was several times higher than that at 13.56 MHz and showed gradual increase with increased frequency. Plasma uniformity over 30 cm along the electrode surface was ± 10 % at 80 MHz and ± 25 % at 100 MHz. A preliminary experiment of large-area a-Si deposition demonstrated that the deposition-rate uniformity was better than ± 10 % over a 30 cm x 30 cm substrate with an average deposition rate of 6.4 Å/s at the frequency of 60 MHz, power of 150 W, flow rate of 150 sccm and pressure of 80 mTorr.

10:30

BM2 3 Plasma breakdown in a capacitively-coupled radiofrequency argon discharge H.B. SMITH, C. CHARLES, R.W. BOSWELL, *Plasma Research Lab, Australian National University* Low pressure, capacitively-coupled rf discharges are widely used in research and commercial ventures. Understanding of the non-equilibrium processes which occur in these discharges during breakdown is of interest, both for industrial applications and for a deeper understanding of fundamental plasma behaviour. The voltage required to breakdown the discharge V_{brk} has long been known to be a strong function of the product of the neutral gas pressure and the electrode seperation (pd). This paper investigates the dependence of V_{brk} on pd in rf systems using experimental, computational and analytic techniques. Experimental measurements of V_{brk} are made for pressures in the range 1 – 500 mTorr and electrode separations of 2 – 20 cm. A Paschen-style curve for breakdown in rf systems is developed which has the minimum breakdown voltage at a much smaller pd value, and breakdown voltages which are significantly lower overall, than for Paschen curves obtained from dc discharges. The differences between the two systems are explained using a simple analytic model. A Particle-in-Cell simulation is used to investigate a similar pd range and examine the effect of the secondary emission coefficient on the rf breakdown curve, particularly at low pd values. Analytic curves are fitted to both experimental and simulation results.

Invited Paper

10:45

BM2 4 Enhancing Ionisation by Electron Injection into Low Temperature Plasmas.

NICHOLAS BRAITHWAITE, *The Open University, Oxford Research Unit, Oxford, OX1 5HR, UK*

Gas discharges are sustained in the steady state by processes which ensure a balance between the production and loss of charged particles. At low and medium pressure ionization is often associated with the high energy tail of the electron energy distribution (EEDF). When electron impact is the an important mechanism, the characteristic temperature of the energy distribution for electrons must be consistent with the ionization rate required for the given physical conditions, including geometry. However, it is not always the case that ionization is associated with a simple Maxwellian form of EEDF: for instance, secondary emission from negatively biased surfaces can be the major source of ionizing species, as in the negative glow of DC discharges and in the gamma mode of RF discharges. Under these circumstances, the mean energy of electrons is substantially reduced. Deliberately adding controlled amounts of 'ionizing' electrons (from a filament, a surface or a secondary discharge) can therefore be used to tailor the bulk EEDF. In capacitive discharges, modest amounts of externally controlled ionization alter the overall electrical structure of the discharge, increase the electron density several fold and decrease the bulk electron temperature to well below 1 eV. This has been investigated experimentally and through modelling. Calculations for inductive discharges also show a similar scope for manipulating the EEDF. http://www-tec.open.ac.uk/materials/epsrc/pstu3.html

Contributed Paper

11:15

BM2 5 Large-Area Plasmas Formed by Magnetically Confined Electron Beams* RICHARD FERNSLER, ROBERT MEGER, MARTIN LAMPE, WALLACE MANHEIMER, DONALD MURPHY, ROBERT PECHACEK, *Naval Research Laboratory* Magnetically confined electron beams can create plasmas in gas with less heating and greater control and uniformity than sources that produce ionization by heating the plasma electrons. Control is greater because the beam is generated separate from the plasma and steered using an external magnetic field. Uniformity is high because the beam current is constant along the propagation direction and confined magnetically in the transverse direction. And last, heating is reduced because energetic beam electrons ionize efficiently. That is, beam electrons typically require 30 eV of discharge energy per plasma electron formed, whereas conventional plasma sources require 100 eV and often much more. Based on these concepts, a Large Area Plasma Processing System (LAPPS) reactor has recently been built at the Naval Research Laboratory.[1] This reactor utilizes a long hollow-cathode glow discharge to generate a sheet electron beam of several keV in energy, and this beam produces planar plasmas up to 60 cm on a side by 2 cm thick with densities as high as $5x10^{12}$ cm^{-3} in 30 mtorr of oxygen. Various aspects of beam-produced plasmas will be discussed including confinement and stability, efficiency of ionization and dissociation, cathode operation, and the effects of a low and adjustable plasma electron temperature.

*Work supported by the Office of Naval Research

[1]R. A. Meger et al., this conference

Invited Paper

11:30

BM2 6 Fundamentals and Applications of Ion-Ion Plasmas

D.J. ECONOMOU, *University of Houston**

Ion-ion plasmas are formed in the late afterglow of pulsed discharges in electronegative gases. It has been recognized that pulsed discharges can ameliorate such undesirable effects as charge-induced etch profile distortions (e.g. notching) that can occur in traditional continuous-wave discharges used for semiconductor manufacturing. It has been hypothesized that the extraction of negative ions, and the interaction of these ions with the wafer surface, are critical to realizing the above benefits. Ion-ion plasmas are also important in continuous wave discharges in strongly electronegative gases. A bounded

plasma in an electronegative gas with hot electrons and cold ions tends to separate into an ion-ion plasma in the core of the discharge, and an electron-positive ion plasma near the periphery. Despite their importance, the dynamics of ion - ion plasmas and the mechanism of negative ion extraction are poorly understood. This paper will discuss (a) the fundamentals of formation and spatiotemporal dynamics of ion-ion plasmas in pulsed and continuous wave electronegative discharges at very low pressures, (b) the mechanism of negative ion extraction and acceleration under the influence of an externally applied bias, and (c) applications of ion-ion plasmas in semiconductor manufacturing and other fields. A novel "plasma four point probe" for detecting the transition from an electron-ion plasma to an ion-ion plasma in the afterglow of pulsed electronegative discharges will also be presented.

*Co-Authors V. Midha, University of Houston and L. Overzet, University of Texas at Dallas.

SESSION BM3: ENERGY DISTRIBUTION DIAGNOSTICS
Monday morning, 19 October 1998
South Pacific Ballroom, Aston Wailea at 10:00
Harold Anderson, University of New Mexico, presiding

Contributed Papers

10:00
BM3 1 Measurements and Simulations of the Energy Distributions of Ions Bombarding Radio-frequency Biased Electrodes in an Inductively Coupled Plasma Reactor ERIK A. EDELBERG, *Department of Chemical Engineering; University of California Santa Barbara* ANDREW PERRY, *Lam Research Corporation* NEIL BENJAMIN, *Lam Research Corporation* ERAY S. AYDIL, *Department of Chemical Engineering; University of California Santa Barbara* A compact retarding field ion energy analyzer has been designed and built to measure the energy distribution of ions bombarding the surface of radio frequency (rf) biased electrodes in high-density plasma reactors. Specifically, the analyzer was installed in the rf biased electrostatic chuck of a high-density, transformer-coupled plasma (TCP) reactor. The effects of TCP power, rf bias power, pressure, and gas composition on the measured ion energy distributions are demonstrated through Ar, Ne, Ar/Ne, O_2 and CF_4/O_2 discharges. To complement the experimental results, a numerical sheath model that predicts the spatio-temporal variations of the potential across the sheath in a high density plasma has been developed. The energy distribution of ions bombarding the rf biased surface is then calculated using Monte Carlo simulations of the ion trajectories. Bimodal ion energy distributions resulting from ion energy modulation in the sheath were observed and simulated. Multiple peaks in the IEDs measured in gas mixtures were identified as signatures of ions with different masses falling through the sheath. The simulations predict both the energy separation of the bimodal IEDs as well as the ratio of the peak heights as measured by the ion energy analyzer.

10:15
BM3 2 Biased Optical Probe Measurement of Electron Energy Distribution Function in Processing Plasmas H. TOYODA, M. HOSOKAWA, R. FUKUTE, H. SUGAI, *Nagoya Univ.* S. NODA, Y. HIKOSAKA, K. KINOSHITA, M. SEKINE, *Plasma Technol. Lab., ASET* Electron energy distribution function (EEDF) is one of the essential parameters in processing plasma. Especially, a high energy part of the EEDF which causes dissociation and/or ionization is important because production rates of reactive species are determined by super thermal electrons. So far, the EEDF has been measured by a Langmuir probe in Druyvesteyn method, but its reliability is reduced in the measurement of high energy part because the electron current is extremely small, and partly because the effect of secondary electron emission from the probe surface is not negligible. On the other hand, optical emission spectroscopy is a useful way to obtain some information on high-energy electrons, but the measured emission intensity does not give a functional form of the EEDF. To overcome the above problems, we have recently proposed a new method for EEDF measurement, *i.e.*, biased optical probe (BOP)[1]. This is a combination of a retarding bias method with optical emission, and has been successfully applied to rare gas plasmas. In this paper, application of BOP to high-density processing plasmas is presented. Here, an important modification from DC bias to RF bias is made to avoid the influence of thin film deposition on BOP.

[1]H. Sugai, et al., *Plasma Sources Sci. Technol.* **4**(1995)366.

10:30
BM3 3 Electron Energy Measurement and its Control by Plasma Volume/Surface Ratio in Large Volume Reactor K. KINOSHITA, S. NODA, M. OKIGAWA, M. SEKINE, *Plasma Technology Lab.* M. INOUE, *Super-fine SR Lithography Lab., ASET* Plasma parameters, such as electron temperature (T_e; mean electron energy) and electron density (N_e), change according to the plasma volume/surface (V/S) ratio. When the volume was changed by the gap width between the top plate and the wafer stage in a large volume cylindrical plasma, the T_e measured with a single probe had good agreement with a model calculation of uniformly generated plasma in the whole reactor volume. Also, T_e estimated by optical emissions from Ar and He atoms decreased such as the probe result when gap width increased. In contrast, T_e estimated from Xe and Ar emission lines had a slight increase. The differences in these tendencies results from the differences of the energy window of each technique. Next, the wafer perpendicular distributions of T_e were measured by an optical technique. We observed that T_e decreased in the upper plasma bulk (near plasma generation region) when the V/S ratio increased. However, in th e down flow region near the wafer stage, T_e was independent to V/S ratio and lower than T_e in the bulk. It is concluded that in a large volume plasma reactor, T_e in the bulk region could be controlled by the V/S ratio while keeping lower T_e near the wafer, which is critical for the charging phenomena on the wafer. This work was supported by NEDO.

10:45
BM3 4 Evaluation of High Energy Tail in The EEDF of Rare Gas Mixture Plasmas by OES S. NODA, K. KINOSHITA, H. NAKAGAWA, M. OKIGAWA, M. INOUE, M. SEKINE, *Association of Super-Advanced Electronics Technologies (ASET)* The high energy portions of the EEDFs of Ar/Xe/He (0.90/0.05/0.05) gas mixture plasmas were compared for different types of plasma sources at a driving frequency of 13.56 - 500 MHz and a gas pressure of 1 - 13 Pa by an OES technique. The overall EEDF profiles were speculated by combining two classes of electron temperatures, T_{el} and T_{eh}, which were the electron temperatures of the lower and the higher portion in the EEDF, assuming a double Maxwellian distribution function. The T_{el} values were calculated from the ratios of the emission line intensities of Xe ($2p_3$, $2p_6$:10eV-) and Ar ($2p_1$, $2p_5$:13.5eV-) with due consideration

given to the contribution of stepwise excitation (1.5eV-) from metastable states. The T_{eh} values were derived from the emission lines of Ar ($2p_1$) and He (3^3P :23eV-). The ΔT differential between T_{el} and T_{eh} is considered to determine the difference in the EEDF profile from the Maxwellian distribution. When ΔT is zero, it can be said that the observed EEDF is exactly equal to the Maxwellian distribution throughout a wide energy range. In this study, T_{eh} was always larger than T_{el}. This is evidence indicating the existence of high energy tails and we considered that the value of ΔT corresponds to the extent of the high energy tail. The high energy tail extended as the driving frequency increased while it shortened as the gas pressure increased. At a certain point at the frequency of 13.56 MHz and at the pressure of 7 Pa, the ΔT value was reduced to zero when the driving frequency was close to the electron-electron Coulomb collision frequency. This work was supported by NEDO.

11:00

BM3 5 The Role of EEDF in Reactive Plasma Chemistry
HARMEET SINGH, JOHN W. COBURN, DAVID B. GRAVES, *University of California at Berkeley* Understanding plasma chemistry is vital to the integrated chip processing industry. The relationship between electron energy distribution function and plasma chemistry has not been systematically investigated in reactive plasma processes. The focus of this research is to use an inductively coupled plasma system as a test-bed for developing and validating plasma chemistry models by systematic comparison of experimental and modeling results. A Langmuir probe is used to measure the radial variations of the electron energy distribution function, plasma density and plasma potential. Simultaneously, modulated beam appearance potential mass spectrometry is used to measure the abundance of stable neutrals and radical species in the plasma. A separate mass spectrometer is used to measure mass resolved ion energy distribution using an electrostatic energy analyzer. Optical emission spectroscopy and argon actinometry are performed to measure the concentration of select neutrals. A model for plasma chemistry is developed using available cross-section data and the measured EEDFs. The EEDF is measured for a variety of plasma chemistries (for example, Ar, O_2, CF_4/O_2, C_2F_6/O_2, $SiF_4/CF_4/O_2$) over a range of power and pressures.

11:15

BM3 6 Electron Density Measurement by a Novel Probe Usable in Contaminated Environment
K. NAKAMURA, H. KOKURA, I. GHANASHEV, H. SUGAI, *Nagoya University* In most reactive plasmas, surfaces of a Langmuir probe are promptly contaminated with thin non-conducting films, which makes reliable measurement difficult. A plasma oscillation method[1] which is based on electron-beam excited plasma oscillations is available even in such environment. In some cases such as fluorocarbon plasmas, however, this method suffers a short lifetime of hot filament used to generate electron beam. Here we developed a novel probe, *"plasma absorption probe"* which gives an accurate local electron density even when the probe surface is contaminated with thick polymer films. Briefly, the probe is constructed as follows: A 6 mm diam. glass tube with a closed front end is immersed in a plasma. A tiny antenna jointed to one end of 50 Ω coaxial cable is inserted into the tube while the other end of the cable is connected to a network analyzer. The network analysis of the antenna-plasma system showed several peaks in the frequency spectrum of power absorption coefficient. Among them, the lowest frequency of the absorption appears at the surface wave resonance, i.e., $\omega = \omega_p/\sqrt{1+\epsilon}$ (ω_p: electron plasma frequency, ϵ:dielectric constant of glass), which in turn gives the electron density. The electron density measured in this way is compared with Langmuir probe and plasma oscillation probe results.

[1]Shirakawa and H. Sugai, Jpn. J. Appl. Phys. 32(1993)5129.

Invited Paper

11:30

BM3 7 Optical Measurements of Electron Temperatures and Species Concentrations in Several Types of Chlorine-Containing, High Density Plasmas.
VINCENT M. DONNELLY, *Bell Laboratories, Lucent Technologies, Murray Hill, NJ**

High charge density, chlorine-containing plasmas are widely used to etch the small features in silicon and aluminum that are required for state-of-the-art microelectronic devices. With the advances in the ability to etch smaller features come new problems such as "micro-trenching", "notching", and plasma-induced damage. Increased understanding of the plasma is needed to solve these problems and anticipate new ones. Both modeling and measurements are needed. Some of the most critical required parameters are electron temperature (T_e) and concentrations of Cl_2 and Cl. We have recently developed an optical emission method for obtaining these parameters and have applied this technique to a variety of chlorine-containing, high density plasmas. Briefly, a small amount (1and optical emission is recorded from selected Paschen 2p levels of the rare gases. This emission is excited by electron impact with the rare gas ground states and metastable states. By modeling this excitation process, the best fit to the observed, relative intensities is obtained by varying the only adjustable parameter (T_e). Electron temperatures measured by this method are mostly characteristic of the tail of the electron energy distribution function (EEDF). This part of the EEDF is mainly responsible for dissociation, excitation, and ionization. T_e's measured for several transformer-coupled plasmas (TCP), other inductively-coupled plasmas (ICP), and ultrahigh (500MHz) frequency (UHF) plasmas will be discussed and contrasted. This optical measurement of the tail T_e also makes it possible to improve on actinometry for measurement of concentrations of species in plasmas. In this case, quantitative measurements of Cl_2 and Cl have been made, corrected for changes in T_e and contributions by metastables to the rare gas emission. From the complimentary decrease in Cl_2 and increase in Cl densities with increasing power, absolute calibration constants were obtained, and the role of dissociative excitation of Cl emission was clarified. Measured T_e's and Cl_2 percent dissociations will be compared to predictions from simple models.

*Bell Labs co-authors: M. V. Malyshev (also at Princeton Univ.), A. Kornblit, N. A. Ciampa, and J. I. Colonell; NEC Corp. co-author: S. Samukawa

SESSION CM1: FOUNDATIONS OF GASEOUS ELECTRONICS
Monday afternoon, 19 October 1998; Plumeria/Jade/Maile Room, Aston Wailea at 13:30
Steve Buckman, Australian National University, presiding

13:30
CM1 1 Electron Swarms.
ROBERT W. CROMPTON, *Australian National University*

Swarm experiments provide an invaluable link between gaseous electronics and atomic physics, that is, between the collective behavior of electrons in gases in electric and magnetic fields and the collision processes that determine that behavior. Early swarm experiments were made to gain an understanding of the basic physics of electrical conduction in gases and electrical breakdown. Subsequent peaks of activity have been associated with attempts to explain quantitatively electromagnetic wave propagation in the ionosphere and in high temperature air, and with applied research in such diverse areas as gas lasers, health physics, gas insulation for high voltage transmission lines, plasma processing, and particle detectors . Through improved experimental techniques and the application of numerical techniques to unravel the complex connection between the individual electron-neutral collisions and the transport coefficients that characterize the properties of the swarm, swarm experiments now contribute accurate, and sometimes unique, cross section data for low-energy electron-atom/molecule collisions. Alternatively they can provide self-consistent sets of cross sections that enable reliable forecasts of the collective behaviour to be made. In the talk I shall aim to provide an understanding of the basic principles underlying swarm experiments, and the interpratation of the results from them, through a description of their development and application up to the present day.

SESSION DM1: LAMPS AND DISPLAYS
Monday afternoon, 19 October 1998; Plumeria/Jade Room, Aston Wailea at 14:45
John Curry, University of Wisconsin, presiding

Invited Paper

14:45
DM1 1 Fluorescent Lamps with Controllable Color Temperature.
GARRIT KROESEN, *Eindhoven University of Technology, the Netherlands*

This abstract was not submitted electronically.

Contributed Paper

15:15
DM1 2 High intensity UV emission from cold-cathode mercury-argon lamps SHINJI KOBAYASHI, *Power and Industrial systems R&D Center, Toshiba Corporation* TAKAAKI MURATA, KIYOHISA TERAI, *Power and Industrial systems R&D Center, Toshiba Corporation* A high intensity UV source is required in the field of the sterilization of bacilli and the material processing. When a continuous sinusoidal voltage waveform between electrodes of a mercury-argon lamp is applied, the UV radiation shows the saturation effect because of a resonance line of mercury. It is caused by the plasma condition such as electron temperature and density. We tried to control the plasma condition by using a pulsed power supply. A cold-cathode mercury-argon lamp used was 180mm long and 6.0mm in diameter. A square-like pulsed waveform of which frequency was 70kHz and duration was 5us, was alternately applied between electrodes. The emission at a wavelength of 254nm was measured by using a photomultiplier tube with a spectrometer. As a result, the UV emission intensity of 30 times higher than that obtained by applying 30kHz continuous wave form was achieved.

Invited Paper

15:30
DM1 3 Research and Development of Large Area Color AC Plasma Displays.
TSUTAE SHINODA, *Peripheral System Laboratories, Fujitsu Laboratories Limited*

Plasma display is essentially a gas discharge device using discharges in small cavities about 0. 1 m. The color plasma displays utilize the visible light from phosphors excited by the ultra-violet by discharge in contrast to monochrome plasma displays utilizing visible light directly from gas discharges. At the early stage of the color plasma display development, the degradation of the phosphors and unstable operating voltage prevented to realize a practical color plasma display. The introduction of the three-electrode surface-discharge technology opened the way to solve the problems. Two key technologies of a simple panel structure with a stripe rib and phosphor alignment and a full color

image driving method with an address-and-display-period-separated sub-field method have realized practically available full color plasma displays. A full color plasma display has been firstly developed in 1992 with a 21-in.-diagonal PDP and then a 42-in.-diagonal PDP in 1995 Currently a 50-in.-diagonal color plasma display has been developed. The large area color plasma displays have already been put into the market and are creating new markets, such as a wall hanging TV and multimedia displays for advertisement, information, etc. This paper will show the history of the surface-discharge color plasma display technologies and current status of the color plasma display.

Contributed Papers

16:00

DM1 4 RF plasma characteristics in a micro-cell in Xe by using RCT model * M. KURIHARA, N. NAKANO, T. MAKABE, *Keio University, Japan* Plasma display panel(PDP) is one of the flat display devices, expected to be a large size, hanging, and high-definition TV monitor. PDP uses ultraviolet light emitted from a noble gas discharge in a micro-cell to excite phosphors. One of the disadvantages of the present PDP is a low efficiency of UV radiation inherent in the low frequency discharge. In this work, we numerically investigate a high frequency(HF) operation of a micro-cell plasma in Xe by using the relaxation continuum-(RCT) model. HF is chosen to improve the efficiency of UV radiation. The external condition of $fd > v_{d_e}/\pi$ is one of the criterion to sustain the micro size plasma between fixed electrodes (f:frequency, d:electrode distance). Capability for maintaining a micro-cell plasma under $fd < v_{d_e}/\pi$ is investigated. One of the capabilities sets up a long path of the electron by the use of ring electrode. γ effect becomes dominant for the production of electrons with decreasing of fd.

*Supported by MESC in Japan, B(2)-09450146 and -9555111

16:15

DM1 5 Optimization of a Plasma Display Panel Cell* SHAHID RAUF, MARK J. KUSHNER, *University of Illinois, Dept. of Electrical and Computer Engr., Urbana, IL 61801, USA* The performance and efficiency of Plasma Display Panels (PDPs) are functions of the cell geometry, gas composition, pressure, material properties and applied voltage format. To investigate the interdependencies of these parameters on PDP performance, a 2-dimensional hybrid PDP simulation, PDPSIM, has been developed. PDPSIM uses fully-implicit time integration techniques to enable simulation of both the current pulse and the long interpulse period. A radiation transport model is employed to evaluate visible light emission and a Monte Carlo simulation is used for transport of secondary electrons accelerated through the cathode fall. Results from the model are used to investigate the operation of a coplanar-electrode PDP cell operating with He/Ne/Xe gas mixtures while varying gas mole fractions, electrode layout, and material properties. Performance is evaluated based on total light fluence and energy efficiency. It was found that PDP cells operate more efficiently at high pressure due to more efficient production of Xe_2^*, the major species which contributes to visible light emission.

*Work was supported by LG Electronics and NSF.

16:30

DM1 6 An Experimental Gas Study in a Model PDP Pixel Cell J.R. GOTTSCHALK, O. SHVYDKY, A.D. COMPAAN, C.E. THEODOSIOU, *Department of Physics and Astronomy University of Toledo* W. WILLIAMSON JR., *Embry Riddle Aeronautical University*† We have built a vacuum chamber for the study of gas mixtures in plasma display panels. The vacuum chamber is designed to deposit the MgO secondary electron layer in situ onto the electrode structure and then to backfill the chamber with a gas mixture. The electrode structure can then drive a gas discharge. We can then measure electrical and optical properties of the discharge as a function of pressure and gas composition. By depositing the MgO layer *in situ* we can insure that the MgO surface is clean, and near simulates real PDP conditions. We will present data on the break down voltage, window of bistability, and light emission all as a function of pressure and composition.

*Funded by NSF.
†In collabartion with EPI

16:45

DM1 7 Kinetic effects in ac plasma display panels* JOHN P. VERBONCOEUR, PEGGY J. CHRISTENSON, *Univeristy of California-Berkeley* GREG. J. PARKER, *Lawrence Livermore National Laboratory* The study of collisional processes in an ac plasma display panel (PDP) cell is motivated by the requirement for accurate rates for rapidly converging fluid codes. A single pulse in an ac PDP cell is modeled as a self-extinguishing dc discharge, with the kinetics of the transient cathode fall determining much of the physics. The resulting rates are temporally and spatially dependent, requiring a kinetic model for complete description. In this research, the collision rates and other physical parameters in a PDP cell are obtained using a PIC-MCC code, and compared to the local field and mean energy approximations. Both pure neon and a neon-xenon mixture are examined.

*This work supported in part by Hitachi Ltd., the Miller Institute for Basic Research in Science, and Lawrence Livermore National Laboratory under U.S. DOE contract W-7405-ENG-48.

17:00

DM1 8 Hydrodynamical and Hybrid Modeling of Plasma Display Panel Cell G.J. PARKER, *LLNL* P.A. VITELLO, *LLNL* J.W. SHON, *LLNL* Plasma display panels (PDP's) consists of arrays of microdischarges which either produce visible or UV light to activate individual pixels of the display. We show two sets of calculations of a typical parallel geometry for a PDP cell. First, the typical efficient hydrodynamical approach assuming a Maxwellian electron energy distribution function (EEDF) is shown to quantitatively give the correct particle densities and resulting fields, though the temporal behavior is not correct. Next, a hybrid approach which evolves the EEDF during the evolution of the discharge via Monte Carlo techniques replaces the assumption of a Maxwellian distribution while agrees quantitatively with the purely hydrodynamical approach, exhibits a substantially different temporal behavior. The two approaches are compared in detail to each other and to the available experimental data.

SESSION DM2: PULSED & MICROWAVE GLOWS
Monday afternoon, 19 October 1998
Maile Room, Aston Wailea at 14:45
Shunjiro Shinohara, Kyushu University, presiding

Contributed Papers

14:45

DM2 1 Characterization of a Pulsed Microwave Plasma in Argon and Oxygen A. BROCKHAUS, ST. BEHLE, A. GEORG, CH. SOLL, J. ENGEMANN, *Forschungszentrum für Mikrostrukturtechnik-fmt, University of Wuppertal, Germany** Pulsed plasmas are gaining interest, both from a fundamental and an application-oriented point of view. Advantages over traditional continous plasma processes may be obtained from a tuning of pulse frequency and duty cycle. We study a slot antenna (SLAN) 2.45 GHz microwave plasma used for polymerization of hexamethydisiloxane. Film quality can be significantly improved by plasma pulsing. In order to understand this empirical result we investigate pulsed plasma properties by time-resolved diagnostics. Pulse frequencies vary from 0 to 20 kHz. Process gases are either argon or oxygen. Diagnostics include (i) Langmuir probe methods, (ii) microwave interferometry, (iii) two-dimensional optical emission spectroscopy, and (iv) two-photon laser-induced fluorescence for the quantitative determination of the atomic oxygen density. We present experimental results with special emphasis on plasma ignition. The time dependencies of relevant densities—in particular atomic oxygen—are discussed by considering the governing rate equations.

*Work supported by BMBF

15:00

DM2 2 Production of Large-Diameter Uniform Plasma in mTorr Range Using Microwave Discharges Y YASAKA, T NOZAKI, K KOGA, *Kyoto University* M ANDO, T YAMAMOTO, *Tokyo Institute of Technology* N GOTO, *Takushoku University* N ISHII, T MORIMOTO, *Tokyo Electron Limited* A large-diameter uniform plasma is obtained by microwave discharges without using magnetic fields at a pressure of a few mTorr. The discharge chamber is 50 cm in diameter and 30 cm in depth with a quartz glass window of the same diameter on the top. A radial line slot antenna (RLSA) is located at 1 − 3 cm above the window and fed by a 2.45-GHz microwave source via coaxial line. The RLSA has a large number of transverse slots over the entire area of the glass window and radiates microwave fields uniformly downwards. Typical plasma parameters are; density 2 − 5 $\times$ 10^{12} cm^{-3}, electron temperature 2 − 3 eV, and ± 3 − 4 % uniformity of ion saturation current over 30-cm diameter for Ar pressure of 5 mTorr and microwave power of 2 kW. The discharge can be started up at a pressure as low as 0.5 mTorr, and can be sustained by 0.5-kW microwave power at that pressure. The mechanism of the efficient production of over-dense plasmas is investigated by measuring wave propagation in the system. The possibilities of surface wave excitation and/or electrostatic wave excitation are considered.

15:15

DM2 3 The Tuning System in the Large Area Microwave Planar Plasma Source JOZEF KUDELA, *Graduate School of Electronic Science and Technology, Shizuoka University, Johoku 3-5-1, Hamamatsu 432-8561, Japan* IGOR ODROBINA, *Institute of Physics, Faculty of Mathematics and Physics, Comenius University, 842 15 Bratislava, Slovakia* MASASHI KANDO, *Graduate School of Electronic Science and Technology, Shizuoka University, Johoku 3-5-1, Hamamatsu 432-8561, Japan* Surface wave sustained discharges have re-attracted the significant attention among the researchers in recent years. Although for many years these discharges have been studied in narrow cylindrical dielectric tubes, now they are appearing in the connection with the large area plasma processing. The researchers found the surface waves to be suitable for the enlargement of microwave discharges and several large area plasma sources based on the surface waves have already been developed. Recently we presented one design of such plasma source with 312 mm diameter. Our source operates at pressures from 1mTorr up to several Torr (argon) and yields the plasma with densities in order of 10^{12} cm^{-3}. However, similarly like all sources of this family, the source exhibits resonant behavior, which results in the electromagnetic mode jumps when the plasma density is changed. This makes it difficult to control smoothly the plasma parameters. To achieve the continuous control of the plasma parameters in microwave discharge in general, a special tuning systems have to be applied. We have already proposed and tested one tuning system on our plasma source, which enabled the continuous change of plasma density within a small plasma density range. In this work, we will present another solutions for the tuning of the discharge in the large area microwave plasma source along with the effect of this tuning system on the discharge behavior and the plasma parameters.

15:30

DM2 4 Effect of Slot Antenna Structure on Production of Planar Surface Wave Plasmas M. NAGATSU, A. ITO, S. MORITA, I. GHANASHEV, H. SUGAI, *Department of Electrical Engineering, Nagoya University* N. TOYODA, *Nissin Inc.* Characteristics of planar surface wave plasmas (SWP) produced by a 2.45 GHz microwave via slot antennas have been studied[1,2]. Effect of antenna-plasma coupling was investigated for various slot antennas by measuring plasma characteristics against an incident microwave power. Four types of slot antenna, that is, inclined, vertical, transverse and radial slots, were tested. At high pressure of say 1 Torr, optical emission patterns of various TM modes were observed in respective slots as expected by theoretical dispersion relations[3]. At low pressure of 10 mTorr, uniformly broadened plasma emission was observed regardless of the antenna structure. An attempt of reducing dielectric window area for vacuum sealing has been made to develop economical etching or CVD plasma sources with less impurities[4]. Recent results of SWP experiments in a larger chamber using 2.45 GHz and 915 MHz waves will be also given. This work was supported by Toshiba Corp., Nissin Inc, and also by a Grant-in-Aid for Science Research from the Ministry of Education, Science, Sports and Culture in Japan.

[1]M. Nagatsu et al *Plasma Sources Sci. Technol.* **6** (1997) 427.
[2]H. Sugai et al *Plasma Sources Sci. Technol.* **7** (1998) 192.
[3]I. Ghanashev et al *Jpn. J. Appl. Phys.* **36** (1997) 337.
[4]S. Morita et al *Jpn. J. Appl. Phys.* **37** (1998) L468.

15:45

DM2 5 Surface-Wave Excitation in High-Density Planar Plasma Sources I. GHANASHEV, S. MORITA, M. NAGATSU, H. SUGAI, *Department of Electrical Engineering, Nagoya University* N. TOYODA, *Nisshin Inc.* Electromagnetic surface waves

introduced into a metal chamber through large[1] or slot-type[2] apertures of various shapes can sustain overdense plasmas in a wide range of gas pressures. A simple cavity model[3] successfully identifies the eigen-modes in the case of single-mode operation and small slot antennas, while neglecting the latter. The stability analysis[4] suggests that the source performance is governed by the dependence of the chamber power reflection coefficient R on the plasma density n_e. The values of R depend on the geometry of the coupling aperture(s) and thus cannot be suggested by a simple theory neglecting them. In this communication we present a full-wave electromagnetic analysis taking into account the aperture(s), along with experimental results for the character of the $R-n_e$ dependence. The simulation results suggest, in accordance with the experimental observations, that, depending on the operating conditions, both single- and multi-mode regimes can be realised. This work was supported by Toshiba Corp. and Nisshin Electronic MFG Co., Ltd.

[1]K. Komachi *J. Vac. Sci. Technol. A* **11** (1993) 164.
[2]H. Sugai et al *Plasma Sources Sci. Technol.* **7** (1998) 192.
[3]I. Ghanashev et al *Jpn. J. Appl. Phys.* **36** (1997) 337.
[4]I. Ghanashev et al *Jpn. J. Appl. Phys.* **36** (1997) 4704.

16:00
DM2 6 Numerical analysis of dynamic behavior of surface wave coupled plasma by the particle-in-cell method NAOKI MATSUMOTO, *Sumitomo Metal Industries Ltd.* The present paper describes a numerical work on dynamic behavior of surface-wave coupled plasma (SWP) that is becoming a popular source for plasma-assisted LSI fabrication technologies such as etching processes and resist stripping processes. The electromagnetic field energy in an SWP sustained by microwaves at 2.45 GHz without external magnetic are calculated by a particle-in-cell (PIC) method. The SWP model consists of a dielectric line and a vacuum chamber filled with discharged argon gas. Oscillating behavior of the plasma is characterized in terms of the power spectral structure of the electromagnetic field energy estimated by fast Fourier transform. The spectra exhibit sharp peaks as a sign of the oscillating field, whose characteristic frequency increases as a function of the plasma density. These observations are discussed from the standpoint of the electron plasma frequency, i.e., the fundamental characteristic oscillations of the discharge that can be induced by the restoring force stemming from the difference in the mobility between electrons and positively charged ions. The distance of the oscillating region of the plasma from the dielectric line is found to correspond to the skin depth of the discharge. These imply that electrons are generated underneath the dielectric line. The PIC method is thus demonstrated to be a powerful tool for analyzing the dynamic behavior of SWP.

Invited Papers

16:15
DM2 7 Basic Concepts in Pulsed Plasmas.
ROD BOSWELL, *Plasma Research Laboratory, ANU*

For plasmas in general there are a number of important time scales: avalanche breakdown of less than one msec, ion diffusion to the walls of some tens of msec, molecular disassociation and gas pumping are less than one msec and gas residence times in a reactor of some hundreds of msec. To this can be added characteristic times in the afterglow: electron cooling being a few tens of msec, density decay increasing from hundreds of msec to msec, the Debye length leaving the system at almost ten msec and the last charged species in the gas phase recombining after a few hundreds of msec. It capacitevly coupled systems there is the additional time scale of the bias (tune) capacitor charging up few msec after breakdown and its discharging in the afterglow up to some tens of msec. Generally it is the rf power supplied to the plasma which is pulsed and its rise and decay times range typically from less than 1 msec to somewhat less than one hundred msec which can severely effect the matching of the power. This talk will give examples of these time scales and show how they can be estimated.

16:45
DM2 8 Characterization of pulse-modulated inductively coupled plasmas.
G. A. HEBNER, *Sandia National Laboratories*

Pulsed plasma processing of microelectronic materials has a number of possible benefits from modifying the discharge radial concentration to neutralizing surface charge. While the measurements will focus on the characteristics of pulse-modulated inductively coupled plasmas in argon and chlorine, measurements in fluorine containing plasmas will also be presented. Measurements were performed for peak rf powers between 150 and 400 W at 13.56 MHz, duty cycles between 10 and 70 frequencies between 3 and 20 kHz. Over this parameter space, measurements were performed of the time dependent forward and reflected rf powers into the matching network, coil voltage, rf variation of the plasma potential, electron density, and negative ion density. A key feature of this work was the use of high bandwidth techniques to capture the transients that occur at plasma turn on. These measurements indicated that for the first 5 - 30 rf cycles of each pulse, the discharges probably were operating in a capacitivly coupled discharge mode with rf variations in the plasma potential of several hundreds of volts and relatively low electron density. Measurements of the electron density in pulse-modulated chlorine discharges indicated that the plateau electron density was a function of the duty cycle; the plateau electron density was lower for higher duty cycles. This may indicate that the ratio of Cl to Cl_2 was changing with duty cycle. In addition, a microwave radiometer was used to provide an indication of the time dependent electron temperature. Large spikes in the microwave radiation temperature were noted at the turn-on of the rf power pulses and, in some cases, at the transition from a capacitivly coupled to an inductively coupled plasma. This work was supported by the United States Department of Energy (DE-AC04-94AL85000). Sandia is a multiprogram laboratory operated by Sandia Corporation, a Lockheed Martin Company, for the United States Department of Energy.

Invited Paper

14:45
DM3 1 Industrial applications of silent discharge plasmas.
MASAKI KUZUMOTO, *Mitsubishi Electric*

New industrial plasma apparatuses were developed. These consist of an ozone generator, a CO2 laser, and a plasma display panel (PDP) excited by silent discharge(SD). The SD is a capacitively coupled discharge and also called dielectric barrier discharge. The electrode system where at least one of the electrodes is covered by a dielectric layer. The dielectric limits current flow, so that even at atmospheric pressure non-thermal and diffused plasma can be easily realized. This feature is quiet suitable for the above-mentioned industrial applications. Measurements of the discharge characteristics on these SD applications by using V(applied voltage)-Q(electric charge) Lissajous' figure were performed. The figure obtained was of a special shape for each application resulting from the differences between applied voltage waveforms. In the ozone generator, which is characterized by lower frequency (1-10 kHz) applied voltage, the figure shows a parallelogram with two slopes. The slopes correspond to non-discharge and discharge periods, respectively. In the CO_2 laser however, which is characterized by high frequency (100-300 kHz) applied voltage, the figure transforms into an ellipse with increase in frequency. Furthermore in PDP, which is characterized by short front impulse (100ns) applied voltage, the figure has another type of parallelogram. In the symposium, the characteristics and properties of silent discharges and their applications will be presented.

Contributed Papers

15:15
DM3 2 A promising plasmatron-produced highly ionized plasma source for research/industrial demand. A.A. BELEVTSEV, V.F. CHINNOV, E.KH. ISAKAEV, A.D. ISEROV, V.I. KALININ, V.K. KOROLEV, A.V. MARKIN, D.I. RYAZHSKY, O.A. SINKEVICH, S.A. TERESHKIN, A.S. TYU, *Science and Engeneering Centre for Energy Efficient Processes and Equipment, Associated Institute for High Temperatures, Russian Academy of Sciences* Presents the design features and basic parameters of an industrially important plasma jets source developed from a high-current arc pasmatron (I< =3D500A, G=3D1-4g/s, jet diameter at a minimum-6mm). The system has been realized of to collect and process data on plasma radiation in the 200-950nm region (resolution=3D0.01nm) allowing securing of a great body of information on atomic/ionic line characteristics (radiation transition probabilities, Stark constants, etc.) as well as deducing the plasma species distributions over electronic, vibrational and rotational degrees of freedom. The source is the basis around which extensive studies of arc current and voltage fluctuations have been performed that strongly suggests that it holds promise for investigating turbulent phenomena in highly ionized plasmas. The work as a whole opens the way to setting up a database on turbulent highly ionized plasma jets.

15:30
DM3 3 Making the Surface of the Polyolefin Fibers Non-Woven Fabric to Hydrophilic by Low Temperature Plasma and the Application to the Separator of the Nickel-Metal Hydrogen Cell YORI IZUMI, *Gunma College of Technology* MASAHIKO TSUKIASHI, *Toshiba Battery Co., Ltd.* HIROHITO TERAOKA, *Toshiba Battery Co., Ltd.* TAKEO OHTE, *Gunma College of Technology* AKIRA KOJIMA, *Gunma College of Technology* Polyolefin fibers non-woven fabric has been used as a separator for nickel-metal hydrogen (Ni-MH) cells. The separators are made to hydrophilic by graft copolymerization or sulfonation and improve the cell characteristics. However, a method which makes the separator hydrophilic conveniently with low-price is requested. In this study, the polypropylene separator was made to hydrophilic with rf plasma treatment and the influence of the characteristics of Ni-MH cell was investigated. Wettability of the separator surface was estimated by the contact angle of water. Initial capacity and self-discharge characteristic of the Ni-MH cell using the plasma-treated separator were measured. The contact angle on the surface of the separator before plasma treatment was in the range of $120^o \sim 130^o$ and decreased after oxygen, nitrogen and argon plasma treatment. The cell using the separator with the contact angle under 80^o gave over 95% initial capacity and over 90% rate of the capacity retention compared with the cell using the graft copolymerized separator. In summary, plasma treated polypropylene separator maintains the necessary electrolytic for Ni-MH cells and controls the reduction of the positive electrode surface.

15:45
DM3 4 Negative potential solitons in a positive ion-negative ion plasma T.E. SHERIDAN, *Plasma Research Lab, Australian National University* We investigate negative-potential (i.e., rarefactive) solitons and solitary waves in a plasma containing positive ions, negative ions and electrons. When the soliton amplitude is small (< < Te), there are parameter regimes for which Korteweg-deVries (KdV) and modified KdV solitons exist. In addition, there is a region of parameter space where non-KdV solitons can be found. Results from a one-dimensional particle-in-cell simulation demonstrate that such solitons are preserved during overtaking collisions, though they are not described by the KdV equations. We derive a KdV-like equation for these solitons having three terms in the effective potential: negative quadratic, negative cubic and positive quartic. This represents a generalization of the KdV equation (negative quadratic, positive cubic) and mKdV equation (negative quadratic, zero cubic, positive quartic). In contrast to KdV solitons, the amplitude of these new solitons remains finite as their speed approaches the ion acoustic speed.

16:00

DM3 5 Photoexcitation and Photoionization of Irradiated Large-gap Thermionic Energy Converter by Xenon Lamp WEI ZHENG, AKIHISA OGINO, MASASHI KANDO, *Graduate school of electronic Science and technology, Shizuoka Universty* This study is concerned with low temperature operated thermionic energy converter (TEC). To reduce the negative space charge, an auxiliary discharge by photo irradiation is proposed to produce cesium ions for space charge neutralization. Cesium has not only the lowest ionization potential of 3.89eV among all materials, but also low excitation potentials about 1.4eV. Excited cesium atoms with low energy can be further ionized through the mutual collisions. Such excitations can be induced by high-energy electrons or by photon resonance absorption with wavelengths shorter than 900nm. Thus, the excitation by solar irradiation can be expected to contribute to the output increase by atomic and molecular cesium ion production. In the present work, the effect of xenon lamp irradiation on the output I-V characteristics of TEC has been investigated, using a TEC with the gap length larger than 10mm. It is found that the irradiation increases the short circuit current of TEC from 3mA to 90mA operated in unignited mode at the emitter temperature of 1280K and cesium pressure of 0.1Torr. The enhancement of the transition from the unignited mode to ignited mode was also observed. By increasing emitter temperature up to 1600K, the short circuit current in ignited mode reached to 1.7A and increased 20% with irradiation at the same cesium pressure.

16:15

DM3 6 Negative ions detection using electrostatic probes P. CHABERT, *Lab. PRIAM, Unité Mixte de Recherche CNRS-ONERA, Fort de Palaiseau, F-91761 Palaiseau Cedex, France* R.W. BOSWELL, *Space plasma group, RSPhysSE, ANU, Camberra ACT 0200, Australia* J. PERRIN, *Balzers Process Systems, 5 rue Léon Blum, F-91124 Palaiseau Cedex* A qualitative description of a helicon plasma with SF_6 gas has been previously proposed[1] and has shown that a significant proportion of negative ions may exist when a highly electronegative gas such as SF_6 is used, although these sources operate at rather low pressure. We now present results obtained in the helicon diffusion chamber on the relative variations of negative ion to electron density ratio ($\alpha = n^-/n_e$) when changing the pressure and the radiofrequency power. Electrostatic probe measurements have been used to deduce α from the ratio $R = I_{th^-}/I_{sat^+}$ where I_{th^-} is the negative particles thermal current and I_{sat^+} the positive ion saturation current. This method has been suggested by Braithwaite and Allen[2] who have established the new expression for the Bohm flux in an electronegative plasma. Results obtained with this simple technique are in fairly good agreement with those published by St-Onge et al[3] and show that a significant amount of negative ions ($\alpha > 1$) seems to be present when $P > 2$ mTorr.

[1]Chabert P, Boswell R W and Davis C *J. Vac. Sci. Tech.* **A16** 78, 1998
[2]Braithwaite N St J and Allen J E *J. Phys. D.* **21** 1733, 1988
[3]St-Onge L, Margot J and Chaker M *Appl. Phys. Lett.* **72** 19, 1998

16:30

DM3 7 An Optically-Pumped Rb Electron Spin Filter* H. BATELAAN, A.S. GREEN, B.A. HITT, T.J. GAY, *University of Nebraska, Lincoln, NE 68588-0111* Intense beams of polarized electrons have been produced in an optically-pumped cold cathode discharge. Either helium or nitrogen can be used as the primary discharge gas. A small partial pressure of Rb (density = $10^{13}/cm^3$) in the discharge is optically pumped with a standing-wave dye laser operating at 795nm. This produces Rb that is spin polarized; the free electrons in the discharge become polarized through spin-exchange collisions with the Rb. The discharge gas also serves to reduce radiation trapping in the Rb[1]. Electron polarizations in excess of 0.3 with beam currents of 5 microamperes and energy widths of less than 1 eV have been obtained with a first apparatus. These results are compared with other standard sources of polarized electrons.

*Supported by NSF Grant PHY-9732258

[1]D.Tupa and L.W.Anderson, Phys.Rev.A 36, 2142(1987)

16:45

DM3 8 $O_2(b^1\Sigma_g^+)$, $O(^1D)$, and $O_2^+ + e$ Recombination in the Lower Thermosphere* D. L. HUESTIS, T. G. SLANGER, *SRI International* J. P. FULBRIGHT, D. E. OSTERBROCK, *University of California Observatories/Lick Observatory* Night-sky spectra taken with the HIRES spectrometer at the Keck I telescope on Mauna Kea have revealed emissions from $O_2(b^1\Sigma_g^+)$ in vibrational levels up to $v'=15$. Previously only $v'=0$ was known in the nightglow. Emissions from $v'=1$ are unexpectedly strong, comparable to $v'=2$, and variable from scan to scan. $v'=1$ emissions are visible up to $J'=50$ (requiring a temperature of more than 500 K, such as in the thermosphere), while $v'=2$ emissions are restricted to $J' < 25$ (consistent with a temperature of 200 K near the mesopause, where O + O recombination would peak). Considering that quenching of $v'=1$ is about ten times faster than $v'=2$, we infer that separate mechanisms are responsible for production of $v'=1$ and the other vibrational levels. The principal source of $v'=1$ appears to be $O_2^+ + e \rightarrow O(^1D)$, followed by $O(^1D) + O_2 \rightarrow O_2(b^1\Sigma_g^+)_{v'=1}$. At twilight, this process should have a maximum emission yield below 150 km, rising to about 250 km as the night progresses. Simultaneous observation of $O(^1D)$ and $O_2(b^1\Sigma_g^+)_{v'=0,1,2}$ should provide new information about kinetics in the thermosphere.

*Supported by NSF and NASA

SESSION EMP1: POSTER SESSION: DUSTY PLASMAS
Monday afternoon, 19 October 1998
Haku/Pikake Room, Aston Wailea at 17:15
Irving Langmuir, General Electric, presiding

EMP1 1 Simulation of dusty plasma crystals in presence of dipole moments GIOVANNI LAPENTA, *Politecnico di Torino* JERRY BRACKBILL, *Los Alamos National Laboratory* Under proper experimental conditions, dust particles immersed in glow discharge reactors arrange in regular patterns resembling macroscopic crystals. In the typical experimental apparatus, the dust crystal is formed at the sheath edge. Two dipoles can develop under such conditions: the field induced dipole and the ion flow induced dipole[1]. The two dipoles are pointed in opposite directions and their relative importance depends upon the material properties of the dust particles. In the present contribution, we decribe two principal results. First, a simple analytical model is derived for the total dipole moment of a dust particle immersed in a plasma with parameters representing actual experimental devices. The effect of charge migration due to a finite resistivity of the dust material is considered. The analytical results are compared with accurate computer simulations of the coupling of dust and plasma. Second, the effect of dust dipole moments on the

structure of dusty plasma crystals is investigated with a molecular dynamics (MD) code. The MD simulations use an interparticle potential obtained from a simple but accurate analytical model[1]. The interaction includes the effect of the dipole moments and of the plasma shielding. [1] G. Lapenta, J.U. Brackbill, Consequences of Sheath Ion Flow on Dusty Plasma Crystals, Phys. Rev. Lett., submitted, 1998.

EMP1 2 Study on Particle Formation in Germane RF Discharges by Photon-Counting Laser-Light-Scattering Method H. KAWASAKI, *Department of Electrical Engineering, Sasebo National College of Technology, Japan* K. SAKAMOTO, S. MAEDA, T. FUKUZAWA, M. SHIRATANI, Y. WATANABE, *Graduate School of Information Science and Electrical Engineering, Kyushu University, Japan* Nucleation and initial growth of particles formed in low pressure and low power GeH_4 rf discharges are studied using a high sensitive photon-counting laser-light-scattering method. [1] Particles of a few nm in size are detected mainly around plasma/sheath boundary near the rf electrode at an early time of 0.3 s after the discharge initiation and the corresponding density of 5×10^{10} cm^{-3} is by about two orders of magnitude higher than the ion-density. Spatial profiles of particle amount are very similar to those of Ge emission intensity, which is related to radical production rate. These results indicate that short-lifetime radicals such as GeH_2, having a high production rate, are key species contributing to the nucleation and initial growth of particles, even for a low pressure (10-13 Pa) and low power density (0.1 W/cm^2). Furthermore surface reflection probabilities of particles below 10 nm in size measured after rf-power-off are found to be above about 95%.[1]M. Shiratani and Y. Watanabe, Rev. Laser Eng. Vol. 26, No. 6 (1998) in press.

EMP1 3 Effects of Gas Flow on Particle Growth in Silane RF Discharges Y MATSUOKA, M SHIRATANI, T FUKUZAWA, Y WATANABE, *Kyushu University, Japan* K KIM, *Kangwon National University, Korea* Effects of gas flow on particle growth in silane rf discharges are studied mainly using a polarization-sensitive laser-light-scattering method. Gas of $He+SiH_4(5\%)$ is supplied from the rf shower electrode and exhausted from the grounded mesh electrode. For 80 Pa and rf power (6.5 MHz) of 80 W, particle growth rate increases to a maximum value of 40 nm/s when increasing the gas flow rate from 2 to 10 sccm, then the rate decreases considerably with further increasing the flow rate to 30 sccm. The former increase is mainly attributed to the increase in supply of short-lifetime radicals contributing to the rapid particle growth. The latter decrease suggests that neutral clusters, a diffusion time of which is longer than a gas residence time in the particle growth region, play a significant role in particle growth. For all the flow rates, particles begin to be observed around plasma/sheath boundary near the rf electrode and some of them flow to the grounded electrode after they grow above 100 nm and then trapped around plasma/sheath boundary there. Moreover some particles above 120 nm flow through the grounded mesh electrode ito the downstream region at a certain time in the discharging period. This result implies that some large particles may deposit on the film surface in CVD reactors having shower rf electrode.

EMP1 4 Trajectory of Particle Injected from Plasma Reactor Wall Y. WATANABE, T. FUKUZAWA, M. SHIRATANI, *Graduate School of Information Science and Electrical Engineering, Kyushu University, Japan* In etching plasmas, significant source of particulate contamination is believed to be due to flaking of films deposited on reactor wall, electrodes and wafers. To prevent such particles from depositing on the substrate surface, behavior of a particle injected from the plasma reactor wall is studied in H e dc glow discharge. For this purpose, we have developed a method to visualize trajectory of one particle injected from the wall. A particle of 20 μm in size injected, at an injection velocity v_p=10 cm/s, from an upper wall biased by -200 V against anode is reflected in the wall sheath and returns to the upper wall, while particles of $v_p >$ 20 cm/s passes through the sheath and goes into the plasma. Particles are considered to be charged positively in the sheath region close to the wall as the density of ions is much higher than that of electrons there. Thus when electrostatic potential energy of the positively charged particle in the sheath region near the wall is larger than its initial kinetic energy, the particle returns to the wall. These results are reproduced by a simple simulation concerning the particle trajectory. For a lower pressure and more negatively biased wall, which are often used in etching discharges, particles of an even higher v_p tend to reflect in the sheath toward the wall.

EMP1 5 Observation of Cu Submicron Dust Particles Trapped in a Diffused Plasma produced by a Low Pressure rf Discharge N. HAYASHI, T. KIMURA, H. FUJITA, *Saga University, Saga 840-8502, Japan* Submicron dust particles (Cu, ϕ 0.05 μm) were observed to be trapped in a diffused radio frequency (rf, 13.56 MHz) plasma. The particles were supplied by the simple speaker system set on the end of a chamber (ϕ = 160mm, L = 500mm). The rf plasma with the power of 20 $\sim$ 80 W was produced by introducing the Ar gas for the pressure range of 20 $\sim$ 60 mTorr. The injected dust particles were localized in the diffused region of the chamber without additional electrode for confinement. They were trapped for a period longer than one hour after switching off the speaker vibration at relatively low pressure, 20 mTorr. When the rf power was reduced gradually, the location of dust trapping moved toward the rf electrode. Electron density estimated from the Langmuir probe characteristcs decreased due to the electron attachment to dust particles. The reduction of electron temperature using a magnetic filter lead to the enhancement of dust plasma production. These results suggested that the dust particles were charged up negatively and maintained against gravity force by some mechanism of the plasma such as a spontaneous formation of potential well.

EMP1 6 Growth of Nano-Particles in an Acetylene RF-Discharge G. CHANDHOKE, C. EGGS, U. KORTSHAGEN, *University of Minnesota, Mechanical Engineering, 111 Church St. S.E., Minneapolis, MN 55455* The growth mechanism of nano-sized carbon particles has been investigated. Particles were grown in a capacitively coupled rf discharge. Pure acetylene (C_2H_2) as well as argon diluted acetylene have been used as feed gases at different flow rates, pressures, and discharge powers. Growth behavior of particles was studied by transmission electron microscopy (TEM) measurements after different plasma-on times t_{on} ($1s < t_{on} < 60s$). For $t_{on} >$ 10 s these measurements clearly show two different size groups of particles. The average size of the smaller particles remains constant at approximately 30 nm whereas larger particles of the second group continue to grow. The particle surface grows at a constant rate and for t_{on} = 60 s the particle diameter is approximately 350 nm (at $P_{discharge}$ = 50 W, p = 100 mTorr). The elemental composition of the particles was determined by x-ray photoelectron spectroscopy (XPS). From the infrared spectra of the particles the hydrogen content and the amount of double and triple C bonds was estimated and compared to the feed gas C_2H_2.

EMP1 7 Characterization of particle growth in a silane plasma M. A. CHILDS, ALAN GALLAGHER, *JILA, NIST and University of Colorado - Boulder.* Particles grow in silane plasmas used to make amorphous silicon films, and some particles escape the plasma and become incorporated in the film. We report measurements of particle size and density as a function of discharge parameters in the initial stages of a RF, parallel plate discharge. When the particles are large enough to be observable (radius $R > 4$ nm), the particles usually grow linearly in time at a rate consistent with growth by SiH_3. The data indicate that more rapid growth occurred for $R < 2$ nm; possible causes for this will be presented. An exception to linear growth for $R > 4$ nm occurs at higher pressures and RF voltages: the growth rate increases after an induction period, perhaps due to Si_mH_j with $m > 1$. We thank A. V. Phelps for valuable suggestions and the National Renewable Energy Laboratory for support.

EMP1 8 A Plasma-Chemical Model for Particle Growth in Silane Discharges ALAN GALLAGHER, M. A. CHILDS, *JILA, NIST and University of Colorado - Boulder.* A model encompassing radical, ion and electron collisions follows the growth of neutral and charged Si_mH_j radicals from inception ($m = 1$) to observable particles ($m > 10^4$). The SiH_3 and electron densities are determined from the film growth rate. The positive ion density results from requiring a balance between production and collisional neutralization of negative ions. Neutral radicals are lost by diffusion to surfaces, Si_mH_j and $Si_mH_j^-$ populations are closely coupled for $m > 20$, and radical collisions dominate growth for $m > 10$. Attrition of negative clusters is smaller for an initial window of a few milliseconds before the positive ion density grows to its steady state value. We thank A. V. Phelps for valuable suggestions and the National Renewable Energy Laboratory, the Department of Energy, for support.

EMP1 9 Study on Growth Mechanism of Particles in Cluster-Size Range in SiH_4 RF Discharges Using Threshold Photoemission Method T FUKUZAWA, S KUSHIMA, Y MATSUOKA, M SHIRATANI, Y WATANABE, *Kyushu University, Japan* Growth mechanism of particles in a cluster-size range has been studied using a threshold photoemission method together with microwave interferometry. For SiH_4, 13 Pa, gas velocity of 68.5 cm/s, 14 MHz and 10 W(0.18 W/cm^2), particles grow up to Si_6H_x ($\approx$ 0.4 nm), $Si_{22}H_x$ ($\approx$ 0.7 nm) and $Si_{200}H_x$ ($\approx$ 1.4 nm) for a discharging period T_{on} of 0.1, 0.2 and 0.5 s respectively, that is, the particle size increases with a constant growth rate of 2.5 nm/s. The constant particle growth rate indicates that the cluster-size particles grow due to deposition of species smaller than the particles on them. The particle density increases up to 1.5×10^{11} cm^{-3} for T_{on}=0.02 s and then decreases down to 1×10^{10} cm^{-3} for T_{on}=0.5 s, while positive ion density is a constant value of 1×10^9 cm^{-3}. Therefore, most particles are neutral and main species contributing to the particle growth are not negative ions but neutral species having a high gas phase reactivity and high production rate, even under low rf power and low pressure conditions. We have revealed that modulation of the rf discharge voltage is effective to reduce considerably both size and density of particle larger than a few nm in size. Effects of the modulation on suppression of cluster-size particles will be presented.

EMP1 10 Development of Photon-Counting Laser-Light- Scattering Method for Size- and Density-Measurements of Nano-Particles Formed in Processing Plasmas S. MAEDA, K. SAKAMOTO, T. FUKUZAWA, M. SHIRATANI, Y. WATANABE, *Kyushu University, Japan* A high sensitive photon-counting laser-light-scattering (PCLLS) method for detection of nano-particles formed in processing plasmas is developed to get information on nucleation and subsequent initial growth of particles. Two different methods are employed to deduce particle-size and -density from time evolution of LLS intensity after turning off the discharge. In one method, size of particles is deduced from their diffusion after turning off the discharge and their density is obtained using the size and absolute LLS intensity.[1]. In the other method, density of particles is deduced from their coagulation after turning off the discharge and their size is obtained using the density and absolute LLS intensity. Results obtained by both the methods agree fairly well with each other. Using the developed method, we demonstrate detection of small particles down to a few nm in size and find the corresponding particle density is above 10^{10} cm^{-3} even in low pressure silane rf discharges of low rf power, which are commonly used to deposit high quality a-Si:H films[1]M. Shiratani and Y. Watanabe, Rev. Laser Eng. Vol. 26, No. 6 (1998) in press.

SESSION EMP2: POSTER SESSION: CHARGED PARTICLE DIAGNOSTICS
Monday afternoon, 19 October 1998
Haku/Pikake Room, Aston Wailea at 17:15
Irving Langmuir, General Electric, presiding

EMP2 1 Langmuir Probe Measurements in an Inductively Coupled GEC Reference Cell Plasma J.S. JI, *Stanford University/NASA-Ames Research Center* J.S. KIM, *Stanford University/NASA-Ames Research Center* M.A. CAPPELLI, *Stanford University/NASA-Ames Research Center* S.P. SHARMA, *NASA-Ames Research Center* Measurements of electron number density, electron temperature, and electron energy distribution function (EEDF) using a compensated Langmuir probe have been performed on an inductively (transformer) coupled Gaseous Electronics Conference (GEC) reference cell plasma. The plasma source is operated with Ar, CH_4, CF_4, or their mixtures. The effect of independently driving the lower electrode on the probe data is studied. In particular, we find that the plasma structure depends on both the phase and power coupled through the lower electrode relative to that of the upper transformer coil. The Langmuir probe is translated in a plane parallel to the lower electrode to investigate the spatial structure of the plasma.

EMP2 2 New Langmuir probe analysis algorithm based on wavelet transform GON-HO KIM, WON-HO JUNG, *Department of Physics* DAI-GYOUNG KIM, *Department of Mathematics, Hanyang University-Ansan, Kyunggi-do, 425-791, Korea* A new algorithm for automating the analysis of Langmuir probe traces from ECR plasmas is developed through a wavelet transform. This approach minimizes the operator-specified inputs and provides denoised data with keeping important information. Such processed data are clearly partitioned into three regions: the ion saturation, the intermidate, and the electron saturation region. Un-

like the usual probe analysis algothim based on averaging with statistical treatments, the ion and electron saturation lines are obtained directly from the low frequency information of the processed data. The differentiation of the processed data also gives clear inflection points corresponding to the plasma potential and the end point of the ion saturation region, so that the intermediate region could be easily determined. The electrons are modeled by the bi-Maxwellian with hot and bulk temperatures, which could be determined in the intermediate region. We will present the test results of this new algorithm. This work is partially supported by 98 Hanbit User Develpment Program and Next Generation FPD Development Project of EDIRAK.

EMP2 3 Errors of Floating Probe System to Measure Fluctuating Plasma Caused by Loading Effect SHOSAKU MATSUMURA, KEISUKE HOSOE, *Musashi Institute of Technology* Floating probe systems such as double probe are used in order to avoid errors caused by the space potential fluctuation of plasmas, however, measured time averaged floating probe characteristics is deformed by rectifying current through the stray capacitance and the input impedance of instruments. Simplified equivalent circuits are applied to estimate the potential and the current fluctuations of the probes cause by the loading when the space potential varies sinusoidal. Time averaged probe current is also estimated to get the probe characteristics. The equivalent circuit model is assured by the experiments. As for the double probe, the spherical probe is most erroneous even if the resistive component of the loading impedance is enough high because the insufficient saturation of ion current results large current fluctuation. The estimated electron temperature by the conventional graphical method reaches up to 70%. As for the symmetrical triple probe, the differences of loading impedance between probe causes serious error. If the loading impedance of the floating probe and the other biased probe is differ few times, the electron temperature cannot estimate. When the floating probe is applied for RF plasma, the loading impedance of floating probe system is low for shielding or filtering the noise, therefor, the loading effect can not neglect.

EMP2 4 A Self-Biassing Planar Probe Technique for Electron Temperature* ALEC GOODYEAR, NICK BRAITHWAITE, *The Open University, Oxford Research Unit, UK* PAUL BOOTH, *LSP,Universite de Grenoble,France* A technique has been proposed to monitor ion flux in low pressure plasmas using a small, wall-mounted capacitively coupled planar probe. This minimally perturbing technique was developed for use in reactive gases where DC current measurements are made difficult or impossible owing to the deposition of insulating layers. The probe is biassed with respect to the plasma by RF bursts so that the probe alternates between floating conditions which are DC and RF-enhanced. This work aims to extract information about the energetic electron population from the same probe. In planar geometry it is relatively easy to extract the electron contribution from the complete current/voltage behaviour of the probe as the probe returns to the DC floating condition following an RF burst. The temperature of the tail of the electron population is determined from the electron current. This method has many advantages over conventional Langmuir probes and is better suited to following experiments in which the EEDF is tailored.

*Work supported by the EPSRC, Grant No. GR/L82380.

EMP2 5 Growth Mechanism of Electron Density in Pulse-Modulated RF Plasma YASUNORI OHTSU, KOJI SHIMIZU, HIROHARU FUJITA, *Department of Electrical and Electronic Engineering, Saga University, 1 Honjo-machi Saga 840-8502, Japan* Few experimental studies on behaviors of charged particles have been done in pulse-modulated plasmas, especially in a short time after the power is switched off. We have reported that electron density grew at $t \leqslant 100\mu s$ and then decreased in a pulsed-modulated RF plasma with a period of 1.2ms and a duty cycle of 40%. In the negative ion plasma with the mixed gases of He and SF_6, the density growth disappeared due to the electron attachment with SF_6 gas. In this work, the density growth mechanism was investigated in the pulse-modulated RF plasma using He and Ar gases. With increasing the gas pressure ($p=0.015 \sim 1$Torr), both of density growth rate and saturation time increased, while the decay rate decreased. These results might suggest that the growth mechanism was caused by the collisional ionization of metastable atoms. It was also observed in the mixed gases of He and SF_6 that the saturation time and decay rate had minimum and maximum values at the certain mixed ratio, respectively, while the density growth rate was almost independent on the ratio.

EMP2 6 Experimental Studies on Electric Currents Flowing into the Hollow Dug on the Substrate Surface in an Argon Plasma I. ARIKATA, K. KONISHI, T. KUBOTA, *Electrical Engineering, Himeji Institute of Technology, Himeji, Japan* The studies on the electric currents flowing into the hollow are of crucial importance for plasma etching. In this work, the sheath structures and the currents flowing into the hollow are measured by using a hollow probe, which consists of an envelope forming a hollow and of a collector movable along the axis. Here, we assume the envelope a substrate. An argon plasma was produced by hot cathode discharge. The typical plasma parameters are $T_e = 1.5$ eV, and $n_e = 1.2 \times 10^{+7}$ cm^{-3}. The inner diameters D of the hollows were 1 mm (smaller compared to the Debye length λ) and 3.0 mm (comparable to λ). Results obtained in the case of the $D \simeq 3$ mmID envelope are as follows: (1) At collector potential Vp is equal to Vwall, the Ven-Ip curves (en: envelope, Ip: the collector current) are sensitive to the location d of the collector. (2) At the sufficiently deep point $d = -15$ mm, only electrons flow into the collector.

EMP2 7 Is there structure in electron energy distribution functions in capacitively coupled H_2 discharges? J. McFARLAND, *Dept. of Pure and Applied Physics, Queen's University of Belfast, BT7 1NN, N. Ireland.* C.M.O. MAHONY, P.G. STEEN, W.G. GRAHAM, *Dept. of Pure and Applied Physics, Queen's University of Belfast, BT7 1NN, N. Ireland.* We report the first extensive study of H_2 and D_2 eedf measurements in 13.56 MHz driven plasmas and discuss reliability issues. A capacitively coupled GEC rf reference reactor was used with plasma properties typical for GEC reference reactors. Different passively compensated Langmuir probes were used to measure time-averaged eedfs via the second derivative technique. The eedfs are consistent with those seen in inert gases under similar conditions, but with an extra peak occurring at an energy of eV_{plasma}-eV_{float}. Issues commonly associated with reliable probe measurement in rf plasmas include; design, compensation, impedance, contamination, long term plasma changes and data analysis. We will discuss how these have been addressed in the current experiment. Our results show we can discount inadequate probe compensation as the root cause of the extra eedf feature. We will discuss other processes which may cause this feature including probe surface effects,

negative ions, temporally modulated electron production and electron collisionality.

EMP2 8 Analysis of Fast Neutrals and Plasma Ions with Quadrupole Mass Spectrometry JIAN WEI, *ABB Extrel* RANDALL PEDDER, *ABB Extrel* Plasma process generates charged molecules as well as fast moving neutrals. In-depth analysis of all these species from the plasma process demands high performance from the quadrupole mass spectrometer. For example, the kinetic energy of the fast moving neutrals can be as high as a few hundred electron volts. Our calculations show the ionization efficiency for these fast neutrals is inversely proportional to their velocity. Thus analysis of these neutrals requires high sensitivity from the ionizer, high transmission from the mass filter for the high energy ions created from the fast neutrals and the capability perform ion energy analysis with the instrument. We will present the results on the analysis of plasma ions and fast moving neutrals. The quadrupole mass spectrometer is equipped with a biasable quadrupole mass filter and an energy analyzer for energy analysis of ions and neutrals. With the combination of an energy analyzer and a biasable mass filter, we can either slow down all ions through a bias potential or select only the ions at a given kinetic energy range and then slow them down to a sufficiently low kinetic energy for the optimum transmission through the quadrupole mass filter. This minimizes the ion transmission loss through the quadrupole and improves overall detection sensitivity in the analysis of the fast neutrals and energy analysis of the plasma ions. When there is mass interference from the residual background in the detection of the fast neutrals, the energy analyzer can also be used to differentiate the fast neutrals from the residual species.

EMP2 9 Impacted Ion Energy Distribution Functions in ECR Plasma YASUNORI OHTSU, KEIICHI MORI, KUNIHIRO YOSHINAGA, HIROHARU FUJITA, *Department of Electrical and Electronic Engineering, Saga University, 1 Honjo-machi Saga 840-8502, Japan* Impacted ion energy distribution functions (IIEDFs) in Ar ECR plasma have been measured with a conventional retarding analyzer mounted in the substrate biased negatively by applying the DC voltage. Effects of ion-neutral collision probability on IIEDFs in the substrate sheath were examined by changing gas pressure (p=1 ~ 50 mTorr) or ion mean free path and biased voltage (V_{dc} = -200 ~ -10V) or sheath thickness. Ions incident to the substrate were confirmed to be accelerated by sheath potential. The IIEDFs were found to spread only toward the low energy side and to have double peaks with increasing the probability. At high probability ($P_c \geq$ 80%), ion density at low-energy peak became higher than that at high-energy peak. The temperature of impacted ions increased from 0.4 to 1eV with the collision probability.

EMP2 10 Ion Energy Distributions and their relative Abundance in Inductively Coupled Plasmas J.S. KIM, *Stanford University/NASA-Ames Research Center* M.V.V.S. RAO, *Thermosciences Institute/NASA-Ames Research Center* M.A. CAPPELLI, *Stanford University/NASA-Ames Research Center* S.P. SHARMA, *NASA-Ames Research Center* Study of kinetics of ions and neutrals produced in high density inductively coupled plasma (ICP) discharges is of great importance for achieving a high degree of plasma assisted deposition and etching. In this paper, we present the ion energy distributions (IEDs) of various ions arriving at the grounded lower electrode. The ions were energy as well as mass analyzed by a combination of electrostatic analyzer-quadrupole mass spectrometer for pure Ar and CF_4/Ar mixtures. The measurements have been made at gas pressures ranging from 30 to 100 mTorr. In addition, the IEDs were measured when the lower electrode was also rf-powered and the effect of the self-bias was observed in the energy distributions of ions. The shapes of the IEDs are discussed and related to the sheath properties and measured electrical waveforms, as a function of pressure and applied power. Relative ion intensities were obtained by integration of each ion kinetic energy distribution function over its energy range.

EMP2 11 Mass Spectrometric Investigations of Ionic Species in RF Discharges in Cl_2, N_2, O_2, and Their Mixtures with Ar YICHENG WANG, *NIST* JAMES OLTHOFF, *NIST* We report the measured ion fluxes and ion energy distributions in radio-frequency (rf) discharges in Cl_2, N_2, O_2, and in their mixtures with Ar. A Gaseous Electronic Conference rf reference cell with an inductively-coupled plasma source is used to produce the discharges, with gas pressures ranging from 0.33 to 6.7 Pa and applied rf powers from 100 to 300 W. Ions are sampled through a 10 μm diameter orifice in the center of the ground electrode and analyzed with a 45^o electrostatic energy analyzer in tandem with a quadrupole mass spectrometer. The total ion fluxes through the orifice are measured by configuring the first few electrostatic elements of the mass-energy analyzer system to form a Faraday cup. We find that for all three molecular gases, the dominant ion is the molecular ion, which exhibits energies reflecting the plasma potential. The fragment ion flux was observed to increase significantly compared to the molecular ion flux when Ar is introduced into the discharges.

SESSION EMP3: POSTER SESSION: CORONAS/BREAKDOWN

Monday afternoon, 19 October 1998
Haku/Pikake Room, Aston Wailea at 17:15
Irving Langmuir, General Electric, presiding

EMP3 1 Experimental Investigation of an Atmospheric Pressure Barrier-Discharge RAVISANKAR SANKARANARAYANAN, BIJAN PASHAIE, SHIRSHAK DHALI, *Southern Illinois University** Atmospheric pressure non-thermal plasma is now being used for various applications such as pollution control, sterilization, and light sources. For the efficient use of electrical power, the discharge characteristics should be more like a diffused Townsend-like discharge instead of a filamentary streamer discharge. Simulations have shown that Townsend-like discharge is more efficient in producing OH radicals which is essential for oxidation reactions. We present the experimental results of OH generation in a dielectric-barrier discharge. The Laser Induced Fluorescence (LIF) measurements are used to determine the OH concentration in the discharge. The setup consists of a tunable dye laser and an Princeton Instruments image intensified CCD camera. This is done for various discharge parameters such as voltage, frequency, and gas flow. We find that increased gas flow makes the discharge more uniform. In addition, impedance matching also helps the uniformity of the discharge.

*Supported by National Science Foundation

EMP3 2 Two dimensional simulation of positive streamer corona under consideration of radical reactions HIDEYUKI ARAI, FUMIYOSHI TOCHIKUBO, TSUNEO WATANABE, *Tokyo Metropolitan University* TIMM H. TEICH, *Swiss Federal Institute of Technology Zurich* Corona discharge is useful tool for removal of gaseous pollutants such as NO_x. Numerical simulation of chemical process enables us to examine the reaction path. Most of these works have been carried out by assuming uniform space with uniform elecric field, however, it is far from the real column discharges in atmospheric pressure. In this work, we calculated two dimensional streamer of positive corona discharge in the point-plane electrode configuration under the consideration of radical reactions. We considered the excited species with short radiative lifetime such as $N_2(B)$ and $N_2(C)$ in addition to radicals such as N, O and $N_2(A)$ because the radiative species contribute metastable generation by cascading or they can react with parent gases without spontaneous radiation in high pressure discharges. Calculation was performed until 500 ns after the discharge initiation. Although the radical production rate is high in the streamer head, considerable amount of radicals are generated after the streamer bridging between electrodes, especially for species with low excitation/dissociation energy. The influence of radiative species is also discussed.

EMP3 3 Discharge Parameters for Engineering Application of a Magnetic Switch* GOVINDA RAJU, *Electrical Engineering, University of Windsor, Windsor, Ont., N9B 3P4* In several engineering applications use of a magnetic switch provides advantages since the operation of such a switch does not involve mechanical motion. A magnetic switch essentially consists of a discharge gap between two electrodes and a magnetic field is applied in a direction perpendicular to the electric field. If the pressure of the gas is low ($<$ 500 Pa) application of a magnetic field reduces the sparking potential of the gap and this way the switch, which is normally open before the application, is closed. A theory for the operation of such a switch, previously developed by the author is used to demonstrate the influence of parameters such as drift velocity, ionization co-efficient and secondary electron emission from the cathode in the presence of magnetic field. The influence of the nature of the gaseous medium is discussed by considering air and argon. The discharge time lag is theoretically calculated which predicts two modes of operation of the switch.

*Parameters of a Magnetic Switch

EMP3 4 Charge Accumulation Effects on Breakdown Condition of Capacitive Discharges in DC-biased RF Field M. SHOJI, M. SATO, *Department of Electrical and Information Engineering, Yamagata University, 4-3 Jonan, Yonezawa 992-8510, Japan* Breakdown characteristics of capacitively coupled argon dc-biased rf (13.56 MHz) discharges are measured using an insulated electrode (IE) system made from glass-covered aluminum disk plates. In the IE system under the influence of a dc-biased rf field, charged particles generated in the discharge space will accumulate at the glass surface without leakage, which may weaken the dc electric field strength. After the dc-biased rf voltage is applied, a time lag T_l until breakdown is observed and the rf breakdown voltage V_{rf} is considerably lowered. For example, V_{rf} decreases by more than 10 % at $T_l = 1000$ sec. The values of V_{rf} which cause breakdown within $T_l = 20$ sec. in the IE system are compared with those for the bare metal electrode (BME) system for which no charge accumulation takes place. At low dc biases, they are almost the same for both systems. As the dc bias is increased, V_{rf} of the BME system becomes much smaller than that of the IE system. The decrease in V_{rf} can be explained by the occurring of secondary electron emission from the metal surface.

EMP3 5 Breakdown Characteristics of RF Capacitive Discharges in Argon-Nitrogen Mixture N. SASAKI, M. SATO, *Department of Electrical and Information Engineering, Yamagata University, Japan* Y. UCHIDA, *Toshiba Environmental Equipment Engineering Laboratory, Japan* Breakdown conditions of Ar-N_2 mixture in an RF electric field at 13.56 MHz are measured using a pair of aluminum parallel plates, 26.4 mm apart and the role of excitation electron energy losses (EEEL) on breakdown is investigated based on a numerical analysis of the Boltzmann equation. The breakdown voltages V_B measured against the total gas pressure p (0.03-11 Torr) show the well-known V-shaped characteristics at given mixture ratios x ($=N_2/(Ar+N_2)$). When replotted as a function of x (0-100%) at a fixed p, the values of V_B increase almost linearly and gradually with x at small p (less 1 Torr). As p is made larger, an initial steep rise takes place and V_B increases slowly with x as above. The value of x at this breaking increases with p, reaching 20 % at $p \approx$ 10 Torr. The numerical result implies that with increasing x, the mean electron energy ε decreases monotonously at small p where the dominant EEEL is not vibrational but electronic, while ε at higher p decreases noticeably due to the rapid increase in vibrational EEELs and then decreases slowly above x near the breaking of V_B. From these results, such energy loss dependences on p and x are considered to influence the electron production which governs breakdown.

SESSION EMP4: POSTER SESSION: DEPOSITION
Monday afternoon, 19 October 1998
Haku/Pikake Room, Aston Wailea at 17:15
Irving Langmuir, General Electric, presiding

EMP4 1 The deposition of SiOF film with low dielectric constant in a helicon plasma source HONG-YOUNG CHANG, *KAIST, Korea* CHI-KYU CHOI, *Cheju National University, Korea* SiOF films deposited by a helicon wave plasma chemical vapor deposition method has been characterized using Fourier transform infrared spectroscopy and ellipsometry. High density plasma of $10^{12} cm^{-3}$ can be obtained on a substrate at low pressure(,10 mTorr) with rf power $>$ 400 W with a helicon plasma source. A gas mixture of SiF_4,O_2, and Ar was used to deposit SiOF films on 5 in. Si(100) wafers not intentionally heated. Optical emission spectroscopy was used to study the relation between the relative densities of the radicals and the deposition mechanism. It was found that the addition of Ar gas to the SiOF/O2 mixture greatly increased the F concentration in the SiOF film. Discharge conditions such as gas composition, sheath potential, and the relative densities of the radicals affect the properties of the film. The dielectric constant of the SiOF film deposited using the helicon plasma source was 3.1, a value lower than that of the oxide film by other methods.

EMP4 2 Plasma Copolymerization of Fluorocarbon Sources and Hexamethyldisiloxane for the Application to Low Dielectric Constant Interlayer Dielectric Films TATSURU SHIRAFUJI, YASUO MIYAZAKI, YUKO NAKAGAMI, YASUAKI HAYASHI, SHIGEHIRO NISHINO, *Department of Electronics and Information Science, Kyoto Institute of Technology* The plasma copolymerization of tetrafluoroethyelene (TFE) and

hexamethyldisiloxane (HMDSO) was investigated for the purpose of application to low dielectric constant interlayer dielectric films. The films were prepared by using a conventional capacitively coupled RF (13.56 MHz) plasma enhanced chemical vapor deposition method. Fourier transform infrared (FT-IR) spectroscopy and X-ray photoelectron spectroscopy on the films have revealed that the film composition can be controlled gradually by changing the proportions of TFE/HMDSO. The dielectric constant of the films has ranged from 2 for the pure TFE films and 4 for the pure HMDSO films. Thermal treatment on the films has revealed that IR absorption peak intensity for C-H and C-H_2 decreases by the treatment, and dielectric constant of the films increases at the same time. Film deposition mechanisms are also discussed with the aid of *in situ* FT-IR gas-phase absorption spectroscopy on the plasma during film deposition. The results obtained for TFE/HMDSO gas are compared to those for commercially available C_4F_8/HMDSO gas.

EMP4 3 Sputter Deposition of Carbon Nitride Films by Reactive High-Density Plasmas with Excitation of m=0 Mode Helicon Wave* S. MIYAKE, Y. SETSUHARA, K. SHIBATA, *JWRI, Osaka University, Osaka Japan* M. KUMAGAI, *Kanagawa High-Technology Foundation, Kawasaki Japan* K. OGATA, *Nissin Electric Co. Ltd., Kyoto Japan* Y. SAKAWA, T. SHOJI, *Nagoya University, Nagoya Japan* Studies on the synthesis of carbon nitride (β-C_3N_4) films have attracted great interests due to the theoretically-predicted extreme properties similar or even superior to those of diamond. Motivated by the desire to establish a nitridation environment with extremely high reactivity for the synthesis of this metastable covalent material, we have developed a sputtering deposition system with installation of high-density helicon wave-excited plasma source to supply high concentration of atomic nitrogen. Carbon nitride films have been deposited on Si and WC substrates using reactive sputtering of carbon in N_2 and Ar mixture gas around 0.1 Pa. High-density plasmas of 10^{12}-10^{13} /cm^3 were produced even in pure N_2 using a helical antenna, where the excitation of m=0 mode helicon wave was verified to propagate. The composition, structure and bonding states of the films were characterized by XPS and FTIR. The nitrogen to carbon (N/C) ratio in the films was found to be controlled up to 0.9. The XPS analysis suggested the formation of sp^3 bonding, which consistently correlated with the film microhardness.

*Work supported by Grant-in-Aid for Scientific Research from the Japanese Ministry of Education, Science, Sports and Culture

EMP4 4 RF-Compensated Langmuir Probe Measurements in an IPVD System DANIEL R. JULIANO, DAVID N. RUZIC, *University of Illinois-Urbana* The experimental apparatus consists of a commercial-scale magnetron with an RF coil between the target and substrate holder. This coil creates a secondary inductive plasma that ionizes a significant portion of the sputter flux en route from target to substrate. In order to understand and predict the ionization of the sputter flux arriving at the substrate, Langmuir probe measurements of this secondary inductive plasma were made under various combinations of powers (magnetron and RF), pressures, and working gas mixtures. The probe apparatus is RF-compensated in order to keep the voltage difference between the probe tip and plasma constant throughout the RF cycle. In order to yield accurate measurements in the dirty depositing environment of the IPVD system, the back of probe tip is recessed in a small ceramic tube, preventing shorting. Further, the potential on the probe tip is kept low except during the data-collecting voltage sweeps in order to continuously clean it and maintain stable electrical characterisitics.

EMP4 5 Characterization and Performance of a High-Current-Density Ion Implanter with Magnetized Hollow-Cathode Plasma Source ZORAN FALKENSTEIN, DONALD REJ, *Los Alamos National Laboratory, P.O. Box 1663, Los Alamos, NM 87545, USA* NIKOLAI GAVRILOV, *Institute of Electrophysics, Ural Division of the RAS, 620049 Yekaterinburg, Russia* In a collaboration between the Institute of Electrophysics (IEP) and the Los Alamos National Laboratory (LANL), the IEP has developed an industrial scalable, high-power, large-area ion source for the surface modification of materials. The plasma source of the ion beam source can be described as a pulsed glow discharge with a cold, hollow-cathode in a weak magnetic field. Extraction and focusing of positive ions by an acceleration and ion-optical plate system renders the generation of a homogeneous, large-area ion beam with an averaged total ion current of up to 50 mA at acceleration voltages of up to 50 kV. The principle set-up of the ion beam source as well as some electrical characteristics (gas discharge current and the extracted ion beam current) are presented for a lab-scale prototype. Measurements of the radial ion current density profiles within the ion beam for various discharge parameters, as well as results on surface modification by ion implantation of nitrogen into aluminum and chromium are presented. Finally, a comparison of the applied ion dose with the retained ion doses is given.

EMP4 6 Deposition of a-SiC:H Films on Si Substrate by 50Hz Plasma CVD using Hexamethyldisilane + H2 M. SHIMOZUMA, *College of Medical Technology, Hokkaido University* M. YOSHINO, *Hokkaido Polytechnic College* H. DATE, *College of Medical Technology, Hokkaido University* H. TAGASHIRA, *Muroran Institute of Technology* Hydrogenated amorphous silicon carbide (a-SiC:H) films have been deposited on Si substrates by 50Hz plasma using Hexamethyldisilane [$((CH_3)_3Si_2(CH_3)_3)$:HMDS] + H_2 gas mixtures. Hexamethyldisilane has nonpyrophoric and nontoxic nature, and the plasma CVD method using HMDS is a safe process of SiC film deposition. Deposition rate, refractive index, Vickers hardness and IR spectrum of the deposited a-SiC:H films have been measured for various deposition temperature Tsub with a constant gas flow rates of the HMDS and H_2 (12.5sccm and 250sccm). As T_{sub} increases, the deposition rate of the a-SiC:H films decreases, and becomes constant value of about 100nm/h at above T_{sub} =350 °C. The refractive index of the films was 2.4 for T_{sub} =350 °C, while the Vickers hardness was 2200Hv for T_{sub} =350°C. The infrared transmission measurement shows that the films contain both Si-C and Si-CH_3 bonds. The composition of deposited a-SiC:H films was measured by XPS method. It was found that Si, C and O atom were contained in the deposited a-SiC:H films. From these results, it seems that high quality a-SiC:H films was obtained with above Tsub =350°C using HMDS+H_2 gas mixture by 50Hz plasma CVD.

EMP4 7 Plasma Parameter Control of the Spatially Afterglow Plasma for the Growth of 3C-SiC Epitaxial Films by Triode Plasma CVD ABDUL MANAF BIN HASHIM, MASAHIDE KIMURA, KANJI YASUI, TADASHI AKAHANE, *Nagaoka University of Technology** To grow epitaxial SiC films at low temperature, plasma parameters in the afterglow plasma region of hydrogen gas were extensively controlled using rf triode plasma CVD. Under negative grid biases, the discharge region was effectively confined between cathode and grid. The average sheath potential of anode surface drastically decreased from 60V at positive grid bias of 50V to about 1V at negative grid bias of -50V. The electron temperature in the afterglow plasma region also decreased to less than 1eV. The reduction of the rf plasma potential

fluctuation was also investigated by the addition of bypass condensers between grid and grounded chamber. The amplitude of the potential fluctuation in afterglow plasma region decreased from several tens volts to less than 2V at grid bias of -100V with the bypass condenser. At the same time, the electron temperature decreased to less than 0.2eV. Using dimethylsilane diluted with hydrogen as the source gas, 3C-SiC films were epitaxially grown on hydrogen terminated Si substrates placed on the anode at 1000°C under the above plasma conditions.

*The authors would like to thank Professor A. Matsuda of Department of Innovative and Engineering Materials, the Graduate School at Nagatsuda, Tokyo Institute of Technology and Electrotechnical Laboratory for useful suggestions and comments. This work was supported in part by a Grand-in-Aid for Scientific Research from the Ministry of Education, Science, Sports and Cult ure.

EMP4 8 Preparation of ZnO thin films by remote plasma enhanced CVD method K. HAGA, M. KAMIDAIRA, H. WATANABE, *Sendai National College of Technology* Highly transparent ZnO films were successfully prepared by remote plasma enhanced CVD of $Zn(C_2H_5)_2$ and carbon dioxide. $Zn(C_2H_5)_2$ contained in a temperature-controlled bath was bubbled with H_2. Carbon dioxide flowed through a coaxial low-frequency discharge chamber, and then into a reactor. The $Zn(C_2H_5)_2$-H_2 mixture was introduced to the reactor separately. The flow rates of H_2 and carbon dioxide were set to 10 sccm and 100 sccm, respectively. The pressure in the chamber was kept at 3.75 Torr. Plasma excitation in carbon dioxide was critical in being able to deposit transparent films. The films deposited on glass substrates at temperature around 450 °C show polycrystalline nature with (0002) preferred orientation. Measurement by the X-ray Photoelectron spectroscopy (XPS) indicates that the deposited films are free from carbon contamination. The resistivity of the films is $10^6\ \Omega \cdot$ cm range and high photosensitivity in near ultraviolet radiation. In addition, we found that ZnO was epitaxially grown on sapphire single crystal substrate using this simple system. Reflection high-energy electron diffraction (RHEED) and X-ray diffraction patterns show that ZnO $(11\bar{2}0)$ plain is formed on a sapphire $(1\bar{1}02)$ plain.

EMP4 9 Growth and Characterization of Polycrystalline $Ge_{1-x}C_x$ Thin Films* JASON T. HERROLD, VIKRAM L. DALAL, *Iowa State University* ALI BADAKHSHAN, *University of Northern Iowa* Polycrystalline $Ge_{1-x}C_x$ thin films have been prepared by ECR reactive plasmas. Systematic investigations were made into how deposition parameters affected the material properties of the resulting films. The films were grown from 300 to 500°C, pressures between 5 and 25 mT, and microwave powers between 100 and 200 W. The substrates were glass, stainless steel, and [100] oriented Si wafers. The optical properties were measured by UV/VIS/NIR photospectroscopy and Photoreflectance Spectroscopy, the lattice parameters were measured by X-Ray Diffraction, the crystallinity was characterized by Raman Spectroscopy, and the atomic percent C in the films was measured by X-Ray Photoelectron Spectroscopy. The films displayed excellent crystallinity, approximately 0 to 3 at. percent C, and the values of the bandgap and lattice dimensions could be varied continuously with the amount of C alloyed in the films. $Ge_{1-x}C_x$ films are of particular interest to the microelectronics industry because they offer a new option for the design of Group IV heterojunction devices.

*Supported by the Iowa Space Grant Consortium under a contract from NASA

EMP4 10 Trench Filling and Deposition of High Quality Cu Thin Films Using CVD Plasma Reactor with H Radical Source H. JIN, M. SHIRATANI, T. FUKUZAWA, Y. WATANABE, *Kyushu University, Japan* Effects of H radicals on removing impurities in Cu thin films during plasma enhanced metal organic chemical vapor deposition (PEMOCVD) are studied using in-situ FT-IR method which is employed for measuring relative impurity concentration in the films. The results show that H radicals are very effective for removing impurities in the film as well as on its surface. Based on such knowledge regarding the roles of H radicals, a PEMOCVD reactor equipped with an H radical source is developed to control both densities of H radicals and Cu-contained radicals independently. High purity ($\approx$ 100%) Cu films of a low resistivity of 2 $\mu\Omega$-cm can be deposited for a H_2 dilution rate of 50-67% by using the H radical source, while the high purity films were obtained only for a very high dilution rate above about 90% for the reactor with no radical source as reported previously. This feature opens up a new possibility of deposition of high quality Cu films at a high rate using the reactor equipped with the H radical source, since a concentration of Cu metal organic material can be increased by more than 5 times. In addition, when using the plasma CVD reactor with H radical source, high quality Cu films can be deposited in trench of 0.7 μm width and 3 μm depth with good step coverage.

EMP4 11 Formation of diamond films by intermittent DC plasma chemical vapor deposition using sub-electrode M. MIKIO, *Aichi University of Education* When diamond film was formed by intermittent DC plasma chemical vapor deposition (CVD) from methane-hydrogen gas mixture, wherein the waveform of the power supply was half-wave-recrified, it was found that the crystalline quality of the film became superior with increasing the distance between the electrodes. However, the discharge at longer electrode distance became unstable or impossible because the voltage to start the discharge became very high. Then, to perform stable discharge at longer electrode distance, subelectrode having short distance to the cathode was laid, and the substrate (anode) was biased with another DC power supply. The crystalline quality of the films deposited on Si substrate became superior when the electrode distance was about 20 to 25 mm, in comparison with those when the electrode distance was 10 and 30 mm. This method was also effective to change the discharge current widely and to perform the stable discharge at very low discharge current.

EMP4 12 The Relationship between C_{60} Mass Spectrum Intensity and C_2 Vibrational Temperature in Microwave Helium Plasmas KENGO UEDA, KIYOSHI KUWAHARA, HIROSHI FUJIYAMA, *Faculty of Engineering, Nagasaki University, Japan* The soot containing C_{60} and C_{70} was synthesized in helium plasmas generated in a quartz tube by microwave discharge. We used reticulated vitreous carbon (RVC) that was heated by electric field of TE_{10} mode microwave and the plasma. During soot deposition, optical emission of plasmas was observed with a monochromator. The soot deposited on the quartz tube was analyzed by the laser desorption time-of-flight mass-spectroscopy (LD-TOF-MS). Up to the present, the most intense C_{60} mass spectrum intensity was obtained for the condition of absorbed microwave power 200W and pressure 100Torr, where C_2 vibrational temperature was about 5500K.

EMP4 13 Characteristics of Scanning Mirror-type Magnetic Field Coaxial ECR Plasma for Inner Coating of Slender Tubes TEPPEI NAGANO, HIROSHI FUJIYAMA, *Faculty of Engineering, Ngasaki University, Japan* We have developed an inner coating system by using scanning coaxial electron cyclotron resonance (ECR) plasma. In this system, plasma was generated inside the coaxial metallic or insulated tubes by ECR method that was possible to discharge at low pressure and narrow gap. ECR plasma was transported along the tube axis using the control system for applied magnetic field that consists of a computer, switching regulator and five solenoid coils. The coils were set around a long process chamber at equal spaces apart. Low pressure discharge with mirror-type magnetic field were realized in the tube of 30 mm in inner diameter at the pressures of 3×10^{-5} Torr even for less than 150 W microwave power. Increases of the electron density and the deposition rate were achieved by generating mirror-type magnetic field. Using the developed plasma source, it could be coated by titanium nitride (TiN) thin films on inner wall of tube with use of a reactive sputtering.

EMP4 14 Extended Anode Effect in Coaxial Magnetron Pulsed Plasmas for Inner Coating of Narrow Tubes SEIKI SUGIMOTO, KIYOSHI KUWAHARA, HIROSHI FUJIYAMA, *Faculty of Engineering, Nagasaki University, Japan* HAJIME KUWAHARA, *Nissin Electric Co.Ltd., Japan* For coating thin films onto inner walls of narrow tubes, we developed a coaxial magnetron pulsed plasma (CMPP) device. The most advantage of this device is that deposited conductive films play the role of an anode. As a result, the plasma position shifts away from an anode set at the tube end and the distribution of film thickness spreads with increasing deposition time. We call this extended anode effect. The moving velocity of the plasma position is dependent on film materials, i.e. sputtering yields and film resistivities. In order to reveal this phenomenon, we deposited films which are different in these, such as titanium, tangsten and gold films onto inner walls of narrow insulated glass tubes.

EMP4 15 Electromagnetic Acceleration Plasma Spraying Applied to Ceramic Coating TETSUJI SHIBATA, HIROKAZU TAHARA, TOSHIAKI YASUI, YOICHI KAGAYA, TAKAO YOSHIKAWA, *Graduate School of Engineering Science, Osaka University, Japan* Electromagnetic acceleration plasma generators, which are called Magneto-Plasma-Dynamic (MPD) arcjet generators, can produce higher-velocity, higher-temperature and higher-density plasmas than those of conventional thermal plasma torches, because MPD arcjet plasma is efficiently accelerated by electromagnetic body forces in MW-class input power operation. For applications of MPD arcjet generators to ceramic spray coatings, an MPD arcjet generator that has a continuous supply mechanism of ceramic materials was developed. In the present study, calcia-stabilized zirconia (CSZ) and titanium nitride (TiN) are sprayed onto steel substrates. At CSZ spraying, argon was used as working gas. However at TiN spraying, nitrogen gas and titanium rod were used as working gas and cathode, respectively. The phase structure and the composition of the coating were analyzed by means of x-ray diffraction and scanning electron microscopy. The results showed that the MPD arcjet generator could successfully prepare a dense ceramic coating. Consequently, the MPD arcjet generator was found to have a high potential for ceramic spray coatings.

EMP4 16 Effect of ion bombardment on the initial growth in low temperature poly-Si formation K. MURATA , K. KAMIYA, R. NOZAWA, M. ITO, M. HORI, T. GOTO, *Quantum Engineering, Nagoya University, JAPAN* Recently, poly-Si films have attracted much attention in the application for TFT of LCD. PECVD is a candidate for the low temperature poly-Si formation. However, the films with good crystallinity are hard to be obtained at lower temperatures ($<$ 300 ° C). In this study, firstly, in ECR SiH_4/H_2 plasma CVD, poly-Si films were deposited by removing the charged species by using permanent magnets to clarify the effect of ion bombardment. The crystalline fraction of films without charged species was about twice as high as that with charged species from Raman spectra. Moreover, poly-Si films were successfully formed on plastic substrates at a low temperature (150 ° C) by eliminating charged species. Furthermore, two step growth method was performed to evaluate the effect of the ion bombardment at the initial stage on the film quality. For the first step, the seed layer was formed without charged species, and the growth layer was formed on the seed layer with charged species. The surface roughness and the crystalline fraction were improved to be 2.5nm and 73% with almost the same deposition rate as that of the conventional ECR PECVD. These results indicate that the ion bombardment prevents the growth of nuclei at the initial stage and affect the roughness and crystallinity of the films.

EMP4 17 Photo Luminescence from Si Films fabricated by Double Tubed Coaxial Line Type Microwave Plasma CVD Apparatus ISAMU KATO, *Waseda Univ.* YOSHIO KAWAHARA, *Waseda Univ.* In this study, we used a double tubed coaxial line type microwave plasma CVD apparatus. Under the low gas pressure ($\sim$ \mtorr), a-Si:H film is fabricated and photo luminescence (PL) is not observed at room temperature. However, under the high gas pressure ($\sim$ \100mtorr), a-Si:H nanoball film is fabricated and PL is observed at room temperture. The diameter of a-Si:H nanoball is about 20nm. It is judged by X-ray diffractmeter that there are nanocrystal Si (nc-Si) in this a-Si:H nanoball. The diameter of nc-Si is about several nm. In this work, we fabricated the a-Si:H nanoball films varying the substrate DC bias voltage from -80V to +40V, the substrate temperture during deposition from R.T. to 400^{o}C and the gas flow rate of SiH_4 per total gas flow (which consists of SiH_4 and Ar) from 7% to 36%. When the films are oxidized at 80^{o}C for more than the several hours, the PL ($\sim$ \800nm) is observed at R.T.. We discuss how the deposition circumstances affect the property and the film characteristics. The result will be presented at the meeting.

EMP4 18 Plasma Dynamics in a Large Area, Rectangular, Inductive Reactor for CVD * J.L. GIULIANI, V.A. SHAMAMIAN, *Naval Research Laboratory* R.A. RUDDER, R.E. THOMAS, R.C. HENDRY, *Research Triangle Institute* A.E. ROBSON, *Berkeley Scholars, Inc.* An advanced plasma reactor for chemical vapor deposition of diamond films over large flat areas ($\sim$ 1/3 m^2) is discussed. The reactor essentially is a single strap coil surrounding a metal box with slots running perpendicular to the current in the coil. The plasma within the box is coupled inductively by the magnetic flux penetrating through the slots while the interior surface of the box is the growth substrate. Typical operating conditions are $\sim$ 20 W/cm^2 surface power density and $\sim$ 1 Torr pressure. The discharge objective is a large uniform plasma so that constant deposition will occur throughout the chamber. In the present paper a global discharge model for the reactor is developed to demonstrate that classical resistivity holds for the plasma and the gas flow is diffusion dominated. Using these conditions a 2-D model is presented which self-consistently

treats the electromagnetic coupling, plasma diffusion, and non-equilibrium hydrogen gas dynamics. Results are compared with experimental data on the plasma length electron and gas temperature profiles, and hydrogen dissociation fraction. The observed trends in the first three of these quantities are reproduced by the model.

*Supported by BMDO and ARPA.

EMP4 19 The influence of uncontrolled carbon sources on diamond nucleation and synthesis using magneto-active microwave plasma CVD HYEONGMIN JEON, TOSHIMICHI ITO, *Department of Electrical Engineering, Osaka University, Osaka 565-0871, Japan* AKIMITSU HATTA, *Department of Electronic and Photonic Systems Engineering, Kochi Unversity of Technology, Kochi 782-8502, Japan* It is found that carbon films substantially deposited on reactor walls significantly influence on diamond nucleation and growth using magneto-active microwave plasma CVD, indicating that carbon-related sources originated from the unintentionally deposited materials on the chamber wall and substrate holder make an important effect to nucleation density and growth rate and quality of diamond films. In order to clarify the effect, a reproducible cleaning process of the growth equipment used should first be required. In the present study, the dependences of etching rate of the carbon films on treatment time, working pressure, microwave power, and substrate holder bias voltage have been examined using magneto-active microwave oxygen plasma as well as a mechanical cleaning method. On the other hand, the time dependences of various molecular species have been investigated using mass spectroscopy, infrared laser absorption spectroscopy, and plasma optical emission spectroscopy. The gas phase synthesis using additional solid sources of nanometer-sized carbon materials beside the source gas usually employed have brought forth an additional information about the influence of the uncontrolled carbon-related sources, especially the particle-related effect, in the plasma CVD growth chamber.

EMP4 20 Dependence of the TiN hard coating properties on the substrate position MIHAI BALACEANU, *National Institute of Laser, Plasma and Radiation Physics, P.O.Box MG-36, Bucharest, Romania* DUMITRU PANTELICA, PETRE MARIN RACOLTA, *National Institute of Physics and Nuclear Engineering - Horia Hulubei, P.O.Box MG 6, Bucharest, Romania* GABRIELA PAVELESCU, *National Institute of Materials Physics, P.O.Box MG 7, Bucharest, Romania* AUREL POPESCU, *Gas-Petroleum University, Ploiesti, Romania* EMIL GRIGORE, PETRICA CRISTIAN LUNGU, *National Institute of Laser, Plasma and Radiation Physics, P.O.Box MG 36, Bucharest, Romania* TiN coatings were deposited by hollow cathode discharge deposition process on samples mounted in various positions within the deposition chamber. Some microchemical, mechanical and tribological characteristics of the layers were investigated by Rutherford backscattering spectroscopy (RBS), spectroscopic ellipsometry (SE), X-ray diffraction analysis, thickness and microhardness measurements and tribological tests. The observed differences between the film properties for the substrates differently positioned can be accounted for by variations both of the coating flux arrival rate and of the ion bombardment intensity on the substrates.

EMP4 21 Silicon Nitride Ultra Thin Film Formation by Electron Cyclotron Resonance Plasma and its Application to Gate-Insulator HIROYUKI OHTA, *Nagoya University and Fujitsu* ATUSHI NAGASHIMA, MASAFUMI ITO, MASARU HORI, TOSHIO GOTO, *Nagoya University* TETSUO IZAWA, *Fujitsu* The silicon nitride film attracts much attention as scaled gate dielectric films, because of low gate leakage current. In this study, we have investigated the properties of the silicon nitride ultra thin films produced by ECR-PECVD method employing SiH_4 and N_2 gases, and ECR N_2 plasma nitridation on silicon substrates. The silicon nitride films were formed by ECR plasma nitridation on silicon substrates at 300W, 0.5Pa, a N_2 flow of 100sccm. The bias and temperature of the substrate were floating and 350 degree C. The film properties were studied by Fourier Transform Infrared Spectroscopy(FT-IR), ellipsometry and in-situ X-ray Photoelectron Spectroscopy(XPS). In-situ XPS analysis showed that the peaks of Si2p and N1s were saturated in 60 min. N_2 plasma duration. The silicon nitride layer was 3.5nm in thickness and the stoichiometric composition(Si_3N_4) without hydrogen content. The films synthesized by ECR-PECVD indicated the nearly stoichiometric composition(SiN_1) without hydrogen content. These results suggest that those nitride films are applicable for the gate insulator in next generations ULSI.

EMP4 22 Ellipsometric Monitoring of First Stages of Diamond Nucleation in a Bias-Enhanced Microwave Plasma YASUAKI HAYASHI, MASAAKI NAGAHIRO, SHIGEHIRO NISHINO, *Kyoto Institute of Technology, Japan* Appropriate negative bias to a substrate in plasma chemical vapor deposition enhances diamond nucleation, i. e., increases the nucleation density and enables highly oriented diamond growth, scattered heteroepitaxy. In order to improve the method into complete heteroepitaxy, the mechanism should be analyzed. However the analysis has hardly been performed because of the difficulty of in-process monitoring in a microwave plasma. We have developed a new diamond synthesis system of surface wave-excited microwave plasma with a slotted antenna, in which an ellipsometric monitor is installed. The first stages of diamond nucleation in a bias-enhanced CH4/H2 plasma were monitored with the use of the monitor, and carbonization, incubation, nucleation, and nuclei growth stages have been able to be distinguished from the changes of the ellipsometric parameters. Ellipsometric monitoring is a useful method for the control of diamond nucleation stages in a bias-enhanced plasma process.

SESSION EMP5: POSTER SESSION: PLASMA-SURFACE INTERACTION AND SHEATHS

Monday afternoon, 19 October 1998
Haku/Pikake Room, Aston Wailea at 17:15
Irving Langmuir, General Electric, presiding

EMP5 1 Angle resolved velocity distributions of sputtered tungsten atoms ANDREAS GOEHLICH, NORBERT NIEMÖLLER, H.F. DÖBELE, *Universität GH Essen, Institut für Laser- und Plasmaphysik, 45117 Essen, Germany* Angle resolved velocity distributions and relative angular distributions of tungsten atoms sputtered by the bombardment of argon ions in the energy range between 0.2 to 5 keV are reported. Tungsten is chosen as the target material because of its importance as a wall material in fusion research. The velocity distributions are determined using Doppler shifted laser induced fluorescence spectroscopy (DSLF) in connection with a detection geometry which allows to vary the angle of emission independently from the angle of incidence. The dependence of the velocity distributions on the beam energy and on the angle of incidence is studied. With an oblique angle of incidence of the ion beam the experimental distributions observed

in forward direction exhibit a broadening and a shift of the maximum (as compared to the Thompson formula). The experimental velocity distributions are also compared with TRIM.SP (ver. TRVMC95) simulations. Good agreement between experimental data and simulation is obtained.

EMP5 2 Ion bombardment effects on boron nitride film synthesis by reactive sputtering with electron cyclotron resonance plasmas M. WAKATSUCHI, *Osaka University* Y. TAKABA, *Osaka University* K. KANAI, *Osaka University* Y. UEDA, *Osaka University* M. NISHIKAWA, *Osaka University* Boron nitride (BN) films are synthesized by reactive sputtering with electron cyclotron resonance (ECR) plasmas. Ions necessary for both sputtering of a target material and bombardment on film surface are supplied by ECR discharge. Pure boron disk is used as a target and dc biased in the Ar/N_2 mixed plasma. Sputtered boron atoms react with excited species of nitrogen to form BN compounds. It is well known that energetic ion bombardment is necessary to synthesize sp^3-bonded cubic phase BN (c-BN) in thin-film form. For this reason, rf bias is applied to a substrate. BN film with high cubic phase content of 78% is obtained at the substrate self bias larger than 175 V under the conditions of ion/boron atom flux ratio to the substrate of 12, Ar/N_2 mixing ratio of 1, substrate temperature of 500°C. As the ion/boron atom flux ratio is increased to 30, the threshold value of self bias to synthesize cubic phase decreases to 75 V. However, c-BN content of the film deposited under this high ion flux condition is 18% at most. Films are resputtered away at the self bias larger than 100 V. It appears that the optimum values of the self bias and the flux ratio exist to synthesize BN films with high cubic phase content.

EMP5 3 Numerical simulation of interactions between pulsed laser and soild targets in an ambient gas ROBERT E. PETERKIN, JR., *Air Force Research Laboratory: Directed Energy Directorate* When a GW/cm^2 repetitively pulsed laser strikes a solid target that is immersed in a gas at 1 atm, numerous interesting plasma phenomena are observed. To help us understand these observations, we perform time-dependent numerical simulations of the propagation and partial absorption via inverse bremsstrahlung of a pulsed CO_2 laser beam through He and N, and the interaction with a solid copper target aligned at various angles with respect to the incident laser beam. For this numerical study, we use the general-purpose 2 1/2-dimensional finite-volume MHD code MACH2. The early portion of the laser pulses is deposited into the solid target and produces a jet of target material that is almost aligned with the target normal. Most of the subsequent laser energy is deposited into the ambient gas at the critical surface. For a repetitive pulsed laser, we observe a series of laser supported detonation (LSD) waves each of which originates at the instantaneous location of the critical surface. The space- and time-dependent electron number density defines this surface. For the numerical code to reproduce accurately the relevant physics, the overall energy budget must be computed accurately. The solid ejecta interacts with the LSD waves in a complex fashion, allowing the spontaneous generation of a magnetic field via the grad(P) term of a generalized Ohm's law. We illustrate the dynamics with graphical results from MACH2 simulations.

EMP5 4 Finite Pulse Rise Effect on Time Dependent Sheath in PSII GON-HO KIM, GUN-WOO KIM, *Department of Physics, Hanyang University-Ansan* SEUNG-HEE HAN, *Advanced Analysis Center, Korea Institute of Science and Technology* MUN-PYO HONG, *AMLCD Division, Samsung Electronics, Seoul, Korea* In a plasmas source ion implantation, the target is sucessively biased by negative voltage pulses with an intrinsic finite rise time to implant ions from plasma to target surface, resulting in a time-dependent sheath around the target. In this work, Langmuir probe was used to study the sheath motion around a planar target biased by a negative pulse with various plasma and pulse conditions. It was observed that the time-dependent sheath consisited of two parts: the ion matrix sheath development during the pulse rise time and the dynamic sheath motion after being attained the full voltage. The ion matrix sheath development was in proportional to square root of pulse rise time and rise rate over plasma density but independent of the ion mass. A new model for the ion matrix sheath development was proposed to explain these results which were discrepant in the previous models. The dynamic sheaths were faster than the ion sound speed in the pulse rise time and eventually slowed down to approximately 1/3 of the speed. We also present the results of target geometry effect on these sheath formation.

EMP5 5 Ion energy distribution function in pulsed discharges. RAMANA VEERASINGAM, *Applied Materials Inc. Santa Clara, CA 95054* In plasma processing equipment, the ions play an important role in determing etch rates for ion assisted etching and sputter rates in physical vapor deposition systems. In processes that rely on physical ion bombardment rather the chemical reaction mechanisms, key parameters include the ion flux and the ion energy distribution function (iedf). In this paper, we present calculated ion energy distributions for varying pulsed waveforms and circuit parameters. The model includes a description for a multizonal plasma sheath and a simple RLC matching circuit. The model indicates that the ied is a strong function of the impedance match and the RF voltage. When the match is poor, the ied does not respond to the applied RF voltage instead has an ied that corresponds to the plasma potential. In the presence of harmonics in the circuit currents, the ied has multiple peaks reflecting the impact of the harmonics on the ion energy.

EMP5 6 Helium Discharges at High E/N. B.M. JELENKOVIĆ,*A.V. PHELPS, *JILA, U. of Colorado and NIST* We investigated He discharges[1] at high electric field to gas density ratios E/N between parallel-plate electrodes (80 mm dia. and 10 mm gap) of graphite and gold-plated cooper. The E/N were 270 Td to 10 kTd for pressures from 2 to 1.1 Torr. Plots of discharge voltage versus pressure times electrode spacing pd are similar for both voltage polarities. The plots are multiple valued[2] at pd near 1.5 Torr cm. Voltage-current data using a pulsed discharge at pd = 2 Torr cm on the low-voltage branch show a linear voltage decrease of 60 mV/μA for 8 to 75 μA and a constant voltage change of -20 V above 200 μA. At low currents and E/N above 4 kTd, absolute values of optical emission coefficients versus distance for the 501.6 nm line (3^1P state) and for the 587.6 nm line (3^3D state) show strong heavy-particle excitation peaking near the cathode. Heavy-particle excitation of the triplet state is much larger relative to electron excitation than for the singlet state. Model results will be presented.

*Permanent address: Institute of Physics, University of Belgrade, Belgrade, Yugoslavia.

[1]A. Strinić, G. Malović, and Z. Lj. Petrović (unpublished) have made similar measurements for 20 Td $< E/N <$ 3 kTd.

[2]M. J. Druyvesteyn and F. M. Penning, Rev. Mod. Phys. **12**, 87 (1940).

EMP5 7 Upgrade of Long-chain Hydrocarbons by Low Pressure Oxygen Plasmas PEDRO PATIÑO, BERNARDO MÉNDEZ, GLORIA GAMBÚS, *Escuela de Química, Facultad de Ciencias, Universidad Central, PO Box 47102, Caracas 1041A, Venezuela** Huge known heavy oil deposits in many countries remain largely untapped. The API gravity of crude oils has been decreasing by about 0.17% per year, this meaning that there will be an urgent need for economically viable new technologies to upgrade the heavy oil for the refineries. The same applies to the residues of several refineries processes. This work will present the results of the application of a plasma process to upgrade long-chain hydrocarbons, namely, tridecane, tetradecane, and squalane (shark oil). They are high boiling point alkanes, the latter being a $C_{30}H_{62}$ with six methyl groups attached to various carbon positions on the chain. An oxygen plasma, created by a high voltage glow discharge, reached the low vapor pressure surface of each liquid hydrocarbon. This (2 mL) was cooled down to temperatures close to its freezing point in a glass reactor. Applied power was 24 W for times of reaction between 30 and 60 minutes and oxygen pressures from 0.1 to 0.4 mbar. Products were analyzed by IR and NMR spectroscopies. The ^1H and ^{13}C NMR spectra showed that the most important products were secondary alcohols and the corresponding ketones, for tridecane and tetradecane. For squalane, tertiary alcohols were first. Total conversions are tipically 90 to 100%

*Thanks to CDCH-UCV for financial support through Grant # 03-12-4083-98

EMP5 8 Characterisation Of Low Pressure Plasma Textile Processing* S. GOMEZ, *Dept. of Pure and Applied Physics, Queen's University of Belfast, BT7 1NN, N. Ireland* E. COSTA BRICHA, P.G. STEEN, W.G. GRAHAM, *Dept. of Pure and Applied Physics, Queen's University of Belfast, BT7 1NN, N. Ireland.* There is increasing interest in the plasma processing of textiles. Here the effects of introducing textile materials into low pressure plasmas are reported. Polypropylene and polyester material has been placed on the lower electrode of an inductively coupled GEC reference reactor. This had to be operated at low power and hence in the capacitive mode to avoid toasting the material. A Langmuir probe was used to measure the plasma potential and electron energy distribution functions (eedfs) and a spectrometer with an ICCD detector was used to make time and space resolved emission studies. The present measurements contrast operation in oxygen and argon gas comparing measurements with a bare stainless steel electrode and one loaded with the sample materials. At power inputs of from 20 to 50 W and gas pressures of 50 mTorr, the eedfs show some structure at low energies but the high energy region can be described by a Maxwellian in Oxygen and a Dryvesteyn in Argon. The shape of the eedf remains essentially unchanged when material is introduced but the electron density decreases in Argon. One indication of plasma interaction with the substrate is emission from CO and hydrogen. This is found to commence about one second after plasma ignition.

*Work supported by the EU BRITE programme

EMP5 9 Ion Sheath Structure around Metal Plates Located in Plasma Flows HIROKAZU TAHARA, TOSHIAKI EDAMITSU, TETSUJI SHIBATA, TOSHIAKI YASUI, TAKAO YOSHIKAWA, *Graduate School of Engineering Science, Osaka University, Japan* In general, a complicated ion sheath is created around a metal plate applied a negatively biased voltage in a plasma flow. This phenomenon can be observed around a substrate in a plasma reactor for material processing and around a high voltage solar array of spacecraft on an Earth orbit. In order to understand the interaction between plasma flow and a metal plate, i.e., the ion sheath formation and its structure, oxygen plasma flow was exposed to a sample plate, which of the one side is an electrode collecting ions and of the other side is a dielectric side. The ion current was measured for variations in the biased voltage and an attack angle of the plate against the plasma flow. The plasma potential around the plate was measured with an emissive probe. The distributions of the ion current density and the plasma potential were found to be drastically changed by the biased voltage and the attack angle.

EMP5 10 Large-Area Uniform Surface Treatment of Polymeric Materials using a Scanning Plasma Method YANG SUNG-CHAE, *Venture Business Lab., Shizuoka Univ.* YANAGI JUNICHI, *Faculty of Engineerinr, Nagasaki Univ.* YAMAMOTO KYOICHI, *Toppan Printing Co. Ltd.* UYAMA HARUO, *Toppan Printing Co. Ltd.* FUJIYAMA HIROSHI, *Faculty of Engineering, Nagasaki Univ.* We have investigated the efficiency of a crossed magnetic field method, called by Scanning Plasma Method (SPM) i.e., using a magnetic field B perpendicular to discharge electric field E, in the field of surface treatment of polymeric meterials such as polyethylene terephthalate(PET) and polypropylene (PP). In this study, it is found that SPM is very useful to control plasma for surface treatment, because plasma is transported in the direction to the EXB drift. From these experimental results, it can be expected that uniform surface treatment extend over large area will be realized.

EMP5 11 Boundary layers in front of an oblique end-plate in a magnetized sheet plasma AKIRA TONEGAWA, MASATAKA ONO, *Department of Physics, School of Science, Tokai University* KAZUTAKA KAWAMURA, KAZUO TAKAYAMA, *Research Institute of Science & Technology, Tokai University* TUGUHIRO WATANABE, HAJIME SUZUKI, NOBUYOSHI OHYABU, *National Institute for Fusion Science, 322-6 Oroshi, Toki Gifu 509-52, Japan* This abstract was not submitted electronically.

SESSION EMP6: POSTER SESSION: INDUCTIVELY COUPLED PLASMAS

Monday afternoon, 19 October 1998
Haku/Pikake Room, Aston Wailea at 17:15
Irving Langmuir, General Electric, presiding

EMP6 1 Simulation of Low Pressure Glow Discharges with DSMC including Electron Kinetic Effects* S.J. CHOI, T.J. BARTEL, R.B. CAMPBELL, *Sandia National Laboratories* A two-dimensional massively parallel plasma DSMC (Direct Simulation Monte Carlo) model called ICARUS has been developed. Neutral and ion transport with chemistry are directly simulated with computational particles; a local charge neutrality assumption is used to determine the electron density. Electron impact rates are separately obtained by iteratively running a Monte Carlo electron simulation with the species densities and the electric fields calculated from the model. The inductive electric fields are updated many times during the calculation from a module called ORMAX (developed at Oakridge National Lab.). In this manner the non-equilibrium nature of the electron energy distribution (EED) is

well represented. Faster and stable convergence with better statistics is observed with a reduced version of the electron kinetic model in which only the electron energy moment ("temperature") affects the source terms. Results will be presented with "well developed" Cl2 chemistry in the GEC Reference Cell.

*This work performed at Sandia National Laboratories supported by the U.S. Department of Energy under contract DE-AC04-94AL85000.

EMP6 2 Three-Dimensional Simulation of Inductively Coupled Plasma Reactors T. L. PANAGOPOULOS, V. MIDHA, D.J. ECONOMOU, *University of Houston* MPRES-3D, a three-dimensional version of the Modular Plasma Reactor Simulator (MPRES), has been developed to study plasma transport and chemistry in inductively coupled plasma reactors of arbitrary geometry. Special attention was paid to azimuthal asymmetries of the etch rate introduced by gas injection and pumping ports, and by non-uniform power deposition profiles. The finite element method using higher order elements allowed accurate representation of complicated reactor geometries. A 3-D Maxwell solver was also implemented to self-consistently account for azimuthal variations of the power deposition in the plasma. The chlorine plasma etching polysilicon was taken as a system for study. Gas inlets were found to introduce some local azimuthal asymmetries. In general, however, gas inlets jetting parallel to the wafer did not contribute substantially to non-uniformities at the wafer level. The effect of pumping port(s) and non-uniform power absorption were more important since significant disturbances of all essential plasma species can be introduced. The implementation of a focus ring was found to yield practically azimuthally symmetric etching profiles. Overall, 3-D simulation tools are viewed as critically important for the design and optimization of upcoming 300 mm wafer plasma processing tools.

EMP6 3 Production of Negative Ion Plasma Using an Internal Helical Antenna in Uniform Magnetic Field MAHMOOD NASSER, HIROHARU FUJITA, *Department of Electrical and Electronic Engineering, Saga University, Honjo 1, Saga 840-8502, Japan* Intensive studies on the inductively coupled plasma (ICP) and the helicon discharges had been made because they can meet with most of the plasma processing requirements. In the ICPs so far, the inductive coupling element has been physically outside the discharge region except for few application, where the coupler was placed inside the discharge region. Here, we are representing an immersed type antenna and in addition an axial magnetic field was applied as an external control parameter. The ICP discharge was generated in a stainless steel cylindrical vacuum (10^{-6} Torr) chamber. The discharge was realised at a very low pressure (2 mTorr) and a rf (13.56 MHz) power of 50 W using an internal helical antenna (3 turn) with a uniform axial magnetic field. The experimental results revealed that oscillating amplitudes and space potential in the plasma were increased and decreased, respectively, with increasing concentration of SF_6 gas in Ar gas. The electron energy distribution functions (EEDFs) and the excited rf magnetic fields were also investigated in both electropositive and electronegative gas discharges.

EMP6 4 Capacitance Termination Effect on Plasma Density in Inductive RF Discharge E. KONISHI, K. SUZUKI, K. NAKAMURA, H. SUGAI, *Nagoya University* A one-turn circular discharge antenna (inductance L) is immersed in a plasma in a 50 cm diameter metal chamber. A capacitance (C=250~ 2000 pF) is inserted in series between a terminal of the antenna and a ground point of 13.56 MHz RF power source. For the different values of C, the plasma is generated in argon at 2 mTorr with the net input power kept constant at 500 W. When the capacitance is chosen to satisfy the condition $\omega^2 LC = 2$, the plasma density is observed to increase by 50~ 100 %, in comparison with a conventional discharge with the antenna terminal grounded (effectively, $C \rightarrow \infty$). The plasma potential oscillation at 13.56 MHz detected by a capacitive probe showed the minimum value (4 V peak-to-peak) in that condition which is much lower than the value (27 V peak-to-peak) in the conventional case. Furthermore, the measurement of power transfer efficiency[1] revealed that such dramatic increase in the plasma density is attributed to reduction of electrostatic coupling from antenna to plasma. Thus, the observed plasma density increase is interpleted by a decrease in the power loss carried by ions to the antenna and the chamber wall. The physical meaning of the above condition between C and L is explained with a distributed voltage along the antenna taken into account.

[1]K. Suzuki, *et al.*, Plasma Sources Sci. Technol. **7**(1998) 13.

EMP6 5 Production of Inductively-Coupled Large-Diameter Plasmas with Internal Antenna Y. SETSUHARA, S. MIYAKE, *JWRI, Osaka University, Osaka Japan* Y. SAKAWA, T. SHOJI, *Nagoya University, Nagoya Japan* Trends in plasma processing of large diameter substrates typically used in fabrications of microelectronic devices such as advanced integrated circuits and flat-panel displays are toward the development of high-density plasma sources with uniform plasma parameters over a large area. In this work large-diameter rf plasmas have been produced by inductive coupling of internal-type double half-loop antennas electrically floated with blocking capacitors. Major objectives of this investigation include the minimization of antenna impedance and the reduction of terminal rf voltage to avoid the anomalous rise of the plasma potential. A double half-loop antenna 360 mm in outer diameter was immersed in the discharge chamber with 400mm inner diameter and 200mm high. The double half-loop antenna was coupled to an RF power generator at 13.56 MHz via a matching network. A blocking capacitor was inserted between the low-voltage side of the antenna conductor and the ground to electrically float the antenna and to balance the rf voltage amplitudes to ground potential at both ends of the rf feedthrus. The plasma source can be stably operated at RF input powers up to 3 kW with densities as high as 10^{12} /cm^3 at Ar pressures around 1Pa.

EMP6 6 Influence of a low frequency bias voltage on a wafer in inductively coupled plasma* H. KOBAYASHI, N. NAKANO, T. MAKABE, *Keio University at Yokohama, Japan* An inductively coupled plasma (ICP) sources in a collision dominated mode are being developed as reactors for high plasma density, low pressure etching of semiconductors and metals for microelectronics fabrication. Wafer for dry etching is usually biased by a low frequency (LF) source to accelarate ions to the wafer. By using previously developed two dimensional ICP model, considering the electron transport under both time varying electric and magnetic fields, we have investigated the influence of the LF (800 kHz) bias voltage on both the wafer and the structure of ICP as a function of bias amplitude. The interaction between both frequencies, 13.56 MHz and 800 kHz on the plasma is discussed. The electron transport to the wafer is also discussed in comparison with that under the high sheath field in the CCP-reactor.

*Work is partly supported by STARC in Japan.

EMP6 7 Tomography of Optical Emission Intensities of Inductively Coupled Plasma Source and the Comparison with Simulations TSANG-LANG LIN, CHUNG-JEN HSU, WHE-YI CHIANG, YUAN HU, K.-C. LEOU, C.-H. TSAI, *Department of Engineering and System Science, National Tsing-Hua University** A CCD pinhole camera is used to record the optical emission intensity from inductively coupled plasma source. The radial distribution of the optical emission intensity can be determined by maximum entropy method (MEM). This inversion method is a non-linear least square fitting plus a constraint of maximum entropy for the probabilities of the intensity distribution. Such a inversion method has been successfully used in many other types of problems. The radial distribution of the optical emission intensity will be discussed in comparison with the radial plasma density distribution obtained by computer simulations and probe measurements. The experiments will be carried out for different gas pressures and rf powers to investigate the effects of operation conditions on the uniformity of ICP plasma source.

*This work is supproted by National Science Council, ROC

EMP6 8 Inductively Coupled Radio Frequency Discharge as a Source of Hydronium Ions* G. BROOKE, S. POPOVIC, L. VUSKOVIC, *Old Dominion University* Inductively coupled discharge in a mixture of water vapor and argon was compared to the hollow cathode discharge with respect to breakdown characteristics, efficiency and stability of operation. Objective was to search for an optimal source for hydronium ions to be used in the proton transfer studies. In the same time, we intend to circumvent the dual-mode operation of hollow cathode discharge, if possible. Spatial distribution of electron density and temperature were measured using Langmuir probes, while hydronium ion density distribution was determined using a variable-position orifice valve and a quadrupole mass spectrometer. The results will be compared with simulations based on a kinetic model of the discharge.

*Supported by Jeffress Foundation

EMP6 9 A Pulsed Inductively Coupled Plasma Source for Atomic Hydrogen Ion Implantation MICHEL TUSZEWSKI, *Los Alamos National Laboratory, Los Alamos, NM 87545* BRIAN CLUGGISH, *Los Alamos National Laboratory, Los Alamos, NM 87545* A pulsed inductively coupled plasma source has been developed to generate highly-dissociated hydrogen plasmas with gas pressures in the range 0.1 - 1 Pa. Such plasmas will be used to implant atomic hydrogen ions into single crystal silicon with energies up to 100 kV. The hydrogen implants will stimulate the cleavage of a thin layer of silicon, which will be bonded to an insulating substrate for the production of economical silicon on insulator devices. The pulsed plasma source operation consists of radio frequency (rf) bursts of 10 - 100 cycles at 100 kHz rf frequency applied to a coil wound around a 0.2-m radius hemispherical quartz dome. The bursts are repeated every few ms to generate dense plasmas with duty cycles of 1 - 1014 kW peak rf power. Plasma densities of about 1.4x1017 m-3 are measured with Langmuir probes and with microwave interferometry 0.15 m downstream from the dome. The ion species content at the same location will be measured with a small ion mass spectrometer. Neutral species from the discharges will be analyzed with optical emission spectroscopy and with a quadrupole mass spectrometer. These data will be presented for various hydrogen pressures and peak rf powers.

EMP6 10 Investigation of the capacitive to inductive mode transition in an rf driven discharge P.G. STEEN, *Dept. of Pure and Applied Physics, Queen's University of Belfast, BT7 1NN, N.Ireland.* S. GOMEZ, C.M.O. MAHONY, W.G. GRAHAM, *Dept. of Pure and Applied Physics, Queen's University of Belfast, BT7 1NN, N. Ireland.* The transfer from the capacitive to the inductive mode has been studied in an inductively driven GEC reactor. The antenna is a five turn planar copper coil coupled through a silica window and the lower electrode 165mm diameter. Operating with Ar at pressures varying from 0.7-67 Pa, spatially resolved optical emission spectroscopy, and compensated Langmuir probe eedf measurements were used to characterise the system. The capacitive to inductive transition occurs suddenly as rf power is increased. When the inductive mode is reached the power can be reduced to similar levels as when running capactively while still remaining in inductive mode. The optical emission increased 30-fold on transition from capacitive to inductive mode and the relative intensity of particular emission lines changed but with little change in the axial variation. At electron energies below about 10 eV the shape of the eedf is essentially the same in both modes. The magnitude increases by about 100 on transition to inductive mode while for the high energy region this factor is only about 10.

EMP6 11 Ion Bombardment Heating Effects HAN-MING WU, E. JACK McINERNEY, VIKRAM SINGH, MICHAEL KILGORE, *Novellus Systems, Inc.* During the plasma enhanced material processing, ion bombardment energy flux (IBEF) is very important. Especially in a high density plasma (HDP) reactor, heating by ion bombardment plays a significant role on the wafer temperature distribution, amongst other effects. In this work, using CFD-PLASMA, the bell-jar plasma reactor for Ar, O2 and He discharges is simulated. Bulk plasma information is used in conjunction with the Godyak collisionless sheath model to calculate the ion energy distribution function (IEDF). The total power of IBEF on wafer is obtained by the integral of IEDF across the wafer. It is found that the IBEF is obviously dependent on neutral species, bias power and frequency, when other operation parameters are fixed. The simulation results indicate the power input to the wafer. When coupled with a heat transfer model for wafer cooling, the wafer temperature is determined. Comparison is being made for wafer heating for the different gases at operating conditions of interest for HDP-CVD.

EMP6 12 Characteristics of a Novel ICP Source with a Deformable Bifilar Coil* K.C. LEOU, *Engineering and System Science Department, National Tsing Hua University, Taiwan* J.H. CHENG, T.S. CHEN, C.R. HSU, W.C. WU, W.Y. CHIANG, T.L. LIN, C.H. TSAI, *Engineering and System Science Department, National Tsing Hua University, Taiwan* The characteristics of a low pressure inductively-coupled plasma (ICP) source which employs a novel coil design to maximize the source's operation window will be described. A uniform plasma density over an area larger than the wafer size is one of the most important requirements for the plasma sources used in ULSI processing tools. By making the coil deformable, the plasma density uniformity can be maintained over a wider operation window as system's parameters, such as gas chemistry, gas pressure, and chuck RF bias power, are varied to meet different process requirements, as compared to the ICP sources based on conventional fixed coil design. The other feature of the new coil design is that it has two sets of winding connected in parallel but 180 degrees opposite azymuthally. This arrangement in principle provides a better azymuthal symmetry than the conventional single winding planar coil. The

system was characterized with several plasma diagnostic tools: a 2D RF-compensated Langmuir probe, a B-Dot probe, a heterodyne interferometer and spectroscopy/imaging of plasma-induced emissions. A wafer-type grided ion energy analyzer has also been developed to measure ion energy distribuition at different locations on the wafer. Experimental results show that the radial profile of plasma density changes as the coil is deformed. The effect is more pronounced at higher gas pressures where electron's mean free path becomes shorter and the plasma density profile is basically determined by the distribution of RF power deposition. The detailed experimental results will be presented.

*Work supported by NSC grant No. 86-AFA04J0010031 and 86-2622-E-007-007R, ROC

EMP6 13 Studies on Electron Behavior in a Magnetic Neutral Loop Discharge Plasma Y. M. SUNG, K. UCHINO, K. MURAOKA, *Kyushu University, Japan* T. SAKODA, *Kumamoto Institute of Technology, Japan* A new type of plasma called a magnetic neutral loop discharge (NLD) has been proposed as a plasma source for processing applications.[1] In order to characterize the electron behavior in the NLD plasma, laser Thomson scattering was applied to diagnose the plasma.[2] Also, laser-induced fluorescence measurements were performed to measure atomic densities at excited states and metastable states. Analysis of these data showed that electron heating and ionization on the neutral loop was essential for the formation of the NLD plasma. In addition, a new type of the NLD plasma, based on capacitive RF power coupling, has been proposed for sputtering applications. Initial results obtained using this new discharge will be presented.

[1]T. Uchida, Jpn. J. Appl. Phys. 33, L43 (1994)
[2]T. Sakoda, et al, Jpn. J. Appl. Phys. 36, 6981 (1997)

EMP6 14 Transformer circuit model including ferrite cores in inductively coupled plasmas S. LLOYD, *Dept. of Electrical Engineering, Colorado State University* D. M. SHAW, *Dept. of Electrical Engineering, Colorado State University* M. WATANABE, *Dept. of Electrical Engineering, Colorado State University* G. J. COLLINS, *Dept. of Electrical Engineering, Colorado State University* We have investigated the effect of two different rf core materials on the primary rf coil in a cylindrical inductively coupled plasma (ICP). Argon feedstock pressure ranges from 1 to 20 mTorr, and rf power is varied from 25 to 500 W. The rf impedance of the core/coil/plasma circuit has been measured both with a plasma and with no plasma present. The effects of the core have been added to the transformer circuit model of Piejak et al. When using the core, the resistive power loss in the primary rf circuit increases as does the coupling coefficient k. Comparisons of plasma electron density, with and without the cores present, have been made and included in the transformer circuit model.

EMP6 15 Effects of the Induced Magnetic Field and Nonlinear Diffusion in Inductively Coupled Discharges* A SMOLYAKOV, I KHABIBRAKHMANOV, M HRYCAY, C SOTEROS, *Department of Physics and Engineering Physics, University of Saskatchewan, 116 Science Place, Saskatoon SK, S7N 5E2 Canada* The influence of the induced magnetic on the collisional skin effect is analyzed. Nonlinear equations are derived for the evolution of the magnetic field in weakly ionized plasmas where the main dissipation is the collisional friction of charged particles with neutral atoms. It is shown that the Lorentz force associated with the induced magnetic field contributes convective term to the magnetic induction equation. Depending on plasma collisionality the effect of plasma flow leads to the wave like propagation of the magnetic field or to the nonlinear diffusion similar to the diffusion in porous medium. It is shown that these nonlinear effects enhance the penetration of the external periodic magnetic field into inductively heated plasma.

*Work is supported by NSERC Canada

EMP6 16 Accelerated Particle Simulation of High Density Discharges M. M. TURNER, *EECS Dept, University of California, Berkeley, CA** Simulation of dense discharges using particle methods is difficult because of the disparity between the plasma frequency and Debye length and the scales of the problem, such as the ion transit time and the device size. Implicit particle in cell algorithms are problematic because of increased algorithmic complexity and the difficulty of minimizing the dissipation inherent in such methods. This paper discusses an alternative approach, exploiting the insensitivity of the problem physics to the exact values of the plasma frequency and Debye length when the former is much the largest frequency and the latter is much smallest length. Some further constraints are usually satisfied in dense discharges: Displacement current should not be important and the magnetic field energy should be large compared to the electric field energy. With these conditions, a fictitious relative permittivity may be introduced to relax the accuracy conditions so that larger time steps and cell sizes may be used in an explicit algorithm. For an inductive discharge with density $\sim 10^{11}\text{cm}^{-3}$, this method can reduce the amount of computer time required by a factor $\sim$ 100, and the amount of memory by about $\sim$ 10. Larger improvements are likely for more ambitious problems.

*Present affiliation: Dublin City University, Ireland

SESSION EMP7: POSTER SESSION: HEAVY PARTICLE COLLISIONS
Monday afternoon, 19 October 1998
Haku/Pikake Room, Aston Wailea at 17:15
Irving Langmuir, General Electric, presiding

EMP7 1 Electron capture from Ni surface resulting from H+ ion impact REIKO SUZUKI, *Hitotsubashi University* REIKO SUZUKI, *Hitotsubashi University* HIROSHI SATO, *Ochanomizu University* MINEO KIMURA, *Yamaguchi University* Electron capture from Cu and Co surfaces by H^+ and He^+ ion bombardment has been investigated theoretically by using the molecular representation. Since an experimental condition was that the incoming particle was introduced on the surface with a large angle, the binary collision would be satisfied. We have obtained electronic states of the colliding pair by the ALCHEMY, and the scattering dynamics was solved by using the semiclassical close coupling treatment. We have included trajectories of compete recoils of the projectile through the coupling of electronic and nuclear motions. The preliminary result obtained shed much light on the understanding of the experimental finding.

EMP7 2 Stark l-mixing in Rydberg atom collisions with slow charged particles D. VRINCEANU, M.R. FLANNERY, *School of Physics, Georgia Institute of Technology, Atlanta, GA 30332-0430** Angular momentum redistribution is the key process in ultracold electron-ion recombination. In the initial stage electrons are captured into high Rydberg states $n > 100$ with high

angular momentum $l \approx n - 1$. The rapid radiative decay to the lowest electronic levels completes the recombination only if low angular momentum states are attained. A classical treatment of Stark mixing of l states by slow collisions with large impact parameter between the Rydberg atom and the charged particles is described. Analytical results are presented. A comparison between the effects of electron and ion collisions with the atom is also presented.

*This Research is supported by the U.S. Air Force Grant No. F49620-96-1-0142

EMP7 3 Ion-Molecule Reactions in CF_4 Discharges BRIAN PEKO, *College of William and Mary* ILYA DYAKOV, *College of William and Mary* ROY CHAMPION, *College of William and Mary* RAO MANGINA, *NIST* JAMES OLTHOFF, *NIST* Cross sections have been measured for ion-molecule reactions relevant to the analysis and modeling of electrical discharges in CF_4. The reactions investigated include electron detachment, collision induced dissociation, and dissociative electron transfer resulting from collisions of CF_3^+, F^+, and F^- with CF_4. Measurements are presented for impact energies ranging from threshold to 200 eV. The cross section data are used to interpret measurements of the kinetic energy distributions and relative fluxes of positive and negative ions striking the electrodes of dc Townsend discharges in CF_4. The relative fluxes of the ions sampled from the discharge are shown to be strongly affected by collision induced dissociation collisions experienced as they travel through the discharge.

EMP7 4 The motive force to settle gas particles in the Maxwell velocity distribution N. IKUTA, *Chiba Inst. of Tech.* A. TAKEDA, K. YAMAMOTO, *Shikoku Univ* It seems generally believed that the Maxwell velocity distribution of neutral gas particles in steady state is given by the maximum value of entropy. However, the authors consider that there must be other motive force directly acting on gas particles to settle them in the Maxwell distribution regardless of the relative velocity dependence of collision frequency. As is easily understood, the velocity distribution of gas particles can change only through collisions. In both the FTI analysis and the Monte-Carlo simulation, we obtained the Maxwell distribution only assuming the isotropic scattering in the center of mass frame. That is, the probability of velocity dispersion through a collision conserving the kinetic energy gives irreversible relaxation into the Maxwell distribution. This fact implies that the direct motive force acting on gas particles toward the Maxwell distribution is solely the law of energy conservation in collisions. The transport properties of gas particles are also determined through collisions conserving energies and momenta with given collision frequencies. The quantities of state such as entropy can not be considered directly giving influences on gas particles but are the results of sequential collisions statistically independent to each other. This idea is also supported by mathematics in solving the Boltzmann equation.

EMP7 5 Three Dimensional Analysis for Loss Prosesses of $N_2(A^3\Sigma_u^+)$ S. SUZUKI, H. ITOH, H. SKIZAWA, N. IKUTA, *Chiba Institute of Technology* Behavior of the loss processes of the metastable nitrogen molecules $N_2(A^3\Sigma_u^+)$ in the cylindrical cavity is analyzed by the three dimensional diffusion equation by using the boundary condition of the third kind that can take account of the reflection at the electrode surface and the cylindrical side. Previously, we have carried out the same analysis in the one dimensional diffusion equation[1]. The results of these theory were compared with the experiments[2,3], and the reasonable agreement was recognized in both results. By this analysis, we can discuss the diffusion of $N_2(A^3\Sigma_u^+)$ from the radial direction to the axial direction in including the transition region for both directions. Furthermore, we report on the behavior of τ_1 due to the each variation of the reflection coefficient at the electrode surface and the cylindrical side.

[1]S.Suzuki, H.Itoh, N.Ikuta and H.Sekizawa: J.Phys.D: Appl.Phys., 25, 1568 (1992).
[2]S.Suzuki, H.Itoh, H.Sekizawa and N.Ikuta: J.Phys.Soc.Jpn., 62, 2692 (1993).
[3]S.Suzuki, H.Itoh, H.Sekizawa and N.Ikuta: Jpn.J.Appl.Phys., 36,Part 1, No.7B, 4744 (1997).

EMP7 6 CW Laser-Induced Fluorescence Study of SiH_2+ SiH_4 Reaction: Evidence for Two-Body Reaction Channel AKIHIRO KONO, *CCRAST, Nagoya University* SATOSHI HIROSE, TOSHIO GOTO, *Dept. Quantum Eng., Nagoya University, Nagoya, Japan* The rate constant of the reaction between SiH_2 and SiH_4 in low-pressure SiH_4/H_2 mixture plasma was studied using laser-induced fluorescence spectroscopy with cw ring dye laser excitation. The decay of the SiH_2 density in the afterglow plasma at various partial H_2 and total pressures was measured. The resulting reaction rate constant showed no significant dependence on the H_2 partial pressure (with SiH_4 partial pressure fixed at 20 mTorr). Thus, although the SiH_2+SiH_4 reaction has been regarded as to take place via three-body process (producing Si_2H_6), the present results indicate that below $\sim$ 40 mTorr the two-body process (presumably producing $Si_2H_4+H_2$) becomes dominant; the results also indicate that H_2 molecule cannot act as an efficient third-body in the three-body reaction channel because of its light mass.

EMP7 7 Theoretical and experimental studies of line broadening in Na vapors* J.F. BABB, H.-K. CHUNG, A. DALGARNO, V. KHARCHENKO, K. KIRBY, W.H. PARKINSON, M. SHURGALIN, K. YOSHINO, *Harvard-Smithsonian* We are investigating theoretically and experimentally line broadening in vapors consisting of Na and buffer gas mixtures. Our progress in high-resolution spectroscopy, measurements of absorption coefficients, and in calculations will be reported.

*Supported in part by the NSF.

EMP7 8 Chemical Generation of NCl($a^1\Delta$) Molecules by the Reaction of Chlorine Atoms with Azide Radicals and Measurements of Quenching Rate Constants of NCl($a^1\Delta$)* K.B. HEWETT, G.C. MANKE II, D.W. SETSER, *Dept. of Chem., Kansas State Univ.* The first electronically excited state of NCl, the $a^1\Delta$ state with a lifetime of $\sim$ 2 s and an energy of 1.15 eV, is a candidate for gas-phase energy-storage applications. The NCl ($a^1\Delta$) molecule can be generated with a high efficiency by the reaction of Cl atoms with the azide radical, N_3, which is generated by the F + HN_3 reaction. The room temperature, gas phase experiments consist of adding F and Cl atoms together with HN_3 to a pre-reactor section of a flow reactor with typical initial concentrations of $[HN_3] = 2.0x10^{12}$, $[F] = 2.5x10^{12}$ and $[Cl] = 2.0x10^{12}$ molecules cm^{-3} in 1 Torr of Ar carrier gas. The flow reactor is a 7.0 cm diameter Pyrex glass pipe of 150 cm length. The reactor walls were coated with halocarbon wax to prevent the loss of F and Cl atoms and NF(a) and NCl(a) molecules by reaction at the walls. The F- and Cl-atom reaction rates with HN_3 and N_3 are sufficiently fast that the HN_3 is converted to NF(a) and NCl(a) in the pre-reactor. The NF(a) and NCl(a) relative concentrations are

monitored along the flow reactor by observing the a-X transitions at 874 and 1077 nm, respectively, with a cooled photomultiplier tube. Quenching reagents are added to the main reactor and the pseudo first-order decay rates of NF(a) and NCl(a) are observed and converted to bimolecular rate constants.

*This work was supported by the U.S. Air Force under Grant F49620-96-1-0110.

EMP7 9 Long-range interactions between metastable rare gases atoms D. VRINCEANU, M. MARINESCU, M.R. FLANNERY, *School of Physics, Georgia Institute of Technology, Atlanta, GA 30332-0430* Knowledge of the long-range interaction between atoms and molecules is of fundamental importance for low-energy and low-temperature collisions. The electronic interaction between the charge distributions of two metastable rare gases atoms can be expanded in inverse powers of R, the internuclear distance. The coefficients C_6, C_8, and C_{10} of, respectively, the R^{-6}, R^{-8}, and R^{-10} terms are calculated by integrating the products of the dynamic electric polarizabilities of the individual atoms at imaginary frequencies, which are in turn obtained by solving a system of coupled inhomogeneous differential equations. The triplet state spectrum of the rare gases atoms is described by precise l-dependent one-electron model potentials. Numerical results for the C_6, C_8, and C_{10} dispersion coefficients for homonuclear and heteronuclear metastable rare gases diatoms are presented.

EMP7 10 Molecular formation of Li_2 by three-body recombination at mK D. VRINCEANU, M.R. FLANNERY, *School of Physics, Georgia Institute of Technology, Atlanta, GA 30332-0430** A theory is developed for molecular formation via the three-body recombination process $^7Li + {}^7Li + {}^7Li \rightarrow Li_2 + Li$ at $T \sim$ mK. Highly accurate Li_2 potential, which accomodate 11 vibrational levels are used, within an impulse approximation to the three body scattering process. An analytical expression is derived for the finite limiting rate of recombination α, a result in accordance with the Wigner Threshold Law. The theory does predict $\alpha \sim a^2$, where a is the zero-energy two body (Li - Li) scattering length.

*This Research is supported by the U.S. Air Force Grant No. F49620-96-1-0142

EMP7 11 Differential Cross Sections for Elastic Ar-Ar Collisions from 0.02 eV to 1 keV. A.V. PHELPS, *JILA, U. of Colorado and NIST* We construct a set ofdifferential cross sections for elastic collisions of Ar with Ar for collision energies used in discharge modeling. At collision energies below 1 eV, viscosity, diffusion, and thermal conductivity measurements, differential scattering measurements, and total cross section theory[1] are used to derive a three-parameter differential scattering cross section that includes an isotropic component. For higher energies, experimental total cross sections[2] for 350 to 1050 eV and calculated diffusion and viscosity cross sections[3] for 10 to 1000 eV yield a two-parameter differential cross section with no isotropic component. At all energies these differential scattering cross sections are sharply peaked in the forward direction. Our viscosity cross section, but not our diffusion cross section, agrees well with that calculated from a recent variable-hard-sphere model.[4] We hope that uncertainties in these results will encourage theorteical and/or experimental work on this topic.

[1]R. B. Bernstein, in *Molecular Beams*, ed. by J. Ross (Interscience, New York, 1971) Chap. 3.
[2]I. Amdur and E. A. Mason, J. Chem. Phys. **22**, 670 (1954).
[3]R. S. Robinson, J. Vac. Sci. Tech. **16**, 185 (1979).
[4]V. V. Serikov and K. Nanbu, J. Vac. Sci. Tech. A **14**, 3108 (1996).

SESSION EMP8: POSTER SESSION: HELICON PLASMAS

Monday afternoon, 19 October 1998
Haku/Pikake Room, Aston Wailea at 17:15
Irving Langmuir, General Electric, presiding

EMP8 1 Ion Temperature Anisotropies in Helicon Plasmas EARL SCIME, MATTHEW BALKEY, ROBERT BOIVIN, PAUL KEITER, JOHN KLINE, *Department of Physics, West Virginia University* Laser induced fluorescence measurements of the ion temperature in an argon helicon plasma indicate a substantial ion temperature anisotropy (perpendicular over parallel). Anisotropies as large as 5 have been observed. We will present evidence that suggests the anisotropies are due to a difference in the parallel and perpendicular particle confinement times. The perpendicular ion temperature scales linearly with the applied magnetic field strength, indicative of Bohm-like particle confinement [Scime et al., Plasma Sources Sci. and Tech. 7, 186-191 (1998)]. The parallel ion temperature is independent of the magnetic field strength. Experimental tests of potential sources of error, such as Zeeman broadening, Stark broadening, power broadening, and frequency hole burning will be reviewed. The West Virginia University Hot hELicon eXperiment (HELIX) is part of a larger experiment designed to experimentally model the high pressure, highly anisotropic plasma of the Earth's magnetosheath. The implications of the observed ion temperature anisotropy control in HELIX will also be discussed with respect to the magnetosheath experiments.

EMP8 2 Resonant Ion Heating in Helicon Plasmas JOHN KLINE, EARL SCIME, MATTHEW BALKEY, ROBERT BOIVIN, PAUL KEITER, *Department of Physics, West Virginia University* A resonant ion heating system has been developed for heating ions and controlling the ion temperature anisotropy in a helicon plasma source. The system uses two rectangular coils placed on either side of the glass cylinder such that it creates a time dependent magnetic field transverse to the steady state axial field. A 1 kW, 25-125 kHz RF generator provides the power to the coils. The parallel and perpendicular ion temperatures in argon plasmas are measured with a laser induced fluorescence diagnostic tuned to a metastable argon ion transition. Ion heating of over 600% has been measured for the perpendicular ion temperatures with an increase of 70% in the parallel direction. This temperature increase occurs for a specific ratio of heating frequency to cyclotron frequency. Ion temperature measurements for multiple neutral pressures will be presented. Some work has been done to provide the basis of a theoretical explanation for the ion heating mechanism. Work supported by the U.S. Department of Energy and the National Science Foundation.

EMP8 3 A rectangular helicon-wave plasma source with parmanent magnets and a simple rf antenna K. SASAKI, T. SHOJI, D. HAYASHI, K. KADOTA, *Department of Electronics, Nagoya University, Nagoya 464-8603, Japan* S. DEN, *Irie Koken Co, Ltd, Japan* Y. SAKAMOTO, *Nichimen Electric Technology Corp, Japan* The conventional helicon-wave plasma sources have a difficulty for the production of large-area plasmas. This is mainly because the conventional helicon plasmas are produced in circular glass tubes with small diameters. In the present work, we show a novel rectangular helicon-wave plasma source. The magnetic field, which is necessary for sustaining the helicon wave, is produced by a pair of parmanent magnets. A straight antenna covered with a glass tube is inserted into the rectangular discharge section made of stainless steel. Because of the simple structure, the present plasma source is suitable for the production of large-area plasmas. A proof-of-principle experiment was carried out in a prototype machine having a relatively small cross section of 100 mm $\times$ 20 mm. A huge jump was observed in the rf power dependence of the electron density. A typical electron density was 5 $\times$ 10^{12} cm^{-3} at a distance of 7 cm from the straight antenna for an rf power of 4 kW (13.56 MHz) and an Ar gas pressure of 10 mTorr. The decrease in the electron density along the axial direction from the antenna was rather small in the high-density operation, which suggests that the plasma was sustained by a helicon wave.

EMP8 4 Profile Control by Biased Electrodes in Large Diameter RF Produced Plasma SHUNJIRO SHINOHARA, NORIKAZU MATSUOKA, TOSHIRO YOSHINAKA, *Interdisciplinary Graduate School of Engineering Sciences, Kyushu University, Japan* Control of the plasma profile has been carried out, using the voltage biasing method in the large diameter (45 cm) RF (radio frequency) produced plasma in the presence of the uniform magnetic field (less than 1200 G). Under the low filling pressure condition of 0.16 mTorr, changing the biasing voltages to the three individual end plates with concentric circular ring shapes, the radial electron density (about 10^{10} cm^{-3}) profile could be changed from the hollow to the peaked one. On the contrary, the nearly flat electron temperature (several eV) profile did not change appreciably. The azimuthal rotation velocity measured by the Mach probe, i.e. directional probe, showed the different radial profiles (but nearly uniform along the axis) depending on the biasing voltage. This velocity became slower with the low magnetic field (less than 200 G) or in the higher pressure regime up to 20 mTorr with the higher electron density. The experimental results by other biasing methods will also be presented.

EMP8 5 RF Plasma Production by Various Antennae with Magnetic Field SHUNJIRO SHINOHARA, TSUTOMU SOEJIMA, *Interdisciplinary Graduate School of Engineering Sciences, Kyushu University, Japan* Plasma production studies excited by the RF (radio frequency) wave (7 MHz) have been tried, using the various configurations of the antennae; six types of the side antennae which were outside the quartz window and two types of the loop antennae inside the large cylindrical chamber, 45 cm in diameter. The ion saturation current I_{is} in addition to the plasma light were measured, changing the filling pressure (0.8 - 16 mTorr), the RF power (100 - 1500 W) and the magnetic field (0 - 1000 G). With the increase in the power and the magnetic field, I_{is} increased in most cases, while some of the antennae showed the maximum I_{is} values under the low magnetic field. Among the side antennae the spiral antenna demonstrated the highest I_{is} value (the electron density was about 4 $\times$ 10^{11} cm^{-3}) in the wide operational window. For the case of the loop antennae the electric field parallel to the magnetic field did not show a main contribution to the plasma production. These results suggest the importance of the loop-like RF induced electric field.With an application of the magnetic field to the loop antennae, the uniformity of the plasma distribution along the radial direction as well as the axial one was improved.

EMP8 6 RF Wave Characteristics in Large Diameter Plasma with Various Magnetic Field Configurations SEIJI TAKECHI, SHUNJIRO SHINOHARA, *Interdisciplinary Graduate School of Engineering Sciences, Kyushu University, Japan* We have been investigating the effect of the magnetic field on the RF (radio frequency) wave phenomenon and the antenna-plasma coupling with an aim to control the plasma parameters in the large diameter (45 cm) plasma produced by a spiral antenna. When the uniform magnetic field was applied, the peaked electron density profile (with the higher density) and the larger antenna-plasma coupling coefficient than those without the field were obtained. The helicon wave with an azimuthal mode number of $m = 0$ was confirmed by the radial and axial profiles of the excited magnetic fields and the dispersion relation. Control of plasma parameters such as the electron density and the uniformity was tried by changing the configurations of the antenna field and the external magnetic field, i.e., uniform, divergent and cusp fields. The effective diameter D_{eff} (ion saturation current was uniform within $\pm$ 5 %) in the cusp field improved drastically, e.g., D_{eff} was up to 27 cm where the electron density was $\sim$ 10^{12} cm^{-3}. The excited wave characteristics depended on the gradient at the line cusp position and the magnitude of the magnetic field, and in the neighborhood of this position showed the different behavior from the observed helicon wave for the case of the uniform field.

EMP8 7 Time-dependent global modeling of helicon plasmas SUWON CHO, *Kyonggi University, Korea** The global balance model is employed to study the time evolution of the electron density and temperature in pulsed helicon plasmas. The power absorption is obtained from the solutions of the Maxwell equations to use in solving the particle and power balance equations. Calculation is performed in a self-consistent manner as the power absorption and plasma parameters are dependent on each other. The numerical results of the uniform plasma model with an assumption of ambipolar diffusion reasonably explain neutral gas depletion and the occurrence of two distinct modes of pulsed helicon discharge which have been experimentally observed. Finally, some preliminary results of the non-uniform density model are presented.

*This work has been supported by Korea Basic Science Institute.

EMP8 8 A 3-Dimensional Model of a Helicon Source* ERIC R. KEITER, MARK J. KUSHNER, *University of Illinois, Urbana, IL 61801, USA* As the semiconductor industry moves to larger wafers (> 300mm) efficient plasma sources which are capable of maintaining process uniformity at large scale lengths will be needed. Helicon sources are being investigated for this purpose due to their high ionization efficiency at low pressures. In this paper, we present results from a numerical investigation of a helicon source using the 3-dimensional Hybrid Plasma Equipment model.[1] HPEM-3D has been improved to include a cold plasma tensor conductivity in the electromagnetics module. A static magnetic field is generated by a solenoid which surrounds the cylin-

EMP8 3 A rectangular helicon-wave plasma source with parmanent magnets and a simple rf antenna K. SASAKI, T. SHOJI, D. HAYASHI, K. KADOTA, *Department of Electronics, Nagoya University, Nagoya 464-8603, Japan* S. DEN, *Irie Koken Co, Ltd, Japan* Y. SAKAMOTO, *Nichimen Electric Technology Corp, Japan* The conventional helicon-wave plasma sources have a difficulty for the production of large-area plasmas. This is mainly because the conventional helicon plasmas are produced in circular glass tubes with small diameters. In the present work, we show a novel rectangular helicon-wave plasma source. The magnetic field, which is necessary for sustaining the helicon wave, is produced by a pair of parmanent magnets. A straight antenna covered with a glass tube is inserted into the rectangular discharge section made of stainless steel. Because of the simple structure, the present plasma source is suitable for the production of large-area plasmas. A proof-of-principle experiment was carried out in a prototype machine having a relatively small cross section of 100 mm $\times$ 20 mm. A huge jump was observed in the rf power dependence of the electron density. A typical electron density was 5 $\times$ 10^{12} cm^{-3} at a distance of 7 cm from the straight antenna for an rf power of 4 kW (13.56 MHz) and an Ar gas pressure of 10 mTorr. The decrease in the electron density along the axial direction from the antenna was rather small in the high-density operation, which suggests that the plasma was sustained by a helicon wave.

EMP8 4 Profile Control by Biased Electrodes in Large Diameter RF Produced Plasma SHUNJIRO SHINOHARA, NORIKAZU MATSUOKA, TOSHIRO YOSHINAKA, *Interdisciplinary Graduate School of Engineering Sciences, Kyushu University, Japan* Control of the plasma profile has been carried out, using the voltage biasing method in the large diameter (45 cm) RF (radio frequency) produced plasma in the presence of the uniform magnetic field (less than 1200 G). Under the low filling pressure condition of 0.16 mTorr, changing the biasing voltages to the three individual end plates with concentric circular ring shapes, the radial electron density (about 10^{10} cm^{-3}) profile could be changed from the hollow to the peaked one. On the contrary, the nearly flat electron temperature (several eV) profile did not change appreciably. The azimuthal rotation velocity measured by the Mach probe, i.e. directional probe, showed the different radial profiles (but nearly uniform along the axis) depending on the biasing voltage. This velocity became slower with the low magnetic field (less than 200 G) or in the higher pressure regime up to 20 mTorr with the higher electron density. The experimental results by other biasing methods will also be presented.

EMP8 5 RF Plasma Production by Various Antennae with Magnetic Field SHUNJIRO SHINOHARA, TSUTOMU SOEJIMA, *Interdisciplinary Graduate School of Engineering Sciences, Kyushu University, Japan* Plasma production studies excited by the RF (radio frequency) wave (7 MHz) have been tried, using the various configurations of the antennae; six types of the side antennae which were outside the quartz window and two types of the loop antennae inside the large cylindrical chamber, 45 cm in diameter. The ion saturation current I_{is} in addition to the plasma light were measured, changing the filling pressure (0.8 - 16 mTorr), the RF power (100 - 1500 W) and the magnetic field (0 - 1000 G). With the increase in the power and the magnetic field, I_{is} increased in most cases, while some of the antennae showed the maximum I_{is} values under the low magnetic field. Among the side antennae the spiral antenna demonstrated the highest I_{is} value (the electron density was about 4 $\times$ 10^{11} cm^{-3}) in the wide operational window. For the case of the loop antennae the electric field parallel to the magnetic field did not show a main contribution to the plasma production. These results suggest the importance of the loop-like RF induced electric field.With an application of the magnetic field to the loop antennae, the uniformity of the plasma distribution along the radial direction as well as the axial one was improved.

EMP8 6 RF Wave Characteristics in Large Diameter Plasma with Various Magnetic Field Configurations SEIJI TAKECHI, SHUNJIRO SHINOHARA, *Interdisciplinary Graduate School of Engineering Sciences, Kyushu University, Japan* We have been investigating the effect of the magnetic field on the RF (radio frequency) wave phenomenon and the antenna-plasma coupling with an aim to control the plasma parameters in the large diameter (45 cm) plasma produced by a spiral antenna. When the uniform magnetic field was applied, the peaked electron density profile (with the higher density) and the larger antenna-plasma coupling coefficient than those without the field were obtained. The helicon wave with an azimuthal mode number of $m = 0$ was confirmed by the radial and axial profiles of the excited magnetic fields and the dispersion relation. Control of plasma parameters such as the electron density and the uniformity was tried by changing the configurations of the antenna field and the external magnetic field, i.e., uniform, divergent and cusp fields. The effective diameter D_{eff} (ion saturation current was uniform within $\pm$ 5 %) in the cusp field improved drastically, e.g., D_{eff} was up to 27 cm where the electron density was $\sim$ 10^{12} cm^{-3}. The excited wave characteristics depended on the gradient at the line cusp position and the magnitude of the magnetic field, and in the neighborhood of this position showed the different behavior from the observed helicon wave for the case of the uniform field.

EMP8 7 Time-dependent global modeling of helicon plasmas SUWON CHO, *Kyonggi University, Korea** The global balance model is employed to study the time evolution of the electron density and temperature in pulsed helicon plasmas. The power absorption is obtained from the solutions of the Maxwell equations to use in solving the particle and power balance equations. Calculation is performed in a self-consistent manner as the power absorption and plasma parameters are dependent on each other. The numerical results of the uniform plasma model with an assumption of ambipolar diffusion reasonably explain neutral gas depletion and the occurrence of two distinct modes of pulsed helicon discharge which have been experimentally observed. Finally, some preliminary results of the non-uniform density model are presented.

*This work has been supported by Korea Basic Science Institute.

EMP8 8 A 3-Dimensional Model of a Helicon Source* ERIC R. KEITER, MARK J. KUSHNER, *University of Illinois, Urbana, IL 61801, USA* As the semiconductor industry moves to larger wafers (> 300mm) efficient plasma sources which are capable of maintaining process uniformity at large scale lengths will be needed. Helicon sources are being investigated for this purpose due to their high ionization efficiency at low pressures. In this paper, we present results from a numerical investigation of a helicon source using the 3-dimensional Hybrid Plasma Equipment model.[1] HPEM-3D has been improved to include a cold plasma tensor conductivity in the electromagnetics module. A static magnetic field is generated by a solenoid which surrounds the cylin-

drical reactor geometry and is simulated by solving for the vector potential. Transport of charged and neutral species is addressed with a fluid simulation. Results from the model show how varying the static magnetic field magnitude, reactor geometry, and coil configuration modifies the power deposition profile, and the downstream ion and neutral flux uniformity. We find that for larger magnetic fields, the power deposition penetrates more deeply into the bulk plasma.

*Work supported by Applied Materials, SRC, and the University of Wisconsin ERC

[1]M. J. Kushner, J. Appl. Phys. v.82, 5312 (1997).

SESSION FT1: ELECTRON / ION TRANSPORT

Tuesday morning, 20 October 1998; Plumeria/Jade Room, Aston Wailea at 7:30; H. Date, Hokkaido University, presiding

Invited Paper

7:30

FT1 1 Electronic Quenching Rate Constants for Kr($5s[3/2]_1$ and $5s'$ $[1/2]_0$) and Xe($6s[3/2]_1$, $6s'$ $[1/2]_1$ and Selected 6p, 6p′ and 7p) States by Various Reagents at 300K.* D.W. SETSER, *Department of Chemistry, Kansas State University, Manhattan, KS 66506*

Various laser-based techniques, including pulsed one-photon excitation from the Xe($6s[3/2]_2$) and Kr($5s[3/2]_2$) metastable states, optical pumping[1] from the metastable state, pulsed two-photon excitation from the ground state and pulsed two-photon amplified stimulated emission (ASE), have been used to selectively prepare a broad distribution of electronically excited states of Xe and Kr. Subsequent monitoring of the fluorescence from these states in the presence of added reagents permits two-body quenching rate constants to be measured. In many cases the products also have been identified, and state-to-state rate constants have been assigned. Examples of Kr* and Xe* excited states with different reagents will be selected to display various collisional properties of the Xe* and Kr* states, such as the role of the $Xe^+(^2P_{3/2})$ and $Xe^+(^2P_{1/2})$ ion-cores in intramultiplet relaxation processes and in reactive quenching with halogen containing molecules. The systematic increase in magnitude of quenching constants for a common reagent with increasing electronic energy of the Xe(6s, 6s′, 6p, 6p′, 7p) states will be presented. Two pairs of Xe(6p′,7p) states have very large ($\sim$ 200 Å^2) cross sections for intramultiplet transfer by collision with He and Ar; these large cross sections can be explained by a Demkov coupling mechanism. The majority of the presentation will be a description of the time-resolved two-photon ASE experiments, which provide a pulsed laboratory source of the Xe($6s[3/2]_1$), Xe($6s'$ $[1/2]_1$) and Kr($5s[3/2]_1$) resonance states. By monitoring their resonance fluorescence in the vacuum ultraviolet, the decay rates of these Kr* and Xe* resonance states can be observed in the presence of added reagent gas and the two-body quenching rate constants can be measured with excellent reliability. The two-body rate constants for the resonance states obtained from these experiments will be compared to those for the Xe and Kr metastable states, which have been available for about 20 years.

*This work was supported by the U.S. National Science Foundation Grant No. CHE-9505032.

[1]The optical pumping experiments were done in collaboration with Dr. N. Sadeghi, Universite Joseph Fourier-Grenoble I.

Contributed Papers

8:00

FT1 2 Effect of Excited Particles and Laser Absorption on Plasma Parameters in Xe/Ne Mixtures SATOSHI UCHIDA, TSUNEO WATANABE, *Tokyo Metropolitan University* YOSUKE SAKAI, *Hokkaido University* It is well-understood that reactions of excited particles play an important role in characterization of discharge plasmas in experiments of laser spectroscopy. Especially in Xe/Ne plasmas under the effect of Penning ionization, plasma parameters strongly depend on excited particle densities. However, because of complicated interactions between excited particles and laser absorption, it is difficult to understand the influence of the excited particles on the parameters in detail through experimental approaches by laser spectroscopy. In this work, as an analysis of the interactions, plasma parameters in Xe/Ne mixtures were calculated using the Boltzmann equation considering reactions of excited particles and laser absorption. The calculation is carried out under the following conditions; E/N = 1 $\sim$ 700 Td, p_0 = 1 $\sim$ 760 Torr, K(= N_{Xe}/N_{Ne+Xe}) = 0 $\sim$ 1, n_e = 1 $\sim$ 10^{12} cm^{-3}, and N_{ph} = 0 $\sim$ 10^{14} cm^{-3}. With the increase in n_e, the average electron energy ($\bar{\epsilon}$) tends to decrease gradually. Influence of p_0 on $\bar{\epsilon}$ for K around 10^{-2} becomes remarkable due to the increase of the Penning ionization rate. The laser absorption effect for each excited level is also changed by varying pressure. In contrast with low pressure cases ($\simeq$ 1 Torr), the absorption rates of the atoms in the metastable and resonance levels are comparable to each other at high pressures ($\geqslant$ 100 Torr).

8:15

FT1 3 Behavior of Electron Swarms in Spherically Symmetric Electric Fields H. DATE, *Hokkaido University* P.L.G. VENTZEK, *Motorola Inc.* M. SHIMOZUMA, *Hokkaido University* H. TAGASHIRA, *Muroran Institute of Technology* A spherically symmetric electric field model is used to study the behavior of electron swarms in non-uniform field conditions generated around fine wires, tips of whiskers or micro-protrusions from material surfaces. Under these conditions, the developing electron swarm may initiate a corona discharge and, in some cases, electrical breakdown. In this study, we have calculated the EEDF and swarm parameters (e.g. drift velocity and ionization frequency) as a function of time and location from the center of a spherical electrode (positively biased) using a Monte Carlo simulation. The results show that the EEDF converges to a steady-state in the potential around the spherical electrode although the total number of electrons varies and the spatial energy distribution is strongly influenced by the background gas inelastic collision thresholds. In addition, we propose similarity laws for swarm parameters that take into consideration the radius of a spherical electrode and gas pressure. Non-locality in this model will also be discussed as will the mechanism of the transition to corona discharges taking into account distortion by space charge near the electrode.

FT1 4 Abstract Withdrawn.

8:30

FT1 5 The relaxation process of the velocity distribution function and transport coefficients of electron swarms in SF6* K. KONDO, *Anan College of Technology* H. DATE, *C. M. T. Hokkaido University* H. TAGASHIRA, *Muroran I.T.* The relaxation

process of the one dimensional electron swarms in SF6 from an initial Maxwellian velocity distribution to the hydrodynamic regime was calculated by solving the initial value problem of the Boltzmann equation. The new Boltzmann-code based on the matrix eigenvalue procedure and a dispersion relation was adopted for the calculation. The time evolution of the velocity distribution function as well as the time dependent transport parameters and relaxation time have been obtained under several conditions of initial mean energy and the values of the electric field upon the gas number density E/N. It was shown that, in the low E/N regime where the effective ionization coefficient is nearly equal zero, when electrons are released with lower initial mean energy, the number of electrons decrease in initial stage and after a time delay turn to increase toward the hydrodynamic creation. In this E/N regime, relaxation time may become quite large as compared with one in the regime of high E/N. This can be understood as the result of the transient enhance of the attachment effect in the initial relaxation process.

*Numerical matrix analysis of the Boltzmann equation

8:45

FT1 6 Electron Thermalization and Attachment in SF_6/Ar Mixtures BERNIE D. SHIZGAL, *University of British Columbia* KEN-ICHI KOWARI, *Inst. of Phys. & Chem. Research (RIKEN)** The relaxation of a nonequilibrium distribution of electrons in a mixture of SF_6 and Ar is studied. Electron-SF_6 and (e^-, Ar) elastic collisions, (e^-, SF_6) vibrationally inelastic collisions and attachment reactions are included in the analysis. The time dependent electron distribution function is determined from the Boltzmann equation and the electron energy relaxation times are calculated. The coupling of the thermalization process and the attachment reaction are studied as a function of the SF_6 mole fraction. The results of the calculations are interpreted analogous to previous experimental work and the methodology of the experimental data reduction is analyzed.

*This research was supported in part by a fellowship to BDS from the Japanese Society for the Promotion of Science for a visit to Hokkaido University where this work was done.

SESSION FT2: LASER DIAGNOSTICS

Tuesday morning, 20 October 1998; Maile Room, Aston Wailea at 7:30
Toshiki Nakano, National Defense Academy, Japan, presiding

Invited Paper

7:30

FT2 1 Laser-Aided Plasma Diagnostics Research at Kyushu University. KIICHIRO UCHINO, *Kyushu University, Japan**

In discharge plasmas, the electrical input power first forms an electric field, which accelerates the electrons. The electrons then collide with gas particles to form various reaction products, such as radicals, excited molecules/atoms and ions. These reaction products execute useful actions for industrial applications. In order to understand the discharge processes systematically, we have to be able to measure (1) the electric field, (2) the densities and velocity distribution functions of the charged particles and (3) these same properties for the neutral particles. At our laboratory, we have been developing laser diagnostics which can be applied for measurements of these three items. For item (1), laser fluorescence techniques have been used to yield the electric field intensity using the Stark effect on spectral profiles. For (2), the capability of Thomson scattering has been greatly expanded so that measurements of very low electron density ($< 10^{16}\,m^{-3}$) plasmas are possible by accumulation of scattered photons. For item (3), reaction products in molecular form have been detected to a very low detection limit ($< 10^{19}\,m^{-3}$) using Raman scattering. In addition to these three items, atomic hydrogen detection has been carried out using two-photon excitation from the ground level.

*This research was carried out in collaboration with Drs. K. Muraoka, M. Maeda, T. Okada, T. Kajiwara and M. D. Bowden

Contributed Papers

8:00

FT2 2 Novel laser spectroscopic method for sensitive electric field measurements in atomic hydrogen U. CZARNETZKI, D. LUGGENHÖLSCHER, H.F. DÖBELE, *Institut für Laser- und Plasmaphysik, Universität GH Essen, D-45117, Germany** In recent years there has been a growing interest in the diagnostics of the sheath region of DC- and RF-discharges by electric field measurements based on laser spectroscopy. A novel technique is presented allowing the measurement of both, very low and very high electric fields with good spatial and temporal resolution: The Stark splitting of Rydberg states in atomic hydrogen is probed by taking advantage of an optical double resonance. Subsequent to Doppler-free two-photon excitation from the ground state to $n = 3$ ($\lambda = 205$ nm) fluorescence at the Balmer-α line ($\lambda = 656$ nm) is observed. A second laser in the near IR (830 nm to 1100 nm) is tuned over the Stark-split resonance between $n = 3$ and a Rydberg state. If the IR-laser is in resonance, population is transferred from $n = 3$ to the Rydberg state, and the fluorescence intensity at Balmer-α is consequently decreased. The Stark spectrum manifests itself, therefore, in a series of dips in the fluorescence spectrum at 656 nm. The electric field strength is deduced by comparing measured and calculated spectra. Rydberg states up to $n = 55$ can be excited, and the minimum detectable electric field is $E = 5$ V/cm. The temporal resolution is determined by the pulse width of the IR-laser of about 4 ns.

*Supported by the ''Bundesminister für Bildung und Forschung''

8:15

FT2 3 ICP-Cavity Ringdown Spectroscopy G.P. MILLER, *Mississippi State University* C.B. WINSTEAD, *Mississippi State University* Cavity ringdown spectrometry (CRS) differs from stan-

dard absorption spectroscopic methods in that it is a measurement of the rate of light absorption within a closed optical cavity. CRS's very high sensitivity, due to very long effective pathlengths and the relaxed constraints on the measurement of the time decay, would appear to make this technique an ideal analytical and diagnostic tool. This presentation will discuss the results obtained when an atmospheric-pressure 1.6 kW 27.12 MHz argon ICP is placed within such a cavity. A Nd:YAG laser pumped tunable dye laser with pulse duration of approximately 10 ns and repetition rate of 10 Hz was used as the light source. The effect of the plasma on optical cavity, especially with regard to fluctuations, will be discussed. The stability of both near confocal (0.5 m) and near planar (5 m) cavity geometries will be shown to yield a standard deviation in baseline ringdown times of better than 1does not significantly impact the measured time constant stability, it does reduce the magnitude of the time constant. This loss mechanism is discussed with respect to scattering and photo-ionization occurring within the plasma. Finally, the introduction of trace contaminates into the plasma is shown to cause the ringdown time to clearly decrease as the trace concentration increases. This result clearly demonstrates the analytical potential of this technique.

8:30

FT2 4 Advanced Cavity Ringdown Diagnostic Methods ANTHONY O'KEEFE, *Los Gatos Research* It is demonstrated that direct optical absorption measurements with sensitivities better than one part in a million can be made using pulsed light sources and employing theCavity Ringdown Spectroscopy optical configuration, but without the need for fast temporal analysis and fitting of the resulting ringdown decay curve. A simple model is presented which demonstrates that the resulting direct absorption signal provides a quantitative total attenuation measurement if the cavity mirror reflectivities are known. This approach to making absorption measurements provides a sensitivity which is comparable to that realized us ing the time domain Cavity Ringdown approach, although with a significant reduction in complexity. This new technique is demonstrated using the weak forbidden oxygen absorption band near 690 nm.

Invited Paper

8:45

FT2 5 Diagnostics of Electronegative Plasmas Using Microwave Resonance and Laser Photodetachment Techniques.

AKIHIRO KONO, *CCRAST, Nagoya University, Nagoya 464-8603, Japan*

Results of basic diagnostic studies of electronegative plasmas are presented with emphasis on a C_4F_8 plasma. Capacitively-coupled RF plasma was produced inside a cylindrical microwave cavity to measure the electron density from the shift of the microwave resonance frequency; negative ions were detected as the electron density-change induced by laser photodetachment. Dependence of the electron and negative-ion densities on the pressure, RF power and other parameters, and their loss kinetics in the afterglow were studied. C_4F_8 was found to be a strongly electron attaching gas, but was found to be easily dissociated in the plasma to be less electronegative. The above-mentioned measurement technique limits the study to low-density capacitively-coupled plasmas because the plasma must to be produced inside the cavity and the electron plasma frequency must be lower than the low cavity resonance frequency ($\sim$ 3.6 GHz). To extend measurements to high-density plasmas as well as to obtain flexibility in the plasma excitation method, a Fabry-Perot type open microwave resonator was designed, which can be operated at higher microwave frequencies, yet maintaining high sensitivity for detecting small electron-density change caused by photodetachment. A preliminary measurement showed that despite the use of a high microwave frequency ($\sim$ 35 GHz), it was possible to detect an electron density as low as 10^8 cm^{-3}. Diagnostics results for C_4F_8 plasma using this technique will also be presented.

Contributed Papers

9:15

FT2 6 Absolute Line Integrated Densities of CF, CF_2, and CF_3 in a GEC Reference Cell* ION C. ABRAHAM, R. CLAUDE WOODS, *UW-Madison Plasma ERC* GREG A. HEBNER, *Sandia National Labs* Tunable diode laser absorption spectroscopy, in the region around 1250 cm^{-1}, was used to measure line integrated densities of CF, CF_2, and CF_3 in a GEC reference cell, modified for inductively coupled plasma operation. The addition of a quartz ring around the source region stabilized and confined the plasma, making the plasma chemistry more like that found in industrial etch tools. Two common etching gas chemistries, C_2F_6 and CHF_3, and two wafer surfaces, bare silicon and blanket photoresist, were investigated across a range of power and pressure. Substantial amounts of undissociated C_2F_6 were also found in the C_2F_6 plasma. The determination of the absolute density of CF led to a reexamination of the literature data on the value of the transition dipole moment for this radical. Our conclusion from this investigation is that recent large scale ab initio calculations currently provide the only reliable value of this parameter, which is required in any calculation of absolute CF densities. The Plasma ERC is supported by NSF Grant No. EEC-8721545. GAH was supported by the United States Department of Energy under contract DE- AC04-94AL85000.

*Funded by SEMATECH Contract No. 38010430

9:30

FT2 7 Cavity Ringdown and Ringdown Spectral Photography for Radical Detection JAMES SCHERER, *Los Gatos Research* The application of Cavity Ringdown Spectroscopy for the study of plasmas is presented, including emphasis on strengths and practical limitations of the approach. Examples in various environments are presented, including laser vaporization plasmas, flames, and microwave discharges. Additionally, a new technique, Ringdown Spectral Photography (RSP), is presented which enables high resolution studies as demonstrated above with cavity ringdown spectroscopy to be performed in a real-time fashion utilizing broadband light sources and multielement arrays. This new method is well suited for studies of transient species in plasma environments, as species concentrations can be inferred on a microsecond timescale.

SESSION FT3: INDUCTIVELY COUPLED PLASMAS I
Tuesday morning, 20 October 1998
South Pacific Ballroom, Aston Wailea at 7:30
A. Bogaerts, University of Antwerp, presiding

Contributed Papers

7:30
FT3 1 Numerical Analysis of Electron Energy Distributions in Inductively Coupled Plasmas S. YONEMURA, K. NANBU, *Inst. Fluid Science, Tohoku Univ.* T. MORIMOTO, *Central Research Laboratory, Tokyo Electron Ltd.* K. SAKAI, *Tohoku Univ.* One of the most important quantities in processing plasmas is the electron energy distribution function (EEDF) because all rate constants are determined from the EEDF. There were many works on the analysis of the EEDF for conventional parallel-plate radio-frequency plasma etcher. However, the realization of electronic devices with quarter micrometer patterns of high aspect ratio requires the change in plasma sources. A recent trend in plasma-assisted materials processing is towards ''low gas density and high plasma density'' as seen in inductively coupled plasma reactors. A typical plasma density is $10^{11} - 10^{12}/cm^3$. This means that the Coulomb collisions are important in such high density plasmas and that only the particle approach makes sense in such low gas density less than 10 mTorr. The objective of the present work is to clarify the effect of the Coulomb collisions on the EEDF by use of the particle-in-cell method. The Coulomb collisions are treated based on the theory of Nanbu[1]. The preliminary results without Coulomb collisions shows that the EEDF has a peak at an energy lower than the peak position of the Maxwellian distribution, whereas it is higher than the Maxwellian distribution in a high energy tail. The effect of Coulomb collisions in the EEDF is presented at the Conference.

[1]K. Nanbu, Phys. Rev. E. **55**, 4642 (1997).

7:45
FT3 2 A coupled plasma dynamics and gas flow model for semiconductor processing DEEPAK BOSE,* *Thermosciences Institute, NASA Ames Research Center* T.R. GOVINDAN, M. MEYYAPPAN, *NASA Ames Research Center* A continuum modeling approach by self-consistently coupling plasma dynamics and gas flow will be presented for the analysis of high density plasma reactors. Experimental data [Khater et. al. JVST-B, 16(2), 1998] shows that gas flow distribution affects the etch rate uniformity even at low pressures (6-20 mTorr) and flow rates (20-70 sccm). This study will investigate the effects of gas flow and gas energy on bulk plasma densities and temperatures using a continuum model. The model solves multidimensional equations of mass balance for neutrals and ions, gas momentum, separate energy equations for electrons and neutrals and Maxwell's equations for power coupling. A test case of N_2 plasma in a 300mm TCP etch reactor, for which hybrid model and Langmuir probe data are available [Collison et. al. JVST-A 16(1),1998], is chosen for this analysis. Our preliminary results show that modeling gas flow and energy improves the predictions of electron density and its spatial variation in the reactor when compared with the experimental data. The aim of this study is to identify the operating conditions for the TCP reactor when a self-consistent modeling of gas flow is important.

*Work supported by NASA contract NAS2-14031 to Eloret.

8:00
FT3 3 A transport model for non-local heating of electrons in ICP reactors C.H. CHANG, DEEPAK BOSE,* *Thermosciences Institute, NASA Ames Research Center* A new model has been developed for non-local heating of electrons in ICP reactors, based on a hydrodynamic approach. The model has been derived using the electron momentum conservation in azimuthal direction with electromagnetic and frictional forces respectively as driving force and damper of harmonic oscillatory motion of electrons. The resulting transport equations include the convection of azimuthal electron momentum in radial and axial directions, thereby accounting for the non-local effects. The azimuthal velocity of electrons and the resulting electrical current are coupled to the Maxwell's relations, thus forming a self-consistent model for non-local heating. This model is being implemented along with a set of Navier-Stokes equations for plasma dynamics and gas flow to simulate low-pressure (few mTorr's) ICP discharges. Characteristics of nitrogen plasma in a TCP 300mm etch reactor is being studied. The results will be compared against the available Langmuir probe measurements [Collison et al. JVST-A 16(1),1998].

*Work supported by NASA contract NAS2-14031 to Eloret.

8:15
FT3 4 Modeling MultiCoil ICPs V.I. KOLOBOV, N. VAIDYA, A. KRISHNAN, *CFDRC* Plasma processing of 300 mm wafers and flat panels places stringent demands on plasma uniformity across large surfaces. A natural solution towards an uniform plasma in a minimum discharge volume is to maintain the plasma by an array of individual sources. Although the design of the individual sources can differ considerably, there is a common feature for all such devices which have been recently suggested by several groups: their essentially 3D geometry. Engineering design of these devices is a challenging task and computational modeling could be a very useful tool. CFD Research Corp. has developed a comprehensive software for virtual prototyping of ICP sources designed for complex 3D geometries with unstructured solution-adaptive mesh. In this paper we shall present the results of our simulation of the multipole high density source [1] which is an example of MultiCoil ICP. We shall describe the procedure of solving the electromagnetic part of the problem using magnetic vector potential and analyse design issues such as the size of dielectric windows. We shall present results of parametric studies of the source for different geometries, gas pressures and plasma densities for simple argon chemistry. [1] J.Ogle. Proc. VI Int. Workshop on Advanced Plasma Tools and Process Engineering, pp. 85-90, May 1998, Millbrae, USA.

Invited Paper

8:30
FT3 5 Power Deposition in Advanced Plasma Sources.*
J.B.O. CAUGHMAN, *RF Group, Oak Ridge National Laboratory*

The amount of power that is coupled into the plasma is a critical processing parameter in microelectronics manufacturing. For high density inductively coupled plasmas, the power coupling from both the source and the wafer biasing system can

affect the ion energies at the wafer and the plasma uniformity, chemistry, and stability. The power coupling has been studied for a large area plasma source that consists of two coupling coils and for capacitively coupled wafer biasing systems. For the large area system, power coupling and efficiency is determined by measuring the matching network losses, the load impedance, and the level of rf current flowing through the coils. Power coupling efficiency ranges from 50% to 90%, depending on process conditions. Plasma uniformity can be achieved by controlling the current distribution on the coils and by balancing the power deposition between the two coils. For wafer biasing systems, the power coupling efficiency is determined by using a surrogate plasma load simulator to measure the output power as a function of the values of the tuning elements in the matching network. Efficiencies can vary from 30% to 90%, depending on processing conditions. Measurement techniques and processing conditions will be reviewed.

*Research sponsored by the Laboratory Directed R and D Program of ORNL, managed by Lockheed Martin Energy Research Corp. for the U.S. Department of Energy under contract no. DE-AC05-96OR22464

Contributed Papers

9:00

FT3 6 Plasma Properties of a Negative Ion Plasma RIE System JOHN H KELLER, *IBM, Microelectronics Division, Hopewell Jct., NY 12533, USA* In high density Reactive Ion Etching, RIE, systems it has been found that there is an aspect ratio charging effect which causes damage, RIE lag and loss of ion current to the bottom of high aspect structures. It has been shown by a number of authors, that one way of reducing these effects is to reduce the electron temperature of the plasma which is above the wafer. We have characterized the plasma properties of a medium to high density plasma system which uses a magnetic filter in an Inductively Coupled Plasma, ICP, to produce a low temperature, negative ion plasma above the wafer. At 4 mTorr, the electron temperature of this negative ion plasma is 1/3 of that for the same system without the filter. We will present uniformity data and electron temperature data versus pressure and magnetic potential.

9:15

FT3 7 Pre-sheaths and Instabilities in Electronegative Plasmas PETER VITELLO, *LLNL* In electronegative plasmas Coulomb scattering between positive and negative ions can lead to the formation of a pre-sheath boundary layer containing the bulk of the negative ions. A negative ion boundary layer forms when momentum transfer from positive to negative ions dominates the negative ion acceleration from the electric field. As the momentum transfer to negative ions from positive ions tends to be in the opposite direction to their acceleration by the electric field, negative ion flow may become unstable in regions where the two effects nearly balance. This condition is met in Inductively Coupled Plasma reactors that operate at low pressure and high plasma density. Simulations of the GEC reactor for Chlorine show the pre-sheath boundary layer structure as a function of applied power and neutral pressure.

9:30

FT3 8 A 2D Self-Consistent Model for Chemically Reacting Plasmas TIMOTHY BARTEL, *Sandia National Labs* JUSTINE JOHANNES, *Sandia National Labs* MICHAEL GALLIS, *Sandia National Labs* Low pressure, inductively coupled, high-density plasma reactors are expected to play a key role in next generation 0.25 μm semiconductor manufacturing. This work focuses on the development and validation of a 2D, kinetic based model to simulate these systems. Since the sheaths are very small, we model the bulk of the reactor using a local charge neutrality assumption for the electron density. We use an electron energy equation to determine the electron temperature using ICP power, electron conduction, and inelastic electron impact reactions. Neutral-neutral and neutral-ion collisions and chemistry are directly simulated; neutral-electron and ion-electron chemistry are also simulated. The electro-static fields are determined by a Langmuir-Tonks relationship. The ICP power is determined by an external code from ORNL, ORMAX, and used as a boundary condition; the remainder of the interactions are treated in a self-consistent manner. We will present validation comparisons for two electro-negative gas systems: pure Cl2 and C2F6. Data will be compared for a GEC Test Cell geometry and for a industrial reactor geometry.

SESSION GT1: POST-DEADLINE SESSION
Tuesday morning, 20 October 1998
Plumeria/Jade Room, Aston Wailea at 10:00
Shahid Rauf, University of Illinois, presiding

10:00

GT1 1 Time resolved monitoring of Xenon ions in plasma jet by LIF N. SADEGHI, *Universit de Grenoble-CNRS, France* C. KADLEC-PHILIPPE, A. BOUCHOULE, *Universit d'Orlans-CNRS* L. BAKKER, *Tech. Univ. Eindhoven, Netherland* Xenon is used as an efficient propellant in plasma thrusters. The velocity distribution of Xe^+ ions in the jet can be characterized from the Doppler-Shifted-Laser-Excitation profile of the 605.11 nm ion line. Saturated absorption method was used to determine the exact rest frequency of the this line for the isotope 132, $^{132}\nu_0 = 16521.299\ cm^{-1}$. In plasma jet extracted from a Helicon source the axial and radial velocity distributions of ions have been recorded for different extraction potentials (V_e =50 to 300 V). V_e was then square wave modulated at 30 kHz and time resolved velocity profiles have been obtained with a resolution of about 100 ns.

10:15

GT1 2 Energy Transfer Studies in CO-Laser Pumped Gases and Liquids* K. ESSENHIGH, E. PLÖNJES,[†] P. PALM[2], I. V. ADAMOVICH, V. SUBRAMANIAM, J. W. RICH, *The Ohio State University* Energy transfer mechanisms of vibrationally excited diatomic molecules in cool enviornments are studied for different compositions (CO, N_2, O_2, Ar) in the gas and liquid phases. The lower excited vibrational levels of the diatomic molecules are prepared by resonance absorption of CO infrared laser radiation. Diffusion of the energy by V-V energy exchanges populates the upper levels of the diatomic[1]. This method of preparing vibrationally excited molecules, as opposed to one with an electrical discharge, provides a cleaner environment in which more precise kinetic measurments and studies of the mechanisms of energy transfer can be made. Particular studies have focused on the mechanisms and kinetic rates of energy transfer by the vibrational up-pumping[2] in the different diluents. For a mixture of two diatomic isotopomers the energy exchanges favor storage of en-

ergy in the heavier molecule. These results are compared and show remarkable similarities in the gas and liquid phases.

*Research is primarily funded by AFOSR and DDRE (Air Plasma Rampart MURI) and by AFOSR Space Propulsion and Power Program.

†Visiting Scholars at OSU, permanently at the Institute für Angewandte Physik der Universität Bonn

[1]C. E. Treanor, J. W. Rich, R. G. Rehm, J. Chem. Phys. (1968), 1798.

[2]I. V. Adamovich, J. W. Rich, C. E. Treanor, AIAA 96-1982, 27th AIAA Fluid Dynamics Conf., New Orleans, LA, June 17-20, 1996.

10:30

GT1 3 Vibration-Vibration Energy Transfer and Associative Ionization of CO in Optically Pumped Plasmas* E. PLÖNJES, *The Ohio State University, permanently at the Institut für Angewandte Physik der Universität Bonn, 53115 Bonn, Germany* I. ADAMOVICH, P. PALM, *Ohio State University, permanently at the Institut für Angewandte Physik der Universität Bonn, 53115 Bonn, Germany* J.W. RICH, *Ohio State University*† In a CO-Ar, CO-Ar-N_2, or CO-Ar-O_2 gas mixture carbon monoxide is excited into low vibrational states v=1,...,10 by absorption of CO laser radiation. Vibration-vibration (VV) exchange pumping results in the diffusion of energy into very high vibrational states up to level v=40. Also vibrational energy is transferred to the vibrational modes of N_2 and O_2. Ionization in optically pumped CO occurs by associative ionization mechanism in collisions of two excited CO molecules when their total vibrational energy exceeds the ionization energy. A master equation kinetic model which takes into account vibration-vibration, vibration-translation, vibration-electronic energy transfer processes, radiative decay, and coupling with electrons has been developed and will be compared to measurements of kinetic rates for the VV-transfer. The diffusion of energy through the vibrational states is observed by time resolved step-scan FTIR spectroscopy on the Δv=2 emission of CO with spectral resolution of 8 cm^{-1} and time resolution of 5 μs.

*Research is primarily funded by AFOSR and DDRE under the Air Plasma Rampart MURI and the AFOSR Space Propulsion and Power Program, Grant F49620-96-1-0184

†Elke Plönjes and Peter Palm are visiting scholars at OSU, permanently at the Institut für Angewandte Physik der Universität Bonn, 53115 Bonn, Germany

10:45

GT1 4 Modeling of Vibration-to-Vibration and Vibration-to-Electronic Energy Transfer Processes in Optically Pumped Plasmas IGOR V. ADAMOVICH, ELKE PLOENJES, PETER PALM, J. WILLIAM RICH, *Department of Mechanical Engineering, The Ohio State University, Columbus, OH* ANDREY CHERNUKHO, *A.V. Lykov Heat and Mass Transfer Institute, Minsk, Belarus* The paper presents the results of modeling of the optical pumping experiments in CO/N2/O2/Ar mixtures. In these experiments, the low vibrational levels of carbon monoxide (v< 12) are excited by resonant absorption of the CO laser radiation. The high vibrational levels, up to v=40, are populated by the CO-CO vibration-to-vibration (V-V) energy exchange. Time-resolved CO infrared and ultraviolet radiation from the excited electronic states is measured by a high-resolution step-scan Fourier transform spectrometer. The kinetic model incorporates coupled master equation for the CO, N2, and O2 vibrational level populations, and Boltzmann equation for the electrons. The comparison of the experimental and synthetic time-resolved spectra allowed inference of the V-V exchange rates for CO-CO up to v=40, cross-sections for the energy transfer between the highly excited CO molecules and electrons, and V-V transfer rates for CO-N2 and CO-O2.

11:00

GT1 5 Discharge Physics and Chemistry in Atmospheric Pressure RF Glow-like Plasmas JAEYOUNG PARK, *Los Alamos National Laboratory* G.S. SELWYN, *Los Alamos National Laboratory* IVARS HENINS, *Los Alamos National Laboratory* J.Y. JEONG, *UCLA* Steady-state, homogeneous discharges at atmospheric pressure have been produced using radio frequency (RF) electric fields. The discharges operate in a capacitively coupled configuration with several gas mixture, such as pure helium, helium with oxygen, and a mixture of helium, oxygen and carbon tetrafluoride. At the fundamental frequency of the RF electric field, the I-V characteristic of the discharge closely resembles a low pressure DC glow discharge. With increasing RF power, the discharge becomes unstable and a transition to an arc occurs. A 1-D, 2 moment fluid model using 'local field approximation' has been developed to study the discharge physics. Good agreement was obtained between the experimental results and code outputs. The code predicts that the pure helium discharge produces 0.2-2x10^{11} cm^{-3} electrons, with an average energy of 2 -3 eV in a volume of 16 cm^3 for input powers between 50 W and 400 W. Introduction of a small fraction of oxygen, up to 3 percent, improves the stability of the discharge and also generates a large flux of reactive species. With an input power of 300 watts and O_2 fraction of 1absolute concentration of ozone is 1-10x10^{15} cm^{-3} and the second molecular oxygen metastable state (O_2 $b^1\Sigma_g^+$) is 0.5-2x10^{12} cm^{-3}, as measured both inside and outside of the discharge region using optical emission and absorption spectroscopy. In addition, the presence of the long-lived first molecular oxygen metastable state (O_2 $a^1\Delta_g$) was also observed and its concentration is expected to be comparable to that of ozone. From these measurements, the concentration of atomic oxygen was estimated to be 0.5-5x10^{15} cm^{-3} inside the discharge volume. The abundant concentration of these reactive species helps to explain the observed etch rate of Kapton^{TM} polyimide film of 0.5 μm/min inside the discharge region over areas of about 100 cm^2 and of 5 μm/min for material exposed to the plasma effluent over areas of 1 cm^2.

11:15

GT2 6 A Model of the D. C. Positive Column based on the Elliptic Representation of the Boltzmann Equation EDWARD A. RICHLEY, *Xerox* The low pressure D.C. positive column is a fine example of a discharge in which the electron velocity distribution function can have highly symmetric angular dependence in some regions of phase space, and, simultaneously, highly distorted dependence in others. The application of the elliptic angular moment model to this problem will be presented in which the spatially dependent EVDF is found simultaneously with the electric field and solutions to the transport equations of ions. This solution is obtained by treating the equations as if they represented a time-dependent reactive flow both in phase space, for electrons, and in configuration space, for all other quantities. By utilizing the elliptic representation, both the highly symmetric EVDF found at low energy near the axis, and the asymmetric EVDF near the walls and at high energy, will be accurately represented.

11:30

GT2 7 Modelling of Ar/Hg Induction Lamps with PLASIMO J. VAN DIJK, G. M. JANSSEN, J. A. M. VAN DER MULLEN *Eindhoven University of Technology, The Netherlands*—In the last years various induction lamps have been announced by the major lighting companies. Examples are the Philips QL lamp, Osram's

Endura and GE's Genura. In order to improve our understanding of such light sources some modelling has been done with the plasma simulation toolkit PLASIMO, which is being developed at the Eindhoven University of Technology. PLASIMO has been designed as a general-purpose modelling tool for two-dimensional non-LTE plasmas. It consists of various submodels for the inductive coupling, the particle densities and velocities, the temperatures, the radiative transfer and others. Some results of the PLASIMO application to Philips' QL, lamp will be shown. Comparisons will be made with the little experimental data which are available.

SESSION GT2: NUCLEATION AND GROWTH OF DUST PARTICLES

Tuesday morning, 20 October 1998; Maile Room, Aston Wailea at 10:00; Helen Hwang, NASA, presiding

Invited Paper

10:00

GT2 1 Particle Formation in RF Discharges.

M. SHIRATANI, *Graduate School of Information Science and Electrical Engineering, Kyushu University, Japan*

Particles in processing plasmas are responsible for yield reduction of devices and quality degradation of films deposited by plasmas. Recently, they have also attracted much attention as new materials. Most previous studies regarding this field have reported growth and behavior of particles above about 10 nm in size. Such large particles are usually charged negatively, suspended in the plasma and hence have less chance to deposit on the film surface at least during discharging period. Information on very small particles below 10 nm in size is important to understand nucleation and initial growth processes of particles formed in the plasma and also their contribution to film-growth and -quality. Size and density of particles of 1-10 nm and below about 1 nm in size formed in silane rf discharges are obtained using a newly developed photon-counting laser-light-scattering and threshold photo-emission methods respectively. Even for a low pressure (13 Pa) and low power density (about 0.1 W/cm^2), particles begin to be observed around the plasma/sheath boundary near the rf electrode and principally grow in the same region. Size of particles below 10 nm linearly increases with time at a growth rate of 10 nm/s, much higher than a typical film deposition rate of 0.1 nm/s, and their density is above about 10^{10} cm^{-3}, which is more than 10 times as high as the positive ion density. These results indicate that highly reactive neutral radicals having a high production rate significantly contribute to nucleation and growth of particles even under the low pressure and low power density conditions. Some of such small particles may be incorporated in films during discharging period as most of them are neutral, although their reflection probability at the surface is a quite high value above 95%. We also investigate effects of pulse modulation on particle growth. The modulation is effective to reduce considerably both particle-size and -density. Suppression of particle growth by the modulation can be explained by diffusion of small polymerized species through the radical generation region where they grow during the discharging period.

Contributed Papers

10:30

GT2 2 Investigation of powder formation in capacitively coupled RF plasmas by infrared absorption spectroscopy, emission spectroscopy and mass spectrometry CH. HOLLENSTEIN, CH. DESCHENAUX, D. MAGNI, A. AFFOLTER, *Centre de Recherches en Physique des Plasmas/EPFL, CH-1015 Lausanne (Switzerland)* Despite of the existence of various powerful plasma and in-situ particles diagnostic methods, the plasma chemistry leading to powder formation in reactive RF plasmas is still not fully understood. Since individual application of these diagnostic methods gives in most cases only restricted information, infrared absorption spectroscopy, emission spectroscopy and mass spectrometry have been simultaneously applied to the plasma. New insights on important process parameters and on powder in RF plasmas in methane, acetylene, ethylene and in helium diluted oxygen/hexamethyldisiloxane (HMDSO) gas mixtures have been obtained. In particular the gas consumption, radical production, powder composition and powder formation mechanism have been investigated. The combination of ir absorption spectroscopy and mass spectrometry allows to identify precisely the chemical composition and structure of the most relevant plasma produced neutral species. The influence of the chemical structure of the monomer gas on the neutral and charged plasma species and on possible polymerization reactions leading to powder precursors will be discussed.

10:45

GT2 3 Spatial distribution and formation of particles in silane rf plasmas K. SATAKE, O. UKAI, M. NODA, Y. TAKEUCHI, *Mitsubishi Heavy Industries, Ltd.* We have developed the numerical model for particle formation and transport in silane radio-frequency (rf) plasmas. The model includes plasma kinetics which provides plasma properties in rf discharges and plasma chemistry which simulates the formation, charging and transport of particles, and is linked to commercial finite-volume code to use gas velocity and temperature fields as input for the particle transport calculations. The model has predicted the spatial distribution and formation of particles in the plasma reactor where the plasma generated by the ladder electrode. The results show that the electrostatic force and the gas drag force are important factor of the spatial distribution of particles. The calculated spatial distributions of particles show good agreement with experimental ones. We also have examined the effect of the gas flow patterns, rf frequency and magnetic fields on the spatial distribution and formation of particles and find that higher rf frequency reduces the electrostatic trapping of particles due to a decreasing the plasma potential and

magnetic field perpendicular to the discharge electric field induces spatial inhomogeneous plasma potential which influences transport and density of the particles.

11:00

GT2 4 Modeling of Contaminant Particulate Nucleation in SiH_4 Plasmas* U. BHANDARKAR, S.-M. SUH, M. T. SWIHART, S. L. GIRSHICK, U. KORTSHAGEN, *University of Minnesota, Mechanical Engineering* In this presentation we report progress on the development of a plasmas–chemistry–nucleation model to predict the nucleation of contaminant particles in silane plasmas. The model couples different modules which describe the electron kinetics, the silane plasma chemistry, and the silicon hydride clustering. Electron distribution functions are determined by solution of the electron Boltzmann equation. A simple silane plasma–chemistry model is used to predict the concentrations of particle precursors. A detailed mechanism was developed for silicon hydride clustering leading to particle nucleation, and this mechanism was coupled to an aerosol dynamics model to predict particle growth, coagulation and transport. The clustering model uses a thermodynamic data base for a large set of Si_nH_m clusters, obtained from ab initio calculations extended to larger sizes using group additivity. Differences are explored between clustering during thermal pyrolysis of silane and clustering during PECVD from silane.

*Work supported by NSF grant ECS-9731568

11:15

GT2 5 Modeling of particle coagulation in low pressure PECVD* U. BHANDARKAR, U. KORTSHAGEN, *University of Minnesota, Mechanical Engineering* Contaminant particles generated in plasmas used to manufacture semiconductor devices can potentially destroy micro-electronic circuits. Particles of micrometer-size in a plasma are usually negatively charged due to the higher mobility of electrons. Like charges on the particles should inhibit growth by coagulation. However, the coagulation rates of nanometer-sized particles observed experimentally are even higher than the thermal coagulation rates of uncharged particles. This observation implies the presence of positively charged nano-particles along with the negative ones such that the mutual attraction enhances coagulation. We propose photo-detachment of electrons due to UV radiation as a potential path for the generation of positively charged particles. We have developed a self-consistent plasma-coagulation model based on the General Dynamic Equation which is well-known from aerosol research. Plasma properties are determined self-consistently using a global plasma model. The particle charge distribution is calculated using a charging module which also accounts for UV photo-detachment. Preliminary results of this model yield coagulation rates consistent with those observed experimentally.

*Work supported by NSF grant ECS-9731568

Invited Paper

11:30

GT2 6 Effects of Crossed Magnetic Field on Silicon Particles in Plasma CVD Process.

HIROSHI FUJIYAMA, *Faculty of Engineering, Nagasaki University, Japan*

Applying a scanning magnetic field(**B**) perpendicular to low frequency discharge electric field(**E**) is effective for large area and uniform thin film deposition. However, for high rate deposition, the generation of particles during deposition becomes a serious problem. This scanning plasma CVD method has the possibility of particle-free large area film deposition. In this paper, we propose a new particle-free CVD process with same frequency and phase of **E** and **B** for the preparation of large-area uniform a-Si:H thin films. Particle behaviors have been experimentally investigated in magnetized dusty plasmas. Particles were formed in argon-diluted silane gas discharge in the presence of crossed weak magnetic field **B** perpendicular to DC or low-frequency discharge electric field **E**. Temporal evolution of two-dimensional profiles of silicon particles has been observed. Silicon particle's behavior in a silane plasma and the particles collected on the substrates set up both sides in **E×B** and opposite direction were observed by laser light scattering(LLS) method using a He-Ne laser and field emission scanning electron microscopy(FESEM). In DC plasmas, silicon particles were transported in the direction opposite to **E×B** drift of plasmas, and the spatially integrated Mie scattering intensity(SIMSI) was decreased with increasing applied magnetic flux density. On the other hand, in low frequency plasmas, the SIMSI was rapidly increased after the discharge-on and was also decreased over the critical magnetic flux density. When a crossed magnetic field with same frequency of discharge electric field was applied, the particles grown in an argon-diluted silane dc plasma are also transported in the direction opposite to the **E×B** drift of plasmas. The deposited film with no serious particles and the silicon particles of around 20nm diameter with high surface density, $5\times 10^{10}cm^{-2}$ were obtained in the **E×B** and the opposite side, respectively. Such effects were also seen in the results under the condition of the same frequency and same phase of the discharge electric field and the crossed magnetic field. From the calculation of equations of motion for negative electrons, positive ions and negatively charged particles, it has been suggested that the particles drift in the direction opposite to **E×B** drift of plasmas by the space charge effect. When the particle radius is increased and the electron density is decreased, the drift velocity of particles is decreased by the decrease of space charge electric field.

SESSION GT3: INDUCTIVELY COUPLED PLASMAS II
Tuesday morning, 20 October 1998
South Pacific Ballroom, Aston Wailea at 10:00
J. Caughman, Oak Ridge National Lab, presiding

Contributed Papers

10:00
GT3 1 3-dimensional Modeling of Electromagnetic and Physical Sources of Aziumuthal Nonuniformities in Inductively Coupled Plasmas for Deposition* JUNQING LU, ERIC R. KEITER, MARK J. KUSHNER, *University of Illinois, Urbana, IL 61801, USA* Inductively Coupled Plasmas (ICPs) are being used for a variety of deposition processes for microelectronics fabrication. Of particular concern in scaling these devices to large areas is maintaining azimuthal symmetry of the reactant fluxes. Sources of nonuniformity may be physical (e.g., gas injection and side pumping) or electromagnetic (e.g., transmission line effects in the antennas). In this paper, a 3-dimensional plasma equipment model, HPEM-3D,[1] is used to investigate physical and electromagentic sources of azimuthal nonuniformities in deposition tools. An ionized metal physical vapor deposition (IMPVD) system will be investigated where transmission line effects in the coils produce an asymmetric plasma density. Long mean free path transport for sputtered neutrals and tensor conducitivities have been added to HPEM-3D to address this system. Since the coil generated ion flux drifts back to the target to sputter low ionization potential metal atoms, the asymmetry is reinforced by rapid ionization of the metal atoms.

*Work was supported by SRC, Tokyo Electron/Arizona, U of Wisconsin ERC for Plasma Aided Mfg. and NSF.

[1]M. J. Kushner, J. Appl. Phys. v.82, 5312 (1997).

10:15
GT3 2 Studies on Magnetron Sputtering Assisted by Inductively Coupled RF Plasma for Enhanced Metal Ionization Y. SETSUHARA, M. YAMASHITA, S. MIYAKE, *JWRI, Osaka University, Osaka Japan* M. KUMAGAI, *Kanagawa High-Technology Foundation, Kawasaki Japan* J. MUSIL, *University of West Bohemia, Czech Republic* Trends in microelectronics device fabrications toward sub-quarter micron regimes require development of a metallization technology with enhanced ionization of metal atoms for highly directional deposition of interconnects filled into high aspect ratio contact holes. In this work we have developed the magnetron sputtering system additionally assisted by inductively coupled plasma (ICP) at 13.56 MHz, which is sustained by a helical rf coil immersed in the plasma[1] Use of the technique significantly enhances plasma density and ionization of the sputtered atoms. The effects of antenna termination (directly grounded/floating) have been investigated. The floating antenna regime effectively suppresses the anomalous rise of the plasma potential to produce a stable and dense ICP as high as $10^{12}/cm^3$ at Ar pressures 2-5Pa and a rf power of 800W. Properties of Al and Cu films are also investigated using XRD, RBS and FE-SEM examine the ionized deposition performance.

[1]Y. Setsuhara et al.; Proc. 2nd Int. Conf. on Reactive Plasmas, Yokohama, Japan, 1994, p. 549; Jpn. J. Appl. Phys. 36, 4568 (1997).

10:30
GT3 3 A Comparison of Results between PIC and RCT Model in a Collisional Inductively Coupled Plasma JIN-SUNG OH, T. MAKABE, *Keio University, Japan* A comparison is made between one dimensional particle-in-cell(PIC) model and relaxation continuum(RCT) model simulation of an inductively coupled plasma(ICP) in a collision dominated region at 50mTorr and 100mTorr in Ar. Up to 10^4 particles per species are loaded in one-dimensional cylindrical spatial mesh($\mathbf{r}$), along with three velocity components($\mathbf{v_r}$, $\mathbf{v_\theta}$, $\mathbf{v_z}$). The simulation generates spatially dependent plasma potential, magnetic and electric fields, density of electrons and ions, and power density. We found that there is agreement in the overall discharge behavior between two models with the exception of the plasma potential. We discuss the diffusion of electrons close to the insulating wall in ICP under a collision dominated region.

10:45
GT3 4 Two-dimensional mapping of electron distribution functions and kinetic modeling of low-pressure ICP* U. KORTSHAGEN, B. HEIL, *University of Minnesota, Mechanical Engineering, 111 Church Street SE, Minneapolis, MN 55455* Development of large-scale uniform low pressure ICP discharges is important to the development of next-generation semiconductor processing tools for 30 cm and 45 cm wafer technology. Efficient plasma modeling is needed for the computer aided design of these discharge tools. The non-equilibrium character of low pressure ICP discharges requires a kinetic description of the typically space-dependent, non-Maxwellian EEDF (Electron Energy Distribution Function). Experimental measurements of the EEDF were performed using a Langmuir probe capable of moving in two dimensions in a Faraday-shielded Argon ICP. These measurements are compared to numerical calculations using a ''Hybrid Approach'' that uses the Non-Local approximation in the elastic range and a rigorous kinetic approach in the inelastic range of electron energies. Reasonable agreement between experiment and model is found.

*Work supported by NSF grant ECS-9713137

11:00
GT3 5 A Traveling Wave Driven, Inductively Coupled Large Area Plasma Source YAOXI WU, M.A. LIEBERMAN, *University of California, Berkeley* Measurements are reported on an inductively coupled large area plasma source (LAPS) driven by a 13.56 MHz traveling wave. Launching a traveling wave eliminates standing wave effects to obtain a uniformly excited processing plasma. The plasma is generated inside a rectangular box 71.1 cm $\times$ 61.0 cm $\times$ 20.3 cm containing a substrate holder large enough to study processing of 300 mm diameter silicon wafers and 360 mm $\times$ 465 mm glass substrates. The driving coil consists of a series (serpentine) connection of eight parallel rods embedded in the plasma inside thin quartz tubes. The ion saturation current to a Langmuir probe was measured as a function of discharge power and pressure for powers up to 2500 watts and pressures from 1 to 100 mTorr. The coil has been instrumented with a set of eight voltage pick-up probes to determine the standing wave ratio on the antenna under plasma-loaded conditions. We found that it was possible to tune the system to launch a traveling wave for a wide range of powers and pressures. The measured plasma densities ranged up to 3×10^{11} cm^{-3}, indicating an inductive coupling mode. The efficiency of delivery of the rf power to the plasma was 77% at 500 watts and 18 mTorr. Further measurements are under way to characterize the plasma density uniformity.

11:15

GT3 6 3D Analysis of CF and CF_2 Radical Densities in CHF_3/Ar Inductively Coupled Plasma H. NAKAGAWA, S. MORISHITA, H. HAYASHI, S. NODA, M. OKIGAWA, K. ITO*, M. INOUE, M. SEKINE, *Association of Super-Advanced Electronics Technologies (ASET) *Matsushita Electric Industrial Co., Ltd.* The three-dimensional (3D) distribution of CF and CF_2 radical densities in CHF_3 / Ar inductively coupled plasma (ICP) was evaluated by using laser induced fluorescence (LIF), appearance mass spectrometry (AMS), and infrared semiconductor laser absorption spectroscopy (IR-LAS). A multi-spiral ICP coil for the 13.56 MHz wave is located on the top quartz plate of the reactor having a diameter of 400 mm. Both the external diameter of the coil and the electrode on which the 8-inch Si wafer is held are about 250 mm, and the gap between the top plate and the electrode is 97 mm. We investigated the space from 5 mm to 45 mm above the electrode. LIF measurement results revealed that both 3D distributions of CF and CF_2 radical densities have a extreme hollow structure. As the ICP power increases, the radical densities decrease in the region inside the diameter of about 250 mm but the radical densities increase in the region outside. The electron density (around 2e+11 cm^{-3} at an excitation power of 2 kW in 3 Pa) measured by a Langmuir probe has indicated that the plasma is concentrated in the inside region. The electron temperature is almost uniform in the radial direction and its value is about 3 eV. These results indicate that the radical densities are enhanced by the dissociation acceleration in the outside region as the electron density increases, but that the radical densities in the inside region is reduced by excessive dissociation because the electron density in the inside region is significantly higher than that in the outside region.*

*This work was supported by NEDO.

Invited Paper

11:30

GT3 7 Magnetic Neutral Loop Discharge (NLD) Plasma and Application to Oxide Etching Process.

TOSHIO HAYASHI, *ULVAC Japan Ltd., 2500 Hagisono, Chigasaki, Kanagawa 253-8543, Japan*

The NLD plasma, which is characterized by the plasma production in a magnetic neutral loop consisted of a zero magnetic field points connected around a circle, was applied to the 0.1 micrometer wafer process. The feature of the NLD plasma is mainly characterized by two points. One is the controllability of position of plasma production which is most useful for some programmed processing like as uniform etching, and the other is the specific thermalization effect due to meandering electrons around the neutral loop which means the higher antenna power application brings forth the faster thermalization of electrons. As an evidence, the NLD plasma generation at lower gas pressure under higher antenna power results in a high density and low temperature plasma. The applicability to the 0.1 micrometer wafer process was verified through the experiments. The uniformity of the etch rate within 3 value) is obtained for a silicon dioxide film on 8 inch wafer by applying sinusoidal or exponential functional current (around 0.1 Hz) to the middle magnetic coil. Silicon dioxide etch rate and selectivity to photo-resist and Si in the NLD plasma were remarkably progressed in a pressure range of 0.1 to 1 Pa, comparing with those in the ICP plasma. A fine ditch pattern with 20 nm width and 800 nm depth was successfully fabricated with an electron beam resist mask (ZEP) in a C_4F_8+CH_2F_2 plasma at 0.4 Pa.

SESSION HT1: ICRP DISTINGUISHED LECTURER
Tuesday afternoon, 20 October 1998; Plumeria/Jade/Maile Room, Aston Wailea at 13:30
R. Itatani, Niihama National College of Technology, presiding

13:30

HT1 1 High-Density Plasma Sources and Technology for the Next Generation.

HIDEO SUGAI, *Department of Electrical Engineering, Nagoya University, Nagoya 464-8603, Japan*

These days, rapid progress in semiconductor devices such as LSI, flat panel displays and solar cells requires technical innovation in plasma-aided deposition and etching. Due to the primary importance of plasma sources, a great deal of effort has been made to develop high-density large-diameter sources and to control reactive plasmas for the next generation. Here I briefly review high-density sources developed so far, focusing mainly on current understanding of nonlinear coupling from RF antenna to high density sources, and on chemistry control of highly dissociated plasmas. First of all, I introduce various high density sources such as ECR, helicon, inductively-coupled and surface-wave plasmas; then they are classified into three categories depending on the antenna-induced electromagnetic fields. In general, antenna-plasma coupling is nonlinear, which causes plasma density jump with a discharge power increase in most high-density sources. I describe such examples of helicon,[1] and surface wave discharges along with a model explaining the mechanism. In the case of inductive RF discharge, power transfer efficiency measurements[2] enable discrimination of electrostatic coupling from inductive coupling, and a few methods to reduce the electrostatic coupling will be presented. The wave excitation and absorption processes in surface wave discharge[3] will then be discussed, but only qualitatively as the physics involved there is not clearly understood yet. Besides the discharge physics described above, plasma chemistry significantly influences the processing performance in high density plasmas. The radical composition is markedly different from the low density case, due to secondary processes accompanied with electron-impact dissociation of radicals and strong plasma-wall interactions. I outline several attempts to modify the radical composition of high density plasma:

control of residence time of radicals, control of electron energies in space (downstream processing) and in time (pulsed power processing), and control of radical loss on walls (temperature, materials, ion impact).

[1]H. Sugai et al., *Plasma Phys. Control. Fusion* **39** (1997) A445.
[2]K. Suzuki, K. Nakamura, H. Ohkubo, H. Sugai, *Plasma Sources Sci. Technol.* **7** (1998) 13.
[3]H. Sugai, I. Ghanashev, M. Nagatsu, *Plasma Sources Sci. Technol.* **7** (1998) 192.

SESSION IT1: HEAVY-PARTICLE INTERACTIONS

Tuesday afternoon, 20 October 1998; Plumeria/Jade Room, Aston Wailea at 14:45
Geoffrey James, Jet Propulsion Lab, presiding

Invited Papers

14:45
IT1 1 Collective Few-Body Coulomb Dynamics.
JIM FEAGIN, *Department of Physics, California State University–Fullerton, Fullerton CA 92834**

We analyze few-body fragmentation as collective motion about the saddles in the Coulomb potential that define *unstable* dynamical equilibria in the breakup configuration. This point of view fundamentally distinguishes the few-body Coulomb problem from most phenomena in physics, which are frequently characterized by oscillations about stable equilibria. We base our approach on the Wannier formalism which seeks to construct the exact few-body wavefunction albeit near threshold and in a limited region of configuration space about the dynamical instability. Advances in bright, high-energy light sources have promoted photoionization as a basic tool for studying the few-body Coulomb problem and in particular double escape near threshold. Recent observations[1] with recoil-ion spectroscopy of *internal* modes in the electron-pair wavefunction will be reviewed. Extensions of this description to new experiments on the photo double ionization of molecular hydrogen[2] will also be presented.

*Supported by the Offices of Energy Research and Basic Energy Sciences, Chemical Sciences Division, U.S. Department of Energy. Email jfeagin@fullerton.edu.

[1]R. Dörner et al, Phys. Rev. Lett. **77**, 1024 (1996); R. Dörner et al, Phys. Rev. A **57**, 1074 (1998).
[2]T. J. Reddish et al, Phys. Rev. Lett. **79**, 2438 (1997); R. Dörner et al, Phys. Rev. Lett., submitted (1998).

15:15
IT1 2 Correlations Among the Three Equal Mass Coulomb Interacting Particles $H^+ + H^+ + H^-$.
L.M. WIESE, *University of Nebraska at Lincoln*

A fundamental problem of physics is how conserved quantities, such as energy and angular or linear momentum, are dynamically shared among the constituent particles in a many body system. Interactions among the particles govern the partitioning of conserved quantities and can give rise to correlated motion in the system. For a continuum three body Coulomb interacting system, the effect of the interaction among the particles and any resulting correlated motion is reflected in the partitioning of available energy. The probability distribution of the correlation angle θ_{12}, the angle between the center of mass (c.m.) frame momenta of two particles with same polarity charge, also describes the correlated motion of the system. We have observed correlated motion in the three body Coulomb interacting system of $H^+ + H^+ + H^-$. By colliding 4 keV H_3^+ with He, we produce the $H^+ + H^+ + H^-$ system a few eV above the dissociative limit. All three fragments are laboratory energy and angle resolved. By detecting all three in triple coincidence, we determine unambiguously the final state dynamics for each triply coincident event. Transforming our results to the c.m. frame, we determine the total available energy, the partitioning of available energy among the three particles, and the correlation angle θ_{12} between the two H^+. We discuss the variety of observed correlated motion resulting from the evolution of this Coulomb interacting three particle system. This work is supported by NSF Grant Number 9419505.

15:45
IT1 3 Lattice Schrödinger Equation Approach for Atomic Collisions.
DAVID R. SCHULTZ, *Physics Division, Oak Ridge National Laboratory, Oak Ridge, TN 37831-6373**

By utilizing contemporary computational techniques and high-performance computers, significant advances have been made toward fully determining theoretically the behavior of few-body quantum systems. After a brief précis of work performed by a number of groups pursuing such treatments, this presentation will describe our work using a lattice approach to solving the time-dependent Schrödinger equation in multiple dimensions for the description of electron- and ion-impact of atoms. Our goal has been to create an implementation with a uniform, unbiased basis set which intrinsically contains a good representation of both bound and continuum states and can be used in a routine manner. Thus, our computer codes operate on large workstation-class machines, but also have been implemented to explore physical atomic

systems requiring massively parallel computing. A perspective on potential future development of lattice and other large-scale computational approaches will be given.

*This work performed in collaboration with D.H. Madison, M.S. Pindzola, M.R. Strayer, and J.C. Wells, and supported by the U.S. DOE Office of Fusion Energy Sciences and Office of Basic Energy Sciences through grants to Oak Ridge National Laboratory managed by Lockheed Martin Energy Research Corp. under contract DE-AC05-96OR22464.

Contributed Papers

16:15

IT1 4 Lyman-α emission via resonant energy transfer* J. WIESER, M. SALVERMOSER, L. H. SHAW, A. ULRICH, *Technische Universität München, D-85747 Garching, Germany* D. E. MURNICK, H. DAHI, *Rutgers University, Newark NJ 07102* Very intense hydrogen Lyman-α ($2p\ ^2P_0$ - $1s\ ^2S_0$) light emission (λ =121.567nm) is observed from neon gas, near atmospheric pressure, containing small admixtures (per mil) of hydrogen when this gas mixture is excited by ionizing particle beams. A dc- beam of 15keV electrons or a pulsed beam of 100MeV ^{32}S ions were used in different experiments for excitation. An energy transfer rate constant from neon to H* of $(3 \pm 1) \times 10^{-11} cm^3/s$ has been measured using time resolved optical spectroscopy on the Lyman-α line. Conversion efficiencies of particle beam power into Lyman-α light on the order ot 10% have been observed. No other significant radiation was emitted in the entire VUV, UV, and visible spectral region. The source appears optically thin with no self reversal or radiative trapping observed. The selective excitation of the H(2p) level is interpreted as arising from a resonant energy transfer between Ne_2^* excimers and hydrogen molecules.

*Supported in part by NSF, NATO and INTAS

16:30

IT1 5 Alpha Particle-Hydrogen Atom Charge Exchange by Numerical Solution of the Time-Dependent Schrodinger Equation M. E. RILEY, *SNL, Alb., NM 87185-1423* A. B. RITCHIE, *LLNL, Livermore, CA 94550* An alternative to atomic-molecular basis expansions for solution of the time-dependent Schrodinger equation (TDSE) is a direct numerical representation of the wavefunction. We present an implicit split-operator procedure (ISOP) for solving the TDSE in 3D. The algorithm combines implicit Crank-Nicolson and split-operator FFT methods[1]. Comparisons with the conventional exponentiated split-operator procedure (ESOP)[2] show that the ISOP is more stable than the ESOP for Coulombic problems using practical grids. A full scale application of ISOP is made to alpha particle collisions with H. The results help to resolve a question in the literature regarding the relative amount of capture to the n=2 and n=3 levels of the Helium ion. Finally we point out that multiprocessor versions of FFT are available, and we will discuss tentative results on the application to correlated two-electron self-consistent-field TDSE solutions for H on H scattering.

[1]A. B. Ritchie & M. E. Riley, Sandia Labs Tech Report SAND97-1205, June 1997

[2]M. Feit, J. Fleck, Jr., and A. Steiger, J. Comput. Phys. 47, 412 (1982)

SESSION IT2: LAMPS

Tuesday afternoon, 20 October 1998; Maile Room, Aston Wailea at 14:45; W. Lee Perry, University of New Mexico, presiding

Invited Paper

14:45

IT2 1 Low Pressure Electrodeless Discharges for Lighting.

R. B. PIEJAK, *OSRAM SYLVANIA Development Inc.*

This talk consists of two main parts. In the first part of the talk the history of low pressure, electrodeless discharges for lighting is reviewed. Early history (when no commercial lamps existed) is presented through the patent literature while more recent history (since 1991) is presented in terms of commercially available low pressure, electrodeless lamps. In this part of the talk, the three electrodeless lamp discharge types (capacitive, surface wave and inductive coupling) are considered along with a discussion of why only inductive discharge lamps are found in commercial products. In the second part of the talk we will introduce the ICETRONTM (ENDURATM in Europe) lamp, a new inductively coupled electrodeless fluorescent lamp recently announced by OSRAM SYLVANIA INC. The ICETRONTM lamp consists of a closed discharge tube that passes through the center axis of one or more ferrite cores. The ICETRONTM lamp produces about 12,000 lumens at about 80 LPW (system) and is operated at about 250 KHz. In comparison with other electrodeless lamps, it appears to be the most efficacious electrodeless lamp available in the market today. In the remainder of the talk, practical issues, as they relate to the performance of this lamp (such as, electrical characteristics, power transfer efficiency and electromagnetic interference) will be discussed.

Contributed Paper

15:15

IT2 2 The UHP Lamp - New Standard For Video Projection*

GUENTHER DERRA, ERNST FISCHER, HOLGER MOENCH, *Philips Research Laboratories, Weisshausstr.2, D-52066 Aachen, Germany* Point-like light sources of extremely high luminance are required to maximize system efficiency of TV and data projection systems. The Philips UHP (ultra high performance) lamp system (a burner mounted in a reflector plus a dedicated electronic driver) is a big step into this direction. The UHP burner has an electrode gap of only 1.3 mm resulting into an extremely high luminance: 2000 Mcd/m^2 in the hot spots, still 700 Mcd/m^2 in the arc center. This dramatically increases efficiency of projection systems: For

display diagonals < 2″, a 100 W UHP lamp outperforms a 250 W metal halide DC lamp in screen brightness. A second unique feature of UHP is its long life of > 8000 hours. Similar to halogen incandescent lamps, a chemical transport cycle is established, preventing wall blackening and leading to very good stability of light output. The UHP concept has established a new standard for projection systems within short time. Further developments to an even shorter arc will enable more efficient, smaller and cheaper projection systems.

Invited Paper

15:30
IT2 3 Theoretical analysis of spectral characteristics and chemical reactions in HID lamps.
T. ISHIGAMI, *Toshiba Lighting & Technology Corp.*

Theoretical analysis of spectral characteristics and chemical reactions has been done by energy balance equations and thermodynamic calculations in HID lamps assuming local thermodynamic equilibrium. An investigation of time-dependent simulation model for the high pressure sodium arc based upon energy balance equations has been carried out. In this model continuum radiation near 450 nm is treated as NaHg molecular spectrum taking into account its temperature dependent absorption coefficient. By this method calculated increase rates of continuum radiation near 450 nm in pulsed operation are coincident with measured values.Taking account of this effect,calculated result of correlated color temperature increases in pulsed operation is obtained. Tungsten transport from the electrodes to the lamp wall in an Fe iodide lamp is considered.By comparing the calculated gaseous Fe pressure with Fe vapor pressure at the electrode temperature region,the formation of the W-Fe alloy which has a low melting point can be explained and SnI2 additive effect is made clear.

Contributed Papers

16:00
IT2 4 Modeling rare-earth arc visible emission without fundamental data TIMOTHY J. SOMMERER, *General Electric CRD, P. O. Box 8, Schenectady NY 12301 USA* DAVID O. WHARMBY,* *GE Lighting Ltd., Melton Rd., Leicester LE4 7PD UK* The dominant appearance of the rare-earth atom emission spectrum of high-pressure arcs, when viewed at the Angstrom scale, is that of a very dense forest of weak (optically thin) emission lines, punctuated with occasional strong lines. Only a few hundred of the visible emission lines have been characterized in any detail. Unfortunately, prediction of the chromaticity (color coordinates) of the emitted spectrum depends on the total power emitted by these many weak lines, per unit wavelength at low resolution (5 nm), rather than detailed characterization of the strongest emission lines. We have therefore used a semiempirical approach which combines a simple model of the rare-earth atom emission and ordinary integrating sphere photometry with a first-principles model[1] of all aspects of a metal-halide discharge lamp except the rare-earth atom emission data. The result is a model which is able to predict the change in chromaticity of a metalhalide lamp as input factors such as power are varied about some central condition.

*Present address: SLI Lighting Ltd., Shipley, West Yorkshire, UK.

[1]James T. Dakin, Theodore H. Rautenberg, Jr., and Evelyn M. Goldfield, J. Appl. Phys. **66**, 4074 (1989).

16:15
IT2 5 Radiometric Efficiency of Barium Discharge Plasmas* HEIDI M. ANDERSON, J.E. LAWLER, *University of Wisconsin-Madison* Barium in the vapor phase has shown promise as an efficient atomic radiator in a glow discharge. A Barium discharge is a direct source of visible light, with the primary contributions coming from the Ba neutral resonance line at 553 nm, another neutral transition at 650 nm, and two strong Ba ion transitions at 493 nm and 455 nm. Approximately 50 other Ba neutral and ion lines also contribute to the spectrum, to varying degrees. At low buffer gas pressures (below 1 Torr), the discharge emission is dominated by the 553 nm resonance line and is green in color, but at higher pressures (a few Torr), the other portions of the visible spectrum gain in importance and the discharge appears white. We have measured the luminous efficacy of a Barium DC positive column under various temperature and pressure conditions, and have found that the efficacy can exceed 200 lumens/Watt. Current efficacy results will be reported.

*Supported by the NSF.

Invited Paper

16:30
IT2 6 Experiment on a metal hydride light source.
SHIN UKEGAWA, *Matsushita Electric Works R&D Laboratory, Inc.**

The MgH molecule that has the possibility for high efficacy light source was selected by theoretical standpoint. The experimental system is composed of discharge cell system , vacuum system , high frequency power source and inductive coupling system. The discharge cell is made of ceramic and sapphire for preventing attack from Mg and each part is connected by frit (Outer diameter is 25.4mm, inner diameter is 22mm, length is 25mm). RF (13.56 MHz) inductively coupled discharges in Mg, H_2 and Ar vapor have been studied separately at densities of 10^{15}-10^{16}[cm^{-3}]. The observed radiation bands centered at 480, 517.5 and 555nm have been identified by their rotation vibration structure as due to MgH (A state to X state). Visible MgH radiation efficiency and electrical characteristics have been studied from experimental measurement and theoretical consideration. The visible radiation (around 520nm) efficiency of MgH is about 10.4% and

the coupling coefficient between plasma and inductive coil is about 0.5. The electron temperature measured by Boltzmann plots is 0.42 eV. The calculated electrical field in plasma is 3 [V/cm]. The loss of the inductive coil under several condition is 7-27% of input power. This depends on the ratio of hydrogen strongly. The impedance including inductive coil is measured with changing input power. With increasing input power, reactance decreases and resistance increases. For example, the impedance is Z=5+j122.5 [ohm] at 20W and Z=13+j115.3 [ohm] at 50W. (Filling condition is that H_2 is 0.2Torr , total pressure of H_2 and Ar is 2 Torr and the temperature of reservoir is 600 C^o. The coil impedance without load is 1.2+j122.5). Further results including the relationship efficiency and plasma impedance will be discussed.

*This research performed in collaboration with Alan Gallagher in JILA, University of Colorado and NIST.

Contributed Paper

17:00

IT2 7 An Alkaline-earth Discharge for Lighting Applications* J.J. CURRY, J.E. LAWLER, HEIDI ANDERSON, *University of Wisconsin* The alkaline-earth element barium has been considered as a possible atomic radiator for a highly efficient gas-discharge light source. A luminous efficacy of greater than 200 lumens/Watt has been reported for the positive column of a Ba direct-current glow.[1] The low-pressure sodium discharge has a comparable efficacy, but is limited by its nearly monochromatic spectrum. We report here on the observation of 'white' light emission from a radio-frequency inductively-coupled Ba glow-discharge. A balanced visible spectrum is achieved when the BaI 553.5nm resonance line is combined with the BaII 455.4nm and 493.4nm resonance lines as well as strong ion and neutral lines in the red. The luminous efficacy of the discharge can remain high, despite strong ion emission, if conditions are such that the ratio of the ion excitation rate to the ion loss rate is much greater than one. This issue is addressed with numerical modelling as well as experimental observations.

*Supported by the NSF.

[1]H.M. Anderson et al., IEEE Conference Record - 1998 IEEE International Conference on Plasma Science, p. 123.

SESSION IT3: ETCHING AND DEPOSITION SIMULATION

Tuesday afternoon, 20 October 1998
South Pacific Ballroom, Aston Wailea at 14:45
John Helmsen, Applied Materials, Inc., presiding

Contributed Papers

14:45

IT3 1 Mechanism Development for High Density Plasma Modeling JUSTINE JOHANNES, TIMOTHY BARTEL, PAULINE HO, *Sandia National Laboratories* High density plasma (HDP) reactors applied to dielectric etch of fine-line, high aspect ratio features poses a challenge for future technology (below 0.25 μm). The complex nature of HDP reactors and the lack of basic chemical reaction rate data has made it difficult to apply numerical simulation to enhance process development. This work will focus on developing a validated, predictive model for a C2F6 plasma for oxide etch through extensive comparisons to experimental data. The initial mechanism is developed using gas phase and surface etch mechanisms from available data. Sensitivity analysis is applied to reduce the number of species and reactions, this is required for performing 2D simulations. The mechanism and the plasma models are validated and improved through comparisons to diagnostic data. A suite of three simulation tools are used during validation: Aurora, MPRES and Icarus. Validation data included Langmuir probe data, laser diode data, laser induced flourences data, Hiden probe data and oxide etch rate data. Data was taken in both an experimental Gaseous Electronics Reference cell and a commercial HDP reactor. The C2F6 plasma mechanism is then applied to investigate issues of gas injection and 300 mm scale up for a commercial HDP system.[1]

[1]Funding for this project provided by the Sandia/SEMATECH CRADA

15:00

IT3 2 Feature Evolution Simulation of I-PVD Copper Films MICHAEL A. VYVODA, CAMERON F. ABRAMS, DAVID B. GRAVES, *U.C. Berkeley* As the semiconductor industry trends toward the use of copper as a primary metallization material, robust process technologies for depositing this material in high aspect structures must be developed. One technique that has shown promise in accomplishing this task is ionized physical vapor deposition (I-PVD),[1] which can be used to perform the entire fill or provide a seed layer for subsequent copper electroplating. A key need in designing I-PVD processes is controlling the degree of sidewall copper coverage during seed layer deposition and preventing pinch-off during total fill. We have developed a numerical simulation of copper film evolution during I-PVD processing that addresses these issues. The simulation uses as inputs distribution functions of plasma ions (Ar^+ and Cu^+) and neutrals (Cu) as well as reflection and sputtering distributions of energetic species impacting copper surfaces.[2] This methodology allows for the proper tracking of reflected and sputtered material as it redeposits elsewhere within the feature. Independent variables include ion-ion and ion-neutral flux ratios as well as wafer bias voltage. We show that for a given initial feature aspect ratio, optimal conditions for achieving high film conformality and pinch-free fill can be determined by proper adjustment of these independent variables.

[1]P.F. Cheng *et al.*, J. Vac. Sci. Technol. B **13**, 203 (1995).
[2]C.F. Abrams, unpublished.

15:15

IT3 3 Scattering and Sputtering Processes of Ar^+ and Cu^+ Ions on Cu Surfaces: Molecular Dynamics Simulations CAMERON ABRAMS, DAVID B. GRAVES, *University of California, Berkeley* A better understanding of how energetic Ar^+ and Cu^+ ions from plasmas interact with copper surfaces is crucial for further development of metallization technologies. We present results of molecular dynamics (MD) simulations of Ar^+ and Cu^+ ions impacting model Cu surfaces with a variety of impact energies (50 - 200 eV) and angles. We modeled Cu-Cu interactions using the EAM potential energy function (PEF) and Ar-Cu interactions using the ZBL PEF.[1] We report the total sputtering and reflection yields for these energies and angles. We report spatial distributions of sputter and reflection yields with respect to angle of ejection,

and compare our MD results to recent experimental findings.[2] The effects of changing ion energy and angle on these quantities are discussed. For example, we observe that the sputter yield for Ar^+ on Cu decreases as the Ar^+ ion's incident angle is increased from 30° to 60° from normal. These results shed light on the dynamics of low energy ion/metal surface interactions and provide a useful databases for use in profile evolution simulations of Cu seed layer deposition and trench/via fill.

[1]K. Gärtner *et al.*, Nucl. Instr. Meth. Phys. Res. B **102**, 183 (1995).
[2]C. Doughty, S. M. Gorbatkin, and L. A. Berry, J. Appl. Phys. **82**, 1868 (1997).

15:30

IT3 4 Combined Monte Carlo and Fluid Sputter Transport Model in an Ionized PVD System with Experimental Plasma Characterization DAVID N. RUZIC, *University of Illinois-Urbana* DANIEL R. JULIANO, *University of Illinois-Urbana* DOUGLAS B. HAYDEN, *University of Illinois-Urbana* MONICA M. C. ALLAIN, *University of Illinois-Urbana* A code has been developed to model the transport of sputtered material in a modified industrial-scale magnetron. The device has a target diameter of 355 mm and was designed for 200 mm substrates. The chamber has been retrofitted with an auxilliary RF inductive plasma source located between the target and substrate. The source consists of a water-cooled copper coil immersed in the plasma, but with a diameter large enough to prevent shadowing of the substrate. The RF plasma, target sputter flux distribution, background gas conditions, and geometry are all inputs to the code. The plasma is characterized via a combination of a Langmuir probe apparatus and the results of a simple analytic model of the ICP system. The source of sputtered atoms from the target is found through measurements of the depth of the sputter track in an eroded target and the distribution of the sputter flux is calculated via VFTRIM. A Monte Carlo routine tracks high energy atoms emerging from the target as they move through the chamber and undergo collisions with the electrons and background gas. The sputtered atoms are tracked by this routine whatever their electronic state (neutral, excited, or ion). If the energy of a sputtered atom decreases to near-thermal levels, then it exits the Monte Carlo routine as is tracked with a simple diffusion model. In this way, all sputtered atoms are followed until they hit and stick to a surface, and the velocity distribution of the sputtered atom population (including electronic state information) at each surface is calculated, especially the substrate. Through the use of this simulation the coil parameters and geometry can be tailored to maximize deposition rate and sputter flux uniformity.

15:45

IT3 5 Modeling Operating Points in Atomic Nitrogen Sources* R. E. TERRY, J. L. GIULIANI, *Plasma Physics Division, Naval Research Laboratory* High flux sources of atomic nitrogen are of interest in the fabrication of III-V semiconductor materials and nitride treatments. The cracking of nitrogen in a steady state plasma cell is investigated with regard to optimizing the dissociated fraction and delivered mass. Non-Maxwellian electron energy distribution functions (EEDF) are used in conjunction with known cross section data to compute reaction rate coefficients for electron impact dissociation, vibrational excitation, and ionization of nitrogen. The three couplings [e-v,v-v,v-T] are reflected in distinct temperatures T_e, T_v, and T_g for the model. These rate coefficients themselves vary with the concentration of N and N_2 as well as these temperatures. We incorporate these rates in a simple plasma cell model, coupled to an external circuit, and compute the expected output N concentration for a variety of applied voltages and frequencies, cell size, wall properties, and mass fluxes.

*Work sponsored by BMDO.

16:00

IT3 6 Kinetic Sheath Simulation Using the DSMC Technique M. L. HUDSON, M. E. RILEY, *Sandia National Labs, Albuquerque, NM 87185-0827* A continuing goal of the microelectronics industry is decreasing the size of wafer features for maximum density usage. This effort requires an understanding of the surface evolution on an atomistic scale. We present a first-principles simulation of the rarefied plasma near the wafer surface. The model is based on our Direct Simulation Monte Carlo (DSMC) code with an integral Poisson solver. We include kinetics of all species, feature geometry, gas and surface chemistries, sheath transport, and surface charging of dielectrics and floating conductors. Loading/shielding effects between features can be evaluated since we include transport between features. A large computational domain is used as the code is massively parallel. In principle this will afford a simulation of the reactor covering all scales. Validation efforts for this 2-D sheath-feature topography simulation include a direct simulation of an AC sheath compared with the Unified Sheath Model.[1] This simulation code can then be used to evaluate the effects of process parameters on surface evolution and such problems as notch damage.

[1]P. A. Miller & M. E. Riley, J. Appl. Phys. 82, 3689 (1997)

16:15

IT3 7 Simulation of Etching Profiles Using Level Sets HELEN HWANG,* *Thermosciences Institute* T.R. GOVINDAN, M. MEYYAPPAN, *NASA Ames Research Center* Using plasma discharges to etch trenches and via holes in substrates is an important process in semiconductor manufacturing. Ion enhanced etching involves both neutral fluxes, which are isotropic, and ion fluxes, which are anisotropic. The angular distributions for the ions determines the degree of vertical etch, while the amount of the neutral fluxes determines the etch rate. We have developed a 2D profile evolution simulation which uses level set methods to model the plasma-substrate interface. Using level sets instead of traditional string models avoids the use of complicated de-looping algorithms. The simulation calculates the etch rate based on the fluxes and distribution functions of both ions and neutrals. We will present etching profiles of Si substrates in low pressure (10s mTorr) Ar/Cl_2 discharges for a variety of incident ion angular distributions. Both ion and neutral re-emission fluxes are included in the calculation of the etch rate, and their contributions to the total etch profile will be demonstrated. In addition, we will show RIE lag effects as a function of different trench aspect ratios. (For sample profiles, please see http://www.ipt.arc.nasa.gov/hwangfig1.html)

*Work supported by NASA contract NAS2-14031 to Eloret.

16:30

IT3 8 Effect of electron and ion transport on the charge build-up of the microscopic structure in CCP etcher* J. MATSUI, N. NAKANO, T. MAKABE, *Keio University at Yokohama, Japan* Charging damage, caused by the local charging on a patterned wafer surface exposed to a plasma, is one of the urgent subject to be overcome in plasma processing. There is few theoretical studies considering the phase space transport of electrons/ions incident on the microscopic structure under charge accumulation from the sheath in dry etching. We have developed the numerical model to investigate the effect of the velocity distribution of electrons/ions on the charge build-up of microstructure by

using a direct numerical procedure (DNP) of the Boltzmann equation in conjunction with Poisson's equation. The model is connected at the position close to the wafer with two frequency pulsed capacitively coupled plasma (CCP) by using RCT/Boltzmann equation model[1]. The influence of the low frequency bias operation on the charge neutralization in the wall of the microstructure is demonstrated in 2f-pulsed CCP at 27MHz and 700kHz in CF_4. Time constant for charging in the trench is discussed as a function of external plasma conditions. The suitable duty ratio of pulse operation to reduce the local charging is observed. This duty ratio depends on the background gas and drive/bias frequency.

*Work is supported by STARC in Japan.

[1]J. Matsui *et al*, J. Vac. Sci. and Technol. A, **16**, pp.249 (1998).

Invited Paper

16:45
IT3 9 Simulation of Topography Dependent Charging.
TAKASHI KINOSHITA, *KOBE STEEL, LTD.*

Topography dependent charging (TDC) or electron shading causes significant charging damage on high-aspect structure in high density plasma processes. This charging damage results from the directionality difference between ions and electrons bombarding a surface with topography. Simulation technique is one of the most powerful tool to visualize and understand the mechanism of the phenomena in submicron structures. The ion and electron energy distribution functions (IEDF and EEDF, respectively) also play important roles in charging voltage by this mechanism. Especially, an electron temperature (Te) in the bulk plasma is one of the significant parameter to control the TDC. The low energy peak of the typical double peak IEDF is directly related to Te, and the reducing Te causes less charging in the feature scale structure. Also. recent analysis using the former simulator indicates the importance of EEDF and its modified trajectory in the high aspect structure. A electron focusing effect, where the low energy electrons focused into the high positive potential at the bottom structure, has effective mechanism to reduce TDC. This effect is observed in typical low Te plasma sources, including TCP, UHF plasma, and Pulse Modulated Plasma. The mechanism will be discussed in the paper.

SESSION JTP1: POSTER SESSION: OPTICAL DIAGNOSTICS: ACTIVE SPECIES

Tuesday afternoon, 20 October 1998
Haku/Pikake Room, Aston Wailea at 17:15
Irving Langmuir, General Electric, presiding

JTP1 1 Spectroscopic studies of the CH and NH radicals during laser ablation of graphite in ammonia ALESSIO PERRONE, *University of Lecce, Department of Physics, P.O.Box 193, 73100 Lecce- Italy* ARMANDO LUCHES, *University of Lecce, Department of Physics, P. O. Box 193, 73100 Lecce-Italy* CELINE VIVIEN, JORG HERMANN, CHANTAL BOULMER-LEBORGNE, *University of Orleans/CNRS, P.O. Box 6759, 45067 Orleans Cedex2, France* Reactive pulsed laser ablation (RPLA) is well established technique for the deposition of thin solid films. Problems concerning the nature of the chemical species involved in the mass transfer from target to subtrate, the collision kinetics and the chemistry with the background gas are of large interest. Moreover, the correlation between the properties of the deposited films and the characteristics of the plasma plume created by laser are very important for the optimization and control of the deposition process. Optical emission spectroscopy of chemical species has been largely used during RPLA as diagnostic tool aiming to answer these problems. In this context, we performed plasma diagnostic using time and space resolved emission spectroscopy of CN, CH and NH radicals during the deposition of carbon nitride thin films by KrF excimer laser ablation of graphite at low ammonia pressures. From computer simulations of the molecular spectra we deduced rotational and vibrational temperatures of the above radicals. These values were found to be identical indicating that a collisional equilibrium is established.

JTP1 2 Optical Emission Spectroscopic and Mass Spectrometric Diagnostics in Nitrogen RF Discharges* HIDENORI ITOH, KOHKI SATOH, YOSHITAKA NAKAO, HIROAKI TAGASHIRA, *Muroran Institute of Technology, Japan* The characteristics of radio frequency (RF) plasmas as a function of driving frequency f, 0.1-13.56MHz in nitrogen have been investigated. The spatiotemporally resolved profiles of the net excitation rate of molecules and ions have been deduced from time resolved optical emission profiles of the second positive band and the first negative band. The atomic and molecular nitorgen ions incident on the grounded electrode, have been also measured simultaneously using a quadrupole mass spectrometer. The present results show clearly that the secondary electrons from the electrodes by ions behave an important part in the maintaining mechanism in the RF glow at low frequency as $f < 1.5$ MHz, the displacement current plays an important part at high frequency $f > 10$ MHz, and not only the secondary electrons but the displacement current do an important part at middle frequency as $1.5 < f < 10$ MHz.

*This work was supported by Grant-in-Aid (No.09650338) of the Ministry of Education, Science, Sports and Culture, Japan

JTP1 3 Two-Photon Absorption Laser Induced Fluorescence of Atomic Nitrogen by an Alternative Excitation Scheme S.F. ADAMS, *Air Force Research Lab, Wright-Patterson A.F.B., OH* T.A. MILLER, *The Ohio State University, Columbus, OH* A new two-photon absorption laser induced fluorescence (TALIF) scheme to monitor the ground state atomic nitrogen produced in a gas discharge is characterized. Excitation at 207 nm to the $(3p)^4S^o_{3/2}$ upper state is demonstrated to be superior to the traditional 211 nm excitation to $(3p)^4D^o_{7/2}$. Most striking is the low quenching rate of the upper $(3p)^4S^o_{3/2}$ state by N_2 at $k_q = 6.7x\ 10^{-11}$ cm^3/s, nearly an order of magnitude lower than the traditional technique. The two-photon excitation rate at 207 nm is also measured to be a factor of 3 greater than the traditional scheme. The advantage in signal strength of the new TALIF scheme is

shown to be especially pronounced at N_2 pressures above 1 Torr. The TALIF technique is also compared to the indirect technique of measuring atomic nitrogen density by monitoring the nitrogen afterglow emission. In a discharge through varying mixtures of H_2 with N_2, it is shown that it is necessary to include the quenching effects of H_2 and H atoms on the $N_2(B^3\Pi_g(v=11))$ state for the afterglow measurements to agree with the N-atom TALIF data.

JTP1 4 Time Transients of Roto-Vibrational Energy Distribution in Positive Column of Pulsed Nitrogen Discharge JACEK BORYSOW, *Department of Physics, Michigan Technological University, Houghton, MI 49931, USA.** Time transients of energy stored in vibrational/rotational motion of molecular nitrogen in the ground electronic state were measured in a positive column of pulsed discharge. Discharge was operating at peak current densities up to 25 A/cm^2, pressures up to 6 Torr and pulse duration between 1.0 and 3.0 μs . The measurements were done during the active discharge and in the afterglow. Coherent Anti-Stokes Raman Spectroscopy (CARS) in unstable-resonator spatially enhanced detection (USED) geometry was employed in all measurements. The 30 GHz line width of Nd-YAG laser set the limit on spectral resolution. The resolution was insufficient to observe single roto-vibrational lines. The energy stored in rotational motion was inferred from the width of vibrational bands. It is shown that initially energy is being transfer, primarily into vibrational levels above $v = 1$, resulting in a highly non Boltzmann distribution. The redistribution between vibrational levels takes place within 100 μs after the discharge pulse. The rotational temperature was as high as 4000 K and reached maximum values between 80 and 100 μs after the discharge pulse.

*Supported in part by State of Michigan Research Excellence Fund

JTP1 5 *In Situ* Diagnostics of Metal-Organic Chemical Vapor Deposition by Micro-Discharge Optical Emission Spectroscopy SHUN MOMOSE, TOSHIHIRO NAKAMURA, KUNIHIDE TACHIBANA, *Department of Electronic Science and Engineering, Kyoto Univresity* We developed an optical emission spectroscopic sensor using a micro-discharge plasma for *in situ* monitoring of metal-organic chemical vapor deposition (MOCVD). The distance between the electrodes is only 5mm and the photo emission from the micro-plasma is introduced by optical fibers to a monochromator. Since the size of the sensor head is about 12 mm, the spatial distribution of the source gases can be measured by moving it in the CVD reactor. We applied this technique to the diagnostics of the MOCVD of barium strontium titanate (BST) film, which is the most promising capacitor dielectrics for giga bit scale DRAMs. We used β-diketonate chelates of Ba, Sr and Ti elements dissolved in tetrahydrofuran as the source materials. The plasma-induced optical emission was strongly dependent on the temperature. From the profile of these spectra, the degree of the thermal decomposition of the source gases is investigated, which does influence the electric properties of deposited BST films. At the Conference, we will report and discuss the correlation between the decomposition mechanism of the source gases and the quality of the deposited films.

JTP1 6 Measurements of SiH_3 Density in RF Silane-Contained Gas Discharges Using Ultraviolet Absorption Spectroscopy M. SHIRATANI, A. MINEMOTO, T. FUKUZAWA, Y. WATANABE, *Kyushu University, Japan* An UV light absorption method applicable to transient plasmas is developed to study production and loss rates of SiH_3 in SiH_4 contained CVD plasmas. Measurements of time evolution of SiH_3 density by this method are carried out together with those of Si emission intensity in both pure SiH_4 and SiH_4+N_2 rf discharges. While the Si emission intensity linearly increases with rf power P, the SiH_3 density is proportional to the power for P< 0.275W/cm^2 and tends to saturates P> 0.275W/cm^2 for pure SiH_4 discharges. These features show an enhancement of the SiH_3 loss rate in the high power range. Using this non-linear power dependence and rate equation concerning SiH_3 density, its absolute value is estimated to be 7 $\times 10^{11}$ cm^{-3} at 0.23 W/cm^2, which is close to that obtained by the infrared laser absorption spectroscopy. [1]. Both the Si emission intensity and SiH_3 density in SiH_4+N_2 rf discharges increase considerably for SiH_4 < 30% and slightly for 30-60% and become constant for 60-100%. Hence, the SiH_3 loss rate is insensitive to the N_2 dilution rate, showing that reactions of SiH_3 with N_2 are slow. Moreover the deposition rate for 30-100% SiH_4+N_2 can be explained by the estimated absolute SiH_3 density. [1] N. Itabashi, et al. Jpn. J. Appl. Phys. **29**, 585(1990).

JTP1 7 Effects of Fluorocarbon Films on CF Radical in CF_4/H_2 Plasma T. ARAI, M. GOTO, S. MASHINO, H. AIKYO, *Kanagawa Institute of Technology* The behavior of CF radical in CF_4/H_2 plasma was studied as a function of the fluorocarbon film thickness grown on the inner wall in DC pulsed CF_4/H_2 discharge plasma. The discharge tube was hollow cathode tube consisting of a stainless steel cylindrical cathode (10cm inner diameter, 30cm long) with optical access parts and two tungsten pin anodes (1.5mm diameter). A DC pulsed voltage with a repetition frequency of 10Hz, a width of 0.5ms and discharge current of 300mA was applied between the electrodes. Laser-induced fluorescence was used to examine the temporal behavior and radical distribution of CF radical density. The thickness of fluorocarbon films grown on the inner wall of the discharge tube was measured to investigate the influence of fluorocarbon film formation on CF radical density in the plasma. It was found that the CF radical density increased with increasing film thickness, and that the radial distribution of CF radical density changed to uniform profile.

JTP1 8 Development of incoherent-light absorption spectroscopic technique for measuring atomic species in process plasmas SEIGOU TAKASHIMA, *Nagoya University and Nippon Laser & Electronics Lab.* SHIGEO ARAI, MASAFUMI ITO, MASARU HORI, AKIHIRO KONO, TOSHIO GOTO, *Nagoya University* KATSUMI YONEDA, *Nippon Laser & Electronics Lab.* In process plasmas, atomic species such as Si, C, and H play an important role. We have established the measurement method for C atom densities by ultraviolet absorption spectroscopy(UVAS) employing an incoherent light source, that is, the carbon hollow cathode lamp. In order to apply this method to in-situ monitoring of C atom densities, the development of light source with high intensity and stability is necessary. In this study, the properties of carbon hollow cathode lamp have been investigated by changing the hollow size, the gas composition and the gas pressure. The maximum light emssion intensity of C atom(296.7nm) was obtained in the condition of the hollow diameter of 3mm, the hollow depth of 15mm, the gas composition of Ar/O_2(1:3), the gas pressure of 2Torr, and the discharge current of 10mA. The lamp indicated a good stability for several hours operation. Furthermore, we have been developing a high pressure microdischarge H_2 lamp for measuring H atoms in the plasma. This lamp is designed to prevent broad emssion line profile due to high-speed H atoms arising from dissociation of H_2. The results of the microdischarge H_2 lamp will be also presented.

JTP1 9 Measurements of He metastable atom density profile in front of substrate in ECR plasma flow by laser-induced fluorescence technique. H. TOYOTA, K. TAKIYAMA, T. ODA, *Dept. Appl. Phys., Hiroshima University* Metastable atoms of rare gases affect on the etching processes and the radical formation processes in a reactive plasma because of their high internal energy. Fundamental understanding is required of the creation and annihilation mechanisms of the metastable atoms in the plasma, especially in the boundary region between plasma and substrate. We have measured spatial profile of He metastable (2^1S) atom density in plasma flow from an ECR plasma source by polarized laser-induced fluorescence (LIF) spectroscopy [1]. It has been shown that the metastable atoms near the outlet of the plasma flow are created by collisional-radiative processes. However, the remarkable decrease near the substrate placed in the downstream has not been clearly understood. Observation of the polarized LIF due to forbidden excitation is made with high spatial resolution in the vicinity of the substrate to obtain the detailed density profile. Based on these results, possible annihilation mechanism of the metastable atoms will be briefly discussed. [1] H. Toyota *et al.*; Jpn. J. Appl. Phys. **36** (1997) 4670.

JTP1 10 Measurement of C_2 Radical Density in Low-Pressure Radio Frequency $CH_3OH/H_2/H_2O$ Inductively Coupled Plasma Used for Diamond Formation H. NAGAI, N. HORIO, M. HIRAMATSU, M. NAWATA, *Meijo University* In contrast with conventional methods of diamond chemical vapor deposition (CVD) employing high-pressure plasma ($\geqslant$ 100 Pa), in the case of low-pressure, high-density, and highly dissociated plasmas, carbon dimer (C_2) radicals or carbon atoms instead of methyl radicals might be important species for diamond growth. In this work, C_2 radical density in a low-pressure ($\leqslant$ 13 Pa), radio frequency (rf, 13.56 MHz), inductively coupled plasma (ICP) for diamond CVD was measured using absorption spectroscopy with Xe lamp emitting a continuous spectrum as a light source. A mixture of $CH_3OH/H_2/H_2O$ was fed through a quartz tube of 26 mm i.d. A 5-turn rf coil was mounted on the quartz tube to produce plasma. Transmittance spectra in the ICP and downflow region were obtained around 516.5 nm of (0-0) bandhead of C_2 Swan system. It was found that C_2 radical density increased almost linearly with increasing rf input power or CH_3OH partial pressure, and decreased with increasing H_2O partial pressure.

JTP1 11 Diode Laser Measurements in an Inductively Coupled GEC Cell for Oxide Etching LEE PERRY, *University of New Mexico* GLEN DEERING, *University of New Mexico* LAURE KOLTUNSKI, *University of Orlean* HAROLD ANDERSON, *University of New Mexico* Diode laser absorption measurements have been made on CF, CF_2 and CO radicals in an inductively coupled GEC reference cell. The GEC reference cell was modified with a quartz confinement ring around the source region to stabilize the plasma. Optical emission and Langmuir probe studies indicated this modification resulted in fluorocarbon discharges with a plasma chemistry similar to that found in commercial etch tools. The experiments in this study focused on radical concentrations found in the reactor under typical high-density plasma etching conditions. In a 10 mTorr C_2F_6 discharge at 300 W source power and 100 W bias power, etching proceeded at about 5000 Å min^{-1}. A range of source power and bias power conditions, from 100 to 400 W and from 0 to 130 W, respectively, was employed. The time evolution of CF, CF_2 and CO in a C_2F_6 plasma was monitored during an approximate 2 minute etch cycle. Chamber cleanliness and bias was found to exert a strong influence on radical densities. The data is expected to provide an important database for models of oxide etching in inductively coupled plasma tools.[1]

[1]This work has been supported by SEMATECH

JTP1 12 Effect of surface chemistry on CF, CF_2, and C_2 radical densities in high-density CF_4/H_2 plasmas C. SUZUKI, H. FURUKAWA, K. SASAKI, K. KADOTA, *Department of Electronics, Nagoya University, Nagoya 464-8603, Japan* Laser-induced fluorescence (LIF) spectroscopy combined with absolute density calibration was employed for the measurements of CF, CF_2, and C_2 ($a^3\Pi_u$) radical densities in low-pressure and high-density ($n_e \simeq 10^{12}$ cm^{-3}) CF_4/H_2 plasmas generated by helicon wave discharges. Hydrogen concentration was varied from 0 to 50 % under the constant CF_4 partial pressure of 5 mTorr. The chamber wall was seasoned in each H_2 percentage until all the radical densities reached the steady state values. When the H_2 concentration exceeded a certain percentage, the radical densities largely and slowly increased in several ten minutes. The lifetimes of the radicals in the afterglow became longer simultaneously. These results indicate that the wall condition changes drastically at the threshold H_2 concentration. Since the spatial distributions of the radical densities were hollow shape in each H_2 percentage, the radicals were produced on the chamber wall covered with fluorocarbon films. Strong correlations between the radical densities and the inward radical fluxes estimated from the density gradients suggest that the CF_x and C_2 radical densities in the CF_4/H_2 plasmas were predominantly determined by the radical productions on the wall surface.

JTP1 13 Behavior of Atomic C Species in Inductively Coupled Plasma HARUHIKO ITO, *Nagoya Municipal Industrial Research Institute, JAPAN* MASAYUKI ISHIKAWA, MASAFUMI ITO, MASARU HORI, TOSHIO GOTO, *Nagoya University, JAPAN* TAKASHI TAKEO, TERUMASA KATO, *Nagoya Municipal Industrial Research Institute, JAPAN* CO gas was used for plasma etching and plasma enhanced chemical vapor deposition processes. It is considered that C atoms generated from a dissociation of CO gas play an important role in the plasma process. We have developed the measurement system for absolute density of C atoms using ultra violet absorption spectroscopy (UVAS). The transition line of C atom was $2s2p^3\ ^5S_2$ - $2s^22p^2\ ^3P_2$ at 296.7 nm. In order to measure the absolute density of C atoms, Einstein's A coefficient has been experimentally measured. The C atom density in 13.56 MHz radio frequency inductively coupled pure CO plasma was 5.1×10^{12} cm^{-3}. The diamond has been reported to be synthesized by adding small amount of CH_4 to CO highly diluted by H_2 in the inductively coupled plasma. The behavior of CH and OH species and C and H atoms was measured from optical emission spectroscopy in this plasma. The emission spectra of C decreased considerably with increasing the mixture ratio of CH_4 to CO. The behavior of atomic C species will be discussed on the basis of measurement results using UVAS and their emission spectra.

JTP1 14 Plasma Diagnostic of $CH_4/H_2/O_2$ Micorwave Plasma CVD TOSHIAKI YASUI, HIDEKAZU KODERA, HIROKAZU TAHARA, TAKAO YOSHIKAWA, *Division of Mechanical Engineering, Department of Systems and Human Science, Graduate School of Engineering Science, Osaka University, Japan* Microwave plasma chemical vapor deposition (CVD) using mixture of $CH_4/H_2/O_2$ gases is enable to produce good quality amorphous carbon and diamond films at low pressure ($<$ 5 kPa). To understand the deposition process, the microwave plasma composition

(ions,electorn and radicals) were invesigated. 2.45GHz microwave plasma was produced using cylindrical resonant cavity and diagnosed by optical emission spectroscopy (OES) and electrostatic probe technique. Also, laser-induced fluorescence spectroscopy (LIF) was carried out to evaluate radical species by using a tunable dye laser pumped by a YAG laser. C_2 and CH radicals were detected and its number densities were measured.

JTP1 15 In Situ CF3 Detection in Low Pressure RF Discharges by Fourier Transform Infrared Spectroscopy J.S. KIM, *Stanford University/NASA-Ames Research Center* M.A. CAPPELLI, *Stanford University/NASA-Ames Research Center* S.P SHARMA, *NASA-Ames Research Center* The detection of CFx (x=1-3) radicals in low pressure discharges using source gases such as CF4 and CHF3 is of importance to the understanding of their chemical structure and relevance in reactive ion etching (RIE). These radicals are known to contribute to the formation of fluorocarbon polymer films, which affect the selectivity and anisotropy of etching. In this study, we present preliminary results of the quantitative measurement of trifluoromethyl radicals, CF3, in low pressure radio-frequency (RF) discharges. The discharge studied here is an inductively (transformer) coupled plasma (ICP) source in the GEC RF reference cell, operating on pure CF4 at pressures ranging from 10-100 mTorr. This plasma source generates higher electron number densities at lower operating pressures than obtainable with the parallel-plate capacitively coupled version of the GEC reference cell. Also, this expanded operating regime is more relevant to new generations of industrial plasma reactors being used by the microelectronics industry. Fourier transform infrared (FTIR) spectroscopy is employed to observe the absorption band of CF3 radicals in the electronic ground state X2A1 in the region of 1233-1270 cm-1. The spectrometer is equipped with a high sensitivity HgCdTe (MCT) detector and has a fixed resolution of 0.125 cm-1. The CF3 concentrations are measured for a range of operating pressures and discharge power levels.

JTP1 16 CH3 and CFx Detection in Low Pressure RF Discharges by Broadband Ultraviolet Absorption Spectroscopy M.A. CAPPELLI, *Stanford University/NASA-Ames Research Center* J.S. KIM, *Stanford University/NASA-Ames Research Center* S.P. SHARMA, *NASA-Ames Research Center* The detection of reactive radicals in low-pressure radio-frequency (RF) discharges is of importance to the understanding of the chemical processes involved in discharge applications such as reactive ion etching (RIE) and plasma-enhanced chemical vapor deposition (PECVD). Furthermore, the quantitative measurement of radical concentrations and their spatial distributions provide a test of theoretical models that describe the kinetics of such discharges and their ability to predict the overall reactor-scale performance. In this presentation, we describe preliminary studies of the quantitative detection of CH3 and CF2, which are the products of electron collisional dissociation of methane (CH4) and tetrafluoromethane (CF4), respectively, in low-pressure RF plasma discharges. The discharge studied is an inductively (transformer) coupled plasma (ICP) source, operating on either pure methane or pure tetrafluoromethane, in some cases, with argon dilution. Such discharges are commonly employed in RIE and PECVD applications, and these data contribute to the growing database on properties of such discharges, for which sophisticated models of their operation are presently under development at many laboratories. The detection method employed in these experiments relies on the relatively well studied, X -> B uv-absorption band of CH3 near 216 nm, and the A(0,2,0) -> X(0,0,0) uv-absorption band of CF2 at 234.3 nm.

JTP1 17 Measurements of Charged and Neutral Species in BCl_3/Cl_2 Reactive Gas Discharges for Metal Etching* RAVIPRAKASH J., R. T. MCGRATH, *PennState University* G. A. HEBNER, *Sandia National Laboratories* J. A. SHERWIN, *PennState University* Measurements made using an uncollided beam mass spectrometer (Hiden EQP) have allowed identification of reactive species and etch products within BCl_3/Cl_2 processing gas discharges used for aluminum etching. Reactive discharge composition was monitored as pressure, ICP power, and wafer substrate material were varied. Wafer substrates investigated include combinations of silicon, photoresist, and aluminum. During BCl_3/Cl_2 (2:1) etching discharges with aluminum coated wafers ($\approx$ 70% Al surface coverage), we find that Al^+ is the principal etch product identified, with concentration an order of magnitude larger than those of other etch products detected, which include $AlCl^+$, $AlCl_2^+$, $Al_2Cl_3^+$, $Al_2Cl_4^+$, $Al_2Cl_5^+$. In fact, Al^+ is the principal positive ion in the discharge with concentration about twice that of BCl_2^+. In blanket silicon wafer substrates, we find large concentrations of $SiCl^+$, comparable to those of BCl_2^+, along with smaller concentrations of $SiCl_3^+$, $SiCl_2^+$, and $SiCl_4^+$. These results imply that etch product species (Al_xCl_y and $SiCl_y$) cannot be neglected in model validation efforts which compare simulation predictions to experimental data obtained from BCl_3/Cl_2 discharges operated with aluminum, silicon and resist wafer substrates.

*This work was supported by Sandia National Laboratories and US Dept. of Energy under contract DE-AC04-94AL85000.

SESSION JTP2: POSTER SESSION: OPTICAL DIAGNOSTICS
Tuesday afternoon, 20 October 1998
Haku/Pikake Room, Aston Wailea at 17:15
Irving Langmuir, General Electric, presiding

JTP2 1 Three dimensional Space-resolved optical-emission spectroscopy in an inductively coupled CF_4/Ar plasma* H. HIRATA, K. HIOKI, N. NAKANO, Z. PETROVIC, T. MAKABE, *Keio University, Japan* S. MATSUMURA, *Musashi Inst. Technology, Japan* Inductively coupled plasmas (ICP) are widely used in semiconductor processing, because of high plasma density at low pressures. In our previous work we have investigated the structure of inductively coupled plasma in Ar[1], driven by one turn coil at 13.56 MHz. In this work we study ICP with CF_4(5%)/Ar mixture, which is normally used for etching. ICP in the mixture has different characteristics from the electro-positive gas, Ar. Results of robot assisted tomographic image of optical emission spectroscopy and electron density by double probe are compared with those in pure Ar. At low pressure (15mTorr), the difference between CF_4(5%)/Ar and Ar plasma is small at the same power. On the other hand, at high pressure (300mTorr), the electron density of CF_4(5%)/Ar is one order of magnitude smaller than that of Ar, due to the influence of electron attachment. CT image in CF_4(5%)/Ar shows a sharp peak near the coil and is more localized than for Ar. Azimuthal anisotropy is also much more pronounced in the mixture.

*Work supported by ASET, and Monbusho ISRP (No.08044169).
[1]A.Okigawa et al, Jpn.J.Appl.Phys. **36**, 4605 (1997).

JTP2 2 Spatially resolved electron density measurements in a CCRF with an 1 mm microwave interferometer VOLKER SCHULZ-VON DER GATHEN, CHRISTOPH LUKAS, MICHAEL SPAAN, H.F. DÖBELE, *Universität GH Essen, Institut für Laser- und Plasmaphysik, 45117 Essen, Germany* Three dimensional electron density profiles are measured with an 1 mm heterodyne microwave interferometer[1] at a capacitively coupled rf discharge. The stainless steel electrode assembly (100 mm diameter and 25 or 40 mm separation) can be displaced in both directions transverse to the microwave beam. From a series of line-of-sight measurements a radial electron density profile can be calculated by Abel inversion. A complete 3 dimensional profile is obtained by repeating the measurements at different distances from the electrodes. The minimum distance to the electrodes is about 3 mm defined by the beam diameter. The detection limit is $\sim 2 \cdot 10^{15}\ m^{-3}$. The gas pressure ranges from 10 to 100 Pa; the RF power at 13.56 MHz between 10 and 100 W. Density profiles are presented and discussed for measurements in Argon and Hydrogen. (Funded by the DFG in the frame of the SFB 191)

[1]N.Niemöller et al., Plasma Sources Sci.Technol., 6 (1997) 478

JTP2 3 Enhancement of the Spectroscopic Diagnostics for Low-Density Plasmas Based on Highly Excited Hydrogen Lines EUGENE OKS, *Auburn University* Stark broadening of highly excited hydrogen lines is frequently used for diagnostics of low-density plasmas. However, it was usually assumed that with the increase of the principal quantum number n of the upper atomic level, the Ionic Contribution to the Impact Width (ICIW) tends to zero. In distinction to this paradigm, by finding an exact analytical result for the ion dynamical broadening of hydrogen spectral lines, we show here that with the increase of n, the ICIW goes to a finite limit. Moreover, this "residual" ICIW, being independent of n and of the plasma density N, can be comparable to the standard electron impact width. This novel result leads to: 1) a substantial revision of the past diagnostic conclusions for a variety of low density plasmas; 2) a much better possibility to deduce experimentally not only the plasma density but also the plasma temperature T; 3) a significant enhancement of the accuracy of N and T obtained from experimental line profiles.

JTP2 4 Spectroscopic measurements in inductively coupled RF discharges in hydrogen* MICHAEL L. HUEBSCHMAN, *Fusion Research Center, The University of Texas at Austin, Austin, Texas 78712, USA* ROGER D. BENGTSON, JAMES C. WILEY, *Fusion Research Center, The University of Texas at Austin, Austin, Texas 78712, USA* JOHN G. EKERDT, *Science and Technology Center for the Synthesis, Growth and Analysis of Electronic Materials, University of Texas* VIVEK BAKSHI, *International Sematech, Austin, TX* P.A. VITELLO, *LLNL, Livermore, CA* Spatially resolved electron temperature profiles, $T_e(r,z)$, and plasma electron density profiles, $n_e(r, z)$, were measured with a multi-chord, multi-channel optical emission spectrometry in inductively coupled hydrogen plasmas over a range of RF power and pressure in a semiconductor growth and analysis chamber. The absolute intensities from eighteen simultaneous viewing chords were measured and Abel inverted for eleven hydrogen Balmer lines. These spatially resolved excited level densities are used to estimate the electron temperature and density using collisional-radiative models[1,2] and pressure balance. We also compare the profiles with 2D fluid models[3]. These experiments and models are motivated by the desire to develop accurate computational models of a simple chemical system -hydrogen on silicon- in a simple geometry which could be verified by measurements.

*Research supported in part by the Texas Advanced Research Program.

[1]L.C. Johnson and E. Hinnov, J. Quant. Spectrosc. Radiat. Transfer. 13, 333 (1973)
[2]K. Sawada and T. Fujimoto, J. Appl. Phys. 78 (5) (1995)
[3]INDUCT94

JTP2 5 Influence of Plasma Inhomogeneities on Thomson Scattering Results J. SCHEIN, G. GREGORI, P. SCHWENDINGER, U. KORTSHAGEN, J. HEBERLEIN, E. PFENDER, *University of Minnesota, Department of Mechanical Engineering, Minneapolis, MN 55455* Several attempts have been made in the past to measure the electron density and electron temperature of a plasma spray torch plasma using Thomson Scattering. Unfortunately the results of these experiments are not in agreement with spectroscopic measurements. The temperatures determined by using the electron feature of Thomson Scattering are usually around 5000 K higher and seem to be nearly independent of axial location. For a wider variation of the parameter $\alpha = 1/k\lambda_d$ experiments have been made with scattering angles varied from 40° to 140°. The results indicate that the measured temperature is a function of the scattering angle, with higher temperatures at smaller angles. However, this is in contradiction to the theory. An explanation is given by introducing a broadening mechanism, caused by disturbing factors like macroscopic plasma density fluctuations and gradients. Using this mechanism in the evaluation of the data, temperature values have been obtained, which are in reasonable agreement with the spectroscopic measurements. Experimental data have been obtained with a 20Hz, 10ns pulsed Nd:YAG laser, operated at 532nm. The plasma jet is produced with a Miller SG100 Torch, operated with Argon at 700A.

JTP2 6 Thomson Scattering Measurements in Reactive Plasmas M. D. BOWDEN, H. KUDO, K. UCHINO, K. MURAOKA, *Kyushu University, Japan* In recent years, laser Thomson scattering has been applied to make reliable measurements of electron properties in glow discharges. Until now, measurements have been carried out in various types of discharges using non-reactive gases. In this paper, we describe an experimental system designed for measurements in an etching plasma. The discharge is a low pressure inductively coupled plasma operated in a mixture of CF_4 and Ar. The scattering system uses a YAG laser at 1064 nm as the laser source and a single photomultiplier as the detector. Various steps were taken to check that the high energy laser pulse did not perturb the discharge. Measurements taken with this system will be presented, and the extent to which the EEDF can be measured will be discussed.

SESSION JTP3: POSTER SESSION: PLASMA JETS
Tuesday afternoon, 20 October 1998
Haku/Pikake Room, Aston Wailea at 17:15
Irving Langmuir, General Electric, presiding

JTP3 1 Nitriding of Titanium Using Supersonic Nitrogen and Nitrogen/Hydrogen-Mixture Plasma Jets under a Low Pressure Environment HIROKAZU TAHARA, TETSUJI SHIBATA, YASUTAKA ANDOH, TOSHIAKI YASUI, KEN-ICHI ONOE, TAKAO YOSHIKAWA, *Graduate School of Engineering Science, Osaka University, Japan* Nitriding of titanium using nitrogen and nitrogen/hydrogen-mixture plasma jets under a low pressure environment was investigated from metallurgical and gas dynamical viewpoints. Under a low pressure below 3 kPa, plasma was smoothly accelerated using an optimally designed supersonic expansion nozzle because a shock diamond was not observed in a plasma flame. Even below 3 kPa, a hard titanium nitride layer was constructed on the surface of a titanium sample by only 5 minutes plasma jet irradiation. Although nitride formationability decreased with decreasing pressure at the center of the irradiated region, the nitrided area became larger. These results suggest that plasma jet operations under a low pressure environment is very effective for uniform large-area plasma processing.

JTP3 2 Plasma Features in a Supersonic Ammonia or Nitrogen/Hydrogen-Mixture Plasma Jet Generator HIROKAZU TAHARA, TETSUJI SHIBATA, YASUTAKA ANDOH, TOSHIAKI YASUI, KEN-ICHI ONOE, TAKAO YOSHIKAWA, *Graduate School of Engineering Science, Osaka University, Japan* Spectroscopic measurement was carried out to understand the plasma features in a 10-kW-class water-cooled direct-current arcjet generator with a supersonic expansion nozzle. Ammonia or a mixture of nitrogen and hydrogen was used as working gas. In the mixture of N +nH , the H mole fraction n was varied from 0.5 to 3.0, in which a H mole fraction of 3.0 corresponded to that of simulated ammonia. The NH and N +3H plasmas in the nozzle throat were expected to be nearly in a temperature-equilibrium condition. On the other hand, the plasmas in the expansion nozzle were in thermodynamical nonequilibrium, because the electron number densities rapidly decreased downstream. As a result, the H-atom excitation temperature and the N rotational excitation temperature decreased from 7000-11000 K in the throat to about 4000 K and to 1000-1500 K, respectively, on the nozzle exit at input powers of 7-12 kW, although the NH rotational excitation temperature did not axially decrease significantly.

JTP3 3 Unstable Arc Motion in an Atmospheric Pressure Furnace MAX KARASIK, S.J. ZWEBEN, *Princeton University Plasma Physics Lab* Plasma Arc Furnaces are used extensively in metallurgical processing and hazardous waste remediation. Studies of arc equilibrium and stability are being carried out on an experimental 20 kW 250 A DC open air arc at PPPL. Intermittent arc motion in the frequency range of 200-1000 Hz has been observed on a steel and graphite anodes with a graphite cathode, with frequency varying approximately 10% within a burst. Arc motion is typically accompanied by $\sim$ 10% rms current and $\sim$ 3% rms voltage fluctuations and sometimes leads to arc extinction. Possible sources of the instability are being investigated, including the cathode jet, arc current, and anode geometry and composition effects. Stability measurements in the arc current, arc length parameter space as well as dependence on anode material and geometry will be compared with theoretical model predictions.

JTP3 4 Application of the Computer Tomography Technique to Diagnostics of the Plasma Jet SATOSHI SAKIYAMA, OSAMU FUKUMASA, *Faculty of Engineering, Yamaguchi University, Japan* The thermal plasma jet has a great potential for processing materials, i.e. spray coating, production of fine particles and synthesis of new materials. To realize high quality processing using plasma jet, it is important to measure the plasma parameters with high accuracy. The parameters of the plasma jet have been usually measured using Abel inversion method on the assumption that the plasma jet is axially symmetric. But the processing plasma jet becomes axially asymmetric, because the material gases or powders are injected into the jet. Therefore, Abel inversion method can't be applied. The purpose of this study is to develop the diagnosis of the asymmetric plasma jet. In this paper, the application feasibility of the computer tomography (CT) technique to measuring the heat transfer flux of the asymmetric plasma jet is studied. The shape of the plasma jet is deformed by injecting the material gas perpendicular to the jet axis. Heat transfer flux is measured with the calorimetric probe and algebraic reconstruction method (ART) is used as the reconstruction technique. The heat transfer flux profile obtained shows two off-axis peaks and it is found that CT technique is available for the diagnostics of the asymmetry plasma jet.

JTP3 5 Synthesis of β''-Alumina from Powder Mixtures Using Thermal Plasma Processing OSAMU FUKUMASA, SATOSHI SAKIYAMA, HIROTOSHI ESAKI, *Faculty of Engineering, Yamaguchi University, Japan* Thermal plasma processing, using the plasma jet with high speed and high heat capacity under reduced pressure ($\leq$ 100 Torr), is one of the most promising methods to synthesize new materials. To this end, we have developed the thermal plasma reactor composed of the forced constricted type plasma jet generator and the feed ring, and also confirmed that this reactor generates stable plasma jets with high heat capacity for various operation conditions. With the use of this plasma jet reactor, synthesis of thermoelectric materials (β''-alumina) for the Alkali Metal Thermo-Electric Converter (AMTEC) has been studied. Under not only atmospheric pressure but also low pressure, thin-films of β''-alumina are successfully synthesized from the powder mixtures, i.e. α-Al_2O_3, Na_2CO_3 and MgO. Powder species ratio, jet temperature, jet power and substrate position affect strongly synthesis of β''-alumina.

JTP3 6 Efficient Production of Endohedral Metallofullerenes in Repetitive Gravitation-Free Arc Discharge by Means of a 12m Vertical Swing Tower MIENO TETSU, *Dept. Phys., Shizuoka Univ.* By using an arc discharge in helium gas atmosphere (several 10 kPa), various kinds of fullerenes and endohedral metallofullerenes are produced in large quantities, where sublimated carbon atoms from an anode frequently collide each other and with helium atoms in high-temperature gas phase and they self-organize various kinds of fullerenes. In usual discharge, there is a strong heat convection from the arc plasma region due to the gravity, which reduces production time of fullerenes. In order to confirm this gravitational effect, production of endohedral metallofullerenes in gravitation-free arc discharge is investigated by means of a 12-m-high vertical swing tower, in which thermal convection of hot gas is suppressed and long-duration hot reaction of carbon molecules can be realized. As a result, production rate of lanthanum metallofullerene (LaC82) in gravitation-free condition prominently increases compared with that in steady-state gravita-

tional condition. Ref. : T. Mieno, Jpn. J. Appl. Phys. Vol. 37, Pt. 2, No. 6B (1998) (in press).

SESSION JTP4: POSTER SESSION: MAGNETRON PLASMAS

Tuesday afternoon, 20 October 1998
Haku/Pikake Room, Aston Wailea at 17:15
Irving Langmuir, General Electric, presiding

JTP4 1 Steady State Properties of Magnetron Sputter Simulation C.H. SHON, Y.K. SHIN, J.S. PARK, J.K. LEE, *Pohang Univ. of Science and Technology, Pohang 790-784, Korea* Y.S. MOON, *LG Electronics, Kumi, Korea* T.H. CHUNG, *Dong-A Univ., Pusan, Korea* Results of the particle simulation of a magnetron sputter are presented. By a kinetic code OOPIC, we obtain the spatial profiles of plasma density, potential, and velocity distribution-function along with the electron and ion temperature, the current density, and the deposition profiles at the substrate. The current density from simulation is compared with the Child-Langmuir law applied to the magnetron discharge[1], and the global model[234] to estimate the steady state properties of magnetron sputter. When normalized to above Child-Langmuir law, the current density profile from simulation converges. The velocity distribution-function of electron is Maxwellian, but that of ions is non-Maxwellian near the cathode with majority in the energy range below 50 eV which shows the need for particle simulation.

[1]K. Kuwahara and H. Fujiyama, IEEE Trans. Plasma Sci., 22, 442 (1994).
[2]H.J. Lee and J.K. Lee, Jpn. J. Appl. Phys. Part 1, 35, 6252 (1996).
[3]J.K. Lee, L. Meng, Y.K. Shin, H.J. Lee and T.H. Chung, Jpn. J. Appl., Phys. Part 1, 36, 5714 (1997).
[4]M. Yoon, S.C. Kim, H.J. Lee and J.K. Lee, J. Korean Phy. Soc., 32(5), L635 (1998).

JTP4 2 2D Selfconsistent Simulation of a DC magnetron Discharge and Its Target Erosion Profile K. OKAZAWA, N. NAKANO, T. MAKABE, *Keio University at Yokohama, Japan* E. SHIDOJI, *Asahi glass Co.,Ltd. Yokohama* A two dimensional simulation of a conventional DC magnetron discharge with Al target is performed in Ar by a hybrid model consisting of fluid and particle models, where the fast electrons with $\epsilon > 8$ eV are treated by particle model. The transport of the fast electron is quite important for the spatial net ionization, though the electron affects little the field distribution. The numerical structure close to the target of the magnetron discharge show a reasonable agreement with our optical emission spectroscopy. The ion velocity distribution in the local and narrow sheath region is simulated by the Boltzmann equation under the 2D ion density and field distributions. The 2D velocity profile on the target surface enable us to estimate the erosion profile. The erosion profile and the ion velocity distribution on the surface is discussed.

JTP4 3 Measurement of a Magnetron Plasma Varied by the Superposition Method with Alternating Voltages KIYOSHI KUWAHARA, HIROSHI FUJIYAMA, *Faculty of Engineering, Nagasaki University, Japan* A dc magnetron plasma in a multi-electrode type of magnetron apparatus was investigated with the superposition method that alternating voltages were superposed to the dc voltage to generate the plasma. From the investigation, it was found that the ion acoustic wave propagated in the bulk magnetron plasma at $\omega=\Omega_c$ (ω: a frequency of the superposed signals of alternating voltages, Ω_c: the Larmor frequency of ions). Moreover, the reaction of magnetron plasmas to the various superposed signals is diagnosed for the control of plasma parameters with the ion waves, etc. Especially in the discharge-modified plasma processings, such as a pulse discharge and a plasma immersion, the adjustment of the plasma parameters by means of the wave motion in plasma is considerably favorable due to using the proper motion of the plasma. The effect of the superposed signals to the plasma parameters is described at $\omega=\Omega_c$ in the magnetron plasmas with multi-electrodes.

JTP4 4 Development of Cylindrical ECR Magnetron Sputtering Apparatus AKIRA YONESU, HIROKI TAKEMOTO, NAOKI NISHIMURA, YASUMASA YAMASHIRO, *Ryukyu University* A new magnetron sputtering apparatus employing electron cyclotron resonance (ECR) discharge to achieve high sputter deposition rates at the low gas pressures has been developed. The apparatus is composed of a stainless steel chamber which contains a water cooled electrode, a microwave system. Similarly to a standard cylindrical multipolar magnetron system, permanent magnets are placed inside the electrode. And these magnets have magnetic flux density of about 3.8kG at their surfaces, which is higher than that of the magnets used in usual magnetron system, so that the region of the magnetic field for ECR exists near the electrode surface. The interaction between the microwave and the magnetic field around the electrode surface induced ECR and generated the plasma. Sputtering is done in this apparatus by generating ECR plasma and applying DC negative voltage to the electrode which also serves as the target for the sputtering. The maximum target current in this apparatus is about high of 1.0A at even low gas pressure of 0.2mTorr. An impurity free sputtering with the high deposition rate can be expected in this apparatus.

JTP4 5 Analyses and Design of Magnetic Field in a Magnetron Sputtering System SHUNJI IDO, *Saitama University* MASANORI KAWASHIMA, *Saitama University* MIEKO KASHIWAGI, *Saitama University* The magnetic field analyses are carried out for a magnetron sputtering plasma with a ferromagnetic target by using a FEM(Finite Element method) code. When a ferromagnetic target is used, the plasma is generated locally due to the magnetic field configuration affected by the existence of a ferromagnetic material. Then, the erosion is advanced quickly in the localized narrow area resulting in the shortening of lifetime of a ferromagnetic target. In this study, the magnetic field configurations are studied by using a FEM code. To compare with the experimental results, the procedure of the erosion advance is divided into several time steps. The computational results show the good agreement with the experimental results. The target configuration is examined and designed to improve the lifetime of a ferromagnetic target. In the design, the ferromagnetic material is placed near the target. The magnetic field is affected by this additional material, and the magnetic field configuration is modified. In the magnetic field analyses by FEM, the useful mesh generation method is applied because the target configuration is change. Especially, this method is useful in the analysis that the erosion profile is changed by sputtering with the time advance.

JTP4 6 Computational Studies of Plasma Generation and Control in a Magnetron Sputtering System SHUNJI IDO, *Saitama University* MIKIHIKO TAKAHASHI, *Satiama University* MIEKO KASHIWAGI, *Saitama University* Recently, the magnetron sputtering system is widely used in the field of thin film deposition. It is useful to study the feature and control methods of plasmas in a magnetron sputtering system. The computational studies on the plasma generation problem and the erosion generation are carried out by the particle code. The magnetic field is studied by Finite Element method(FEM). Electrons are traced by solving the equation of motion. Collisions between electrons and neutral atoms, ions and electrons are calculated by Monte Carlo method. The distributions of ionization collision points are assumed to show the plasma distribution. The problems of plasma generation and diffusion are examined in the simulations. The results are compared with the experimental ones. The effects on the plasma distribution by the sheath thickness and the target configurations are analyzed. Electromagnetic features of the magnetron system are examined for several designs of electrodes, additional magnetic field configuration, and materials.

JTP4 7 Production Of Multi-magnetron Plasma By Using Polyphase Ac Glow Discharge In An Improved Multi-pole Magnetic Field KAZUNORI MATSUMOTO, KENTARO MOTOKI, MASAHIRO MIYAMOTO, *Electronics and Informatics, Toyama Prefectural University* YASUHIRO UETANI, *Research Institute for Technology, Toyama Prefectural University* Effects of an improved multi-pole magnetic field on a plasma production generated by a polyphase ac glow discharge with multiple electrodes have been investigated. Conventional configuration of the multi-pole magnetic filed has been modified to suppress plasma losses at both ends of the chamber due to ExB drift motion. The modified multi-pole magnetic field has enabled us to produce a multiple magnetron-plasma at a considerably low pressure less than mTorr. The low temperature plasma has been widely used as the fine processing technology of a dry etching and as the thin film formation technology of a sputtering coating. Large-scale plasmas which can be generated at a low gas-pressure have been desired for more wider dry etching and greater sputter coating. The purpose of this study is to develop a large-scale and low-cost plasma generator by using a polyphase ac power source with the low frequency. In this session, we will present the experimental result as to a multiple magnetron-plasma generated in the modified twenty-four poles magnetic field by using the twenty-four-phase ac power source with the commercial electric power frequency of 60Hz. The ac power is supplied to twenty-four electrodes which are fixed to the water-cooled chamber-wall through sheet insulators so that the electrodes can be cooled indirectly.

SESSION JTP5: POSTER SESSION: ETCH
Tuesday afternoon, 20 October 1998
Haku/Pikake Room, Aston Wailea at 17:15
Irving Langmuir, General Electric, presiding

JTP5 1 SiO_2 Etching Characteristics in DC and RF Magnetron Plasmas with an External Magnetic Field HIROSHI YAMADA, KIYOSHI KUWAHARA, HIROSHI FUJIYAMA, *Faculty of Engineering, Nagasaki University, Japan* Using an external magnetic field type of magnetron plasma equipment, we compared of SiO_2 (cultured quartz crystal) etching characteristics in DC and RF magnetron plasmas. The etching rates were about the same in both DC and RF magnetron plasmas at the same power level, but the etching uniformity in RF magnetron plasma was better than that in DC. In addition, it was found that the etching mechanisms were ion assist etching in DC magnetron plasma and chemical etching in RF magnetron plasma, respectively. In the mixed gas (CF_4+Ar, CF_4+O_2) plasmas, it was confirmed that the creation of C_xF_y polymer in RF magnetron sputtering decreased comparing with that in DC, which is based on an observation of FE-SEM on the surface of etched substrate and an investigation on the elimination effect of C_xF_y polymer by the feedgas of O_2. In this study, we obtained the optimum etching characteristics for 200W in RF power, 236gauss in magnetic flux density and 1.7×10^{-3}torr in operation pressure. Furthermore, crystal resonators by using inverted mesa blanks (etched culture quartz crystal) was created in RF magnetron plasma and their electrical characteristics as a crystal resonator were measured. As a result, it was found that the fundamental mode of the crystal resonators was about 120MHz for 13.8μm in thickness.

JTP5 2 Behaviors of CF_x(x=1-3) and polymeric species in electron cyclotron resonance fluorocarbon plasmas KUNGEN TEII, MASAFUMI ITO, MASARU HORI, TOSHIO GOTO, *Department of Quantum Engineering, Nagoya University, JAPAN* NOBUO ISHII, *Tokyo Electron, Ltd., JAPAN* Film formation on the etched wafer or the reactor wall is known to give significant influences on the plasma and plasma-surface chemistries. Extensive studies on the surface irradiated in fluorocarbon plasmas have suggested that polymeric species produced in conventional low density plasmas are the predominant contributors to the film-forming flux. Therefore, analysis of the behavior of the polymeric species as well as CF_x(x=1-3) radicals is highly desired for the advancement of the radical controlled etching technique. In this study, polymeric and CF_x(x=1-3) species in electron cyclotron resonance fluorocarbon plasmas were analized by using low-energy ($\leq$ 10 eV) electron attachment mass spectrometry (EAMS) and infrared diode laser absorption spectroscopy (IRLAS). In addition to the most abundant F^-, resulted exclusively from dissociative electron attachment to various fluorocarbons, $C_3F_7^-$ and $C_4F_9^-$ were detected in C_4F_8 plasmas near the reactor wall at 40 mTorr, 500W, and relatively long gas residence time on the order of 10 $\sim$ 100 s. This fact confirmed the existence of C_3F_7 and C_4F_9. The behaviors of these polymeric species are discussed on the basis of those of CF_x(x=1-3) radicals.

JTP5 3 FTIR Ellipsometric Measurement of Chemical Bonds Formed on SiO_2/Si Surfaces Treated by Inductively Coupled Plasmas in Fluorocarbon Gases HIDEKI MOTOMURA, KUNIHIDE TACHIBANA, *Department of Electronic Science and Engineering, Kyoto University* We have been performing *in situ* diagnostics of chemical bond states on the surfaces exposed to fluorocarbon gas plasmas by using our developed FTIR phase modulated ellipsometric technique. On Si substrates we succeeded in the detection of CF_x, CHF_x, C=C, Si–C and SiF_x bonds, and investigated the dependence of those bond strengths on the treatment conditions such as kinds of fluorocarbon gases, operating gas pressure, substrate bias voltage etc. In the second step, similar measurement must be done on SiO_2 surfaces for fully understanding the selective etching mechanisms of SiO_2 over Si. However, in our method a severe interference occurs due to large SiO_2 bond signal around the wavenumber region of 1100–1300 cm^{-1} in which CF, CHF_x and C=C bonds have been detected. One effective method for avoiding this interference is to search for alternative wavelength region for those bonds. Thus, we changed the

central wavenumber for the phase modulation from 1000 cm^{-1} to 2800 cm^{-1}, and succeeded in the detection of C=C bond at 1700 cm^{-1} with better sensitivity. A systematic measurement is under progression.

JTP5 4 Vacuum Beam Studies of Photoresist Etching Kinetics FRANK GREER, GOWRI KOTA, JOHN COBURN, DAVID GRAVES, *UC Berkeley* One factor limiting the development of quantitative models of high density, low pressure oxide etch plasmas is the relatively poor understanding of the plasma-photoresist interactions. In particular, the relatively high rates of photoresist loss experienced in fluorocarbon plasmas is a significant problem. To develop reliable models of these etch tools, it is necessary to predict etch loss rates as a function of the neutral to ion flux ratio as well as the ion energy dependence. This research models the complicated chemistry of these fluorocarbon plasmas with independent, well-characterized beams of energetic argon ions and neutral fluorine atoms intersecting at the surface of a photoresist sample. We will present experimental evidence showing that the etch yield of photoresist (carbon atoms removed per incident argon ion) is characterized by three main regimes: an ion flux limited regime, a fluorine atom flux limited regime, and an intermediate transition regime. The effect of hydrogen on the photoresist surface reactions has also been explored through the addition of a hydrogen atom flux, and the etch yield has been quantified. In addition, the relative reactivity of hydrogen and fluorine atoms towards heteronuclear abstraction on the photoresist surface has been measured.

JTP5 5 In situ Measurement of Resist Etch Rate with Submicron Pattern H. KAWATA, H. FUKUDA, T. MATSUNAGA, M. YASUDA, K. MURATA, *Osaka Prefecture University, Japan* The etch rate often depends on the aspect ratio of the etched pattern when very fine patterns are etched. Then, it is very important to know the time dependence of the etch rate. In our report the reflection intensity of the laser beam which is irradiated to the sample is examined experimentally and theoretically. The tri-level resist film is prepared on silicon wafer. The 0.5μm period grating is etched in the the bottom layer ($\sim$ 1.2μm positive photo resist) by O_2 plasma with a conventional parallel plate type reactor at the pressure of 1.3Pa. The laser beam with 670nm wavelength is irradiated to the sample. The time variation of the reflection intensity is periodical but the amplitude is not constant. The reflection intensity is simulated assuming that the etched line profile is rectangular. Good agreement can be obtained between the simulation and the experiment. The etch rate is estimated about 110nm/min. We can demonstrate the in situ monitor of the etch rate in the submicron grating etching.

JTP5 6 Influences of the modified materials on plasma parameters in plasma surface treatment MASAAKI KATOH, TAKAYUKI KOUNO, *Gunma College of Technology* KIYOSHI MIYASHITA, *Gunma Prefectural Industrial Technology Research Laboratory* TAKEO OHTE, *Gunma College of Technology* AKIRA KOJIMA, *Gunma College of Technology* SUGIO OHTANI, *Tokai University* Influences of the modified materials on plasma parameters in plasma surface treatment have been investigated by using various plasma diagnoses. Many analyses about the effects of plasma on materials have been carried out till now. However, on the other hand, how plasma changes in case a treated material exists, compared with plasma itself, is not much examined. This study becomes important in next cases. (1) Large quantities of materials are treated simultaneously. (2) Time for modifying is long. After the plasma is generated and stabilized on condition that there is no material within the chamber, change of plasma parameter was measured by using quadruple mass-spectrometer, emission-spectrometer and lagmuer probe in case that the modified material is inserted into its plasma. Then, the same measurements are carried out when it is removed from the treatment chamber. We show topical results. We used carbon material and O_2 plasma. By means of mass spectra measurement, both the peak magnitudes of O^+ and O_2^+ decreased to 15% of peak magnitudes without the material 1 sec. after the carbon was inserted into the chamber and their magnitudes kept constant for 5 min. at least. In case of removing the material from its chamber 5 min. after inserting the material, the peak magnitudes of O^+ and O_2^+ increased and returned to the value i before insertion, 2 min. (O^+) and 4 min. (O_2^+) after removal.

JTP5 7 Direct Simulation Monte Carlo Analysis of Flows and Etch Rate in a Model Inductively Coupled Plasma Reactor K. NANBU, *Inst. Fluid Science, Tohoku Univ.* T. MORIMOTO, *Central Research Laboratory, Tokyo Electron Ltd.* M. SUETANI, *Tohoku Univ.* The etch rate of a silicon wafer is calculated by coupling the Direct Simulation Monte Carlo analysis of the rarefied flow of etchant with the Particle-in-Cell simulation for the production of etchant in an inductively coupled plasma source. Chlorine gas is fed from the shower head at the top of a model reactor. The chlorine gas, etchant, reaction product are pumped from an annular duct between the substrate edge and chamber wall. The species considered are electron, Cl_2, Cl, Cl^-, Cl_2^+, and $SiCl_2$, where $SiCl_2$ is the reaction product. The etchant is assumed to be Cl and/or Cl_2. The objective of our work is to examine the effects of several factors on the etch rate and its uniformity. For example, these factors are the mass flow rate of the source gas Cl_2, the reaction probability of Cl_2 on the wafer, and the recombination probability of Cl on the chamber wall. As the mass flow rate increases, the etch rate increases and also its uniformity becomes better.

JTP5 8 Modeling of Aluminum Etching in a Commercial High Density Plasma Reactor Using BCl_3/Cl_2/Ar Gas Mixtures* S.J. CHOI, P. HO, A. TING, *Sandia National Laboratories* E. MEEKS, *Reaction Design, Inc.* The predictive capability of numerical plasma reactor models depends sensitively on the accuracy of the plasma chemistry mechanisms, the database, and the surface chemistry that are included in the models. A comprehensive plasma-etch mechanism has been developed to describe the high-density plasma etching of aluminum in a BCl_3/Cl_2/Ar mixture. Results of extensive validation comparisons with experimental data (from various experiments at Sandia) are shown for several different reactor models (Aurora, MPRES, and PROTEUS) employing the aluminum-etch mechanism. Comparisons are made to both diagnostic measurements of the gas-phase as well as to wafer-etch data from a commercial reactor. The gas-phase chemistry and aluminum-etch mechanisms provide very good quantitative agreement between the models and the wide collection of observations and measurements available in this study over wide ranges of power, pressure, and gas mixture. Simulation results from the 2-D model predict well the measured radial uniformity for blanket-aluminum etching.

*This work performed at Sandia National Laboratories supported by SEMATECH and DOE under contract DE-AC04-94AL85000.

JTP5 9 Escape of electrons as a reason for formation of an ion-ion plasma in electronegative pulsed discharges for etching A.A. KUDRYAVTSEV, *Institute of Physics, St.Petersburg State University, Russia* In the recent research on plasma etching (e.g.[12]) it has been pointed out that using a pulsed plasma enables to improve substantially the etching quality. The rapid temporal decrease in the electron density observed experimentally in these plasmas is explained by the mechanism of electron-to-molecule attachment. In our opinion, the interpretation of the above effect which invokes mainly the volume plasmachemical processes, is incomplete. The reasoning is that it ignores other fundamentally important aspects of the transport processes in electronegative gases, which manifest themself via the existence of the two-stage decay of such a plasma[3]. In[4] we have used these aspects to explain the charged particles behaviour observed in a pulsed negative-ion current source. In this report we further demonstrate that whether or not the processes of electron-to-molecule attachment are included does not change the established by us earlier picture explaining the relatively rapid escape of electrons from the volume in the first stage of decay. This circumstance may be of a fundamental importance for understanding the physical mechanisms in high-performance plasmas used for etching. Work supported by RFBR under grant 98-02-17778.

[1]T.H.Ahn et all., Plasma Sources Sci.Technol., 5(1996)139
[2]S.Samukawa et all., J.Vac.Sci.Technol.A 14(1996)3049
[3]S.A.Gutsev et al., Tech.Phys. 40(1995)1131
[4]A.A.Kudryavtsev, Tech.Phys.Lett. 22(1996)693

JTP5 10 Patterned Platinum Etching Studies in an Argon High Density Plasma SÉBASTIEN DELPRAT, *INRS-Énergie et Matériaux* MOHAMED CHAKER, JOËLLE MARGOT, *Univ. de Montréal* HENRI PÉPIN, *INRS* LIANG TAN, TOM SMY, *Carleton Univ.* A high-density surface-wave Ar plasma operated in the low pressure regime is used to study pure physical etching characteristics of platinum thin films. The platinum samples are RF biased so as to obtain a maximum DC self-bias voltage of 150 V. The sputter-etching characteristics are investigated as a function of the magnetic field intensity, the self-bias voltage and the gas pressure. At 1 mtorr, the etch rate is found to be a unique linear function of both the self-bias voltage and the ion density, independently of the magnetic field intensity value. However, even though the ion density increases, the etch rate is found to decrease with increasing pressure. In the low pressure regime, etch rates as high as 2000 A/min are obtained with a good selectivity over resist. Without any optimization of the etching process, we were able to etch 0.5 micron Pt trenches, 0.6 micron thick yielding fence-free profiles and sidewall angles (75) that already meets the present industrial requirements of NVRAM technology.

JTP5 11 Enhancement of Dry-Etching Durabilities by Energy or Etchant Quenching with aliphatic, aromatic and alicyclic homopolymer, polymer blends and copolymer MASAHITO KUSHIDA, *Chiba Univ.* KIEKO HARADA, *Chiba Univ.* KYOICHI SAITO, *Chiba Univ.* KAZUYUKI SUGITA, *Chiba Univ.* Dry-etching rates for O_2 reactive ion etching, O_2 plasma etching, Ar sputter etching, and Ar ion beam etching were descending in the order of poly(methyl methacrylate) [PMMA], poly(isobornyl methacrylate) [PIBMA], poly(α-methyl styrene) [PMSt], and poly(2-vinylnaphthalene) [PVN]. 2-vinylnaphthalene monomer units were found to be more effective for enhancing dry-etching durability, which was defined as the reciprocal of etching rate, and for quenching the etching energy or etchants, than α-methyl styrene units. Dry-etching rates of PMMA, PMSt, and PVN homopolymers increased linearly proportional to reciprocal carbon atom content in a monomer units. However, dry-etching rates of polymer blends (PMMA/ PMSt, PMMA/ PVN) or copolymer (MMA-co-IBMA) did not follow the linear relationship, namely durabilities were larger than the value deduced from the reciprocal carbon atom content in a monomer units. The durability deviation from the estimated value was larger with PMMA/ PVN blends than that with PMMA/ PMSt blends, which means that the etching energy travels or etchants migrate for longer distance in the former blends.

SESSION JTP6: POSTER SESSION: GLOWS
Tuesday afternoon, 20 October 1998
Haku/Pikake Room, Aston Wailea at 17:15
Irving Langmuir, General Electric, presiding

JTP6 1 Abstract Withdrawn

JTP6 2 Spatially and temporally resolved measurements of electron density variations caused by shockwaves in plasmas PETER BLETZINGER, *ISSI, Beavercreek, OH* J.T VERDEYEN, *Univ.of Illinois* B.N. GANGULY, *AFRL, WPAFB, OH* A focused beam microwave interferometer was designed to measure spatially resolved electron density (N_e) variation in 10 to 40 Torr, 30 to 150 mA DC discharges in nitrogen. The discharges were between cylindrical electrodes spaced 20 cm apart in a 5 cm dis. Pyrex tube. The objective was to obtain maximum spatial resolution and still have enough sensitivity for N_e in the 10^9 - 10^{10} cm^{-3} range. The X-band frequency range was selected. Spatial resolution was provided by a pair of spherical mirrors, arranged to focus microwave beam on the discharge axis. The interferometer was used to measure changes in N_e produced by shockwaves from a 100 Joule spark discharge outside the cathodic electrode. At the expected arrival time of the shockwave, the N_e showed a pulsed increase to almost 50 percent of the steady-state value followed by a strong decrease. The width of the increase, limited by spatial resolution, was 10^{-4} seconds. The timing of the N_e pulse showed the same increase of the shock velocity with increasing discharge current as observed with simultaneous laser photodeflection measurements. The N_e pulse is interpreted as a consequence of strong electric field modulation caused by the shockwave.

JTP6 3 Non-linear behavior of low-current Townsend discharges J. ŽIVKOVIĆ, I. STEFANOVIĆ, S. ŽIVANOV, S.B. RADOVANOV, Z.LJ. PETROVIĆ, *Institute of Physics, University of Belgrade, Belgrade, Yugoslavia.** Low-pressure, low-current discharges in argon were recently studied in order to identify the effect of space charge on the transition from the low-current diffuse to constricted discharge[1]. In this paper we present two aspects of non-linear behaviour. Under special circumstances the damping coefficient of induced oscillations increases with current only to start decreasing and free running oscillations develop eventually. The damping coefficient and negative differential resistance may be described by a constant and an additional current dependent term. In transition to constrictions, exponential development of the electron number density, as viewed through emission profile, is gradually modified and converted to the profile typical for constricted (normal) glow.

*Supported by MNTRS 01E03 project.
[1]Z.Lj. Petrović and A.V. Phelps Phys. Rev. E **56** (1997) 5920

JTP6 4 Wafer Floating Potential for a High Current Serial Ion Implantation S.B. RADOVANOV, S. WALTHER, P. COREY, G. ANGEL, D. BROWN, *Varian IIS, 35 Dory Road, Gloucester, MA 01930** In situ wafer floating potential measurements were made during high current high dose ion implants. Implants were performed on a large area ribbon beam implanter, that uses a low temperature plasma for charge control. Real time potential variations were monitored simultaneously from different areas of the wafer. The actual device consisted of 400 capacitor sites uniformly distributed on the wafer surface. This allowed spatially resolved probe potential measurements. The device used here is a large planar Langmuir probe whose dimensions, while probably larger than the Debye length associated with the beam provide upper limit positive charging The low-pressure plasma used for ion beam neutralization is modeled using the numerical electrodynamic 2.5 D simulation program. The effect of plasma arc current was measured for different current and energy beams. Results show that, even with the low ion beam density 0.05 A/cm2, "cold" electrons are still necessary to maintain device potentials below 5 volts.

JTP6 5 Spatial Profiles of Charged Particles in Multipolar-Magnetic Confined Ar/O_2 Plasmas T. KIMURA, K. INAGAKI, K. OHE, *Nagoya Institute of Technology* The spatial profiles of charged particles in multipolar-magnetic confined Ar/O_2 plasmas produced by DC discharges are investigated by varying the total pressure from 2 mTorr to 10 mTorr, the discharge current from 10 mA to 90 mA, and the oxygen content from 4% to 20%. The measured spatial negative ion and electron density profiles, which are approximated as a parabolic distribution and a uniform one except in the vicinity of the chamber wall, respectively, allow us to divide the entire discharge into three regions: 1) electronegative, 2) electropositive, and 3) sheath. The ratio of negative ion density to electron density measured at the center increases with the increase in both oxygen content and pressure, while decreasing with the increase in discharge current. Oxygen content- and discharge current-dependences of the electronegative region length are similar to those of the ratio, although the length does not strongly depend on the pressure.

JTP6 6 Nonequilibrium Positive Column II. JOHN H. INGOLD, *One Bratenahl Place #610, Bratenahl, OH 44108* Previous work has shown that the first principles nonlocal kinetic method [1] is closely approximated by the nonlocal moment method [2] in positive column analysis. In the present paper, the nonlocal moment method is compared with two of the most often used local moment methods: (i) local moment method with Maxwell EEDF; (ii) local moment method with 0D EEDF. The form of the Boltzmann equation for electrons in a positive column discharge suggests that each gas has a characteristic curve of positive column E/N versus NR (E is axial electric field, N is gas density, and R is tube radius). This characteristic curve affords a systematic way of comparing various methods because its course depends on the form of the EEDF used to calculate transport coefficients and inelastic collision rates, on whether or not it is assumed that the electrons are in equilibrium with the axial field, on whether or not ion inertia is taken into account, etc. Using an argon-like gas for illustration, it is shown that the characteristic curve based on equilibrium with 0D EEDF is a poor approximation to that based on nonequilibrium for NR less than 1×10^{17} cm^{-2} (PR$<$ 3 Torr-cm), while that based on equilibrium with Maxwell EEDF is an extremely poor approximation at any value of NR.

[1]D. Uhrlandt and R. Winkler, J. Phys. D **29**, 115 (1996).
[2]J. H. Ingold, Phys. Rev. E **56**, 5932 (1997).

JTP6 7 Distribution of Electric Field across Shock Structure Propagating through a DC Glow Discharge* S. POPOVIC, L. VUSKOVIC, *Old Dominion University* A number of experiments confirmed the existence of double electric layer (DEL) due to ambipolar diffusion of electrons and ions in the shock front propagating through partially ionized gas. It was used to visualize shock shapes with an electric discharge transverse to the flow. Charge separation generated local electric field that interacted with the electric field of the discharge, to slow down the electron drift, and resulted in a decrease of luminosity along shock front. DEL effect was used to demonstrate a "bow shock generator." Voltage difference between upstream and downstream region of partially ionized gas depended on shock strength manifested in electron temperature and number density gradients. These two gradients did not necessarily coincide, and more than one DEL could be associated with the shock. Based on these facts, we derived reduced electric field distributions in a planar and oblique shock structure. We also determined the parameters and stability criteria for the regions of enhanced degree of ionization associated with DEL.

*Supported by NASA LaRC

JTP6 8 Parallel Operation of Microhollow Cathode Discharges ROBERT H. STARK, WENHUI SHI, KARL H. SCHOENBACH, *Physical Electronics Research Institute, Old Dominion University, Norfolk, VA 23529* The dc current-voltage characteristics of microhollow cathode discharges has, in certain ranges of the discharge current, a positive slope [1]. In these current ranges it should be possible to operate multiple discharges in parallel without individual ballast, and be used as flat panel excimer lamps [2] or large area plasma cathodes. In order to verify this hypothesis we have studied the parallel operation of two microhollow cathode discharges of 100 micrometer hole diameter in argon at pressures from 100 Torr to 800 Torr. Stable dc operation of the two discharges, without individual ballast, was obtained if the voltage-current characteristics of the individual discharges had a positive slope greater than 10 V/mA over a voltage range of more than 5 to obtain parallel operation over the entire current range of the microhollow cathode discharges, which includes regions of negative differential conductivity, we have replaced the metal anode by a semi-insulating semiconductor, which serves as distributed resistive ballast. With this method, we were able to ignite and sustain an array of dc microhollow cathode discharges over a wide range of pressure and discharge current. [1] K.H. Schoenbach et al. Appl. Phys. Lett. 68, 13 (1996). [2] A.El-Habachi and K.H.Schoenbach, APL. 72, 1 (1998). This work was funded by the Department of Energy, Advanced Energy Division, and by the Air Force Office of Scientific Research (AFOSR) in cooperation with the DDR&E Air Plasma Ramparts MURI Program.

JTP6 9 Dependence of the power balance on the reactor aspect-ratio and magnetic field intensity in high-density plasma reactors JOËLLE MARGOT, *Univ. de Montréal* MOHAMED CHAKER, *INRS-Énergie et Matériaux* SÉBASTIEN DELPRAT, *INRS* OLIVIER PAUNA, *UdeM and Univ. Paul Sabatier* DJEMILA BENHABIB, *INRS* Using the flexibility offered by our low-pressure surface-wave plasma reactor in terms of operating parameters, a series of experiments have been conducted in argon for determining the dependence of the spatial distribution of charged particles and of the power absorbed per electron, θ on the magnetic field intensity and on reactor length. It is found that the plasma density presents a maximum at an axial position corre-

sponding to the middle of the reactor chamber rather than in the source region, which indicates that the axial density profile is dominated by diffusion. In addition, the parameter θ becomes independent of the magnetic field intensity above a given value which depends on the reactor length, the saturation value of θ being higher (i.e. the power balance less favorable) when shorter aspect-ratios are used. This can be explained by the predominance of axial diffusion on the charged particles losses at these high magnetic fields. Preliminary results obtained in chlorine will also be presented.

JTP6 10 2-D modeling of a high-density argon plasma FRANOIS VIDAL, *INRS-Énergie et Matériaux* JOELLE MARGOT, *Univ. de Montral* MOHAMED CHAKER, *INRS* TUDOR W. JONHSTON, *INRS* OLIVIER PAUNA, *UdeM and Univ. Paul Sabatier* A simple 2-D diffusion model applicable to high-density plasmas, magnetically confined or not, has been developed. Using the basic moment equations (number density, flow density and energy density) for singly-ionized argon and for electrons, a simple anisotropic diffusion equation is derived, as in the work of Lieberman and Lichtenberg, together with an integrated power balance equation. Using appropriate diffusion coefficients, the anisotropic diffusion equation has been solved numerically for a geometry which consists in two co-axially abutting cylinders of different diameters. The model provides the spatial structure of the plasma density as well as the discharge power balance, parameterized as the power absorbed per electron θ. We have examined the influence of both the magnetic field intensity and the reactor aspect ratio on the plasma characteristics. The model reproduces the observed axial distribution of plasma density as well as the dependence of the parameter θ on the reactor length L and the magnetic field intensity.

JTP6 11 Mode Investigation in the Large Area Microwave Planar Plasma Source JOZEF KUDELA, *Graduate School of Electronic Science and Technology, Shizuoka University, Johoku 3-5-1, Hamamatsu 432-8561, Japan* IGOR ODROBINA, *Institute of Physics, Faculty of Mathematics and Physics, Comenius University, 842 15 Bratislava, Slovakia* MASASHI KANDO, *Graduate School of Electronic Science and Technology, Shizuoka University, Johoku 3-5-1, Hamamatsu 432-8561, Japan* Recently, much attention has been paid to the investigation of microwave discharges for the large area plasma processing. Many of the large area microwave plasma sources appeared in literature in the connection with the electromagnetic surface waves, which are considered as a suitable means for the enlargement of microwave discharges into the large volumes. These sources work without the use of static magnetic fields and yield the plasma with high very densities, which is very attractive from the technological point of view. However, they exhibit one serious deficiency and it is their resonant behavior with the discrete set of plasma densities bound to the particular electromagnetic modes sustaining the discharge. The azimuthally asymmetrical modes have been reported for the discharges on the large diameters. In our plasma source, we achieved the azimuthally symmetrical discharges on the diameter of 312mm. However, the more detailed study has shown that the azimuthally symmetrical light emission patterns of the discharges do not represent the azimuthally symmetrical modes but they are just the rotations or mode-jumps of azimuthally asymmetrical modes. High-speed camera photograps of the discharges and the electric field measurements indicate that the mode-jumps occur with the frequency of 10-100kHz and this frequency decreases as the gas pressure increases.

JTP6 12 Characteristics of the Interpulse Plasma of a High Power Short Pulse Microwave Discharge S. BHATTACHARJEE, H. AMEMIYA, *RIKEN and Saitama University, Japan* A plasma is produced by using microwaves (3 GHz) of high power (60 - 100 kW), short pulse width (0.05 - 1.0 μs) and a pulse repetition frequency of 10 - 500 Hz. The decay profile and the probe characteristics were measured by a Langmuir probe (plane) using a digital oscilloscope and a Boxcar integrator. Optical studies of the total emitted light were made using an optical fiber and a photomultiplier. Results indicate that the electron temperature T_e lies in the range (6 - 10 eV), and the plasma density builds up after the end of the pulse with a peak value above 10^{10} cm^{-3}. Particular attention has been paid to the plasma state between the pulses, defined as an interpulse plasma. Our studies have shown that the interpulse plasma is distinctly different from the usual afterglows of dc and high frequency pulse modulated discharges with a longer pulse width. One of the important characteristics is the high T_e even during the power off phase of the discharge, which decreased at a time scale much longer than the charged particle decay times. Another one is the thermal nonequilibrium state of the interpulse phase which differs considerably from the active parent plasma. The high T_e of the energy sourceless plasma could be favorable for the formation of radicals, metastables, multicharged ions, negative ions and other plasma-chemical reactions.

JTP6 13 Process Diagnostics of a Pulsed SLAN Microwave Plasma for Polymerizationin of Hexamethyldisiloxane A. BROCKHAUS, CH. SOLL, A. GEORG, ST. BEHLE, D. THEIRICH, J. ENGEMANN, *Forschungszentrum für Mikrostrukturtechnik-fmt, University of Wuppertal, Germany** A remote microwave-excited plasma has been utilized for the deposition of scratch resistant silicon oxide films from polymerization of hexamethyldisiloxane (HMDSO). The primary plasma is excited in a slot antenna (SLAN) geometry. Process gases are mainly oxygen and argon, whereas HMDSO is added downstream. Varying the pulse frequency considerably influences the deposition results, e.g. growth rate and film microstructure. This has been investigated experimentally by ex-situ methods (REM, FTIR) as well as by in-situ plasma diagnostics. For the latter we used imaging spectroscopy with a fast CCD camera system and mass spectroscopy with a plasma process monitor. A specific molecular fragment was found as a precursor. Process dependencies and relations to the atomic oxygen density are discussed. Conclusions for improving film quality are drawn.

*Work supported by BMBF

JTP6 14 Large Area Plasma Processing System (LAPPS)* ROBERT MEGER, RICHARD FERNSLER, MARTIN LAMPE, DARRIN LEONHARDT, WALLACE MANHEIMER, DONALD MURPHY, ROBERT PECHACEK, *Naval Research Laboratory, Washington, DC* The Large Area Plasma Processing System (LAPPS) utilizes a magnetically confined sheet electron beam to generate a planar plasma.[1,2] In present experiments a 3-5 kilovolt, $<$ 50 mA/cm^2, 1 cm x 60 cm area pulsed electron beam ($\leq$10% duty cycle) is produced by a hollow cathode. Electrons extracted from the cathode follow the ~200 Gauss magnetic field as they pass through and ionize the 30-100 mTorr background gas density. The resultant plasma distribution mimics the beam cross section producing a 1.5-3 cm thick planar plasma with peak electron density of up to 10^{12} cm^{-3}. Measurements on this plasma show electron temperatures of $<$ 1 eV with better than 5% uniformity over the area. The plasma can be produced at an arbitrary location relative to a material processing stage and away from chamber walls. The beam production method is very efficient both in

plasma production and in generation of free radicals. Initial testing using oxygen and a small pulsed system without RF bias has demonstrated isotropic ashing of a photoresist patterned by an aluminum mask. The technology is scalable to square meters for large area processing applications. Pulsed or continuous operation is possible depending on the application.

*Work supported by the Office of Naval Research

[1]R. F. Fernsler, et al., this conference

[2]R. A. Meger, et al., Proceedings of the Fourth Inter. Workshop on Advanced Plasma Tools and Process Engineering, PEUG/NCCAVS (Millbrae, CA, May 1998), p. 235.

JTP6 15 Time Resolved Optical Emission Measurement of Nitrogen Time Modulated Inductively Coupled RF Plasma S. TAKAIRA, T. NAKANO, *National Defense Academy, Japan* S. SAMUKAWA, *NEC Corporation, Japan* Pulse-time modulated inductively coupled RF plasmas are diagnosed by spatially and temporally resolved optical emission measurements in order to discuss the electron energy variation caused by the time-modulated power. The plasmas are produced through nitrogen with a helicon-type inductively coupled plasma source. The N_2 pressure is 1.3 Pa or 0.26 Pa. The typical on and off periods of the RF power are 50 μs. The (0,0) bands of the 2nd positive for N_2 and the 1st negative for N_2^+ are measured around the band-head wavelengths. The N_2 and N_2^+ emission intensities increase rapidly after the RF power is on and go through a maximum. It is also found that the emission intensity peak is more pronounced for N_2^+ than for N_2. Concerning to the pressure dependence of the emission intensity peaks of N_2 and N_2^+, the peaks at 1.3 Pa appear in the shorter time after the RF power is on than those at 0.26 Pa. The application of the uniform magnetic field decreases the emission peak significantly. These results suggest that the appearance of the emission peaks after the application of the RF power strongly depends on the electron density and the threshold energy for the emission observed.

JTP6 16 Measurement of $N_2(X^1\Sigma_g^+)$ Vibrational Excitation in a Pulsed RF Discharge* C.A. DEJOSEPH, JR., *Air Force Research Laboratory, Wright-Patterson A. F. B., OH* Measurements of vibrational excitation in the ground electronic state of N_2 have been made in an inductively coupled, pulsed RF (13.56 MHz) discharge using the Penning ionization technique in He/N_2 gas mixtures. A double-pulse system is used in which the first (longer) pulse vibrationally excites $N_2(X^1\Sigma_g^+)$ while a second (short) pulse is used to probe the vibrational populations after some set delay. The delay allows vibrational relaxation to be measured. By varying the pulse length, repetition rate, and N_2 density it is possible to distinguish direct electron pumping from pumping due to v-v exchange. Experimental results will be presented and compared with model calculations. The model includes direct electron pumping, v-v and v-t exchange, and wall deactivation of vibrationally excited molecules.

*Research supported by AFOSR

JTP6 17 Time-Resolved Optical Emission Spectrometry of Pulse -Modulated Surface-Wave Induced Argon Plasma YUKIO OKAMOTO, *Toyo University* Time variations of the optical emission in a pulse–modulated large–area surface–wave induced argon plasma are obtained. The plasma is generated in a quartz dischage tube (16 cm in diameter) by an Okamoto cavity (Jpn. Appl.**37** (1998)L170) and effused into a process chamber. Microwave power (2.45 GHz, 0-1 kW) is modulated by a square wave pulse with duration 20-100 μ sec and 10–80% duty ratio. Time resolved emission spectra of Ar I (355.4, 419.8 and 811.5 nm) are obtained with a time resolved spectrometer as a function of the duty ratio, power, pressure. Upper state energy of these lines are 15.02, 14.57 and 13.07 eV, respectively. In the case of Ar I(355.4 and 419.8 nm) the intensity of these lines were increased rapidly (spike) just after the microwave power was turned on, and just after the power was turned off, the intensity decays rapidly. On the other hand, no spike was observed for Ar I(811.5 nm) over the wide pulse range, and the intensity decays more slowly just after the power turned off. The time variations of these signals are compared with the time variations of the electron temperature and the electron density measured by a Langmuir probe. Good correlations were obtained between these results.

JTP6 18 Transitions and Scaling Laws for Electronegative Discharge Plasma Models A.J. LICHTENBERG, M.A. LIEBERMAN, I.G. KOUZNETSOV, *University of California, Berkeley* T.H. CHUNG, *Dong-A University, Pusan, Korea* The equilibrium of electronegative discharges is studied in the plane-parallel approximation over a wide range of pressures and electron densities, encompassing a number of regimes that have previously been modeled analytically. The transitions between the various regions (models) have been determined in the input parameter space. It is shown that, for a given feedstock gas, these transitions can be found in terms of the two input parameters pl_p and $n_{e0}l_p$, where p is the pressure, n_{e0} is the central electron density, and l_p is the half-system length. Here n_{e0} is used as a convenient input proportional to the power. For each of the principal regions, scaling laws are developed for the most important plasma parameters in terms of the input parameters. The input parameter space is conveniently divided by whether ion flux to the wall or positive-negative ion mutual neutralization is the dominant positive ion loss mechanism. For a capacitive radio frequency discharge, scaling is also given for a complete discharge depending on the main heating mechanism (stochastic heating or ohmic heating dominated) and sheath model.

JTP6 19 Time-resolved structures in electrical discharges in gases: experiment and stochastic model A.D.O. BAWAGAN, *Department of Chemistry, Carleton University* Time resolved discharge patterns generated in gaseous dielectric breakdown (DB) are imaged using a fast optical imaging system (40 ns). The discharge patterns from various gases (He, air, SF6) show general features consistent with their known dielectric strength. A new stochastic pattern-forming model that explicitly includes physical time is presented and is shown to produce theoretical DB patterns in qualitative agreement with the present experimental discharge patterns for air. The stochastic DB model also provides an approximation to the discharge current which is in good agreement with published current wave forms.

SESSION JTP7: POSTER SESSION: ELECTRON/ION TRANSPORT AND CHEMISTRY
Tuesday afternoon, 20 October 1998
Haku/Pikake Room, Aston Wailea at 17:15
Irving Langmuir, General Electric, presiding

JTP7 1 Electron energy distribution function in N_2 Townsend discharges - measurements and Monte Carlo simulation S. VRHOVAC, V.D. STOJANOVIĆ, B.M. JELENKOVIĆ, Z.LJ. PETROVIĆ, *Institute of Physics, University of Belgrade, Belgrade, Yugoslavia.* Electron energy distribution functions (EEDF) in N_2 Townsend discharges for E/N between 1 and $30kTd$ were measured using multigridded energy analyzer behind a small $(0.1mm)$ apperture on the graphite anode. Using the Monte Carlo simulations we h ave calculated the energy of electrons impinging the anode within the solid angle subtended by the detector used for measuring the EEDF. At moderate E/N ($\leqslant 3kTd$) EEDF decreases nearly exponentially with electron energy for both experiment and MC data . At high E/N MC and experimental results are in agreement with measurements throughout the entire energy range including a broad, high energy peak, only when both secondary and backscattered electrons[1] were included in simulation.

[1]R.L. Verma, J. Phys. D **10**, 1167 (1977) ; E.J. Scheibner and L.N. Tharp, Surface Science **8**, 247 (1967).

JTP7 2 A Pure Electron Plasma Colliding with Background Neutrals* EDWARD H. CHAO, STEPHEN F. PAUL, RONALD C. DAVIDSON, *Princeton University - Plasma Physics Laboratory* Single species nonneutral plasmas have robust confinement properties because the conservation of angular momentum in a system with azimuthal symmetry limits the allowed radial positions of the particles. If no external torques act on the plasma, the plasma cannot expand radially to the wall. However, collisions with a background neutral gas exert a torque on the rotating plasma thus allowing radial expansion. Measuring this expansion rate yields information on the electron-neutral collision frequency. In our experiment at the Princeton Plasma Physics Laboratory, a pure electron plasma is confined in a Malmberg-Penning trap and the expansion rate is measured as a function of the background pressure and of the confining magnetic field. The base pressure in the trap is 3×10^{-10} Torr while the magnetic field is normally about 200 Gauss. The plasma densities are typically 1×10^7 cm^{-3} and the temperature is 1 eV. The expansion rates, temperatures, and equilibrium density profiles are compared to theory. In addition, the $m = 1$ diocotron mode amplitude is monitored and the decay rate is also observed to depend on the background pressure.

*Research supported by the Office of Naval Research.

JTP7 3 Effects of CO_2 on electron drift velocities in air PAUL BARNES, *AF Research Laboratory* DOUGLAS ABNER, *AF Research Laboratory* Drift velocities of electron swarms are measured for dry air with varying low concentrations of CO_2. Results are compared with electron drift velocities in dry CO_2-free air. Moist air drift data is also compared using CO_2-free air and air with CO_2. A pulsed Townsend drift tube is used with a quadrupled Nd-YAG laser to determine the drift velocities by time of flight. Electron attachment is also considered.

JTP7 4 Electron Drift Velocities in Moist Air DOUGLAS ABNER, *AF Research Laboratory* PAUL BARNES, *AF Research Laboratory* Drift velocities of electron swarms are measured for moist air at various levels of relative humidity. Results are compared with electron drift velocities in dry CO_2-free air. The data provided for the various levels of humidity allow for some quantitative prediction of drift velocities for other humidity levels . A pulsed Townsend drift tube is used with a quadrupled Nd-YAG laser to determine the drift velocities by time of flight. Electron attachment is also considered.

JTP7 5 Particle Transport in Pure Electron Plasmas.* J.M. KRIESEL, C.F. DRISCOLL, *UCSD* At UCSD we confine pure-electron plasmas in Penning-Malmberg traps, which consist of cylindrical electrodes in an axial magnetic field ($B \sim 100$G). The trap is under ultra-high vacuum (10^{-10} Torr) so that transport due to electron-neutral collisions is negligible. Instead, cross-field particle transport is due to electron-electron collsions or from interactions with external fields. A plasma in one of our traps is roughly cylindrical in shape and rotates about its own axis due to the **E** x **B** drift from the space-charge field. Electron-electron collisions bring the plasma to a thermal equilibrium state of rigid rotation and uniform temperature. We find that the transport is driven by shears in the rotation velocity, and measure a coefficient of viscosity which is as much as 10,000 times larger than classical theory. This transport is driven by long-range "$\mathbf{E} \times \mathbf{B}$ drift Coulomb collisions" with impact parameters on the order of a Debye length rather than a cyclotron radius, as in classical theory. In our plasmas $\lambda_D \gg r_c$, and O'Neil and Dubin have developed theories[1] of transport in this regime. In addition to this work, I will also present measurements on the transport due to externally applied fields. The scalings provide insight into the overall confinement properties of our traps.

*Supported by ONR N00014-96-1-0239 and NSF PHY94-21318.
[1]Daniel H.E. Dubin, Phys. Plasmas **5**, 1688 (1998)

JTP7 6 Properties of electron swarm in PDP cell by Monte Carlo simulation T. FUKUYAMA, H. ITOH, *Chiba Inst. of Tech.* Y. MURAKAMI, H. MATSUZAKI, *NHK Sci. Tech. Res. Lab.* Electron transport and driven rate coefficients in a PDP cell are obtained by a Monte Carlo simulation (MCS) method. Calculations are carried out under the same condition as in the actual PDP cell. The PDP cell is 0.02cm in electrode distance and is filled 40 kPa (300 Torr) He/Xe(10%) mixture. Electron collision cross section sets for He and Xe recommended by Hayashi[1] are used. Position dependent, so called nonequilibrium electron transport and driven rate coefficients are obtained by the MCS using electric field distributions which are calculated by a one-dimensional fluid model under the local field approximation (LFA)[2]. For comparison, the similar calculations are also performed under the uniform electric fields. Discrepancies are recognized between both results. The gradients of electric field are the lager, the differences of coefficients and electron distribution functions are the more evident. This suggests that the LFA is not necessarily suitable for more detailed analysis including the strong nonequilibrium regions in the PDP cell.

[1]*Handbook of Plasma Material Science* (in Japanese), OHM-SHA (1992)
[2]Y.Murakami et al., Proceedings of Euro Display '93, P.555 (1993)

JTP7 7 Temperature Dependence of Electron Drift Velocity and Electron Collision Cross Section Sets for Ground State and Vibrationally Excited State of the CO_2 Molecule M. HAYASHI, *GEI* Y. NAKAMURA, *Keio University* The electron drift velocity in carbon dioxide was calculated at gas temperatures ranging from 193 to 573 K and at E/N values up to 100 Td, assuming that the gas was a mixture of ground state and vibrationally excited molecules and that the mix-ratio was determined by the gas temperature. The elastic momentum cross sections for the ground and the vibrationally excited molecules used in the present calculation were based on the compilation of Hayashi (1990) and recent experiments of Nakamura (1995) and Strakeljahn (1998). We also assumed that all other inelastic cross sections for the ground and the vibrationally excited molecules were the same (Schulz 1969, Srivastava 1983). The calculated electron drift velocity showed marked temperature dependence which agreed fairly well with the measurement of Elford (1980).

JTP7 8 An Elliptic Angular Moment Representation of the Boltzmann Equation EDWARD A. RICHLEY, *Xerox* Many studies have pointed out the limitations of the two-term spherical harmonic expansion of the Boltzmann equation. Typically, these limitations become apparent as the distribution function becomes so distorted that the first two terms of the expansion do not provide an adequate representation. By taking angular moments of the Boltzmann equation based on an ellipsoidal representation of the distribution function, proper asymptotic behavior of the equations is obtained with only slightly greater computational cost than for the two-term SHE. With this elliptic method, the desirable perturbation properties of the two-term SHE expansion are retained for situations of low distortion, while for highly distorted situations, the transition to a highly unidirectional distribution is accurately represented. The derivation of the equations will be shown, along with some discussion of their asymptotic behavior.

JTP7 9 Abstract Withdrawn

JTP7 10 An accurate analysis of ion transport properties by FTI method A. TAKEDA, *Shikoku Univ.* N. IKUTA, *Chiba Inst. of Tech.* The velocity distribution and the transport properties of ions in gas under electric fields are calculated using FTI method.[1] In which, the probabilities of velocity dispersion through a flight and a collision, respectively, are prepared in advance the main analysis. The velocity distribution just after scattering $\Psi s(v_0)$, i.e., just before start for next flights, is first determined through a relaxation procedure. The velocity distribution in flight $F(v_i)$ and the transport properties are accurately obtained from $\Psi s(v_0)$. Under zero field, $F(v_i)$ is, of course, obtained in the Maxwellian form. Most of ion transport properties remain in thermal values in a low range of reduced electric field E/N regardless of the relative speed dependence of the collision frequency $\nu(v_r)$, but vary in proportion to some powers of E/N depending on $\nu(v_r)$ in higher E/N. The values are influenced by not only the reduced mass M_r but also the ion-neutral mass ratio m_i/m_g. The anisotropy in the ion velocity distribution increases in proportion to E/N in a low range but saturates in higher E/N at extremely high values.[2] Such variations are of interest from the view point of the trajectories under electric field.

[1]S. Okuda, R. Kawakami, T. Miyazaki and N. Ikuta: J. Phys. Soc. Jpn. **65** (1996) 1270.
[2]T. Miyazaki, R. Kawakami and N. Ikuta: J. Phys. Soc. Jpn. **67** (1998) 1620.

JTP7 11 Mobilities of He^+, Ne^+, Ar^+, N_2^+, O_2^+, CO_2^+ in Parent Gas over a Wide Range of E/N* EDUARDO BASURTO,[†]JAIME DE URQUIJO, CARMEN CISNEROS, IGNACIO ALVAREZ, *Instituto de Física, UNAM, México.* We have recently improved the performance of a drift tube with a mass spectrometer at its exit end, by adding to it a mass spectrometer to its ion source. Thus we have measured the mobility of He^+, Ne^+, Ar^+, N_2^+, O_2^+, and CO_2^+ in their parent gas over the combined range of gas density normalized electric field, E/N, $0.04 - 12kTd$ ($1kTd = 10aVcm^2$). As regards the monoatomic ions, our mobilities compare fairly well with those of Beatty[1] and Hornbeck[3] in the overlap range up to 1.3, 1.8 and 12 kTd, respectively. Comparisons with the mobility of the molecular ions and those of other authors[3] in the overlap range are also presented.

*Work Suported by DGAPA, Project 1N104795
[†]Also at ESFM-IPN, Grant from CONACyT

[1]See Mason E.A. and Mc Daniel E.W., "Transport Properties of Ions in Gases", Wiley, 1988.

JTP7 12 Chemical Equilibrium Model for an Ar-H_2 Non-Local Thermodynamic Equilibrium Plasma T.G. BEUTHE, *McMaster University* J.S. CHANG, *McMaster University* A chemical kinetic model has been constructed to predict the gas and electron temperature dependence of the neutral and ionic species composition in Ar-H_2 mixtures under thermal plasma conditions. The model includes electron impact, thermal impact, ion-molecule, and recombination reactions as well as accounting for diffusion. Important metastable and excited states of species have been accounted for as well as the presence of neutral molecules, radicals, and atoms, positively and negatively charged atoms and molecular ions, and electrons. All relevant electron temperature, gas temperature and pressure terms have been included. Under thermodynamic non-equilibrium conditions, Ar, H_2, and H, were found to be the dominant neutral species, H_3^+, ArH_3^+, Ar_2^+, Ar^+, or H^+ the dominant positive ion (depending on the temperature range), and H^- and electrons the dominant negatively charged species. Calculations were carried out under constant pressure and constant volume assumptions for electron and gas temperatures between 300 and 15000 K and various pressures and neutral gas compositions.

JTP7 13 Temporal variation of the electron density in afterglow of high-density CF_4, C_4F_8, and CF_4–H_2 plasmas K. SASAKI, K. KADOTA, *Department of Electronics, Nagoya University, Nagoya 464-8603, Japan* The kinetics of electrons in electronegative plasmas is greatly affected by dissociative attachment to neutral molecules, which is a major process for the formation of negative ions. In fluorocarbon plasmas, negative fluorine ions (F^-) are produced by electron attachment to various reaction products as well as the parent gas. In the present work, we have measured the temporal variation of the electron density in the afterglow of high-density CF_4, C_4F_8, and CF_4–H_2 plasmas. A conventional microwave interferometer at 35 GHz was adopted for the measurement. The electron loss frequency was evaluated from the temporal variation of the electron density which was calculated from the interferometry signal digitized with a high sampling rate of 100 MHz. In CF_4 plasmas, the variation of the electron loss frequency roughly corresponded to that of the neutral radical densities. In C_4F_8 plasmas, the electron loss frequency was higher for the discharge condition with lower dissociation degree. These results indicates that reaction products play important roles for the production of F^- in CF_4 plasmas, while in C_4F_8 plasmas, the production of F^- is governed by the parent gas. No correla-

tions were found between the electron loss frequency and the F atom density in CF_4–H_2 plasmas, which suggests that the production of F^- from F_2 is nearly negligible.

JTP7 14 A Model of Hydrocarbon Reactions in Low Temperature Hydrogen Plasmas DARREN A. ALMAN, DAVID N. RUZIC, *University of Illinois* A model of collisional processes of hydrocarbons in hydrogen plasmas has been developed to aid in computer modeling efforts relevant to plasma-surface interactions. It includes 16 hydrocarbon molecules (CH up to CH_4, C_2H to C_2H_6, and C_3H to C_3H_6) and four reaction types (electron impact ionization/dissociative ionization, electron impact dissociation, proton impact charge exchange, and dissociative recombination). Experimentally determined reaction rates or cross sections have been compiled, and estimates have been made for the cases where such information is not available. The electron impact ionization and dissociation cross sections are fit to known graphs using four parameters: the threshold energy, the maximum value of the cross section, the energy at the maximum, and a constant for the exponential decay as energy increases. Proton impact charge exchange reaction rates are calculated from a theoretical model using molecular polarizabilities. The dissociative recombination rates are described by the equation A / T^B where parameter A is fit using polarizabilities and B is estimated from known reaction rates. The resulting set of reactions can be added to computer codes to simulate these hydrocarbon reactions. Currently used in erosion/redeposition studies in controlled fusion devices, the emphasis here is on applications in plasma processing.

JTP7 15 Electron Impact Dissociation of CF_n(n=1,2,3) Radicals* P. C. COSBY, ROBERT P. HODYSS, *SRI International, Menlo Park, CA 94025* Carbon tetrafluoride is a common feedstock gas component for plasma-assisted etching and thin film deposition. Due to its paucity of stable electronically excited states, CF_4 decomposes into highly reactive radicals CF_n(n=1-3) and F in the plasma. We report progress in measuring the products and cross sections for 5 - 200 eV electron-impact dissociation of these radicals into other neutral species. The measurements are made in a fast molecular beam that is produced by charge-transfer neutralization of the corresponding molecular ion. This beam is intersected by an electron beam and the correlated dissociation products produced by the electron-molecule interaction are identified by a time and position-sensitive detector.[1] The present measurements are unique in that they observe the low energy dissociation channels that lead to neutral dissociation products and complement previous measurements of the ionization[2] and dissociative ionization[3] product channels in these species.

*Research supported by NSF Grant CHE-9713238.

[1]P. Cosby, J. Chem. Phys. 98, 7804 (1993).
[2]V. Tarnovsky and K. Becker, J. Chem. Phys. 98, 7868 (1993).
[3]V. Tarnovsky, P. Kurunczi, D. Rogozhnikov, and K. Becker, Int. J. Mass Spectrom. Ion Processes 128, 181 (1993).

JTP7 16 A Rigorous Procedure of Monte-Carlo Simulation for Ion Motion NOBUAKI IKUTA, KOHJI YAMAMOTO, *Shikoku University, Chiba Institute of Technology, Japan* A rigorous procedure of the Monte-Carlo simulation for ion motion in thermal gases with arbitrary collision frequencies dependent on the mean relative speed $< v_r' >$ is developed. In which, the mean relative speed just before collision $< v_r' >$ is determined first as a function of ion speed $v_i'(t)$. The relative velocity $v_r'(t)$ and the velocity of gas atom v_g' both just before collision are determined next. The ion velocity after collisions is determined assuming the isotropic scattering in the center of mass frame. Under zero field, the ion velocity distribution $F(v_i)$ in the Maxwellian format the same temperature of gas is obtained perhaps for the first time. The relative velocity distribution is also found in the Maxwellian form depending on the reduced mass. However, the distributions of ion velocity and of relative velocities just before and after collisions are not in the Maxwellian form except the constant collision frequency (CCF). Under electric fields, the mean collision frequency increases depending on the ion-neutral mass ratio m_i/m_g and gives influences to all the ion transport properties. Large discrepancies between the values of transverse diffusion coefficients defined as the increasing rate of the radial dispersion $d < R^2(t) > /4dt$ and the mean radial square displacements in every flights $d < \Delta R^2 > /4d < \Delta t >$ are found against the agreements for electrons.[1] This may be due to the effects of momentum conservation through collisions due to the large mass ratio. The effects of anisotropic scattering are of interest.

[1]K. Yamamoto et.al., J. Phys. Soc. Jpn. 633 (1994) 954-964.

SESSION KW1: ELECTRON-MOLECULE SCATTERING

Wednesday morning, 21 October 1998; Plumeria/Jade Room, Aston Wailea at 7:30
Kenneth Trantham, Arkansas Tech University, presiding

Invited Paper

7:30
KW1 1 Electron Scattering from NO: Cross Sections and their Implication to NO Excitation Processes Under Auroral Conditions.
M.J. BRUNGER, *Department of Physics, The Flinders University of South Australia, Australia*

We present a selection of our results for differential and integral cross section measurements of elastic, rovibrational ($0 \rightarrow 1,2,3,4$) and electronic-state excitation in NO by electron impact. The energy range of the present measurements was 7.5 - 50 eV. In general these measurements are often the only available data in the literature. However, where possible we compare the current results with those of other experimental groups and with theoretical calculations[1].A subset of these new electron impact cross sections was combined with a measured[2] IBC auroral secondary electron distribution and the electronic-vibrational populations were determined for conditions of statistical equilibrium. The model[3] of statistical equilibrium determines the density of each excited state from the balance between population by electron impact excitation and radiative cascade, and depopulation by radiative cascade and quenching by N_2, O_2 and O. Results of this analysis will also be presented at the meeting.

[1]L.E. Machado, A.L. Monzani, M-T. Lee and M.M. Fujimoto in ''Proc. Int. Sym. El- and Ph- Mol. Coll. and Swarms,'' H32, 1995; and private communication.
[2]P.D. Feldman and J.P. Doering, J. Geophys. Res. **80**, 2808-2812, 1975.
[3]D.C. Cartwright, J. Geophys. Res. **83**, 517-531, 1978.

Contributed Papers

8:00
KW1 2 Dissociative processes in electron-molecular ion collisions NADA DJURIC, GORDON H. DUNN, *JILA, University of Colorado with CRYRING team, Stockholm* There is renewed interest in dissociation of molecular ions, primarily due to needs for modeling plasma generators for etching and deposition and for modeling edge plasmas for fusion reactors. At the same time, there are improvements in experimental techniques; e.g. use of heavy-ion storage rings has opened possibilities in dissociation studies of vibrationally relaxed molecular ions. At electron energies below the dissociation energy (D_e) of a molecular ion, the most importanat process is dissociative recombination (DR). Once the energy is above D_e, dissociative excitation (DE) is allowed, and at even higher energies dissociative ionization (DI) is energetically possible. In JILA we set up an apparatus wherein light fragment ions from DE of heteronuclear molecular ions are detected. In the heavy-ion storage ring at Stockholm (CRYRING) detection of neutral fragments was used for DE and DR studies. We will discuss the techniques and give examples of DE and DI obtainet at JILA and CRYRING [1,2,3]. Work supported in part by the Office of Fusion Energy of the U. S. DOE under Contract No. DE-A105-86ER53237 with NIST and in part by the Swedish Natural Science Research Council. 1. N. Djuric et al., Phys. Rev. A 56, 2887 (1997). 2. J. Semaniak et al., Ap. J. 498, 886 (1998). 3. J. R. Peterson et al., J. Chem. Phys. 108, 1978 (1998)

8:15
KW1 3 Electron Interactions with Cl_2 LOUCAS CHRISTOPHOROU, *NIST* JAMES OLTHOFF, *NIST* The results of a synthesis and an evaluation of data on low-energy electron interactions with the neutral Cl_2 molecule will be presented and discussed. Assessed data will be shown for total, elastic, momentum transfer, ionization, and attachment cross sections, and for the electron attachment rate constant below ~ 1 eV. Cross sections for rotational excitation, dissociation into neutrals, and ion-pair formation have been measured for this molecule, but not for vibrational and electronic excitation. Reliable measurements of the transport coefficients of Cl_2 are lacking. Pertinent information on the Cl_2^+ and Cl_2^- molecular negative ions and the atomic species Cl, Cl^+ and Cl^- produced by electron impact on Cl_2 will be presented also.

8:30
KW1 4 Low-Energy Electron Scattering by BCl_3* T.N. RESCIGNO, *Lawrence Livermore National Laboratory* W.A. ISAACS, C.W. McCURDY, *Lawrence Berkeley National Laboratory* Despite the importance of BCl_3 in plasmas used for commercial etching processes, no calculations or measurements of elastic low-energy electron scattering have previously been carried out. We will describe calculations based on the complex Kohn method for elastic electron BCl_3 scattering at incident energies below 8 eV. We find a number of interesting features in the low energy cross section, including a near-zero energy virtual state, a sharp B_2 negative ion resonance at 0.25 eV and several higher energy resonances, all of which are extremely sensitive to correlation differences between the N- and (N+1)- electron systems. We will comment on the significance of these low-energy features and the consistency between our findings and the limited body of experimental and theoretical information available for this system.

*Work performed under the auspices of the USDOE by LLNL and LBL under contracts W-7405-ENG-48 and DE-AC03-76SF00098, respectively.

8:45
KW1 5 Very Low Energy Electron Scattering from Ozone and Chlorine Dioxide R.J. GULLEY, *Australian National University* T.A. FIELD, *University of Nottingham* W.A. STEER, N.J. MASON, *University College London* J.P. ZIESEL, *Universite Paul Sabatier* S.L. LUNT, D. FIELD, *University of Aarhus* Total cross-sections are reported for the scattering of electrons from

ozone (O_3) and chlorine dioxide ($OClO$) for energies in the range of 9 meV to 10 eV. The measurements were made in transmission experiments using a synchrotron photoionization apparatus with an energy resolution in the incident electron beam of ~ 3.5 meV (FWHM). The cross section for O_3 shows strong rotational scattering at low energy, through the presence of the permanent dipole moment of O_3. Superposed on this strong scattering signal, there is evidence of a weak structure around 50 meV associated with dissociative attachment. A shape resonance, known from earlier work at ~ 4 meV, is also observed. Electron scattering from $OClO$ is dominated by rotationally inelastic scattering decreasing from a peak at essentially zero eV to an energy of 40 meV, where p-wave attachment becomes more important, peaking at 50–60 meV and extending to several hundred meV.

Invited Paper

9:00
KW1 6 Electron-Molecule Collisions in Semiconductor Processing Plasmas.
VINCENT McKOY, *California Institute of Technology**

In the low-temperature, nonequilibrium plasmas used in semiconductor fabrication, collisions with electrons excite, dissociate, and ionize molecular feed gases to produce the reactive fragments that drive the chemistry for etching and other steps in the manufacturing process. Extensive and reliable data on electron-molecule collisions are therefore needed for improved numerical modelling of reactor designs and operating conditions. Yet for gases of interest, electron collision data are sketchy at best, in part because low-energy cross section measurements are often difficult. Although calculating such cross sections quantum mechanically is also challenging, the development of methods that exploit large-scale parallel computers has made such calculations practical. In this talk, I will review the progress we have made in exploiting large parallel computers to generate electron collision cross sections for gases of interest to the semiconductor industry. Following an overview of the method employed in these calculations and its computational demands, I will discuss the strategies used to parallelize the compute-intensive steps of these calculations. Results of applications to a few gases used in semiconductor fabrication will then be presented.

*Work done in collaboration with Carl Winstead and Chuo-Han Lee

SESSION KW2: SURFACE REACTIONS
Wednesday morning, 21 October 1998; Maile Room, Aston Wailea at 7:30; Seiji Samukawa, NEC Japan, presiding

Invited Paper

7:30
KW2 1 Mechanism of high aspect ratio contact hole etching.
T. OHIWA, *Microelectronics Engineering Lab. Tohiba Corp.*

High aspect ratio contact hole RIE is one of the most significant processes used in ULSI fabrication, requiring high selectivity to etch mask material (of resist) and under-layer material. This is realized by a carbon rich fluorocarbon gas chemistry, which also has the drawback of tending to cause etch stop. Deposition of carbon species generated in the carbon rich fluorocarbon gas plasma makes high selectivity to resist and under-layer possible, but it also suppresses the oxide etching reaction at the bottom of holes, by forming fluorocarbon polymer on the oxide surface there. So, it is important to understand and control the oxide etching reaction and the fluorocarbon polymer formation on the oxide at the bottom of holes, which is dominated by the transport of reactive species through the holes to the hole bottom. This paper discusses the mechanism of high aspect ratio contact hole etching regarding the transport of reactive species through the hole to the hole bottom. Reactive species involved which was examined, were, the flux of high energy species of ions and neutrals, fluorocarbon radicals, carbon species sputtered from the hole side wall, and oxygen released by the oxide etching reaction.

Contributed Paper

8:00
KW2 2 Ion and Radical Flux Estimates at Wafer Surface in Dual Frequency Narrow-Gap RIE S. MORISHITA, H. HAYASHI, T. TATSUMI, Y. HIKOSAKA, S. NODA, M. OKIGAWA, M. INOUE, M. SEKINE, *Association of Super-Advanced Electronics Technologies (ASET)* The net flux of ions and radicals at the wafer surface was estimated from the deposition rate of fluorocarbon polymer film in a dual frequency narrow-gap RIE. The frequencies applied to the upper and the lower (wafer) electrodes of the RIE were 27 MHz and 800 kHz, respectively. The electrode gap was 20 mm. A $2.6C_4F_8$, $1.9O_2$ and 95.5Ar gas mixture was used at 4.0 Pa pressure. These conditions were based on an SiO_2 etching process for 0.1-$\mu m\phi$ contact holes with high selectivity to the photoresist mask and Si substrate. In this experiment, an RF power of 800 kHz was not supplied to the lower electrode to deposit ions and radicals on the wafer surface. The deposition rate increased with electron density and gas residence time and it strongly depended on the flux of ions including C atoms not on the radicals. The net flux of the C-inclusive ions was 10^{-16} $cm^{-2}s^{-1}$ and it was greater than that of the radicals. In the

C_4F_8/O_2/Ar system, adding a large amount of Ar in order to reduce excess deposition for the etching process lowers CF_X radical concentration. Argon ion concentration was, however, less than 25 percent in spite of large partial pressure of Ar gas. Furthermore, due to the narrow-gap arrangement, plasma was confined between the two electrodes. Therefore, the net flux of C-inclusive ions became larger than that of radicals. It is supposed that the fluorocarbon ion is main chemical species that control the etch reaction in the RIE system. This work is supported by NEDO.

Invited Paper

8:15

KW2 3 Realistic Etch Yield of Fluorocarbon Ions in SiO_2 Etch Process.

Y. HIKOSAKA, H. HAYASHI, S. NODA, H. NAKAGAWA, S. MORISHITA, T. TATSUMI, M. SEKINE, *Aset*. T. TSUBOI, M. ENDO, N. MIZUTANI, *ULVAC Ltd.*

Energetic ions striking the surface with chemical species, such as ions and radicals, form a reactive layer and an etching reaction occurs. It is thought that etching rate and selectivity are defined by the composition and thickness of the reactive layer which can be controlled by ions and neutral radicals. Our goal is to clarify the relationship of incident parameters (flux, composition and energy) of chemical species with SiO_2 etching characteristics. First, the energy distribution and flux of ions arriving at the wafer were measured using an rf-floating ion energy analyzer with a mass spectrometer equipped inside an rf-biased electrode. The flux of neutral radicals was estimated by the measured spatial distribution of Under the etching conditions to fabricate 0.14-$\mu m\phi$-size contact holes, ion energy exceeded 1 keV and ion flux reached 1.4e16 $cm^{-2}s^{-1}$. The thermal flux of neutral radicals such as F and CF_X were 2-10 times larger than ion flux. Second, we measured the etch yield of SiO_2 as a function of ion energy. We found that the SiO_2 etch yield increased monotonically with ion energy and saturated at around 800 eV where the yield was 1.5 molecules/ion. Next, we investigated the relationship between the etch yield and the flux ratio of chemical species. The flux ratio of CF_X/F was changed by varying the gas chemistry under a constant ion flux. The etch yield of SiO_2 rose with an increase in CF_X flux. However, the etch yield of poly-Si decreased with an increase in the ratio of CF_X/F. Therefore, high rate and high selectivity in SiO_2 etching could be obtained by high incident CF_X flux with the suppression of F atoms under a constant ion flux.[1]

[1]This work was supported by NEDO.

Contributed Papers

8:45

KW2 4 Electron Beam Ablation Plumes: Diagnostic Studies and Thin Film Deposition* S.D. KOVALESKI, R.M. GILGENBACH, L.K. ANG, Y.Y. LAU, *Nuclear Engineering and Rad. Sci., University of Michigan* Material ablation through channelspark electron beam irradiation for deposition of thin films is being studied. The channelspark is a high current, low accelerating voltage e-beam device developed at KFK[1] in Karlsruhe, Germany. The channelspark has the following parameters: e-beam current of 1.5 kA, accelerating voltage of 15-20 kV, and background Ar or N_2 gas pressure of 7.5-30 mTorr for ion focusing. Ablation of UV grade fused silica has been studied through Dye-Laser-Resonance-Absorption-Photography (DLRAP). Through DLRAP, a plume expansion velocity of about 1 cm/μs has been measured and a hydrodynamically complex ablation plume has been imaged. Wavelength-resolved, time-integrated, gated spectroscopy and time-resolved monochromator spectroscopy reveal plume emission from ionization states up to doubly ionized Si and lasting up to 4 μs. Ion focusing plasma emission spectra contain singly, doubly, and triply ionized argon. Fused silica films have been successfully deposited on Cu substrates. Dynamics of low energy e-beams are also being explored.

*Supported by the NSF and Northrop Grumman

[1]G. Muller and C. Schultheiss, Proc. of Beams 1994, Vol. II, p833.

9:00

KW2 5 Materials Processing by High Density Ablation Plasma Produced by Intense Pulsed Ion Beams KIYOSHI YATSUI, WEIHUA JIANG, ALEXANDER POGREBNJAK, *Nagaoka University of Technology, Nagaoka, Niigata 940-2188, Japan* High density ablation plasma has been obtained by the irradiation of an intense pulsed light ion beam on solid target. With such a technique, which was named as ion-beam evaporation (IBE), we have successfully demontrated the preparation of various kinds of thin films, ultrafine nanosize powders and fullerene. The IBE has the following features: 1) Due to high density plasma, the deposition rate is extremely high, 2) A good stoichiometry is obtained between the target and the thin films. 3) The preparation is possible even in vacuum without heating the substrate. The results of characterization of the materials will be presented.

9:15

KW2 6 Characteristics of Electron Density in Ablation Plasma Produced by an Excimer Laser from Functionally Graded Materials YOSHIHISA UCHIDA, *Aichi Institute of Technology* JUN YAMADA, *Aichi Institute of Technology* HIDEO FURUHASHI, *Aichi Institute of Technology* YOSHIYUKI UCHIDA, *Aichi Institute of Technology* Functionally Graded Materials (FGMs) is drawing attention in industrial application fields. For industrial applications, the FGMs require the secondary processing. Since the excimer laser is able to process with precision and fineness, the excimer laser processing is available. When material is exposed to laser beam, ablation plasma is generated. The structure of producing ablation, which differs with materials, influences the accuracy of production. It has not been analyzed enough. The purpose of this study is to analyze the mechanism of the ablation plasma wave and to achieve the precise microprocess and surface treatment of FGMs by controlling the wave appropriately. This paper reports on the electron density of ablation plasma. The laser used in this experiment was an UV excimer laser with a wavelength of 308nm, a maximum pulse energy of 500mJ and a pulse duration of 30ns. Mach-Zender interferometer is used in this ex-

periment. Density dependence of the ablation plasma plumes on the ceramic-metal content of the FGMs is observed.

9:30

KW2 7 Characterization of Film Thickness Using Off-Normal Spectral Reflectometry BROOKE S. STUTZMAN, FRED L. TERRY JR., *University of Michigan** Spectral ellipsometry (SE) is one of the most accurate thin film characterization techniques which can be applied in situ. However, SE's are too expensive to be used on every plasma system in a semiconductor fabrication facility. We designed, built and tested an optical system capable of measuring film thicknesses in situ with better accuracy than normal incidence reflectometry at a much lower cost than SE. This system, an off-normal spectral reflectometer (ONSR), has no moving parts and is mounted on the ellipsometer ports of a modified GEC reference cell. Our instrument uses linearly polarized white light directed at the sample through strain free windows. A Wollaston prism simultaneously resolves the reflected light into its s and p components. From the magnitudes of Rs and Rp, we extract the film thickness using conventional thin film optics analysis. We will present real-time thickness measurements made during etches and discuss the benefits of our ONSR system in terms of speed, accuracy and cost.

*Research funded in part by SRC contract FC-87-85.002 and MURI F49620-95-1-0524.

9:45

KW2 8 In-Situ Optical Detection of Etch-Induced Defects in GaAs and Si Etched in a Chlorine/Ar Plasma O.J. GLEMBOCKI, *Naval Research Laboratory, Washington DC 20375* R.T. HOLM, *Naval Research Laboratory, Washington DC 20375* D. LEONHARDT, *Naval Research Laboratory, Washington DC 20375* C.R. EDDY, *Boston University, Boston, MA 02215* D.S. KATZER, *Naval Research Laboratory, Washington DC 20375* Plasma processing of semiconductors uses energetic ions (100 to 500 eV) as a key component of the etch process. The impinging particles penetrate beyond the surface layer and in losing their energy produce lattice defects such as vacancies, interstitials and antisites, which act as free carrier scattering or recombination centers, and charge traps. This degrades optical and electronic device performance. We show that the modulated optical technique of photoreflectance (PR) can be used as an in-situ monitor of etch induced damage in semiconductors exposed to a chlorine/Ar plasma generated by an ECR source. Because the intensity of the PR signal is directly proportional to the surface photovoltage produced by a pump laser, we can detect in-situ, the formation of defects generated by the plasma. We have determined the limits of ion energy for reversible etch damage and explored the use of a low energy Cl plasma to heal etch damage. Measurements were benchmarked using a specially design GaAs test structures, for which we can measure not only the surface photovoltage, but also the Fermi-level pinning position. This allows us to calibrate the photovoltaic changes and to extend the measurements to Si. We will discuss the ion energy range of damage free etching in both GaAs and Si.

SESSION KW3: ENVIRONMENTAL APPLICATIONS

Wednesday morning, 21 October 1998; South Pacific Ballroom, Aston Wailea at 7:30

J. Norman Bardsley, U.S. Display Consortium, presiding

Invited Papers

7:30

KW3 1 Abatement of Perfluorocompounds (PFCs) in a Plasma Reactor Using O_2 as an Additive Gas.

HERBERT H. SAWIN, *Department of Chemical Engineering, MIT, Cambridge, MA 02139*

This paper discusses the abatement of four perfluorocompounds (PFCs) in microwave and inductively coupled reactors - C_2F_6, CF_4, SF_6 and CHF_3. The abatement was carried out using O_2 as an additive gas, and was studied as a function of O_2:PFC ratio, flowrate, power, and pressure. Near 100% abatement was achieved for all the PFCs investigated in the microwave reactor. A detailed characterization of C_2F_6 abatement using GC, GC/MS and inline Mass Spectroscopy showed the major abatement products to be CO_2, COF_2 and F_2. The major products from CF_4 abatement were similar to those from C_2F_6 abatement. Mass Spectroscopy indicated the main products for SF_6 abatement were SO_2F_2, SO_2, and F_2 while those for CHF_3 were CO_2, COF_2, F_2 and HF. The work with an inductively coupled plasma reactor exhibited large emissions of CF_4. The difference in CF_4 emission between these reactors was related to the neutral gas temperatures and the thermodynamic stability of the products.

8:00

KW3 2 Positive Streamers and Glows in Air and Exhaust Gases.

R. MORROW, *CSIRO Division of Telecommunications and Industrial Physics, PO Box 218, Lindfield NSW 2070, Australia*

Theoretical and experimental studies have been made of the effects of sub-microsecond voltage pulses on the plasma chemistry of real flue gases in a test cell. Chemical analysis shows that, for real flue gases, the pulsed system can remove up to 90 % of NO, and 30 % of SO_2, if a residence time of $\sim$ 30s is used. We also find that (i) water vapour is essential to the removal of SO_2, but not for the removal of NO or NO_2; and (ii) that small quantities of N_2O are produced. The removal of SO_2 is primarily due to reactions with OH radicals from water vapour, producing sulphuric acid, whereas nitrogen oxides are reduced by N atoms. When a positive voltage is abruptly applied to a point in air at atmospheric pressure, positive streamers are produced. A theory is presented for the development of the first such streamer by solving the continuity equations for electrons, positive ions and negative ions, including the effects of ionisation, attachment,

recombination, electron diffusion, and photoionisation, simultaneously with Poisson's equation. With an applied voltage of 20 kV across a 50 mm gap, the streamer does not reach the cathode. When the voltage is sustained in the presence of free electrons, the electric field at the anode starts to recover until positive glow pulses develop at the anode. The presence of the positive glow corona precludes any further streamer formation; this limits the number of chemical reactions stimulated by the discharge because the positive glow is confined close to the anode. Thus, a limit is set for the voltage pulse width. A theory is also presented for the current and light pulses of positive glow corona from a point in air; results are obtained by solving the continuity equations, described above, in concentric sphere geometry. A series of ''saw–toothed'' current pulses of period $\sim$ 1 μs are predicted with a dc current level. Accompanying the current peaks are discrete 30 ns wide pulses of light. It is found that if, in the presence of a positive glow corona, the voltage is raised at a rate less than 1 kV/μs, the the positive glow corona adjusts to the positive glow corona conditions at a higher voltage; however, if the voltage is raised at a significantly faster rate, streamers develop and propagate out into the gap. Thus, the need for sub–microsecond voltage pulses in order to produce positive streamers can be shown theoretically, and limits determined for the rise time required for the stimulation of chemical reactions.

Contributed Papers

8:30

KW3 3 Corona initiation from raindrops - a step towards solving the lightning initiation problem VICKI SCHROEDER, *Geophysics Program, University of Washington* M.B. BAKER, *Geophysics Program, University of Washington* JOHN LATHAM, *National Center for Atmospheric Research* The vertical E-fields observed in thunderclouds are an order of magnitude too small to allow for large-scale breakdown of air to occur. Laboratory experiments performed by Latham *et al.* showed that corona was initiated at the surfaces of colliding raindrops for applied E-field values comparable to those observed in thunderstorms. In this study we employ a numerical model of the corona process at the drop surface. Our model results show that negative corona was initiated when the upper surface of the drop became unstable. We examined the amount of positive charge (deposited on the drop by the negative corona) that was necessary for positive corona initiation at the opposite end of the drop - where the surface was observed to remain intact. The experimental data for positive corona initiation from the lower end of the drop was best matched by the model when the charge density on the drop was approximately 0.035 C/m^3. Lightning is generally initiated at altitudes greater than 5 km while the Latham *et al.* experiments were done at surface pressure. The model allowed us to extend their results by predicting the E-fields required to initiate positive corona as a function of both pressure and drop size.

8:45

KW3 4 A Study on NO_2 Decomposition in a Low-Pressure Plasma and 172 nm Xenon Excimer Lamp Radiation* CRISTIAN PETRICA LUNGU, ANA MIHAELA LUNGU, *Hokkaido University (on leave from: Low Temperature Plasma Physics Laboratory, National Institute of Laser, Plasma and Radiation Physics, P.O.Box MG-37, Bucharest, Romania)* GO INOUE, YOSUKE SAKAI, HIROTAKE SUGAWARA, *Hokkaido University, Sapporo 060-8628, Japan* An excimer lamp radiation with λ = 172 nm was used to enhance NO_2 decomposition in a low-pressure (133 $\sim$ 665 Pa) NO_2, dc discharges between parallel plate electrodes. The effects of helium, nitrogen and oxygen on NO*x* decomposition were studied for various composition of the gas mixtures and discharge parameters. The behaviour of decomposed species was investigated by optical emission spectroscopy (OES), quadrupole mass spectrometry (QMS), and gas chromatography. Enhancement effects of helium on NO*x* decomposition were supposed by a fact that the Penning ionization of NO_2 by metastable helium atoms was emphasised by following the N_2^+ emission band ($B^2\Sigma_u^+$, $\nu' = 0 \rightarrow X^2\Sigma_g^+$, $\nu'' = 0$), at 391.44 nm ($\Delta\nu = 0$, first negative system).

*Work in part supported by Grant-in-Aid by the Ministry of Education, Science, Sports and Culture, Japan, under JSPS program No.97191.

9:00

KW3 5 An Air Plasma Off-Gas Emission Monitor (APO-GEM) For On-line Toxic Metal Monitoring G.P. MILLER, *Mississippi State University* Z. ZHU, *Mississippi State University* D.P. BALDWIN, *Ames Laboratory, USDOE* Increasing regulatory demands requiring significant reductions in the emission of hazardous air pollutants have led to the need for techniques capable of providing real-time monitoring of toxic metals in combustion gas streams. These waste streams range from coal-fired boilers, municipal waste combustors to plasma vitrification systems used for the remediation of low level radioactive waste. Our solution to this problem is the development of APO-GEM. This instrument incorporates an atmospheric-pressure inductively-coupled air plasma powered by a 3.5 kW solid-state 27.12 MHz rf generator coupled with an isokinetic sampling system. The detection system includes both a 1-m monochromator and a novel solid-state AOTF high-resolution spectrometer. The air plasma readily tolerates the introduction of combustion gases as well as the significant particle loading that can be present in exhaust streams. Plasma properties and performance characteristics, including results obtained recently at the DOE/EPA-sponsored Demonstration of Toxic Metal Continuous Emission Monitors, will be discussed.

9:15

KW3 6 Investigations for the Optimization of Energy Requirements for Exhaust Gas treatment by dielectric barrier Discharge HOLGER RUSS, *Electric Gas Discharge Group, LTI/University of Karlsruhe, Germany* MANFRED NEIGER, *Electric Gas Discharge Group, LTI/University of Karlsruhe, Germany* The work presented is part of an investigation to remove NOx from engine exhaust gases by plasma treatment. Numerical simulations of 2-dimensional distributions of different radicals produced by nanosecond microdischarges with different geometries are presented and compared with experimental results. The 2-D model for simulation of transient microdischarges uses the so-called Donor-Cell-Method, known from hydrodynamics. The numerical implementation is based on an unstructured grid. The Poisson equation is solved using the Finite Element Method, whereas the continuity equiation is treated by a Finite Volume Technique. With this model we are able to simulate single microdischarges within dielectric barrier discharges for very different discharge configurations. The simulation presented were conducted in an effort to understand vastly different values of energy

requirement for the production of e. g. atomic nitrogen radicals in different discharge configurations and for different exhaust gases. The modelling results are in good agreement with the different efficiencies for different reactor configurations.

9:30

KW3 7 Silicon Oxide Selective Etching and Chamber Cleaning Processes for Preventing Global Warming KAZUSHI FUJITA, SHIGETO KOBAYASHI, MASAFUMI ITO, MASARU HORI, TOSHIO GOTO, *Department of Quantum Engineering, Nagoya University, JAPAN* Fluorocarbon gases and SF_6 gas are used in dry etching processes for the thin film patterning and chamber cleaning after film depositions. The use of these gases, however, will be restricted because of environmental problem, namely global warming. In this study, we have developed a novel fluorocarbon gas source without using fluorocarbon feed gases for preventing global warming, where polytetrafluoroethylene (PTFE) is ablated by a CO_2 laser and the generated fluorocarbon species such as radicals and molecules are introduced into the ECR Ar plasma reactor. This novel gas source has been applied to the selective etching of SiO_2 over Si and the etching of a-Si and W for chamber cleaning process. In SiO_2/Si selective etching process, it was found that higher molecules and CF_x (x=1-3) radicals in the ECR plasma were successfully controllable by the novel gas source. Highly selective etching of SiO_2 over Si was realized at a microwave power of 800 W, a pressure of 0.16 Pa, and a bias voltage (V_{dc}) of -420 V. Therefore, it is expected that this novel gas source replaces the conventional gas source in order to prevent global warming. We will also discuss the etching of a-Si and W using ECR O_2 plasma employing the novel gas source for the chamber cleaning process.

9:45

KW3 8 Point-of-Use Plasma Abatement of PFC's: Modeling and Experiments ERIC J. TONNIS, JARAD DANIELS, DAVID B. GRAVES, *U.C. Berkeley* Perfluorocompounds (PFCs) with high global warming potentials and long atmospheric lifetimes such as C_2F_6 and CF_4 are regularly used for oxide etching and CVD chamber cleaning applications within the semiconductor industry. Due to their potential for long term environmental impacts, efforts are underway within the semiconductor industry to reduce or eliminate their emissions. While significant emissions reduction progress has been made on CVD chamber clean applications using process optimization and gas replacement methods, the stringent requirements of oxide etch have limited similar progress on this processing step. One method under exploration is use of a point-of-use (POU) plasma abatement system which is installed after the main chamber tubomolecular pump and prior to the system roughing pumps. A flow of O_2 is added upstream of the POU abatement plasma, which dissociates the PFC/HFC and O_2 mixture causing the CF_x fragments to react with O atoms to form products that can be removed downstream through caustic water scrubbing processes. We will present experimental evidence suggesting that a POU plasma abatement system may be a viable means for PFC emissions reduction, particularly on high density oxide etch systems. In addition, we will present measurements which indicate that chamber wall film deposition plays an important role in the overall emissions from a high density oxide etch tool.

SESSION LW1: ALLIS PRIZE LECTURE

Wednesday morning, 21 October 1998; Plumeria/Jade/Maile Room, Aston Wailea at 10:15
J. Norman Bardsley, U.S. Display Consortium, presiding

10:15

LW1 1 Three-Body Recombination at Thermal and Ultra-low energies.
M. R. FLANNERY, *School of Physics, Georgia Institute of Technology, Atlanta, GA 30332-0430**

Various aspects of Three-Body Recombination – electron-ion, ion-ion, and neutral-neutral – will be briefly reviewed, together with different applications such as anti-hydrogen formation at 4K and the Bose Einstein Condensate at nK. (A) The microscopic theory developed[1] for three-body ion-ion recombination as a function of gas density and cited in the Allis Prize, will be discussed. This serves as a prototype study not only for collisional ion-ion recombination, but also for transport influenced reactions in general. (B) Three-Body electron-ion recombination[2] in an electron gas $T_e \leq 4K$ will also be discussed. Here recombination proceeds via a very rapid production ($\sim T_e^{-4.5}$) of atoms in highly excited Rydberg levels (n,l), with almost circular orbits $n \approx l - 1$ which are very long lived ($\tau_r \sim n^5$), towards radiative decay and collisional de-excitation. A new theory[3] of l-mixing collisions between Rydberg atoms and ions will be provided. This Stark mixing produces lower l-states. Recombination is then stabilized radiatively by decay ($\tau_r \sim n^3$) to lower electronic levels. This is the rate limiting step. (C) A theory will be provided for the molecular formation by three body recombination ($^7Li + {}^7Li + {}^7Li \rightarrow Li_2 + Li$) of significance to Bose Einstein Condensation at mK. Although, the temperature is insufficient to redissociate the higher vibrational level of Li_2 with binding 0.6K, the energy released by bound-bound vibrational quenching can redissociate the upper levels originally formed by three-body collisional capture.

*Research is partially supported by the U.S. Air Force Grant No. AFOSR: F49620-96-0142

[1]Flannery, M.R., *Phil. Trans. Roy. Soc.* A **304** (1982), 447; *J. Chem. Phys.* **95** (1991), 8205.
[2]Flannery, M. R., *Electron-Ion and Ion-Ion Recombination in Atomic, Molecular and Optical Physics Handbook*, edited by G. W. F. Drake, New York: AIP Press, 1995, ch. 52, pp. 605-629.
[3]Flannery, M. R., and Vrinceanu, D., in *APS Topical Conference on Atomic Processes in Plasmas*, edited by E. Oaks and M. S. Pindzola, AIP Press, *to be published.*

SESSION MW1: GEC BUSINESS MEETING

Wednesday morning, 21 October 1998; Plumeria/Jade/Maile Room, Aston Wailea at 11:15
Mark Kushner, University of Illinois, presiding

11:15
MW1 1 Business Meeting

SESSION NW1: DC AND MICROWAVE GLOWS

Wednesday afternoon, 21 October 1998
Plumeria/Jade Room, Aston Wailea at 13:15
Kenichi Nanbu, Tohoku University, presiding

Contributed Papers

13:15
NW1 1 Plasma Cathodes as Electron Sources for Large Volume, High-Pressure Glow Discharges ROBERT H. STARK, KARL H. SCHOENBACH, *Physical Electronics Research Institute, Old Dominion University, Norfolk, VA 23529* A method to suppress the glow-to-arc transition in high pressure glow discharges is the use of a plasma cathode consisting of microhollow cathode discharges (MHCD) [1]. In our experiment a microhollow cathode discharge with a 100 micrometer diameter cathode hole and identical anode hole was used to provide electrons for a large volume main discharge, sustained between the hollow anode of the MHCD and a third electrode. Current and voltage characteristics, and the visual appearance of the main discharge and MHCD were studied in argon and air by using the micro plasma cathode as electron source. We are able to get stable dc operation in argon up to 1 atm and in air up to 600 torr. The main discharge is ignited when the current in the plasma cathode (MHCD), which is on the order of mA, reaches a threshold value. This threshold current increases with reduced applied voltage across the main gap. Above this transition the current in the main discharge is on the same order as the MHCD current and can be controlled by the MHCD current. Experiments with two MHCDs in parallel have indicated that large area high pressure stable glow discharges can be generated by using arrays of MHCDs as electron sources. [1] K. H. Schoenbach et al, Plasma Sources Sci. Techn. 6, 468 (1997). This work was solely funded by the Air Force Office of Scientific Research (AFOSR) in cooperation with the DDR&E Air Plasma Ramparts MURI program.

13:30
NW1 2 Temperature Measurement in Microhollow Cathode Discharges in Atmospheric Air ROLF BLOCK, OLAF TOEDTER, KARL H. SCHOENBACH, *Physical Electronics Research Institute, Old Dominion University, Norfolk, VA, USA* By reducing the diameter of the cathode opening in hollow cathode discharge geometry to values on the order of one hundred micrometers we were able to operate the discharges in a direct current mode at atmospheric pressure in air. The possibility to operate microhollow cathode discharges (MHCD) in parallel [1] in atmospheric air opens a wide range of applications. At atmospheric pressures, the electric power of a single discharge was measured as 8W. The power density in the microhollow exceeds 1MW/cm^3. This leads to strong thermal loading of the electrodes. In order to study the thermal properties of the discharge we have used a method based on emission spectroscopy. The rotational structure of the emitted lines corresponding to the second positive system of nitrogen contains information on the neutral gas temperature. Taking the apparatus profile into account the temperature of the rotational excited molecules can be estimated by a comparison of simulated and measured data. Measurements on MHCD up to atmospheric pressure show an increase in the neutral gas temperature to values exceeding 1000K. In addition to the gas temperature the electrode temperatures were measured and the thermodynamic behavior of the electrode configuration was calculated. [1] W. Shi, K.H. Schoenbach Parallel Operation of Microhollow Cathode Discharges, ICOPS98, Raleigh, NC, USA, 1998 This work was funded by the Air Force Office of Scientific Research (AFOSR) in cooperation with the DDR&E Air Plasma Ramparts MURI program, and by the Department of Energy, Advanced Energy Division.

Invited Paper

13:45
NW1 3 Shock wave propagation in glow discharges.
B.N. GANGULY, *Air Force Research Laboratory, OH, USA**

The modification of acoustic shock wave propagation characteristics in a 25 cm long positive column low pressure (10 to 50 Torr), low current density (2 to 10 mA/cm^2) argon and N_2 dc discharges have been measured by laser beam deflection technique. The simultaneous multi point shock velocity, dispersion and damping have been measured both inside and outside the glow discharge region. The local shock velocity is found to increase with the increased propagation path length through the discharge; for Mach number greater than 1.7 the upstream velocity exceeded the downstream velocity in contrast to the opposite behavior in neutral gas. The damping and dispersion are also dependent on the propagation distance. The recovery of the shock dispersion and damping in the post discharge region, for a given discharge condition, are functions of the initial Mach number. The optical measurement of the wall and the gas (rotational) temperatures suggest the observed shock features can not be solely explained by the gas heating in a self sustained discharge. The results are similar for both Ar and N_2 discharges showing that vibrational excitation and relaxation are not essential[1]. The explanation of the observed weak shock propagation properties in a glow discharge appears to require long range cooperative interactions that enhance heavy particle collisional energy transfer rates for the measured discharge

conditions. Unlike collisional shock wave propagation in highly ionized plasmas[2,3], the exact energy coupling mechanism between the nonequilibrium weakly ionized plasma and shock is not understood. 1. A.I. Osipov and A.V. Uvarov, Sov. Phys. Usp. 35, 903 (1992) and other references there in. 2. M. Casanova, O. Larroche and J-P Matte, Phys. Rev. Lett. 67, 2143 (1991). 3. M.C.M. van de Sanden, R. van den Bercken and D.C. Schram, Plasma Sources Sci.Technol. 3, 511 (1994).

*work performed in collaboration with P. Bletzinger

Contributed Papers

14:15

NW1 4 Self-Consistent Monte Carlo Simulations of Positive Column Discharges* J.E. LAWLER, *University of Wisconsin* U. KORTSHAGEN, *University of Minnesota* In recent years it has become widely recognized that electron distribution functions in atomic gas positive column discharges are best described as non local over most of the range of $R \times N$ (column radius $\times$ gas density) where positive columns are stable. The use of an efficient Monte Carlo code with a radial potential expansion in powers of r^2 and with judiciously chosen constraints on the potential near the axis and wall now provides fully self-consistent kinetic solutions using only small computers. A set of solutions at smaller $R \times N$ and lower currents are presented which exhibit the classic negative dynamic resistance of the positive column at low currents. The negative dynamic resistance is due to a non-negligible Debye length and is sometimes described as a transition from free to ambipolar diffusion. This phenomenon is sensitive to radial variations of key parameters in the positive column and thus kinetic theory simulations are likely to provide a more realistic description than classic isothermal fluid models of the positive column. Comparisons of kinetic theory simulations to various fluid models of the positive column continue to provide new insight on this 'corner stone' problem of Gaseous Electronics.

*Supported by the NSF.

14:30

NW1 5 Energy-Resolved Particle and Energy Fluxes of Electrons in Positive Column Plasmas U. KORTSHAGEN, *University of Minnesota* J.E. LAWLER, *University of Wisconsin* Recent kinetic caluclations by Uhrlandt and Winkler (J. Phys. D, Appl. Phys., Vol. 29, p. 115, 1996) have revealed the interesting physical phenomenon of radially inward directed energy fluxes in positive column plasmas. However, this study only addressed total, i.e., energy-integrated fluxes. We have used a self-consistent positive column model, based on a highly realistic Monte-Carlo Code, to study this effect in more detail. The results of this study show that the physical picture is far more complex. Electrons with low energies usually exhibit radially outward directed particle and and energy fluxes. In Ramsauer gases, at energies around the Ramsauer minimum, these fluxes can also be directed towards the discharge axis. At energies above the threshold for electronic excitation particle and energy fluxes are usually inward directed. Only close to the wall, at total energies above the wall potential energy, these fluxes point towards the wall. The thickness of this ''wall loss region'' scales with the neutral gas density. The results presented can be qualitatively interpreted in terms of the total-energy-picture for the electrons. The kinetic effects described above are lost in fluid calculations.

14:45

NW1 6 Investigation of Non-local Approach in Positive Column Discharges G.J. PARKER, *LLNL* D. UHRLANDT, *Institute for Nonthermal-Plasmaphysics Greifswald, Germany* A computational study of a neon positive column was performed to study the assumption of the two-term expansion and non-local approximations for a discharge with $pR = 1$ cm Torr. Experimentally determined radial field, axial current and excited species spatial distribution are used to find the reflection coefficient and axial electric field to satisfy particle conservation and specified axial current. Results of the two-term non-local approach is compared and contrasted to two fully kinetic treatments for electrons: Monte Carlo and Convected Scheme simulations. Macroscopic discharge parameters are compared to experiment along with microscopic quantities such as the anisotropic parts of the electron energy distribution functions among the various computational models.

15:00

NW1 7 Consquences of Mode Structure on Ion Fluxes in ECR Sources for Materials Processing* RON L. KINDER, MARK J. KUSHNER, *University of Illinois, Dept. Electrical and Computer Engr., Urbana, IL 61801 USA* Due to their ability to produce high degrees of ionization at low gas pressures ($<$ 5 mTorr), electron cyclotron resonance (ECR) sources are being developed for downstream etching and deposition, and for the production of radicals for surface treatment. The spatial coupling of microwave radiation to the plasma is a concern due to issues related to process uniformity. Studies suggest that certain electromagnetic modes tend to provide better uniformity over larger areas. To investigate these issues, we developed a finite-difference-time-domain (FDTD) simulation for microwave injection and propagation. The FDTD simulation has been incorporated as a module in the 2-dimensional Hybrid Plasma Equipment Model (HPEM). In the FDTD, plasma dynamics are coupled to the electromagnetic fields through a tensor form of Ohm's law. The effects of Doppler shifting have been incorporated by using a modified velocity-space averaged conductivity. Results from parametric studies to determine the dependence of ion flux uniformity on mode, power deposition, and gas pressure will be presented.ECR weblink

*Work supported by SRC and NSF (ECS94-04133, CTS9412-565).

SESSION NW2: LASERS AND EXCIMER SOURCES
Wednesday afternoon, 21 October 1998; Maile Room, Aston Wailea at 13:15
Heidi Anderson, University of Wisconsin, presiding

Invited Paper

13:15
NW2 1 Engineering the kinetics of copper vapor lasers.
JAMES PIPER, *Centre for Lasers and Applications, Macquarie University**

Pulsed copper lasers have a unique capability to produce high average powers at high beam quality (near diffraction-limited) in the visible. Elemental copper vapour lasers (CVLs) have been scaled to very large volumes to give single-device extracted powers of hundreds of watts, but generally this is at the expense of reduced (optimum) repetition rates, lowered efficiencies and lowered specific powers (especially at high beam quality). We recently completed a comprehensive program of experimental and computer modelling studies of CVL discharges, aimed at understanding the complex and interactive processes which determine the power and efficiency of CVLs over a wide range of conditions. Based on these studies we have developed a new technique (called "kinetic enhancement") for power scaling of CVLs using trace gas additives in the laser mixture to moderate key plasma kinetic processes previously limiting performance. Dissociative electron attachment of added hydrogen chloride is used to control interpulse plasma relaxation, and consequently the prepulse electron density, permitting efficient laser excitation to be maintained at elevated metal vapour densities and pulse repetition rate. Output power increases for small-to-medium scale KECVLs of a factor of 3, at wall-plug efficiencies double those of CVLs of similar size, have been demonstrated. Laser power continues to scale to the maximum prf (~ 25kHz) investigated to date, and high-beam-quality performance is greatly improved.

*The author gratefully acknowledges the contributions of co-workers, Drs Daniel Brown, Robert Carman, Richard Mildren and Michael Withford

Contributed Paper

13:45
NW2 2 Modelling the kinetics of a copper vapour laser with H_2-HCl-Ne buffer gas mixtures R.J. CARMAN, *Macquarie University* M.J. WITHFORD, D.J.W. BROWN, J.A. PIPER, *Macquarie University* Following our investigations into the influence of halogens and halogen donor buffer gas additives in high temperature or "elemental" copper vapour lasers, a new sub-class of laser has recently been developed in our laboratory based on H_2-HCl-Ne buffer gas mixtures. This device, known as a kinetically enhanced copper vapour laser (KE-CVL) [1], typically produces laser output powers 2-3 times higher than from a similar sized elemental copper laser employing a standard H_2-Ne buffer gas mix, and at significantly higher wallplug efficiencies. A computer model has been used to simulate the discharge kinetics in a 38mm bore KE-CVL which typically produced 80-100W in the laboratory at pulse repetition frequencies of 4-6kHz. The model is based on a rate-equation analysis of the spatio-temporal evolution of selected atomic, ionic and molecular species population densities, taking into account multiple excitation/afterglow cycles to achieve temporal self-consistency. The halogen donor species HCl(v=0,1), Cl_2, Cl, and Cl^- and associated collision processes have been included in the kinetics scheme for the KE-CVL in addition to the 25 species representing the Cu-Ne-H_2 mixture to investigate their influence on the plasma kinetics during the excitation and afterglow periods. [1] M.J. Withford, D.J.W. Brown, R.J.Carman and J.A. Piper, Opt.Lett., 23, 706-708, (1998).

Invited Paper

14:00
NW2 3 Modeling of Plasma Dynamics in ArF and XeCl Excimer Lasers.
YOSUKE SAKAI, *Graduate School of Engineering, Hokkaido University, Sapporo 060-8628 Japan*

Discharge excited pulsed gas laser plasma is a typical phenomenon of ''pulsed plasma and breakdown.'' In this report the plasma dynamics in ArF and XeCl excimer lasers, which are now increasingly demanded in semiconductor fabrication industry as a UV light source, is presented using a $1D^{12}$ and $2D^3$ models. After a few tens of nanoseconds of the voltage application to a pre-ionized laser medium, the field distortion by the space charge appeared significantly in the vicinity of the cathode, which became up to ~ 300 kV/cm though the maximum of the external field was ~ 20 kV/cm. This high field may suggest the generation of local filament discharges in the cathode sheath by field emission, if microscopic protuberances are on the cathode surface. On the other hand, photo-electron emission from the cathode was shown to moderate the field distortion in the cathode region. The effect of the stimulated emission light on the discharge development characteristics was examined. For example, at times after a maximum in the laser output signal was obtained, the laser light driven interactions made the bulk electron number density increase by a factor of 2 and the electric field adjacent to the cathode by a factor of 1.5. The micro-streamer which was triggered at a protrusion on the cathode surfaces developed in the direction of the anode assisted by the high field induced by space charge. Rise of the gas temperature

in the micro-streamer in the vicinity of a cathode was seen, which played an important role in development of the micro-streamer. The results were explained properly in connection with experimental observations[4].

[1]Akashi H, Sakai Y and Tagashira H 1994 *J.Phys.D: Appl.Phys.* **27** 1097-1106
[2]Akashi H, Sakai Y and Tagashira H 1995 *J.Phys.D: Appl.Phys.* **28** 445-451
[3]Akashi H, Sakai Y and Tagashira H 1997 *Aust.J.Phys.* **50** 655-669
[4]Makarov M 1995 *J.Phys.D: Appl.Phys.* **28** 1083-1093

Contributed Papers

14:30

NW2 4 Particle Modeling of Ion Recombinations Due to Three-Body Coulomb Collisions in a X-Ray Laser Medium K. NANBU, S. YONEMURA, *Inst. Fluid Science, Tohoku Univ.* A. SASAKI, *Kansai Res. Estab., Japn Atomic Energy Res. Inst.* It is probable that a strong nonequilibrium prevails in X-ray laser media pumped by a ultra-short pulse laser. In such a case the particle model makes sense. We consider a particle modeling of the three-body recombination $Li^{3+} + e^- + e^- \rightarrow Li^{2+}(n) + e^-$ due to Coulomb collisions, where n denotes the principal quantum number of hydrogen-like ion Li^{2+}. The rate constant for this reaction is given by A_n/T_e, where T_e is the electron temperature and A_n is the constant that is proportional to n^6. The recombination is treated by dividing into the two stages: $Li^{3+} + e^- \rightarrow Li^{3+} \cdot e^-$; $Li^{3+} \cdot e^- + e^- \rightarrow Li^{2+}(n) + e^-$, where $Li^{3+} \cdot e^-$ represents an imaginary state that Li^{3+} and e^- have just formed a pair. We have found the expression for the probability that an electron participates in a recombination. The probability is inversely proportional to the kinetic energy of electron. Using this probability and Nanbu's theory[1] of Coulomb collisions, we have examined the behavior of electron energy distribution function during a time-evolution of the plasma composed of Li^{3+}, $Li^{2+}(n)$, and e^-.

[1]K. Nanbu, Phys. Rev. E. **55**, 4642 (1997).

14:45

NW2 5 Efficent cw rare gas- halide excimer light sources* A. ULRICH, M. SALVERMOSER, J. WIESER, *Technische Universität München, D-85747 Garching, Germany* D. E. MURNICK, H. DAHI, *Rutgers University, Newark NJ 07102* Extending our work on low energy (10-20keV) dc electron beam excitation of pure rare gases[1] we have begun studies of energy transfer mechanisms in rare gas halogen (RG-H) mixtures. For these systems the thin SiN entrance windows must be coated with halogen resitant films. The system Ar+Cl2 (0-1%) is the first to be studied though other RG-H systems are expected to exihibit similar behaviour. At very low Cl2 concentrations near 1bar the VUV spectrum includes Ar2* excimer radiation, ClI resonance lines and ArCl* radiation. At higher concentrations the ArCl* band at 175nm dominates the spectrum with energy transfer efficiencies exceeding 5% observed. Calculations of threshold pumping power required indicates that compact RG-H lasers based on the e-beam pumped system are feasible with average output powers in the Watt range.

*Supported in part by NSF, NATO and INTAS

[1]J. Wieser, D. E. Murnick, A. Ulrich, H. A. Huggins, A. Liddle, and W. L. Brown, Rev. Sci. Instrum. 68, 1360 (1997).

15:00

NW2 6 Generation of Intense Excimer Radiation from High-Pressure Hollow Cathode Discharges* AHMED EL-HABACHI, *Electrical and Computer Engineering Department, Physical Electronics Research Institute, Old Dominion University, Norfolk VA23529* KARL H. SCHOENBACH, *Electrical and Computer Engineering Department, Physical Electronics Research Institute, Old Dominion University, Norfolk VA23529* By reducing the diameter of the cathode opening in a hollow cathode discharge geometry to values on the order of 0.1 mm, we were able to operate these discharges in noble gases in a direct current mode up to atmospheric pressure. High-pressure discharges in xenon and argon were found to be strong sources of excimer radiation. For xenon, highest intensities at a wavelength of 172 nm were obtained at a pressure of 400 Torr. At this pressure, the Vacuum Ultraviolet (VUV) radiant power of a single discharge operating at a forward voltage of 220 V and currents exceeding 2 mA reaches values between 6% and 9% of the input electrical power. Results of a simple rate equation model indicate that efficiencies of up to 40% may be achievable. Measurements to study the effect of gas flow, gas mixtures, electrode geometry and mode of operation (pulsed versus dc) on the excimer efficiency are under way and will be discussed at the meeting.

*This work was funded by the Department of Energy, Advanced Energy Division

SESSION NW3: TRANSIENT DISCHARGES AND COLLECTIVE EFFECTS IN DUSTY PLASMAS

Wednesday afternoon, 21 October 1998
South Pacific Ballroom, Aston Wailea at 13:15
Andre Bouchoule, GREMI, presiding

13:15

NW3 1 Optical emission from pulsed corona discharge and its related reaction FUMIYOSHI TOCHIKUBO,* TIMM H. TEICH, MAMMEN JACOB, *Swiss Federal Institute of Technology Zurich* When an electrical discharge is initiated, many kinds of excited species may be generated. In high pressure discharges, the reaction time constants of these species can be very short and are reflected in the subsequent reaction processes. In order to investigate some chemical reactions occuring in the early stage of discharges intended for the conversion of nitrogen oxides we studied the time dependence of optical emissions. Special attention has been paid to the decay time constants of species polulations excited by radical-molecule reactions. By systematically changing the partial gas pressure of minor gas components, we estimate the reaction rate contributions of these particular gas constituents. We conclude that NO(B) is predominantly excited by the reaction of $N(^2D)$ with N_2O, while NO(A) and OH(A) are mainly excited by energy transfer from $N_2(A^3\Sigma_u^+)$. The rotational temperature in the active discharge zone was estimated from second positive and first negative band emission of nitrogen to be about 500K. F.T. is

grateful to Swiss National Science Foundation for support during the course of measurements presented in this article.

*Permanet affiliation: Tokyo Metropolitan University

13:30

NW3 2 Femtosecond Study of Ion Kinetics in Laser-Induced Plasmas AMANDA J. ROYBAL, MICHAEL S. DURAN, GRAHAM R. ALLAN, ANDREW V. PAKHOMOV,* *Physics, New Mexico Highlands University, Las Vegas, NM 87701* In this work we report on novel experiments which may lead to a better understanding of the temporal evolution of laser induced plasmas. The plasmas studied were formed on surfaces of solid elemental targets exposed to focussed pulses from Ti:Sapphire mode-locked laser and regenerative amplifier. Energies and yields of various ionic species escaping from the laser-induced plasmas were monitored by time-of-flight and, with femtosecond resolution, by an original ablation scheme, employing two identical excite pulses with variable separation time (second pulse is used also as a probe). Ionic kinetic energies and yields were measured as functions of: atomic mass, irradiance, repetition rate and pulse separation times. Angular distribution of ions, mass-removal rates, ionization ratios and temporal profiles for establishing the so-called "self-regulated" plasma regimes will be reported. This work was supported by New Mexico Space Grant Consortium.

*Author to whom all correspondence should be directed, present address: Department of Physics, The University of Alabama in Huntsville, Huntsville, AL 35899

13:45

NW3 3 Two Dimensional Melting in a Coulomb Crystal of Dusty Plasmas KAZUO TAKAHASHI, *Dept. of Electronic Science and Engineering, Kyoto University* YASUAKI HAYASHI, *Dept. of Electronics and Information Science, Kyoto Institute of Technology* KUNIHIDE TACHIBANA, *Dept. of Electronic Science and Engineering, Kyoto University* Two dimensional melting transitions in a Coulomb crystal of dusty plasmas were analyzed, the crystal treated as macroscopic crystalline model. A simple hexagonal Coulomb crystal formed by carbon particles of 4.5 micrometer in diameter were observed in a methane plasma. The structures depending on gas pressure were analyzed by a method based on KTHNY theory. The analyses showed that an ordered (crystalline) structure changed to disordered (liquid) phase by way of a coexistence phase containing intermediate (hexatic) and disordered phase as gas pressure went up from 64 to 100 Pa. To examine the experimental results, Monte Carlo simulations were employed, because the results having structural fluctuations made it difficult for the structure to be made a decision of the phase. The MC studies found that charged particle system could change from liquid to hexatic and from hexatic to solid as Coulomb coupling parameter increasing. This fact implies that change of Coulomb coupling between particles due to plasma parameter change depending on pressure causes two dimensional melting transitions in a Coulomb crystal of dusty plasmas.

14:00

NW3 4 Crystallographic Study of 3-Dimensional Coulomb Crystals in a Fine-Particle Plasma YASUAKI HAYASHI, AKITO SAWAI, *Kyoto Institute of Technology, Japan* Three-dimensional Coulomb crystals were formed in a carbon fine-particle plasma. The crystal structure and particle arrangement were investigated with the use of CCD video cameras from both the top and the side at the same time, and BCC(body-centered cubic)-like and FCC(face-centered cubic)-like structures have been observed. The BCC-like structure shows (110) planes, alternate particle arrangement in line in the neighboring layers, from the top. The ratio of particle distances, a and b, in the orthogonal two directions in planes is not 1.41 but 1.6-1.7. The inter-layer distance, c, is larger than b/2 and less than a/2. As a result, the BCC-like structure should be mentioned to be face-centered orthorhombic. The FCC-like structure shows (111) planes, close-packed arrangement, from the top. The structure seems to be truly FCC, however, is under investigation more in detail. The two structures have been observed at the same time in close positions or at a close time in the same position. The mutual change of the two structures can be explained by the slip of crystal faces.

14:15

NW3 5 Characterization of Dipole Interactions in Dusty Plasmas H.R. SNYDER, *Los Alamos National Laboratories* M.S. MURILLO, G.S. SELWYN, D. WINSKE, *Los Alamos National Laboratories* We constructed an rf plasma chamber incorporating an electrostatic trap for studying various properties of dusty plasmas. Our plasma system is capacitively coupled with an asymmetrical electrode geometry. We introduce well characterized glass microspheres of various diameters (1.0μm-50μm) into the trap to simulate dust grains and measure properties of the dust using laser light scattering techniques in conjunction with a digitizing video capture system. In particular, we observe a crystalline phase in which the microspheres form strings aligned with the electric field and we measure the intergrain spacing. This alignment, which has been observed in other experiments, appears to be a ubiquitous property of dust in rf plasma chambers. Because the strings behave fairly independently, it has been suggested that the dust has an acquired dipole moment. Such an interaction qualitatively describes vertical alignment of dust within a string and horizontal repulsion between strings. We have developed several estimates for the dipole strength based on nonuniform charging and ion focusing to compare with the suggested mechanism of induced dipoles within the dust. A simple theory has been developed which predicts the lattice spacing for various dipole mechanisms. Comparisons are made with lattice spacings measured in the experiment.

SESSION OWP1: POSTER SESSION: ECR PLASMAS
Wednesday afternoon, 21 October 1998
Haku/Pikake Room, Aston Wailea at 15:15
Irving Langmuir, General Electric, presiding

OWP1 1 Investigation of the Behavior of Electrons in ECR Plasmas Using a Self-Consistent Particle-Wave Model HIROSHI MUTA, *Kitakyushu National College of Technology* In finite-sized and inhomogeneous ECR plasmas for materials processing, the behavior of electrons is usually complicated because there are highly non-linear interactions between the electrons and injected microwaves which can propagate with various modes corresponding to the magnetized plasma. In this paper, the results of numerical simulation for an argon plasma using a self-consistent particle-wave model are presented and the behavior of electrons in the plasma is investigated. In the model, the microwave fields are solved three-dimensionally using the finite-difference time-domain (FDTD) method, and the dynamics of both electrons and ions in the axisymmetric plasma model are calculated two-dimensionally using the particle-in-cell(PIC) with Monte-Carlo(MC) collisions. For neutrals, the data calculated beforehand using the direct simulation Monte Carlo(DSMC) method are used.

The simulations in accordance with the experimental apparatus were carried out and compared with the experimental results of the electron velocity distribution function (EVDF) and electron density measured by Laser Thomson scattering. As a result, it was found that the model presented here reproduced the measured values well.

OWP1 2 Extensive Control of Plasma Parameters in the Afterglow Region of ECR Plasma for the Epitaxial Growth of c-GaN ATUSHI UWABACHI, MASAAKI KIKUCHI, KANJI YASUI, TADASHI AKAHANE, *Nagaoka University of Technology* In order to extensively control the plasma parameters in the afterglow region of ECR plasma for the epitaxial growth of c-GaN, magnetic and electric fields were supplied in the afterglow region. A submagnetic coil and a mesh electrode were set surrounding a growth chamber and between ECR discharge chamber and the growth chamber, respectively. Under mirror field conditions, the electron temperature of NH_3 plasma in the growth chamber was extensively varied from 0.4eV to 5.6eV with mesh electrode bias. The plasma space potential also varied from 0.9V to 41.5V according to the variation in the electron temperature. The lowest electron temperature and smallest space potential were obtained at a negative mesh bias under the mirror field. C-GaN films were grown on GaAs (100) at 550°C in the growth chamber using TMGa and NH_3, after nitridation of the substrates. The crystallinity of c-GaN was best at the negative mesh bias under the mirror condition. The integrated intensity ratio of c-GaN(200) to h-GaN(10-11) also showed the large value under the condition of low electron temperature and low space potential.

OWP1 3 Mode Conversion of Electromagnetic Waves at a Critical Radial Position in a Large Diameter ECR Plasma Y. UEDA, *Kyushu University, Japan* H. MUTA, *Kitakyushu National College of Technology, Japan* Y. KAWAI, *Kyushu University, Japan* Recently, a great interest has been directed toward the uniformity and the area of an electron cyclotron resonance (ECR) plasma as a processing plasma, because the uniformity of the plasma usually depends on experimental conditions. We already reported the experimental results[1]; not only the whistler wave (R wave) but the extraordinary wave (X wave) affected to the plasma uniformity. The wavelength of the X wave became short according to the local electron density around the plasma boundary, which indicates the X wave sustained the uniformity of the ECR plasma due to upper hybrid resonance (UHR). Hence, behaviors of electromagnetic waves around the plasma boundary should be understood in order to control the uniformity of an ECR plasma and to design effective ECR plasma reactors. We measured electromagnetic wave propagation in the ECR plasma by a 2D movable loop antenna. It was found experimentally that mode conversions of electromagnetic waves occurred at a radial edge of the ECR plasma and the position changed depending on the input microwave power.

[1]Y. Ueda and Y. Kawai : Appl. Phys. Lett. 71(15) 1997 p.2100.

OWP1 4 Experimental Comparison of Microwave, Oxygen Plasmas in a Conventional Electron-Cyclotron Resonance, Diverging Magnetic Field and in a Multi-pole Magnetic Field Geometry TETSUYA AKITSU, *Yamanashi University, Kofu, 400-8511, Japan** A plasma-enhanced reactive sputtering was developed for the deposition of oriented thin crustals of metallic-oxide compound. An oxygen plasma was excited with microwave, electron cyclotron resonance discharge at 2.45 GHz and a compact DC magnetron sputtering was combined. The discharge characteristics was compared in two types of magnetic field configurations.using the optical emission spectroscopy and the appearance potential mass-spectrometry. In a divergent magnetic field, the microwave was absorbed in a single electron-cyclotron resonance Layer, 30-45 mm apart from a crystallized ceramic vesse, and the deposition region was exposed to a freely expanding plasma. Next, the end of the magnetic field line was closed with a magnetic circuit and the source plasma was magnetically confined in the local mirror, thus only neutral oxygen was allowed to expand into the deposition region.

*The present work was supported in part by a Grant-in Aid for Scientific Research from the Ministry of Education, Science and Culture of the Japanese Government

OWP1 5 Negative Ion Volume Production in ECR Hydrogen Plasmas OSAMU FUKUMASA, MASANORI MATSUMORI, *Faculty of Engineering, Yamaguchi University, Japan* Production and control of electron cyclotron resonance (ECR) plasmas for negative ion sources have been studied. A new production method using permanent magnets is proposed as one possibility for a large diameter high density uniform microwave plasma. The microwave power is launched by an annular slot antenna into the circumference of a chamber and a line-cusp permanent magnets surrounding the chamber. Advantages of using permanent magnets are that the magnetic field can be applied in the local region, where plasmas can be efficiently generated if the ECR condition is satisfied, and that an almost magnetic free condition can be achieved on the extraction grid. In this paper, we report the structure of the microwave (ECR) -discharge negative ion source, the characteristics of the ECR plasma, the optimization of the plasma parameters in the extraction region, comparison of the ECR plasmas with DC discharge plasmas from a viewpoint of negative ion production and extraction.

OWP1 6 Ion and Neutral Temperatures in Electron Cyclotron Resonance Plasmas AKIRA YONESU, *Ryukyu University* YOKO UEDA, SHUNJIRO SHINOHARA, YOSHINOBU KAWAI, *Kyushu University* Electron cyclotron resonance (ECR) plasmas are being extensively used for etching and deposition of thin films. To understand these ECR plasma processes, It is important to investigate the behavior of ions and neutrals as well as electrons. In this work, we report preliminary measurements of the ion and neutral temperatures in resonance regions of an ECR processing reactor using a optical emission spectroscopy. The measurements were made as a function of gas pressure and microwave input power with Ar gases. The ion temperature increase from approximately 0.4 to 1eV as the operating gas pressure is lowered from 1 to 0.1mTorr and slightly increase with increasing microwave input power. On the other hand, the neutral temperature is lower ($\leq$ 0.3 eV) than the ion temperature, and weakly depends on both gas pressure and microwave input power. Langmuir probes were also used to determine the variations of plasma parameters (electron temperature, density, plasma potential, potential fluctuation). Using the obtained results, mechanism of ion and neutral heating in this reactor is discussed.

OWP1 7 Control of Plasma Parameters Using Magnetic Filter OSAMU FUKUMASA, YASUSHI TAUCHI, NORIHISA MIZUKI, MASANORI MATSUMORI, *Faculty of Engineering, Yamaguchi University, Japan* Electron temperature control is performed on negative ion production using a magnetic filter. Plasma parameters in case of direct current argon, deterium and hydrogen discharges change dramatically across the magnetic filter. The

plasma is divided into two parts, the source plasma region (high density plasmas with energetic electrons) and the diffused plasma region (low electron-temperature plasma without energetic electrons). The effect of the magnetic filter depends on ion species. This method of plasma parameter control is also applied to plasmas produced by electron cyclotron resonance discharge.

OWP1 8 Reactive Sputtering Using ECR Plasma Source with One-dimensional Uniformity TOSHIAKI YASUI, HIROKAZU TAHARA, TAKAO YOSHIKAWA, *Division of Mechanical Engineering, Department of Systems and Human Science, Graduate School of Engineering Science, Osaka University* A 30 cm long electron cyclotron resonance (ECR) plasma source with one-dimensional uniformity was developed for reactive sputter deposition. Slot anntenas are cut on a side wall of 30 cm long rectangular waveguide, and permanent magnets on the waveguide surround the slots to form ECR layer. Microwaves of 2.45 GHz were radiated from the slots and generated plasma along the waveguide. The spatial uniformity of Ar plasma at 0.093 Pa was 13.3 % within 160 mm long at 50 mm downstream from the slot antennas. A sputtering target was placed within the discharge chamber to achieve high deposition rate. Moreover, this plasma source prevents the microwave window contamination from sputtered particles. By using Ti target and mixture of Ar and N_2 gases, TiN films were successfully deposited. The deposited film thickness uniformity was 11.3 % within 160 mm in the long direction.

SESSION OWP2: POSTER SESSION: DISPLAYS, LAMPS, AND LASERS
Wednesday afternoon, 21 October 1998
Haku/Pikake Room, Aston Wailea at 15:15
Irving Langmuir, General Electric, presiding

OWP2 1 Modelling of High Pressure Discharge Lamps including Electrodes* PETER FLESCH, MANFRED NEIGER, *Electric Gas Discharge Group, LTI/University of Karlsruhe, Germany*† The time-independent modelling of high pressure discharge lamps without dividing the discharge into special zones is the subject of this poster. The model equations were first proposed by Fischer [1, Modelling of low-power high-pressure discharge lamps, Philips J. Res. 42, pp. 58-85 (1987)] without giving a rigorous derivation of the equations and boundary conditions. The main point is an enlarged electrical conductivity with respect to its LTE-value near the electrodes, leading to realistic magnitudes of the electric field (→ voltage drop) close to the electrodes. We give a derivation which is partly different from [1] starting from fundamental diffusion equations [2, Hirschfelder, Curtiss, Bird, Molecular Theory of Gases and Liquids, John Wiley & Sons (1964)], clarifying the different approximations. As a result we get new boundary conditions at the electrodes. We compare different boundary conditions by means of modelling results, calculated using the finite element method. Results for Hg and Xe with different geometries are presented and compared with experiment.

*Funded by BMBF, FKZ 13N7107/0
†Special thanks to Hartwig Wiesmann, who implemented the Finite-Element-Program to solve the equations on an unstructured grid

OWP2 2 A Study of Nonlocal Ionization Process in the Thermionic Cathode - Glow Discharge Model YAN-MING LI, *OSRAM SYLVANIA Development Inc., 71 Cherry Hill Dr., Beverly, MA 01915* During high intensity discharge (HID) lamp starting, high cathode fall voltage (200-300 V) observed in the cold cathode glow discharge phase, collapses to 30-70 volts as the cathode heated up to thermionic emitting temperature. This low voltage thermionic arc phase can last up to minutes as the plasma transit to steady state arc discharge closed to local thermodynamic equilibrium. The thermionic arc phase plays an important role in the overall HID lamp starting and lumen maintenance. The hot cathode glow discharge model is being re-examined[1] by including the nonlocal, nonequilibrium ionization process due to the thermionic emitted electrons gaining energy from the cathode fall. The cathode energy balance equation describing the hot cathode and thermionic emission will be set up. Various components of cathode heating power due to discharge ions, electrons, and neutrals will be analysis. The possible role of back diffusion of high energy plasma electron in cathode heating will be studied. Based on the numerical solution of the coupled plasma-cathode system, the current-voltage characteristics are determined and the change in cathode emission charateristics from secondary to thermionic will be explored. The effect of nonlocal ionization of thermionic emitted electrons on current-voltage characteristics of the plasma-cathode system will be presented.

[1]Byszewski W. W., Gregor P. D., Budinger A. B., Li Y. M., ''Tungsten radiation measurement during starting of metal halide lamps'', J. Ill. Eng. Soc., Vol. 21, p. 85(1992)

OWP2 3 Fundamental Research on Rare Gas Fluorescent Pulsed Discharge Lamps for Mercuryless Lamps MASAFUMI JINNO, HISAYOSHI KUROKAWA, MASAHARU AONO, *EHIME Univ.* The characteristics of xenon-neon fluorescent discharge lamps with inner electrodes, and of xenon fluorescent discharge lamps with both inner electrodes and external electrodes were investigated at the pulsed operation. In the case of the inner electrodes type, when the partial pressure of neon is high, the ignition voltage is low because of the Penning effect. Then, the high mixing ratio of neon is desirable to lower the ignition voltage. However, the luminance of the phosphor increases as the mixing ratio of xenon increases. Therefore, in order to get high luminance, xenon should be fill at high mixing ratio. If only xenon is filled in a lamp with inner electrodes, the cathode is bomberd and damaged by the large mass of xenon ions. Consequently, the most suitable mixing ratio of xenon and neon or some other buffer gases should be found for inner electrode type. When the lamp filled only with xenon is operated by external electrodes, the afterglow emission of the phosphor increases as the pressure of xenon increases. These increases following the increase in xenon pressure seem to be caused by the UV light of xenon excimers. However, the starting voltage becomes higher at high xenon pressure. So, the external electrode type requires the optimization of some conditions such as electrodes, pulse frequency, etc.

OWP2 4 Modelling of Low-Pressure Gas Discharges Using Electron Clouds MARTIN DEDEKE, *University of Karlsruhe, Germany* A selfconsistent, time-dependent, hybrid fluid-particle model of a dc low-pressure gas discharge is presented. The description includes all parts of the discharge, the cathode fall, the negative glow, the faraday dark space, and the positive column. The model is based on a microscopic description of the electron kinetics. Electrons are combined in gaussian-shaped clouds as a local distribution. There are two kinds of electron-clouds: the beam-electrons and the plasma-electrons. The beam-electron-

clouds are emitted by the cathode, they gain energy in the cathode fall and generate new electrons: the plasma-electron-clouds. Because of thermal movement plasma-electron-clouds spread slowly. For each cloud, there is a maxwell energy distribution below the first inelastic collision energy. Above this energy limit, the distribution function is represented at discrete points in an irregular mesh. If clouds are too large, the whole electron-distribution in the discharge is divided into new clouds. Time-dependent fluid equations (continuity equations) are used to describe the movement of the ions. The electric field is calculated by the Poisson equation. With a given cold spot temperature, fill gas pressure, current, radius, and length of the lamp, the electric field, the electron and ion density, the electron temperature, and the radiation can be calculated.

OWP2 5 Spatio-Temporally Resolved Measurements of Cu Density in Kinetically-Enhanced Copper Vapour Lasers and Cu:HyBrID Lasers R.P. MILDREN, D.J.W. BROWN, J.A. PIPER, *Centre for Lasers and Applications, Macquarie University, NSW 2109, Australia* There is presently strong interest in understanding the kinetics of copper laser discharges containing hydrogen halides (HX) following the radical improvements in power scaling of high beam quality output observed from Cu:HyBrID lasers (which use HBr additive) and kinetically enhanced copper vapour lasers (KE-CVLs, HCl + H_2 additive). Though the improved performance of these devices is generally attributed to the effects of dissociative attachment of HX during the inter-pulse period, the kinetics have not been investigated in detail and the new limits for output power scaling are not well understood. We show that spatio-temporally resolved measurements of ground-state Cu density during the discharge cycle of KE-CVLs and Cu:HyBrID lasers provide a potent diagnostic for elucidating the effects of HX in the discharge. Though a comparison of Cu ground-state density evolution in a KE-CVL and a Cu:HyBrID laser reveals that the devices are similar with respect to the effects of HX in accelerating inter-pulse plasma relaxation, significant differences in performance arise due to factors that influence the absolute copper density. We discuss how these factors may limit specific output power scaling of KE-CVL and Cu:HyBrID devices.

OWP2 6 A Kinetic Model for Excimer UV and VUV Radiation in Dielectric Barrier Discharges* XUDONG "PETER" XU, MARK J. KUSHNER, *University of Illinois, Dept. Electrical and Computer Engr., Urbana, IL 61801 USA* Dielectric barrier discharges (DBDs) have shown promise as high intensity sources of UV and VUV radiation emitted by dimer and trimer excimers. In this paper, we report on a computational investigation of the kinetic mechanisms, efficiency and scaling of atmospheric pressure DBDs operating in Xe/Cl_2 mixtures. This parameteric study was performed with 1-d and 2-d plasma chemistry and hydrodynamic models while varying gas mixture, applied voltage, gap and gas pressure. The efficiency of reaction mechanisms for excitation of the excimers XeCl* and Xe_2^* will be discussed. We found that emission from Xe_2^* decreased with increased Cl_2 fraction due to quenching and conversion to XeCl*. The emission from XeCl* optimized at Cl_2 fractions of a few percent. Total efficiencies (light power out/discharge power) of > 0.05 are predicted. Increasing capacitance of the dielectric increases total light generation with little loss in efficiency,

*Work supported by NSF.

OWP2 7 Modeling of Micro-Discharge in Xe DBD Excimer Lamp HARUAKI AKASHI, *National Defense Academy, Japan* AKINORI ODA, YOSUKE SAKAI, *Hokkaido University, Japan* Dielectric barrier discharges (DBD) have been applied widely to industrial devices, such as ozonizers, removal of polluted gases, plasma display panels, and so on. Generally, DBD could make energetic electrons by suppressing arc discharges, and accordingly excited species are produced efficiently. Excimer lamps have been developed using DBD as an important VUV light source[1,2] , however the physics of DBD is not understood well. For further development of efficient DBD excimer lamps, understanding of the characteristics of micro-discharges is necessary. In this work, a micro-discharge in Xe DBD excimer lamps has been simulated using a 2D fluid model[3]. 300Torr Xe gas, 1cm distance between the electrodes and 1-2mm thickness of dielectric barrier(ε_r=4) is used. Both electrodes are covered with dielectric barrier and 12kV DC voltage is applied to the electrodes. As a result, peak value of electron density slightly decreases as the thickness of dielectric barrier decreases. On the other hand, the radiation of excimer(172nm) becomes two times larger as the thickness of dielectric barrier decreases. The width of current waveforms becomes two times wider with decreasing the thickness of dielectric barrier.

[1]K Stockwald and M Neiger: Contrib. Plasma Phys., 1995 **35**, 1, 15-22
[2]B Eliasson and U Kogelschatz: IEEE Trans. Plasma. Sci., 1991 **19**, 309-23
[3]H Akashi et al: Aust. J. Phys., 1997, **50**, 655-669

OWP2 8 2-D Modeling of Micro-Discharges in Xe Dielectric Barrier Discharges AKINORI ODA, HIROTAKE SUGAWARA, YOSUKE SAKAI, *Hokkaido University, Japan* HARUAKI AKASHI, *National Defense Academy, Japan* Dielectric barrier discharges (DBD) are composed of many short-lived micro-discharges, with which we can obtain stable glow discharges even under high pressure conditions. Thus, the discharges are utilized in the wide range of applications, *e.g.*, ozone generation, vacuum ultraviolet light sources, plasma display panels, destruction of toxic compounds, *etc*. For optimal control of these applications, it is very important to understand the properties of micro-discharges. In this work, a self-consistent 2-dimensional fluid model[1] was applied to an analysis of micro-discharges in Xe DBD. The calculation was carried out under conditions of the applied voltage V_0 = 12kV (DC), the gas pressure p = 300Torr, and the gap distance d = 6mm between the dielectric barriers (ϵ_r = 4) with thichness of 2mm. As a result, we found that the electron density peak in a micro-discharge appeared in the vicinity of the cathodic dielectric, and it reached the order of magnitude of $10^{14}cm^{-3}$. In addition, the electric field near the electron density peak was distorted up to 70kV/cm in axial and 15kV/cm in radial directions, and the elecron energy was around 9eV.

[1]A.A.Kulikovsky, *J.Comput.Phys.* **119**(1), 149-55 (1995)

OWP2 9 Distribution of Xe(6s[3/2]$_2^o$) Metastable Density in a Xe/He Barrier Type Discharge* MARIA ANTOANETA BRATESCU, *Hokkaido University (on leave from: Low Temperature Plasma Physics Laboratory, National Institute of Laser, Plasma and Radiation Physics, P.O.Box MG-37, Bucharest, Romania)* YOSUKE SAKAI, OHKUBO MITSUYUKI, *Hokkaido University, Sapporo 060-8628, Japan* Two methods of laser absorption spectroscopy: classical absorption and plasma modulation technique are used to study the distribution of Xe(6s[3/2]$_2^o$) metastable density in a barrier discharge generated in Xe/He mixture.

Xe transition from $6s[3/2]_2^o$ to $6p[3/2]_2$ at 823.390 nm, obtained with a diode laser, presents a complex hyperfine and isotopic structure. >From the metastable atom density distributions at different Xe/He ratios, a maximum density of 10^{11} cm^{-3} at $r = [Xe/(Xe + He)] = 20$ % is obtained, while in pure Xe and at $r = 30$ % the maximum density is about 10^{10} cm^{-3}. The quench of $Xe(6s[3/2]_2^o)$ outside of the plasma edge is determined and explained by diffusion of metastable atoms, their interaction with each other and with electrons. The transient behavior of $Xe(6s[3/2]_2^o)$ atom density at plasma modulation with a low frequency (comparing with the a.c. high voltage frequency) is obtained outside of plasma edge.

*Work in part supported by JSPS long term program.

OWP2 10 Ion-Pair XeO Emission from a Microwave Discharge M. CEKIC, J. FRANK, *Fusion UV Systems, Inc.* S. POPOVIC, *Old Dominion University* Molecular structure of the low lying excited states of XeO was studied in more detail in relation of excimer lasers. Rare gas halide excimer lasers established themselves as more efficient ultraviolet sources, and the remaining problems related with molecular structure of XeO were set aside and forgotten. Hence very little information is still available about ion pair and Rydberg states of XeO. Apart of a vague statement about an extended continuum, peaking at 237 nm, and a tentative assignment for a dozen of ion pair states, little is known about their complex structure. In our continuing search for high-intensity, narrow-band ultraviolet light sources as candidates for substituting high intensity mercury lamps in various applications, we performed experiments with high pressure, microwave-excited mixtures of Xe with O_2 and N_2O. Dominant feature in the spectrum is the 237-nm band extending probably rather deep below 200 nm with the characteristic narrow peak near the band's head. Width of the band indicates a very deep potential energy minimum with many vibrational levels, characteristic for the ion-pair upper excited state. Contrary to the previous description of the band, there is a visible structure, showing a probable overlap of two or more different states.

OWP2 11 Studies of Preionization Processes of High Pressure Gases for Excimer Laser Discharges N. KATAOKA, K. UCHINO, K. MURAOKA, T. OKADA, M. MAEDA, *Kyushu University, Japan* E. SUNAKA, T. ENAMI, H. MIZOGUCHI, *Komatsu Ltd.* The aim of this research is to understand and control the preionization process in high pressure discharges used for excimer lasers. For this purpose, a test chamber with a spark light source was designed and fabricated, to achieve ultra high vacuum and to control the base pressure. Photocharge signals produced by the spark light source were collected by pairs of plate electrodes placed inside the test chamber. In order to study the effect of gaseous impurities on the preionization process, measurements were performed for different base pressure conditions. The results showed that the photocharge signal was linearly correlated with the base pressure. Also, the possibility of actively controlling the preionization by adding small amount of Xe gas to the gas mixture was examined. The maximum signal at the Xe partial pressure of 0.1 Torr was 10 times higher than the signal for the Ne and Kr mixture without Xe, suggesting that active control may be possible.

OWP2 12 2-D Simulation and Breakdown Characteristics of PDP Cell Y.K. SHIN, C.H. SHON, H.S. LEE, W. KIM, J.K. LEE, *Pohang Univ. of Science and Technology, Pohang 790-784, Korea* Fluid and hybrid simulations for PDP cell are presented and benchmarked by the comparison with a particle code OOPIC. Fluid simulation based on our previous code[1] has an advantage of saving computation time, but it has an inherent assumption for velocity distributions. Kinetic simulation yields the ion energy distribution which plays an important role in secondary electron emission and MgO sputtering but it is not efficient computationally. Combining the advantages of fluid and kinetic codes, various hybrid methods using the Monte-Carlo collision are employed. The breakdown characteristics of PDP cells in various geometry are compared. The current absorbed at the dielectric above the anode electrode is linearly proportional to the applied voltage but the half width of the current pulse is not. If the cell voltage does not vanish after the discharge-turnoff, quasi-neutrality inside the cell does not hold.

[1]J.K. Lee, L. Meng, Y.K. Shin, H.J. Lee and T.H. Chung, Jpn. J. Appl., Phys. Part 1, 36, 5714 (1997); *ibid*, 36 (5A), 2874 (1997).

OWP2 13 Plasma Display Panel Cell Modeling G.J. PARKER, *LLNL* P.A. VITELLO, *LLNL* J.W. SHON, *LLNL* Plasma display panels (PDP's) consists of arrays of microdischarges which either produce visible or UV light to activate individual pixels of the display.Typical modeling techniques exploit the fact that the neutral gas pressure is close to atmospheric by using the reduced field E/N to determine the electron energy distribution function (EEDF) in order to solve the typical hydrodynamical equations. Further refinements of this approach construct a one-to-one mapping between average energy and E/N results along with a solution of the hydrodynamical electron temperature equation. We present results which show both these methods are not accurate in either spatial or temporal behavior since these microdischarges are not local in nature due to the large variationsover small spatial distances of the fields and particle densities. A hybrid approach is used to find the actual EEDF via Monte Carlo as the discharge develops and is used to closed the moments of the hydrodynamical equations. Results of Paschen curve calculations and parallel geometry PDP's are shown and discussed in relation to the strengths and weakness of each computational approach.

OWP2 14 A Gas Composition Study in PDPs : Experimens and Model Calculations J.R. GOTTSCHALK, O. SHVYDKY, A.D. COMPAAN, C.E. THEODOSIOU, J.M. , *Department of Physics and Astronomy University of Toledo* W. WILLIAMSON JR., *Embry Riddle Aeronautical University** We have made both experimental measurements and model calculations in a plasma display panel pixel cell. We have measured the breakdown voltage, range of bistability, and the light emission from the discharge. The measurements were made in a model chamber where the gas pressures and concentrations were varied. The calculations were made using a 1-D code with variable gas components. Calculations for the breakdown voltage, bistability range, and uv light output have been made.

*Funded by NSF.

OWP2 15 Surface Electronic Structures of Oxidized Metal Electrodes and Flickering of Backlight for Small Flat Liquid Crystal Display KOZO OBARA, NARIAKI IMAMURA, ZU-SHUN XU, *Kagoshima University* RYO-ICHI HIGASHIZONO, *Ueno Manuf. Co.* We present relations between surface electronic structures of metal electrodes and time and spatial dependences of optical characteristics of 3/4-inch flat-type backlight for liquid crystal display of CCD movie camera. The characteristics of the discharge strongly depended on the electronic states of the oxidized electrode and the wall. The electronic states of electrodes

and wall were dominated by the mass transport induced by the external forces; temperature difference and electric field, and kinetic energy of impinging particles. We confirmed two phenomena: one is the time dependence of the discahrge on the oxidized electrode, which is constricted to the thin line-region by the potential of both walls, and its spatial distribution was dispersed as the time proceeds because of the phase transition of cromium oxides induced by the kinetic energies of impinging particles, and another is the temperature and electric field dependences of the flickering. The flickering was generated at low temperature and low potential region. These experimental facts show that the importance of the mass transport on the wall and electrodes induced as the result of the energy dissipation of the input power.

SESSION OWP3: POSTER SESSION: POSITIVE AND NEGATIVE IONS IN PLASMAS
Wednesday afternoon, 21 October 1998
Haku/Pikake Room, Aston Wailea at 15:15
Irving Langmuir, General Electric, presiding

OWP3 1 Laser cooled $^9Be^+$ plasmas in a Penning trap* B.M. JELENKOVIC, J.J BOLLINGER, A.S. BARTON, T.B. MITCHELL, X.-P. HUANG, W.M. ITANO, D.J. WINELAND, *NIST, Boulder* We present results from experiments with cylindrical Penning traps. Near resonant laser light cools 5 x 10^5 ions to 5 mK while laser torque applied to the plasma results in a narrow column along a 6 T magnetic field (0.1mm diameter, 6 mm length) with density close to Brillouin limit of 10^{10} cm^{-3}. We plan to use these long, dense plasmas to trap and sympathetically cool moderated positrons with laser cooled $^9Be^+$ ions. Estimates of the capture efficiency based on Monte-Carlo simulation of cumulative small-angle scattering will be given. Rf potentials with opposite phases, applied to a two-sector electrode near the trap center, were used to control the ion plasma rotation frequency[1]. Low rotation frequency spreads the plasma to large radius, which, together with voltage induced trap anharmonicity, leads to donut shape plasmas with very few ions near trap center[2]. Laser cooled ion plasmas form crystals with the long range order. We show results from Bragg scattering studies and real space images of the observed crystalline order.

*supported by the US Office of Naval Research

[1]X.-P. Huang et al., Phys. Rev. Lett. 80,73(1998)
[2]D. Poulsen and R. Spencer, Phys. Plasma 5, 345 (1998)

OWP3 2 Characterization of Vacuum Arc-Discharge Deuterium Plasma Ion Sources JAMES BROWNING, STEVEN BALSLEY, ROBERT KOSS, *Sandia National Laboratories* ROBERT SHORT, *University of South Florida** Ion and energy distributions from time-of-flight (TOF) mass spectrometry are presented for ions emanating from a vacuum arc-discharge deuterium plasma ion source. A hemispherical energy analyzer is incorporated into a linear TOF instrument for studying ion and energy distributions. Ions emerging from the source are collimated and energy tagged and subsequently imaged onto the entrance slit of the hemispherical analyzer. Also presented are data acquired from experiments evolving high resolution, high sensitivity mass spectrometry. In these experiments gases produced in the operation of the vacuum arc-discharge source are analyzed using a Finnigan MAT 271 mass spectrometer. Together, these data will be used to improve and enhance deuterium ion production.

*Sandia is a multiprogram laboratory operated by Sandia Corporation, a Lockheed Martin Company, for the United States Department of Energy under contract DE-AC04-94AL85000.

OWP3 3 Distributions of Negative Oxygen Ions in a Capacitively Coupled GEC-Reference Cell H.-M. KATSCH, T. STURM, E. QUANDT, H.F. DÖBELE, *Institut für Laser und Plasmaphysik, Universität-GH Essen, 45117 Essen, Germany** Axial density profiles of negative oxygen ions are determined in an RF-discharge with asymmetric capacitive coupling by photodetachment in combination with a Langmuir probe. The densities of charge carriers are axially constant in case of small excitation voltages (for amplitutes < 200 V) and a pressure of 13.8 Pa. With increasing excitation voltage (> 250 V) the charge carriers peak on the center of the discharge as is typical for electropositive discharges. With increasing pressure (50 Pa) and with medium excitation voltages the influence of the DC offset manifests itself by a shift of the maximum of the negative oxygen ion density towards the driven electrode. Pulsing the discharge allows to demonstrate the influence of atomic oxygen and the metastable O_2 ($a^1\Delta_g$) molecules on the balance of the negative oxygen ions. The time behavior of both the negative ions and the emission of O_2^+ ions demonstrate that the O_2 ($a^1\Delta_g$) represent the dominant loss channel for the negative oxygen ions.

*Supported by the 'Deutsche Forschungsgemeinschaft' in the frame of the SFB 191: 'Physikalische Grundlagen der Niedertemperaturplasmen'

OWP3 4 Negative and Positive Ion Energies in an RF Plasma in Nitrous Oxide J.A. REES, C.L. GREENWOOD, D. SEYMOUR, *Hiden Analytical Limited* It is known that negative ions are important in the plasma oxidation of silicon and silicon nitride surfaces and there is growing interest in the use of nitrous oxide instead of oxygen as the plasma gas. The present paper describes an investigation into the distribution of energies with which the O- ions produced in a capacitive RF plasma impinge on the grounded discharge electrode and compares these energies with those of the positive N20+ ions produced under the same plasma conditions. It is shown that the maximum energy of the O- ions is largely determined by the D.C. bias of the driven electrode and is independent of changes in the plasma potential. It is, therefore, possible in such systems to select, independently, the energies of the positive and negative ions. The energy distribution of the O- ions show interesting structure, which for a given D.C. bias, is a function of the input RF signal. The investigation confirms that, for strongly assymetric geometries, negative ions produced in the sheath of the driven electrode of a capacitive RF plasma system travel through the plasma and impact on the counter electrode with a range of energies.

OWP3 5 Measurement of Negative Ion Density in an Oxygen DC Glow Discharge by Optogalvanic Photodetachment Spectroscopy YOSHINOBU MATSUDA, HITOMI NAGAMATSU, HIROSHI FUJIYAMA, *Department of Electrical and Electronic Engineering, Nagasaki University, Japan* We measured the local density of oxygen negative ions (O^-, O_2^-) in an O_2 dc glow discharge by laser optogalvanic photedetachment spectroscopy. The advantages of the photedetachment spectroscopy are its simplicity, quantitative capability for density evaluation, and straightforward data analysis compared with other diagnostics. However,

the use of a probe for collecting photodetached electrons in reactive plasma environment, a careful attention has to be paied because the electron collection efficiency may be changed due to the change of surface condition of the sampling probe. In fact, we often observed an abnormal signal intensity in the laboratory experiments. Therefore, we have chosen gold as probe material and carefully investigated the influence of sputter-deposition and laser irradiation on the electron collection efficiency. As a result, we have succeeded in obtaining a reproducible and reliable spatial distributions of negative ion density. For the 0.2 Torr oxygen dc glow discharge (550V,7mA) in a parallel plate electrodes of diameter 40mm and with gap distance 30mm, we have obtained the following values: $[O^-] \simeq 2 \times 10^8 cm^{-3}$, $[O_2^-] \simeq 10^8 cm^{-3}$, whereas $[n_e] \simeq 1.2 \times 10^{10} cm^{-3}$ at the negative glow region.

OWP3 6 Production and Loss Mechanisms of H^- in Helicon-Wave H_2 Plasmas D. HAYASHI, M. NAKAMOTO, K. SASAKI, K. KADOTA, *Nagoya University, Nagoya, Japan* K. TSUMORI, Y. OKA, O. KANEKO, *National Institute for Fusion Science, Toki, Japan* We have developed a helicon-wave-excited H^- source for NBI heating of thermonuclear fusion plasmas. The H^- ions were efficiently produced by pulsed-discharge operation and optimizing the plasma profile with control of the magnetic field configuration. Major concerns in achievement of the efficient production can be categorized as follows; (1) the contribution of excited H_2 to the enhancement of the volume-production of H^-, and (2) the understanding of the dominant loss process in high-density plasmas. We applied laser-photodetachment technique for the measurements of H^- density. The relative populations for electronic-excited states of H_2, H_2^*, were measured by optical emission spectroscopy combined with a collisional-radiative model for H_2 plasmas. The correlation between the H^- yield and H_2^* density was investigated. The production efficiency of H^- linearly increased with H_2^* density. With regard to the loss processes, the mutual neutralization between H^- and H^+ ($H^- + H^+ \rightarrow H + H^*$) becomes significant, which yields H and H* as products. The optical emissions from H* produced by the mutual neutralization was observed in the afterglow. The relationship between the emission intensity and H^- (or H^+) density was studied.

OWP3 7 Production and Loss Mechanisms of H^- in Helicon-Wave H_2 Plasmas D. HAYASHI, M. NAKAMOTO, K. SASAKI, K. KADOTA, *Nagoya University, Nagoya, Japan* K. TSUMORI, Y. OKA, O. KANEKO, *National Institute for Fusion Science, Toki, Japan* We have developed a helicon-wave-excited H^- source for NBI heating of thermonuclear fusion plasmas. The H^- ions were efficiently produced by pulsed-discharge operation and optimizing the plasma profile with control of the magnetic field configuration. Major concerns in achievement of the efficient production can be categorized as follows; (1) the contribution of excited H_2 to the enhancement of the volume-production of H^-, and (2) the understanding of the dominant loss process in high-density plasmas. We applied laser-photodetachment technique for the measurements of H^- density. The relative populations for electronic-excited states of H_2, H_2^*, were measured by optical emission spectroscopy combined with a collisional-radiative model for H_2 plasmas. The correlation between the H^- yield and H_2^* density was investigated. The production efficiency of H^- linearly increased with H_2^* density. With regard to the loss processes, the mutual neutralization between H^- and H^+ ($H^- + H^+ \rightarrow H + H^*$) becomes significant, which yields H and H* as products. The optical emissions from H* produced by the mutual neutralizatikon was observed in the afterglow. The relationship between the emission intensity and H^- (or H^+) density was studied.

OWP3 8 Estimate of Negative Ion Density in C_4F_8 ECR Plasma MASAKO SHINDO, SHINJI HIEJIMA, YOKO UEDA, YOSHINOBU KAWAI, *Interdisciplinary Graduate School of Engineering Sciences, Kyushu University* SATOSHI KAWAKAMI, *Tokyo Electron Tohoku Limited* NOBUO ISHII, *Tokyo Electron Limited* Fluorocarbon gases such as C_4F_8 have been widely used for SiO_2 etching, but C_4F_8 plasma parameters have not been measured yet. We measured C_4F_8/Ar ECR plasma parameters with a heated Langmuir probe and 8-mm microwave interferometer[1]. Furthermore, the negative ion density was estimated from the following equation:

$$\frac{I_{is}(C_4F_8)}{I_{is}(Ar)} = \left[\frac{I_{es}(C_4F_8)}{I_{es}(Ar)} + \frac{N_-}{n_i(Ar)}\sqrt{\frac{T_e(C_4F_8)}{T_e(Ar)}}\right]\sqrt{\frac{m_i(Ar)}{m_i(C_4F_8)}} \quad (1)$$

where I_{is} and I_{es} is the ion saturation current and electron saturation current, respectively. The negative ion density N_- can be determined when the ion reduced mass $m_i(C_4F_8)$ is assumed. As a result, we found that the ratio of negative ions to positive ions amounts to more than 60%. We also measured CF_4 ECR plasma parameters and found that there were much negative ions. 1)M. Morimoto, Y. Ueda, S. Hiejima, I.Katsumata and Y. Kawai, Jpn. J. Appl. Phys. **36** (1997) 4659

OWP3 9 Accumulation of Negative Ions around Magnetized CF_4 Plasma Column and their Mass Analysis MIENO TETSU, *Dept. Phys., Shizuoka Univ.* KAWAI RYOICHI, *Dept. Phys., Shizuoka Univ.* Electronegative plasmas are widely used in dry etching and another plasma processings. However, properties of negative ions in these plasmas are not clear because the diagnosis of negative ions is not easy. Here, mass distribution and contents of both negative and positive ions in a magnetized CF_4 plasma column are diagnosed by a newly developed cyclotron resonance mass spectrometer and a Langmuir probe. This spectrometer can measure both negative and positive ions in the plasma separately and simultaneously. As a result, large amount of F^- ions are found to be accumulated around the plasma column, where negative ion density is much larger than electron density, the reason of which will be discussed in the presentation. By using a follow type magnetized plasma, we successfully accumulate negative ions at central core of the follow plasma, which is more useful for negative ion sources. Ref.: R. Kawai & T. Mieon, Jpn. J. Appl. Phys. Vol. 36 (1997) L1123.

OWP3 10 Measurement of negative-ions in sheet plasma by photodetached method AKIRA TONEGAWA, *Department of Physics, School of Science, Tokai University* KAZUTAKA KAWAMURA, *Research Institute of Science & Technology, Tokai University* MASAHIRO SATO, *Department of Nuclear Engineering, School of Engineering, Tokai University* KAZUO TAKAYAMA, *Research Institute of Science & Technology, Tokai University* HARUO SHINDOW, *Department of Applied Physics, School of Engineering, Tokai University* TUGUHIRO WATANABAE, HAJIME SUZUKI, NOBUYOSHI OHYABU, *National Institute for Fusion Science, 322-6 Oroshi, Toki Gifu 509-52, Japan* This abstract was not submitted electronically.

SESSION OWP4: POSTER SESSION: INNOVATIVE PLASMA APPLICATIONS
Wednesday afternoon, 21 October 1998
Haku/Pikake Room, Aston Wailea at 15:15
Irving Langmuir, General Electric, presiding

OWP4 1 Plasma hardening of railway wheel surface E.KH. ISAKAEV, P.P. IVANOV, A.S. TYUFTYAEV, *Science and Engeneering Centre for Energy Efficient Processes and Equipment, Associated Institute for High Temperatures, Russian Academy of Sciences* I.L. PARISTYI, A.A. TROITSKY, A.E. YABLONSKY, *Moscow Railways* G.A. FILIPPOV, *I.P. Bardin Central Institute for ferrous metallurgy, Russia* A computer-controlled plasma technology was developed for the treatment of rolling stock wheels, providing the thermal hardening of tread and flange working surfaces. As a result of the plasma treatment the surface hardness of the wheel grows from 255 up to 420-450 HB. Herewith, the wear capability of the wheel metal grows 2-3 times and its resistance to the weariness-driven destruction grows 1.5 times due to the pecularities of the structural state of the steel, arising out of the thermal impact and of the alloying of the steel with nitrogen during the plasma treatment. Installation of several plants based on this technology in engine houses allowed to carry out a full scale experiment in order to assess the running characteristics of treated wheel sets in comparison with plain ones. Wheel life between mounting and truing or dismounting doubles due to plasma hardening.

OWP4 2 Laser Induced Fluorescence Spectroscopy of O- and N- Atoms in a Dielectric Barrier Discharge MICHAEL SPAAN, H.F. DÖBELE, *Institut für Laser und Plasmaphysik Universitätsstr.5, 45117 Essen, Germany* Dielectric Barrier Discharges are being considered as possible systems for exhaust gas cleaning of mobile engines. The knowledge of N - and O - concentrations in these discharges is of crucial importance. Space resolved TALIF measurements performed at a filament localized at a stainless steel tip are reported. Two-dimensional relative radical concentrations are obtained for various parameter combinations. Operating the DBD with fast rising voltages results in well defined ignition and allows time resolved measurements. LIF spectroscopy of NO yields additional information on the gas temperature and NO concentration. Emission spectroscopy of N_2 and O provides information on the longitudinal filament structure. The gas composition at the reactor outlet is monitored by FTIR spectroscopy. (Funding by the "Bundesministerium für Bildung, Wissenschaft, Forschung und Technologie" is acknowledged, Project Number 13 N 7195)

OWP4 3 The Effect of Carbonaceous Deposit for NOx Dissociation KAGEHIRO ITOYAMA, *Nagasaki University* The carbonaceous deposit is formed on the surface of electrodes, when the short gap discharge generates in the mixed gas of CH4 and N2 +NO. After this pre-treatment gave, authors investigated the effect of carbonaceous deposit for NOx dissociation by floating N2 +NO gases with keeping 500Torr or 700Torr of the pressure in the discharge chamber. NOx concentration in this work was 458ppm, 1101ppm and 4502ppm. In the pre-treatment, the ratio of mixed gas was changed 60pressure was 20Torr to 70Torr. From result of measurement by Q-mass, authors clarified that C2H2 increased immediately the beginning of discharge in spite of the difference of pre-treatment. The species of NO decreased as a function of times. Especially, gradient of NO decreases is larger in immediately the beginning of floating and discharge. The carbonaceous deposit is effective for NOx dissociation as the catalyst, because it's ratio in before discharge is higher than in after discharge. Moreover, the results of analysis of the carbonaceous deposit show double or triple combination of carbon and hydrogen.

OWP4 4 Degradation of Gateoxide Exposed to Inductively Coupled Hydrogen Plasma AKIHIRO IKEDA, YUKINORI KUROKI, *Graduate School of Information Science and Electrical Engineering, Kyushu-University, Fukuoka, Zip code 812-8581, Japan* Hydrogen plasma is interested for cleaning of high aspect ratio structure on semiconductor surface at low temperature. We investigate the degradation of MOS capacitor exposed to Inductively Coupled hydrogen Plasma (ICP). Much more electron trap centers which are activated by hot electron injection are introduced into the oxide by hydrogen plasma exposure. Hydrogen plasma generates many defects in oxide lattice structure, also passivates the defects such as dangling bond and makes many Si-OH and Si-H groups in oxide. This hydrogen in the oxide is easily depassivated by non elastic collision to hot electron and generates electron traps. Electron trap density is increased with increasing incident ion energy to the substrate. With increasing gas pressure during plasma exposure, hole trap centers are appeared instead of electron trap centers and charge trap density is decreased as compared with lower gas pressure condition. This is caused by the decrease of incident ion flux to the substrate with decreasing electron temperature.

OWP4 5 Dissociation of Carbon Dioxide in the Martian Simulant Gas Discharge* T. DINH, S. POPOVIC, R. L. ASH, L. VUSKOVIC , *Old Dominion University* Martian atmospheric gas processed by a radio frequency discharge result in a mixture of oxygen, carbon monoxide, residual carbon dioxide, and other minor components. Recombination of oxygen and carbon monoxide into carbon dioxide is slow enough to allow the extraction of oxygen downstream of the radio frequency discharge reactor. In a series of experiments we verified these data, based on a simplified model where a limited number of elementary processes was included. We also compared the efficiency of inductive and capacitive discharges in the same density, temperature and power ranges. Relationship between the average reduced electric field and discharge gap in capacitive discharge was established. Sharp maximum in oxygen flux observed in our earlier experiments[1] was used to determine the optimum operating conditions. The experiments confirm the extensive dissociation of carbon dioxide, in spite of being performed in a limited range of the average reduced electric field.

*Supported by NASA JSC.
[1]Z. Shi, D. Wu, and R. L. Ash, SAE Paper 961598 (1996).

OWP4 6 Low Cost Ozone Generation in Corona Streamer B. POTAPKIN, A. KNIJNIK, S. KOROBTSEV, D. MEDVEDEV, V. SHIRYAEVSKY, *Russian Research Center ''Kurchatov Institute''* There is an interesting experimental result (S. Korobtsev, D. Medvedev et al , ISPC 13,1997, vol.2, p. 755.) for low cost ozone generation (7-8 eV/molec in air) in streamer with dominant energy consumption in streamer channel (where molecular vibrations are excited). For explanation we considered the effect of vibrational pumping saturation, when vibrational energy was increased (due to the super-elastic processes) and the change of electron cross-sections due to vibrational excitation, which could also lead to efficiency growth. Boltzmann equation solution showed that both

effects required too large energy consumption in discharge (> 0.7 eV/mole). Thus we went to conclusion, that some direct energy transfer from vibrational degrees of freedom to electronic degrees should take place. One of the possible new mechanisms is the reaction: $N_2(v)+N_2(v)=N_2(A)+N_2$. Our numerical model of vibrational kinetic in air with this reaction showed that dependence of ozone generation cost upon energy consumption in streamer channel had a minimum with the value of the cost about 8-10 eV/molec.

OWP4 7 Ozone generation by discharge inside the bubbles in water C. YAMABE, S. IHARA, T. MIICHI, S. SATOH, *Faculty of Science and Engineering, Saga University, Saga 840-8502, Japan* The purpose of this research is an efficient utilization of radicals such as atomic oxygen, ozone and OH radical which are generated in the bubbles and in water by discharge. The bubbles are generated at the discharge region between electrodes by a bubling tube. A pulse-power generator which is able to obtain a rapid rise time of applied voltage between electrodes(typical gap spacing 7.6mm) was used as a power supply. The peak value of output voltage, its pulse width and current are about 100kV, 100ns and 1kA, respectivery. Many small oscillations observed on the waveform of the applied voltage suggest that the discharge occurs in bubbles. The light emission produced by discharge from the bubbles was also observed. The input energy to discharge region was about 1J. Blumlein type of pulse-power source was also used for a pair of disk electrodes(diamater of 30mm, gap spacing of 5mm) at the discharge repetiotion rate of 15 pulse per second. The diamater of bubbles is about 1mm. The maximum applied voltage and discharge current of about 25kV and 150A were measured at the charging voltage of 10kV. The measured ozone which comes from the water was about 43mg/Nm^3 at the oxygen gas flow rate of 0.7l/min and 122mg/Nm^3 at 0.6l/min. In latter case, a $TiBaO_3$ plate(relative dielectric constant of 400 and thickness of 4.5mm) was attached on the surface of the electrode.

SESSION OWP5: POSTER SESSION: RF GLOWS
Wednesday afternoon, 21 October 1998
Haku/Pikake Room, Aston Wailea at 15:15
Irving Langmuir, General Electric, presiding

OWP5 1 Electromagnetic Electron Surface Waves in a Non-Uniform Thermal Plasma KEVIN BOWERS, *EECS Dept., Univ. of Calif. Berkeley, CA 94720-1770* The quantitative theory of resonance oscillations in a non-uniform thermal plasma given by Parker, Nickel and Gould and the surface wave theory given by Cooperberg are extended in this paper. The new theory relaxes the electrostatic assumption of both theories and approximately includes the effects of electron-neutral collisions. For a planar plasma slab with no applied magnetic field, the new equations decouple into two distinct types of oscillations. Quasi-electrostatic modes are identical to the resonances predicted by PNG / Cooperberg in the limit of electrostatic theory. Quasi-transverse electric modes are governed by the same equations governing TE electromagnetic modes in the vacuum limit. The coupling of wave behavior in the plasma with external dielectrics and / or conductors is discussed. The equations governing the quasi-electrostatic modes are solved numerically for eigenmodes and dispersion for various plasma slab profiles and material boundaries. Lastly, the predicted heating and impedance of a resonantly sustained discharge experiment are computed and compared with the results from simulation in the accompanying paper.

OWP5 2 Resonant Discharge Simulations; Comparisons with Theory and Experiment C. K. BIRDSALL, K. J. BOWERS, *EECS Dept., Univ. of Calif. Berkeley CA 94720-1770* Discharges driven at the series resonance frequency have a small input resistance. The voltage drive is small (like Te), and the average plasma potential is low (like 10Te). Such were observed experimentally by Godyak et al. (paper 3C9, IEEE ICOPS, Santa Fe NM, 6-8 June 1994). Our PIC-MCC simulations and theory [K. Bowers, accompanying paper, and Cooperberg and Birdsall (PSST, Vol. 7, Feb and May 1998)], show similar results. The electron heating profile (J.E) is different from that of a low pressure capacitive discharge. Our scaling laws, at fixed pressure, show peak electron density proportional to the cube of the drive frequency (cap. have as the square), as derived by Godyak (Sov. J. Plasma Phys. Vol. 2, p.78 1976). The electron energy distribution in the bulk is bi-maxwellian. The ion energy distribution at the target (wall) has a peak at the peak average potential, with a narrow ion angular spread about the normal, at low pressures. Results will be shown for a range of pressures from collisionless to collisional. We are supported by DOE DE-FG03-97ER54446 and AFOSR FDF 49620-96-1-0154.

OWP5 3 Gas Lasers with RF Capacitive Discharge at Different Frequencies NIKOLAI YATSENKO, *Optical engineering, Inc., Institute for Problems in Mechanics, Russian Academy of Sciences.* Radio frequency (RF) capacitive discharges are widely used for a pumping of different gas lasers (atomic, molecular, ion). Their space structure features determine the advantages of lasers with the RF excitation. The important peculiarity of a space structure of the RF capacitive discharge is its dependence upon the RF frequency. The purpose of this work is a systematic study of the RF frequency influence on the RF capacitive discharge space structure and thus on the output characteristics of gas lasers with the RF pumping. The experiments were carried out at frequencies (0.5 - 120) MHz with CO_2, CO, N_2, He, Ne, Ar, Xe, and their mixtures. The pressure was from 0.1 to 200 Torr. The maximum RF power input - 6 kW, the maximum input power density - 100 W/cm^3. Water-cooled flat or profiled RF electrodes with a dielectric cover of a different thickness or without it were used. The maximum area of each electrode reached 0.1 m^2. The influence of additional DC electric and magnetic fields on the characteristics of gas lasers, excited at different RF frequencies, was studied. The experiments have shown, that the main properties of the RF discharge plasma could be explained by its space sheath structure at all the frequencies.

OWP5 4 E to H Transition Dynamics in a Pulsed RF Plasma GILLES CUNGE, BRENDAN CROWLEY, DAVID VENDER, MILES TURNER, *PRL, DCU** The mode transition between a low power capacitive (E mode) and a high power (H mode) inductive discharge is investigated in a inverted geometry where the plasma surrounds the excitation coil. The transition occurs at relatively low power in this configuration and exhibits pressure dependent hysteresis. The hysteresis of the transition current and dynamics of the transition are examined in a time modulated discharge where the injected power is ramped up and down in a triangular waveform. The time evolution of the discharge is diagnosed by a Scientific Systems I/V head which measures the voltage and current in the antenna, a Scientific Systems Langmuir probe operating in boxcar mode, a 50 cm spectrometer to monitor the 750.4 and 420.0 nm argon emission lines, and a directional RF

power meter to measure the instantaneous power delivered to the discharge. The evolution of the transition is found to depend strongly on the matching conditions and the effect of the matching network on the overall behavior of the pulsed discharge is investigated in detail.

*This work is supported by Association EURATOM DCU Contract ERB 50004 CT960011

OWP5 5 rf Driven DC Electron Beam Source D.M. SHAW, M. WATANABE, G.J. COLLINS, *Dept. of Electrical Engineering, Colorado State University* A small area ((2.5 cm diameter) electron beam source using ion-induced secondary electron emission from a rf biased, Al2O3-coated electrode has been demonstrated scientifically. The new electron beam source differs from previous soft vacuum DC electron beam sources in three major ways: 1, a separate, independently powered inductively coupled plasma sustains the discharge and allows lower pressure operation (1—20 mTorr for the new source versus 100–1000 mTorr for the prior art sources); 2, a more robust cathode material is used (Al2O3 for the secondary emitter in the new electron source versus metal or Cermet materials for the old sources); and 3, beam flux and beam energy are set by the ICP power and the cathode voltage respectively. The electrode bias potential sets the electron beam energy, with the maximum beam energy equal to the peak-to-peak rf (13.56 MHz) voltage on the powered electrode. A differentially pumped retarding potential analyzer measures the electron beam flux and energy characteristics, which are related to reactor argon gas pressure (1–20 mTorr), ICP power (125–500 W), and cathode rf and DC self bias potential (0 to 1000 V).

OWP5 6 Circuit Model for Capacitive Coupling in Inductively Coupled Plasmas M. WATANABE, D.M. SHAW, G.J. COLLINS, *Dept. of Electrical Engineering, Colorado State University* H. SUGAI, *Dept. of Electrical Engineering, Nagoya University* A crude circuit model has been developed to illustrate and account for capacitive coupling between the rf coil and the bulk plasma in a stove top inductively coupled plasma source. The circuit model is composed of three levels of capacitance: the dielectric window capacitance, sheath capacitance contiguous to the dielectric window, and the chamber to ground sheath capacitance. The model is verified by quantitative comparison with the measured rf plasma potential in the bulk plasma body, plasma feedstock gas (argon) pressures below 2 mTorr. At higher pressures above 5 mTorr, the measured results diverge from the circuit model due to the transition from a spatially uniform electron density throughout the bulk plasma at pressures less than 2 mTorr to a less spatially uniform electron density at pressures above 5 mTorr.

OWP5 7 Sheath Dynamics and Field Reversal in a Hydrogen RF-Discharge investigated by electric field measurements U. CZARNETZKI, D. LUGGENHÖLSCHER, H.F. DÖBELE, *Institut für Laser- und Plasmaphysik, Universität GH Essen, D-45117, Germany** Anomalous sheath heating and field reversal in RF-discharges with molecular gases like nitrogen or hydrogen have been discussed for some years. A novel laser spectroscopic technique allows the measurement of electric fields in atomic hydrogen below 100 V/cm, typical for field reversal. Time and space resolved measurements of an asymmetric capacitively coupled RF-discharge in hydrogen in the GEC reference cell are presented. The peak-to-peak voltage is 650 V, the self-bias voltage is 245 V, and flux and pressure are 90 sccm and 80 Pa, respectively. Sheath electric fields, charge densities, sheath voltages, displacement and conduction currents are measured at the powered and the grounded electrodes. A negative charge distribution builds up during sheath contraction at the sheath edge that finally forms a 'capacitor field' when the electrode gets positively charged. This charge distribution vanishes when the voltage becomes negative again. The electrons are gaining energy by acceleration within the sheath rather than by being pushed by a sharp expanding sheath front. A simple fluid model is presented that describes the charge disributions and fields during field reversal.

*Supported by the ''Bundesminister für Bildung und Forschung.''

OWP5 8 A Study of Sheath Structure in a Radio-Frequency Discharge in Helium Y. W. CHOI, *Korea Electrotechnology Research Institute* K. KAWAMURA, *Kyushu University,Japan* J. B. KIM, M. D. BOWDEN, K. MURAOKA, In this study, three different methods were used to investigate the sheath region in a capacitively coupled rf discharge. In an experimental study, electric fields were measured using a laser-induced fluorescence technique. The extent of the sheath could be estimated from the position at which the electric field becomes zero. It was found that the measured sheath width depended strongly on pressure. In a separate study, the properties of the discharge were calculated using a particle-in-cell simulation. The electric field and other properties such as electron density were outputs of the simulation. The results of the experimental and simulation studies were then compared with an analytical calculation of the sheath properties, such as the sheath width, which was made using collisional sheath theory. For the analytical calculation, plasma properties such as the electron temperature and density were essential, and these were measured using a Langmuir probe. Comparison of the results of each study was useful for testing the validity of both the simulation and collisional sheath theory.

OWP5 9 Effect of Gas Flow on RF Plasmas N. SATO, *Iwate University* Y. SHIDA, *Iwate University* A Monte Carlo simulation (MCS) technique has been used for investigating effects of gas flow on the characteristic of rf plasmas sustained between parallel plates under a plasma processing condition. In this MCS, for neutral atoms and molecules, a Maxwelliam velocity distribution modified by gas flow is assumed. A typical one dimension spatial variation of the electric field averaged over one rf cycle is used for the calculation. The electron and ion density distributions between the electrodes are obtained by changing the gas pressure. A significant effect of gas flow on the ion density distribution in the bulk region of the rf plasma has been observed under a condition that the velocity is larger than that of the ion diffusion motion. Using the results of the MCS, validity of a fluid model in which the velocity of gas flow is added to the drift and diffusion motion is examined. This shows that such a fluid model may be valid at a pressure above 133 Pa. Under this conditin, using a self-consistent fluid model for silane rf plasmas, the electron and ion density distributions modified by gas flow have been obtaind.

OWP5 10 Plasma sheath electric field strengths above a grooved electrode in a parallel-plate radio frequency discharge G. A. HEBNER, *Sandia National Laboratories* U. CZARNETZKI, D. LUGGENHOLSCHER, H. F. DOBELE, *Universitaet GH Essen, Germany* M. E. RILEY, *Sandia National Laboratories* During plasma etching of microelectronic structures such as deep trenches, the direction and energy of the ions that strike the surface has a major influence on the characteristics of the etch profile. However, the wafer surface is a multidimensional surface with several layers of subsurface dielectrics and structures

that can significantly modify the electric field direction and ion trajectories. To examine the details of the spatial distribution of the electric field strength in the sheath region above an electrode with surface structure, we have measured sheath electric fields above a structured electrode. The magnitude of the sheath electric field above a grooved electrode was measured using a novel, two color, laser induced fluorescence technique. Spatially resolved electric fields in the sheath region were determined by mapping the field induced Stark splitting of the n = 14 level in atomic hydrogen. Measured electric field values are in good agreement with calculated values. GAH thanks the Deutsche Forschungsgemeinschaft for a travel grant in the frame of the SFB 191. GAH and MER were supported by the United States Department of Energy (DE-AC04-94AL85000). Expert technical support by Rainer Fuhrer is gratefully acknowledged.

OWP5 11 Detailed measurements of Radial and Axial Structure of RF Glow Discharge H. SASAKI, K. NANBU, M. TAKAHASHI, *Inst.Fluid Science,Tohoku Univ.* After 1990, main interest in the numerical simulation of materials processing plasmas moved to axisymmetrical or three-dimensional problems. Since then, many papers based on the fluid model or particle model have been published. However, the comparison of obtained numerical data with experimental data is not enough. To promote such a comparison and make it possible to examine the validity of numerical methods employed, we propose a set of detailed experimental data on the structure of axisymmetrical rf argon discharge with a practical dimension. The pressure range of our measurements is 0.05Torr – 0.4Torr. The 13.56MHz rf power through a matching box is 150W. Mass flow rate of argon gas is 50 – 800ccm. The diameter of two copper electrodes is 190mm. The discharge chamber made of stainless steel is 355mm in inner diameter and 500mm in height. Two pumping systems are used. It is possible to change the mass flow rate continuously from low to high rate. After the chamber is evacuated up to 10^{-5} Torr, argon gas is fed up to a given pressure. Then the rf power is applied between the two electrodes. The following properties have become clear after examining all the data. The electron number density shows a spatial oscillation between the electrodes and the amplitude of the oscillation increases as the gas pressure increases. But the ion number density is almost constant in the axial direction.

OWP5 12 Combined Inductively- and Capacitively- Coupled Antenna for Large-Scale Light Sources JUN INOUE, MAMORU MATSUOKA, MOTOICHI KAWAGUCHI, *Mie University* We devised and tested a combined coupling method where both an inductively-coupled antenna and a capacitively-coupled antenna were used to feed an rf power. A coil, surrounding a sphere discharge tube at the equatorial plane, has been used in a long life light source so far. With such an inductively-coupled antenna, the discharge became donut-like and unsuitable for a light source, when the diameter of the discharge tube was enlarged to about more than 5 cm. In addition to the coil located at the equatorial plane, we attached an electrode at both pole positions. Two leads of the coil and two electrodes were connected in parallel. Thus the rf current inductively induced by the coil should flow in the longitudinal direction and the current capacitively induced by the electrodes should flow in the pole-to-pole direction alternately. We obtained a homogeneous plasma in a discharge tube with 13 cm of diameter. A localized discharge was, however, also obtained, depending on the procedure to ignite a plasma. Such a localized plasma would be avoided by optimizing the coupler system and the operating procedure. Large-scale rf-based light sources will be realized by adopting this combined coupling method.

OWP5 13 Reduction of Plasma Potential in an rf Ion Source with a Magnetized Antenna KAZUKI OHNO, MAMORU MATSUOKA, MOTOICHI KAWAGUCHI, *Mie University* One of the key issues to realize rf sources is to reduce high plasma potential, caused by an rf field. Otherwise, frequent arcing occurs and plasmas are contaminated by electrode and wall materials. To overcome this problem, we devised and tested 'magnetized' capacitively-coupled antennas, where a thin magnet is sandwiched in two copper plates in each electrode and thus electrons accelerated by rf field are prevented from impinging on the electrodes. The ion source made use of was of magnetic multipole type. The size of the magnets buried in the electrodes immersed in a plasma was 40mm× 40mm× 3mm. The size of the copper plates attached to the magnets was 60mm× 60mm× 0.5mm. We confirmed the plasma floating potential was reduced from 80 V to 40 V, when the unmagnetized antenna was replaced by the magnetized antenna. The plasma was, however, produced locally near the periphery of the antennas. A grill-like antenna immersed in a plasma was found to be good for obtaining a homogeneous plasma. A grill-like antenna with magnet is, therefore, expected to produce a homogeneous plasma with low plasma potential. This type of antenna is being tested to optimize the geometry.

OWP5 14 Characteristics of VHF Plasma Produced Using a Ladder-Shaped Antenna MASAYOSHI MURATA, HIROSHI MASHIMA, TATSUJI HORIOKA, *Mitsubishi Heavy Industries Ltd., Japan* TSUKASA YAMANE, YOSHINOBU KAWAI, *Interdisciplinary Graduate School of Engineering Sciences, Kyushu University, Japapn* Very high frequency (VHF) discharge plasmas have been used in the field of solar cells and thin film transistors (TFT) because of high density plasma (high deposition rate) and low ion energy (high quality films). We have developed a novel CVD device using an electrode of a ladder-shaped antenna and succeeded the plasma density is uniform within ± 10% over 300mm. Furthermore, increases in the frequency ($\sim 40MHz$) of the RF power source lead to increases in the plasma density.[1] In order to achieve higher deposition rate, we have investigated the effect of higher frequency ($\sim 120MHz$) on the plasma density with a ladder-shaped antenna. The H_2 plasma parameters measured with a movable Langmuir probe are examined as a function of discharge frequency, RF power, gas pressure and gas flow rate. The uniformity of the plasma density parallel to the antenna is achieved ± 13% for the distance of over 300mm at 80MHz.

[1]M.Murata et al, Jpn. J. Appl. Phys. Vol. 36 (1997) pp. 4563

OWP5 15 Two dimensional profiles of a pulsed capacitively coupled plasma Y. TAKEO, T. KITAJIMA, N. NAKANO, T. MAKABE, *Keio University at Yokohama,Japan* Capacitively coupled plasma(CCP) is one of the common tools for microelectronics fabrication. Pulsed plasma operation will be employed in plasma technology as highly selective SiO_2 etching. Experiments were performed in pulsed CCP at 13.56MHz(RF) during a periodic steady state. In the present study, we measured time-averaged and time-resolved two dimensional profiles of the net excitation rate of $Ar(3p_5)$ in pure Ar and in mixture $CF_4(5\%)$/Ar, as the probe of the plasma structure. When the duty ratio, defined by the ratio of the on-time to the total period, was changed from 10/20μs to 2/12μs, the peak of the net excitation rate in Ar at 25mTorr shifted to the outside of the RF electrode due to the diffusion of

charged particles in off time, and self-bias votage dropped from 270V to 230V in a periodic steady state. It was demonstrated that during off-time the sheath collapses and the electron density in front of the electrode increases. In addition, CT image was obtained under the condition that the low frquency bias voltage at 700kHz was applied to the opposite electrode.

OWP5 16 A Simulation of Step Responses of RF Silane Discharges JING YANG, HIROTAKE SUGAWARA, YOSUKE SAKAI, *Hokkaido University, Japan* PETER L.G. VENTZEK, *Motorola* HIROAKI TAGASHIRA, *Muroran Institute of Technology* The behavior of the transient response of electronegative radio frequency (RF) glow discharges is important for process control, better selectivity etch applications and charge free etching. We investigated step responses of silane discharges at 0.5 Torr under a driving frequency of 13.56 MHz. The present discharge model is a 1D fluid model of a capacitively coupled parallel plate reactor. In the case of that an RF voltage of 1100 V is changed stepwise to 700 V peak to peak, the steady state pulsed plasma modulation appears periodicaly with a few kHz. We interpret the transients in terms of both transport and chemistry. First, the gap voltage decreases significantly and the electric fields at any location in the gap begin to decay. The negative ions leave from the bulk and the net charge in the sheath is almost neutralized, then negative ions tend to diffuse less. The diffusion flux for negative ions becomes less than the drift flux, thus the negative ions can gather in the bulk again. Consequently, the plasma shows an oscillation. The transport and chemistry of negative ions and related species are indicated to provide this oscillation.

OWP5 17 Computer Modelling of Plasma Kinetics of RF Glow Discharge in Nitrogen.* KOHKI SATOH, HIDENORI ITOH, HIROAKI TAGASHIRA, *Muroran Institute of Technology, Japan* A self-consistent computer modelling of the plasma kinetics of RF glow discharge in nitrogen gas has been carried out using a one-dimensional Propagator method coupled with Poisson's equation and an external circuit. Gas pressure and applied frequency are assumed to be 1.0 Torr and 13.56 MHz, respectively, and electron-N_2 cross sections shown by Ohmori et al (J.Phys.D,vol.21,724-9) are used. Velocity distributions of charged particles used here have 60 mesh points for energy and 20 mesh points for polar angle. The discharge space is sliced in 100 slabs, and the velocity distributions are defined in each of the slabs. Behaviour of charged particles is described by calculating the balance of the particles in each of cells $f(\epsilon + \Delta\epsilon, \theta + \Delta\theta, x + \Delta x)$ of the velocity distributions in Δt. The spatio-temporal variations of the mean energies, the densities of the charged particles, the collision rate of ionisation and excitation and the electric field are calculated, and these are compared with the results from optical emission spectroscopy measurement.

*This work was supported by Grant-in-Aid (No.09650338) of the Ministry of Education, Science, Sports and Culture, Japan

OWP5 18 Near Sheath Structure in Electron Energy Distributions in an Argon rf Discharge. CATHERINE DEEGAN, DAVID VENDER, MICHAEL HOPKINS, *PRL, DCU** Capacitively-coupled rf discharges operate in three modes. At intermediate pressures and low currents the plasma is ohmically heated. Increasing the current results in a transition to a mode where the primary source of ionisation is secondary electron emission from electrodes. Spatially-resolved Langmuir probe measurements were performed on a capacitively-coupled rf discharge to characterise its spatial structure for each of the heating modes. Plasma parameters and EEDF's are measured both as a function of distance from the powered electrode and radially from the plasma centre to the walls. Charged particle density profiles are compared to the diffusion equation. The EEDF, measured axially and radially, did not vary to any great extent in the low-current mode at either low (25 mTorr) or intermediate (300 mTorr) pressures. Once in the high-current mode, the EEDF shows a marked 'peak' structure near the sheath regions which decreases in energy and disappears as we move away from the powered electrode.

*This work is supported by Association EURATOM DCU Contract ERB 50004 CT960011

OWP5 19 Reduction Parameter of Electron Temperature for Magnetic Filter with rf Plasma Operation N. HAYASHI, D. SATAKE, H. FUJITA, *Saga University, Saga 840-8502, Japan* The reduction parameter of the electron temperature for a magnetic filter was investigated in a radio frequency (13.56MHz) plasma. The magnetic filter was assembled of three parallel rod-type permanent magnets and set at a center of the chamber (ϕ = 160mm, L = 500mm). The chamber was separated into a source region and a diffusion region by the magnetic filter. When the electron flows from the source region to the diffusion region through the magnetic filter, the electron temperature reduced below 1 eV. The reduction rate was found to depend on the ion hole parameter around the magnetic filter, $\omega_{ci}\tau_i$ (ω_{ci}: ion cyclotron frequency, τ_i: ion-neutral collision time), in spite of the electron energy reduction. Several gases (He, N_2, Ar, Xe) were used and the pressure of gases was changed 0.2 ~ 20 mTorr to study the dependency. The curve of the reduction rate Te (diffusion region)/Te (source region) as a function of $\omega_{ci}\tau_i$ seemed to be hyperbolic. It would be concluded that the ambi-polar diffusion around the magnetic filter is a key parameter in the reduction mechanism. Also, the magnetic filter worked as a noise filter that reduces rf noise in the diffusion region effectively.

OWP5 20 Object Oriented Monte Carlo Simulations of Parallel PLate Capacitively Coupled Discharges I. HORIE, *Hokkaido Inst. of Technology* P.L.G. VENTZEK, *Motorola Inc.* K. KITAMORI, *Hokkaido Inst. of Technology* Object oriented models programmed using Java are suited to the modeling and simulation of complex plasma processes as complex physics can be incorporated into the code in a straightforward fashion and the coding structure lends itself to parallelization. This paper describes the details of the object oriented based implementation of the Monte Carlo simulation. In general, the discharge gap is broken down into uniform slabs. Each slab corresponds to a stand-alone Monte Carlo simulation of the plasma species in that slab. After a time-step, statistics are collected using a Legendre Polynomial Weighted Sampling object and the simulation continued by an object that does a B-Spline fit to those statistics. A boundary object deals with the particle transmission to walls or to other slab objects. This process will be described using both electronegative and electropositive gas discharges as examples.

OWP5 21 Parallel Implementation of Object Oriented Monte Carlo Simulations Using Java T. SUZUKI, *Hokkaido Inst. of Technology* I. HORIE, *Hokkaido Inst. of Technology* S. NAKAMURA, *Hokkaido Polytechnic College* P.L.G. VENTZEK, *Motorola Inc.* K. KITAMORI, *Hokkaido Inst. of Technology* One drawback of simulating plasma dynamics using a particle based simulation is that a prohibitively large number of particles are required to couple the particle dynamics to a solution of the electric field and that (usually) the statistics get worse in regions of the

plasma where good statistics are most important. By combining a parallel implementation of a Legendre Polynomial Weighted Sampling scheme, we are able to overcome these limitations. The parallel implementation is done on an array of PC grade computers. The key to the implementation is the synchronization of the PCs for the Poisson equation calculation. This is done using a remote method invocation, java.rmi. This paper will describe the details of the parallel implementation and scaling and speed-up performance.

OWP5 22 Analysis of Electronegative Discharge Plasma Using Equilibrium Model T. H. CHUNG, *Dong-A University* H. J. YOON, *Dong-A University* J. K. LEE, *Pohang University of Science and Technology* To analyze electronegative rf discharge plasmas, one-dimensional equilibrium model which descibes four species(two positive ion, negative ion, and electron) is formulated and solved numerically. A classification of operating regions is performed based on the shape of density profiles, prevailing loss mechanisms (recombination-loss dominated or ion flux-loss dominated), and the ratio of the negative ion density to the electron density. The scaling laws between plasma parameters and control parameters(gas pressure, input power, and system length) are estimated and compared with the results of other models(spatially averaged global model, two-dimensional fluid model, and particle-in-cell simulation). In addition, experimental results which are obtained from an inductively coupled oxygen plasma are discussed.

OWP5 23 Paralleling and Other Methods of Speeding Up Particle Codes Applied to RF Plasma Discharges E. KAWAMURA, C.K. BIRDSALL, *Univ. of Calif., Berkeley, CA* V. VAHEDI, *Lam Research Corp., Fremont CA* We demonstrate, on Ar and O_2 RF discharges, means for speeding up particle codes. In our electro-static 1D3v particle simulations, the field solve is typically only 1 percent of the work load. Hence, we can let one CPU do the field solve while dividing the rest of the work among all the CPUs. We applied this simple paralleling scheme to conduct 1D3v particle simulations on 4 and 8 CPU SMP machines. We observed that speed gains become more arithmetic when more particles are used. Other speedup methods include implicit coding, subcycling of e^-s, use of lighter mass ions, different weights for e^-s and ions, and improved initial density profiles (Symposium on Plasma and Flow Simulation for Materials Processing, Inst. of Fluid Science, Tohoku Univ., Sendai, Japan, July 10-11, 1997). We also tried unsuccessfully to use heavier e^-s and larger ϵ_o in order to decrease ω_p and thereby relax the timestep constraint $\omega_p \Delta t \ll 1$. We are supported by AFOSR ASSERT F49620-94-1-0387 and AFOSR FDF 49620-96-1-0154.

SESSION OWP6: POSTER SESSION: LEPTON COLLISIONS WITH MOLECULES
Wednesday afternoon, 21 October 1998
Haku/Pikake Room, Aston Wailea at 15:15
Irving Langmuir, General Electric, presiding

OWP6 1 Competing pathways in the electron impact dissociation of CF DARIAN STIBBE, WINIFRED HUO, *NASA Ames Research Center, Moffett Field, CA 94035* Plasma etching is one of the most important methods for the manufacture of semiconductor nanodevices. Despite the relevance of the reaction, the database for cross sections of electron impact dissociation of the radicals which actually do the etching is virtually non-existent. In the case of one such radical, CF, there are two likely pathways to dissociation. The first is vertical excitation of the molecule to a dissociative valence state. The molecule can then either decay to an optically accessible lower state or it will follow the potential curve of the valence state to dissociation. The second, indirect possibility is that the molecule predissociates by excitation to a Rydberg state which crosses a dissociative valence state, such as is known to occur in the electron impact dissociation and photodissociation of N_2. We are developing methods to examine both competing pathways in order to find the total electron-impact dissociation cross section of CF at electron temperatures relevant to plasmas used in etching. Progress of this project will be reported at the meeting.

OWP6 2 High Resolution Emission Spectroscopy of the $A^1\Pi$ - $X^1\Sigma^+$ Fourth Positive Band System of CO from Electron Impact L.W. BEEGLE, *JPL* J.M. AJELLO, *JPL* G.K. JAMES, *JPL* D. DZICZEK, *JPL* We report electron impact induced medium resolution fluorescence spectra (310 mÅ and 366 mÅ FWHM) of CO at 100 eV over the spectral region of 1200 to 2050 Å. The features in the far ultraviolet emission spectra correspond to the Fourth Positive Band System, atomic multiplets from C and O and their ions. The absolute electronic transition moment as a function of internuclear distance was determined from relative band intensities. A model of the vibronic structure of the band system based on the laboratory measurement of the electron transition moment and Honl-London factors was developed. In addition, we have obtained high resolution (34 mÅ FWHM) spectra of the (5,1) band at 1435 Å and the (3,0) band at 1447 Å and accurately modeled the rotational line structure. The excitation function of the (0,1) band (1597 Å) was measured from electron impact in the energy range from threshold to 750 eV and placed on an absolute scale using the relative flow techique. The CO A-X band system emission cross section was established from a measurement of the relative band intesities at 100 eV. The high resolution line profile of the 1152 Å atomic O multiplet ($^1D^0$ - ^{1}D) resulting from dissociative excitation was measured at 22 mÅ FWHM and the deconvolved true line profile was analyzed to provide the kinetic energy distribution of the atomic O fragment at 30 and 100 eV impact energies.

OWP6 3 Electron-Impact Ionization Cross Sections of BF_x, BCl_x, (x = 1–3) and WF_6. WINIFRED M. HUO, *NASA Ames Res. Ctr.** YONG-KI KIM, *NIST*† The binary-encounter-Bethe (BEB) model[1] was used to calculate the electron-impact total ionization cross sections of BF_x, BCl_x, (x = 1–3) and WF_6. These molecules and radicals are either currently used in plasma processing or being considered as potential candidates. The electron binding energies in the BEB calculations were determined using CASSCF wave functions for the neutral targets and ions, and the bound electron kinetic energy from SCF calculations. For WF_6, where relativistic effects are important, the SCF and CASSCF calculations were done using a relativistic effective core potential (RECP) of W which represents the core electrons up to n=4. Due to the use of RECP, the BEB calculation of WF_6 is applicable to incident energies below the ionization threshold of the n=4 electrons, i.e., up to approximately 100 eV. The cross sections exhibit the expected trend: the BCl_x cross sections are systematically larger than those for BF_x. Also, the WF_6 cross section curve is

very similar to that of BCl_3 except for a shift in the threshold energy. These calculations represent the first cross sections reported for this group of molecules and radicals.

*Work supported by the NASA Ames IPT on device/process modeling and nanotechnology.
†Work supported in part by the Office of Fusion Sciences, DOE.

[1]Y.-K. Kim and M. E. Rudd, Phys. Rev. A **50**, 3954 (1994).

OWP6 4 Electron Collisions with Perfluoroethene CARL WINSTEAD, VINCENT McKOY, *California Institute of Technology* We have calculated cross sections for low-energy electron collisions with perfluoroethene, C_2F_4, which is of interest as a constituent of fluorocarbon etching plasmas. The Schwinger multichannel method, as implemented for massively parallel computers, was used to carry out the calculations. Cross sections for electronically elastic scattering include the effects of target polarization. Inelastic cross sections obtained in a few-channel approximation are reported for excitation of low-lying electronic states. The influence of resonances on the elastic and inelastic cross sections is analyzed, and comparisons are made to electron scattering by other fluorocarbons and by C_2H_4.

OWP6 5 Elastic differential cross sections of N2O by electron impact HIROSHI TANAKA, *Sophia University* HIROSHI TANAKA, MASASHI KITAJIMA, S WATANABE, *Sophia University* MINEO KIMURA, *Yamaguchi University* Elastic differential cross sections for N2O by electron impact have been studied experimentally and theoretically for the impact energy from 1.5 eV to 100 eV and the scattering angles from 20 degree to 140 degree. Comparing with these results for CH4, CF4 and CH3F systems studied previously, the present data provide further information of the deeper understanding of the florination effect for the scattering dynamics.

OWP6 6 Total and differential cross sections of CH2F2 by electron and positron impacts HIROSHI TANAKA, *Sophia University* HIROSHI TANAKA, MASASHI KITAJIMA, *Sophia University* OSAMU SUEOKA, AKIRA HAMADA, MINEO KIMURA, *Yamaguchi University* Total cross sections of CH2F2 by electron and positron impacts have been measured for the impact energies from 0.7 eV to 600 eV. In addition, differential elastic cross sections have been studied experimnetally and theoretically for the impact energy from 1.5 eV to 100 eV and the scattering angles from 20 degree to 140 degree. Comparing with these results for CH4, CF4 and CH3F systems, the present data provide an additional information of the florination effect for these scattering processes.

OWP6 7 H-Atom Yield in the Dissociative Recombination of $H_3^+ + e^-$* MIROSLAW P. SKRZYPKOWSKI, MICHAEL F. GOLDE, RAINER JOHNSEN, *University of Pittsburgh, Pittsburgh, PA* A flowing afterglow technique coupled with laser induced fluorescence (LIF) diagnostics has been used to determine the H-atom yield from the dissociative recombination of $H_3^+ + e^- \rightarrow (3H \text{ and } H_2 + H)$ at 300K. H atoms were converted to OH radicals in the reaction $H + NO_2 \rightarrow OH + NO$, and subsequently the concentration of OH was monitored by means of LIF. Analysis of calibrated LIF data gave $f_H = 2.2 \pm 0.3$, in good agreement with the results obtained in merged beam[1] and ion storage ring[2] experiments.

*This work was supported by NASA

[1]J. B. A. Mitchell et al., Phys. Rev. Lett. 51, 885 (1983)
[2]S. Datz et al., Phys. Rev. Lett. 74, 896 (1995)

OWP6 8 Very Low Energy Electron Scattering from Molecular Chlorine R.J. GULLEY, *Australian National University* T.A. FIELD, *University of Nottingham* W.A. STEER, N.J. MASON, *University College London* J.P. ZIESEL, *Universite Paul Sabatier* S.L. LUNT, D. FIELD, *University of Aarhus* We report the first experimental measurements of the absolute integral (0–180°) and backward (90–180°) cross-sections for the total scattering of electrons by Cl_2 in the energy ranges of 20 meV to 9.5 eV and 16 to 250 meV respectively. Strong evidence is found for electron attachment at very low impact energies, in agreement with the results of other groups. Data suggest that attachment occurs through the p- partial wave. A resonance in the form of a doublet, with a cross-section of up to 10Å^2, has been observed in the total integral scattering cross-section between 70 and 200 meV. This structure is absent in the backward scattering cross-section. A qualitative mechanism is suggested for the formation of the observed structure, involving virtual excitation of the $\nu = 1$ quantum of Cl_2 and coupling of the Cl_2^- Σ ground state wave function with the excited Π states of Cl_2^-.

OWP6 9 Mode-dependence of vibrational excitation in CO2 by electron and positron impacts MICHIYA TAKEKAWA, *Inst. Space and Astronautical Sci.* OSAMU SUEOKA, *Yamaguchi University* HIDEKI TAKAKI, *Yamaguchi University* MINEO KIMURA, *Yamaguchi University* YUKIKAZU ITIKAWA, *Inst. Space and Astronautical Sci.* Vibrational excitation for (100), (010) and (001) vibrational modes by electron and positron impacts has been studied theoretically and experimentally in the incident energy from 1 eV to 6 eV. We have found that for symmetric stretching (100) mode, the excitation cross section of electron impact is larger by 2-3 orders of magnitude than that of positron impact, while for bending (010) and asymmetric stretching (001) modes, the magnitude of both cross sections for electron and positron impacts is nearly comparable. These results are qualitatively confirmed experimentally.

OWP6 10 The Middle Ultraviolet-Visible Spectrum of H_2 Excited by Electron Impact GEOFFREY K. JAMES, JOSEPH M. AJELLO, *Jet Propulsion Laboratory, California Institute of Technology, Pasadena CA 91109** WAYNE R. PRYOR, *Laboratory for Atmospheric and Space Physics, University of Colorado, Boulder, CO 80303* The electron-impact-induced emission spectrum of H_2 has been measured in the extended wavelength region 175-530 nm at a spectral resolution of 1.7 nm (FWHM). The laboratory spectra observed in the middle ultraviolet (MUV) and visible spectral region are characterized by underlying H_2 ($a^3\Sigma_g^+ \rightarrow b^3\Sigma_u^+$) continuum emission, together with many strong lines assigned to the radiative decay of the gerade singlet states of H_2, and to members of the H Balmer series resulting from dissociative excitation of H_2. Our calibrated MUV spectral data, obtained at 14, 19 and 100 eV electron-impact energies, provide absolute emission cross sections of these H_2 lines and will assist in the

interpretation of planned Galileo Ultraviolet Spectrometer observations of Jupiter's aurora in this wavelength region.

*This work was carried out at the Jet Propulsion Laboratory, California Institute of Technology, and was supported by NASA Planetary Atmospheres Program Office.

OWP6 11 Total and differential cross sections of C3H8 and C3F8 by electron and positron impacts OSAMU SUEOKA, *Yamaguchi University* MASASHI KITAJIMA, Y SAKAMOTO, T SUZUKI, *Sophia University* S SAMUKAWA, *NEC* OSAMU SUEOKA, AKIRA HAMADA, MINEO KIMURA, *Yamaguchi University* Total and differential elastic cross sections in e-/e+ + C3H8 and C3F8 scattering have been investigated experimentally and theoretically. The differential cross section measurement by electron impact has been carried out from 2 eV to 100 eV, while the total cross section measurement by electron and positron has been for 0.7 eV to 600 eV. The theoretical study has been performed by using the continuum multiple-scattering method. The present total cross sections are found to agree reasonably well with those by Wayne State Univ. group, and theoretical rationale for origins of shape resonances are provided.

OWP6 12 Vibrational excitation in CO2 by electron impact MICHIYA TAKEKAWA, *Inst. Space and Astronautical Sci.* MASASHI KITAJIMA, S WATANABE, T ISHIKAWA, *Sophia University* MINEO KIMURA, *Yamaguchi University* YUKIKAZU ITIKAWA, *Inst. Space and Astronautical Sci.* Vibrational excitation for (100), (010) and (001) vibrational modes by electron impact has been investigated theoretically and experimentally in the incident energy from 1 eV to 30 eV. The present theory and experiment agree well for (100)-mode excitation in the whole energy range studied, but disagree with the data proposed by Nakamura above 15 eV where Nakamura's data drop rather drastically. For (001)- and (010)-mode excitations, the present theory and experiment also agree well up to 35 eV.

OWP6 13 Differential and total cross sections in e + OCS scattering HIROSHI TANAKA, *Sophia University* MASASHI KITAJIMA, Y SAKAMOTO, *Sophia University* OSAMU SUEOKA, AKIRA HAMADA, MINEO KIMURA, *Yamaguchi University* Differential elastic and total cross sections in e- + OCS scattering have been investigated experimentally and theoretically. The differential cross section measurement has been carried out from 2 eV to 100 eV, while the total cross section measurement was for 0.7 eV to 600 eV. The theoretical study has been performed by using the continuum multiple-scattering method. The present total cross sections are found to agree reasonably well with those by Wayne State Univ. group, and theoretical rationale for origins of shape resonances are provided.

OWP6 14 Absolute Total-Cross-Section Measurements for Intermediate-Energy Electron Scattering on CHClF2 YOSHITAKA KONDO, TADAHIKO YAMADA, *Daido Institute of Technology* A compact linear electron transmission apparatus has been constructed for the measurement of total electron-scattering cross section for various chlorofluorocarbon, hydrochlorofluorocarbon and hydrofluoro-carbon. As a test of this method, the total electron-scattering cross section for CH4 has been measured in the energy range between 5 and 340eV. The result coincided with one obtained by Dr. H.Nishimura in 5% statistical uncertainty. The same cross section for CHClF2 also has been measured in the same energy range for CH4 . The results for CH4 and CHClF2 show $E^{-0.5}$ dependence at lower energies. The values of total cross section for various molecule at 100eV are 36.6($x10^{-20}m^2$) for CCl4, 31.3 for CCl3F, 27.4 for CCl2F2, 22.7 for CClF3, 18.5 for CF4, 14.2 for CHClF2 and 9.1 for CH4 . This series of total cross section can be explained by using the additivity rule with the values of cross section of each atom.

OWP6 15 Electron Transport Coefficients in pure C_2F_6 and Electron Collision Cross Sections for C_2F_6 S. FUJINO, *Keio University* H. OKUMO, Y. NAKAMURA, We measured the electron transport coefficients, the electron drift velocity W and the product of the gas number density and the longitudinal diffusion coefficient ND_L , over the E/N range from 0.17 to 300 Td and gas pressure range from 0.2 to 165 Torr in pure C_2F_6 by the double shutter drift tube with variable drift distance. We have reported the measurement of the drift velocity and the longitudinal diffusion coefficient in dilute C_2F_6-Ar mixtures and vibrational excitation cross sections of C_2F_6 derived from these swarm parameters (ICAM\DATA97). In the present study we report our new measurement of swarm parameter s in pure C_2F_6 and a new cross section set for the molecule derived by using the present swarm data and our previous vibrational excitation cross sections.

OWP6 16 Electron Transport Coefficients in Pure C_3F_8 and Collision Cross Sections of C_3F_8 with Low Energy Electrons T. SHIBATA, *Keio University* B-H. JEON, Y. NAKAMURA, The drift velocity W, the longitudinal diffusion coefficient ND_L and the attachment coefficient of electrons in pure C_3F_8 gas were measured by the double shutter drift tube with variable drift distance over the E/N range from 0.7 to 250 Td and gas pressure range from 0.2 to 100 Torr. With these transport coefficients and the vibrational cross sections we had determined with transport coefficients measured in C_3F_8-Ar mixtures(ICAMDATA97), a momentum transfer cross section for C_3F_8 molecule was derived by using the multi-term approximation of the Boltzmann equation analysis(Ness and Robson, Phys.Rev.A33,2068, 1986). Also we might find an evidence of unstable negative-ion state of the C_3F_8 molecule in the present measurement.

OWP6 17 A Survey of Electron Impact Cross-sections for Halogens and Halogen Compounds of Interest to Plasma Processing S.P. SHARMA, *NASA-Ames Research Center* M.V.V.S. RAO, *Thermosciences Institute/NASA-Ames Research Center* Published electron impact cross section data on halogens Cl2, F2, and halogen containing compounds such as Cx Fy, HCl, Cx Cly Fz are reviewed and critically evaluated based on the information provided by the various researchers. The paper reports data on electron impact excitation, ionization, dissociation, electron attachment, electron detachment, and photo detachment. Elastic scattering cross sections and data on bulk properties such as diffusion coefficients in various background gases are also evaluated. Since some of the cross sectional data is derived from indirect measurements, such as drift velocity, care has been taken to reconcile the differences among the reported data with due attention to the measurement technique. In conclusion the processes with no or very limited amount of data and questionable set of data are identified and recommendation for further research direction is made.

OWP6 18 Electron-Impact Ionization Cross Sections for Molecular Ions Y.-K. KIM, *NIST** W. M. HUO, *NASA Ames Res. Ctr.*† M. A. ALI, *Howard Univ.* The binary-encounter-Bethe (BEB) model for electron-impact total ionizaton cross sections of

neutral molecules[1] has been modified for ionic targets. For a neutral molecule, the BEB cross section per molecular orbital is given by $\sigma_{BEB} = \frac{4\pi a_0^2 N(R/B)^2}{t+u+1}[\ln t/2\,(1 - 1/t^2) + 1 - 1/t - \ln t/1 + t]$, where a_0 = Bohr radius, N = electron occupation number, R = Rydberg energy, B = orbital binding energy, t = incident electron energy/B, and u = orbital kinetic energy/B. The modification for ionic targets replaces $t + u + 1$ in the first denominator of the above expression by $t + (u + 1)/(q + 1)$, where q is the net charge of the ion, e.g., $q + 1 = 2$ fo singly charged ions. This simple modification leads to BEB cross sections in excellent agreement with indirectly deduced experimental data[2] on CD^+ and N_2^+. Comparisons to these and other experiments will be presented at the conference.

*Work supported in part by the Office of Fusion Sciences, DOE.
†Work supported by the IPT on device/process modeling and nanotechnology.

[1]Y.-K. Kim and M. E. Rudd, Phys. Rev. A **50**, 3954 (1994).
[2]N. Durić et al., Phys. Rev. A **56**, 2887 (1997); J. R. Peterson et al., J. Chem. Phys. **108**, 1978 (1998).

SESSION OWP7: POSTER SESSION: ELECTRON-ATOM COLLISIONS
Wednesday afternoon, 21 October 1998
Haku/Pikake Room, Aston Wailea at 15:15
Irving Langmuir, General Electric, presiding

OWP7 1 Abstract Withdrawn

OWP7 2 Atomic Oxygen Emission Cross Sections resulting from Electron Impact in the FUV C. NOREN, *JPL* I. KANIK, *JPL* G.K. JAMES, *JPL* M.A. KHAKOO, *University of California, Fullerton* The atomic oxygen emissions from astronomical sources provide valuable (perhaps unique) information on densities, gas dynamics, etc. of the atmospheres of the planets and their satellites. For example, the atomic oxygen resonance transition at 130.4 nm is a prominent emission feature in the vacuum ultraviolet spectrum of the Earth's aurora and day glow as well as the atmospheres of Europa, Ganymede, Mars and Venus. In this poster we present our measurements of the electron impact emission cross sections of the 130.4 nm atomic oxygen feature from threshold to 1000 eV impact energy. A high density atomic oxygen beam, created by a microwave discharge source, was intersected at right angles by a magnetically focused electron beam. The experimental apparatus consists of an electron impact collision chamber in tandem with a 0.2m UV spectrometer equipped with a CsI coated channel electron multiplier detector. Emitted photons corresponding to radiative decay of collisionally excited state of the 130.4 nm atomic oxygen feature were detected.

OWP7 3 Electron-Photon Coincidence Studies of the Collisional Excitation of the 4^1P_1 State of Calcium Atoms DARIUSZ DZICZEK, *Jet Propulsion Laboratory, California Institute of Technology, Pasadena, CA 91109** DARIUSZ DYL, MARIUSZ PIWINSKI, MARCIN GRADZIEL, STANISLAW CHWIROT, *Institute of Physics, Nicholas Copernicus University, PL 87-100 Torun, Poland* Experimental values of the electron impact coherence parameters (EICP) are reported for collisional excitation of the 4^1P_1 state of Ca atoms. The results have been obtained using the electron-photon coincidence technique for electron energies of 45, 60 and 100 eV, and scattering angles from 10^o to 45^o. Measurements are compared with results of RDWA calculations. EICP values determined at 45 eV are compared with other experimental data obtained with coincidence and optical pumping technique. Unlike the earlier coincidence results our data show very good agreement with the superelastic scattering measurements, confirming the equivalency of these two methods. The agreement with theoretical results is also good at this energy. However, some discrepancies between our data and RDWA calculations exist at higher impact energies.

*D.D. acknowledges receipt of the National Research Council Resident Research Associateship. This work was supported by a grant from Committee of Scientific Research (KBN, No 2 P03B 068 09).

OWP7 4 Electron Impact Excitation of Argon from the Ground State and the Metastable Excited States. VLADO ZEMAN, *University of Nottingham* KLAUS BARTSCHAT, *Drake University** We have extended our Breit-Pauli R-matrix work [1–3] to model electron impact excitation of the $[3p^5 4s]$ and $[3p^5 4p]$ states in argon from the ground state $[3p^6]^1S_0$ and the metastable states $[3p^5 4s]^3P_{0,2}$. Total cross section results will be presented for incident electron energies between threshold and 100 eV and compared with recent experimental data [4,5] and predictions from other theoretical approaches. 1. V. Zeman *et al.*, Phys. Rev. Lett. **79**, 1825 (1997) 2. V. Zeman and K. Bartschat, J. Phys. B **30**, 4609 (1997) 3. M.J. Brunger *et al.*, J. Phys. B **31**, L387 (1998) 4. J.B. Boffard *et al.*, J. Phys. B **29**, L795 (1996) 5. G.A. Piech *et al.* (1998); submitted for publication

*This work is supported by the National Science Foundation under grant PHY-9605124.

OWP7 5 Collision Strengths for Electron Collisional Excitation of the Fine Structure Levels in SIII G. P. GUPTA, S. S. TAYAL, *Clark Atlanta University* We have calculated collision strengths among the levels of the ground $3s^2 3p^2$ configuration and from these levels to the levels of the excited $3s3p^3$, $3s^2 3p3d$, $3s^2 3p4s$, $3s^2 3p4p$, and $3s^2 3p4d$ configurations of SIII by the use of R-matrix method. Relativistic effects in the intermediate coupling are incorporated by means of the Breit-Pauli Hamiltonian. The low-lying 27 LS states which give rise to 49 fine structure levels are considered in our calculations. In order to delineate the resonance structures in the collision strengths, the collision calculation is carried out at a fine energy mesh in the threshold energy regions. Resonances are found to make substantial enhancements in collision strengths for many forbidden and intercombination transitions in the threshold regions. Collision rates are obtained from the total collision strengths by integrating over a Maxwellian velocity distribution.

OWP7 6 Electron Impact Excitation Cross Sections of Fine-Structure Transitions in OII* S. S. TAYAL, L. M. RICHARDSON, *Clark Atlanta University* Cross sections for electron collisional excitation of fine-structure transitions in OII are calculated in the close-coupling approximation using the R-matrix method. The lowest 28 LS states $2s^2 2p^3\ ^4S^o, ^2D^o, ^2P^o$; $2s2p^4\ ^4P, ^2P, ^2D, ^2S$; $2p^2(^3P)3s\ ^4P, ^2P$; $2p^2(^3P)3p\ ^2S^o, ^4S^o, ^4P^o, ^2P^o, ^4D^o, ^2D^o$; $2p^2(^3P)3d\ ^4D, ^2D, ^2F, ^2P$; $2p^2(^3P)4s\ ^4P, ^2P$; $2p^2(^1D)3s\ ^2D$; $2p^2(^1D)3p\ ^2F^o, ^2D^o, ^2P^o$, and $2p^2(^1S)3s\ ^2S$ which give rise to 62 fine structure levels are included in the close-coupling expan-

sions. These levels are represented by fairly extensive configuration-interaction wave functions which yield excitation energies and oscillator strengths that are in good agreement with available most extensive calculations and experiments. The relativistic effects are included through a part of the Breit-Pauli Hamiltonian. Rydberg series of resonances converging to the excited state thresholds are found to enhance the cross sections substantially in the low energy region.

*Funded by NSF under grant AST-9528945

OWP7 7 Lasers in dense gases pumped by low energy electron beams* J. WIESER, M. SALVERMOSER, A. ULRICH, HIROMITSU TOMIZAWA, CLAUDIA NIESSL, *Technische Universität München, D-85747 Garching, Germany* D. E. MURNICK, H. DAHI, *Rutgers University, Newark NJ 07102* Low energy (11keV) electron beams are used for pumping laser systems in dense gases in a transverse geometry. The laser setup uses thin (300nm) SiN_x ceramic foils as entrance windows for the electron beam. An Ar-Xe infrared laser at a wavelength of 1.73 μm has been operated using a commercially available TV-cathode ray tube as the electron beam source. The electron beam was shaped by a magnetic quadrupole lens and focussed onto the slit entrance foil with an aperture of 30$\times$ 0.7 mm^2. Laser effect has been observed above 300mbar laser gas total pressure. A pumping power threshold of about 15W/cm^3 was measured for a gain length of 2cm, using highly reflective mirrors. Emission spectra perpendicular to the laser beam axis, and kinetic processes in the laser gases, can be studied by time resolved optical spectroscopy from the vacuum ultraviolet to the infrared spectral region.

*Supported in part by NSF, NATO and INTAS

SESSION QR1: PLASMA JETS
Thursday morning, 22 October 1998
Plumeria/Jade Room, Aston Wailea at 7:30
Richard van de Sanden, Eindhoven University, presiding

Contributed Papers

7:30
QR1 1 Scaling Relations of a Flexible Operating Mode Hall Thruster YEVGENY RAITSES, *PPPL, Princeton University, Princeton, P.O. Box 451, NJ 08543, USA* NATHANIEL FISCH, *PPPL, Princeton University, Princeton, P.O. Box 451, NJ 08543, USA* AMNON FRUCHTMAN, *Center for Technological Education Holon, 58102 Holon, Israel* JOSEPH ASHKENAZY, *Soreq NRC, Yavne 81800, Israel* The Hall thruster is a type of electric rocket engine which generates thrust in reaction to the acceleration of an ion jet by an axial electric and a radial magnetic field applied in an annular channel. Having jet velocities in the range 10000-30000 m/s and larger thrust densities than ion thrusters, Hall thrusters can be useful for spacecraft applications on small satellites. Flexible thruster operation, variable thrust and power, might reduce the initial spacecraft mass for various space applications. Experiments with a laboratory Hall thruster at Soreq show that efficient thruster operation under various operating conditions might be achieved by varying the geometry and magnetic field distribution. The scaling of the thruster performance with the discharge parameters and the thruster configuration can be obtained from a simplified analysis of Hall thruster operation under various operating conditions based on one-dimensional fluid model. We show analytically how, by changing the thruster geometry and magnetic field distribution, we can optimize the thruster performance under various operating conditions.

7:45
QR1 2 Time and space resolved analysis of fluctations and oscillations in the plasma channel and in the plasma jet of Hall type ion thruster ANDRÉ BOUCHOULE, FRANCK DARNON, CHRISTELLE PHILIPPE, CLAUDE LAURE, *Laboratoire GREMI, UMR 6066 CNRS - Université d'Orléans* MICHEL LYSZYK, *SEP, Villaroche* STÉPHANE BECHU, PASCAL LAGORCEIX, *Laboratoire Aérothermique, UPR CNRS, Orléans, France* NADER SADEGHI, *Laboratoire de Spectrométrie Physique, UMR CNRS - Université de Grenoble, Saint Martin d'Héres* Efficient crossed fields discharge thrusters (SPT), initially investigated in Russia a long time ago, are characterized by a significant fluctuation level of both discharge channel and plasma plume, mostly in the few tens kHZ domain. A detailed, space and time resolved analysis of these fluctuations has been developed in the frame of a general research program launched recently in France. New insights on this fluctuation have been acquired on a diagnostic equipped thruster (SPT 100, Xenon gas, = 100 mN thrust), through time and space resolved diagnostics of both the active discharge channel and the plasma jet. The study has been performed in the new French thrusters test facility ≪ PIVOINE ≫ (2 m in diameter, 4 m length, operating pressure 10^{-5} mbars). The diagnostics include optical fiber array, fast CCD camera and time resolved ion energy analyser. Time resolved LIF diagnostic (Xe^{+} velocity vector) has been demonstrated. The results lead to new insights on SPT operation and new guidelines for physics and modelling of these thrusters.

Invited Paper

8:00
QR1 3 Review of Non-Equilibrium Plasmadynamics to Predict Energy Transfer in Arcjet Thrusters.
HERMAN KRIER, *Department of Mechanical and Industrial Engineering, University of Illinois at Urbana-Champaign*

Both chemical and thermal processes in an electrothermal arcjet are described as non-equilibrium. Arc current is converted to electron thermal energy through ohmic dissipation. The electrons transfer thermal energy to heavy species in the arc plasma through collisions. This energy is then converted to kinetic energy (and thrust) as the fluid accelerates through the nozzle. The paper presents an axisymmetric, steady, laminar, continuum flow model, supporting a two-temperature kinetic and chemical non-equilibrium, formulated for a direct current arcjet with variabe mixture ratios of nitrogen and hydrogen. Seven species (ions, atoms, electons) assumed with finite rate chemistry accounted for. The model predictions are compared to experiments with a NASA 1 kW hydrazine propellant arcjet.

Contributed Papers

8:30
QR1 4 The Structure and Transient Behavior of Closed-drift Hall Current Plasma Discharges MARK CAPPELLI, WILLIAM HARGUS, NATHAN MEEZAN, *Thermosciences Division, Stanford University* Closed-drift Hall current plasma sources are rapidly emerging as favorable ion thruster technologies in space propulsion applications. These discharges are inherently unsteady, relying on the turbulent plasma transport of electrons across a magnetic field to sustain the discharge. In the past, the structure of these discharges has been ascertained primarily by interrogation of the discharge channel with electrostatic probes. In recent studies in ourelectric propulsion laboratory, we have introduced the use of laser-induced fluorescence (LIF) to directly measure the ion and neutral xenon velocities, and have used these results to measure the fractional ionization, which, in some cases, approaches 100%. The combination of low-impedance ion collection probes, emissive probes, and Langmuir probes together with these LIF measurements have shown that the ionization region is separated from the ion acceleration zone in our present discharge design, resulting in a near-monoenergetic beam of ions, and that coherent, travelling azimuthal disturbances of wavelengths comparable to the discharge circumference (m = 1 mode) are localized between the ionization and acceleration region. The velocities of this long wavelength coherent mode has been estimated to be comparable to the electron drift (E x B) velocity, as has been seen by others in similar discharge devices.

8:45

QR1 5 Computational Analyses of Plasma Generation in a Negative Ion Source MIEKO KASHIWAGI, *Saitama University* SHUNJI IDO, *Saitama University* In a volume-produced negative ion source plasma, the numerical analyses are carried out on the problem of plasma generation. Recently, the progress of the negative ion source techniques is remarkably advanced in the fusion study. In the experiment of Neutral Beam Injection (NBI) of JT-60U, JAERI(Japan Atomic Energy Research Institute), the negative ion beam extracted from a source achieved high power and high current, 500keV and 10A. The authors refer this volume-produced negative ion source in JAERI in the analyses. The gas is H_2 or D_2. H^- or D^- is produced by collisions and extracted as a beam. In a volume-produced negative ion source, an electron behavior and its energy have great effects on the H^- or D^- generation process. The authors have studied the positive ion plasma source by using a particle code. This method is applied to the study of an electron behavior in a negative ion source. The distributions of electrons and the collisions are studied. The magnetic field generated by the permanent magnets, filament currents and a plasma grid filter is analyzed. Then the effects on an electron behavior and the uniformity of plasma by the magnetic field configuration are analyzed.

9:00

QR1 6 Volume-Averaged Model of Inductively-Driven Multicusp Ion Source* KEDAR K. PATEL, M.A. LIEBERMAN, *University of California, Berkeley* M.A. GRAF, *Eaton Corporation* A self-consistent spatially averaged model of high-density oxygen and boron trifluoride discharges has been developed for a 13.56 MHz, inductively coupled multicusp ion source. We determine positive ion, negative ion, and electron densities, the ground state and metastable densities, and the electron temperature as functions of the control parameters: gas pressure, gas flow rate, input power and reactor geometry. Neutralization and fragmentation into atomic species are assumed for all ions hitting the wall. For neutrals, a wall recombination coefficient for oxygen atoms and a wall sticking coefficient for boron trifluoride (BF_3) and its dissociation products are the single adjustable parameters used to model the surface chemistry. For the aluminum walls of the ion source used in the Eaton ULE2 ion implanter, complete wall recombination of O atoms is found to give the best match to the experimental data for oxygen, whereas a sticking coefficient of 0.62 for all neutral species in a BF_3 discharge was found to best match experimental data.

*Work supported by Eaton Semiconductor Equipment Operations Research Agreement No. M2708

Invited Paper

9:15

QR1 7 Modeling the Plasma in a Sonoluminescing Bubble.
WILLIAM C. MOSS, *Lawrence Livermore National Laboratory*

Sonoluminescence arises from the nucleation, growth, and collapse of gas-filled bubbles in a liquid. Although the mechanism of emission from single bubble sonoluminescence (SBSL) has still not been identified conclusively, the ''plasma'' model [Moss et al., Science **276**, 1398-1401 (1997)] appears to explain more features of SBSL than other models. In the plasma model, the gas in the rapidly collapsing bubble is heated and emits a brief optical pulse. Recent measurements of the light pulses from sonoluminescing bubbles show that the pulse widths can vary between 40 and 300ps, exceeding the 50ps upper bound of the earliest pulse width measurements. These new results provide information for improving the modeling of the energy loss and emission mechanisms in the plasma model. In particular, we model the plasma as a ″strongly coupled plasma″ (small Debye screening length), due to its high density and relatively low temperature, which reduces the rate of energy loss by electron thermal conduction, as compared to more typical low density plasmas. This thermal conduction model combined with the dependence of the calculated opacities on the temperature and gas composition in the bubble give rise to longer calculated pulse widths and spectra that are consistent with experimental data. This work was performed under the auspices of the U. S. Department of Energy by Lawrence Livermore National Laboratory under Contract No. W-7405-Eng-48.

SESSION QR2: DEPOSITION

Thursday morning, 22 October 1998; Maile Room, Aston Wailea at 7:30; M. Shiratani, Kyushu University, presiding

Invited Paper

7:30

QR2 1 Advanced Functional Thin Films Prepared by Plasma CVD.
OSAMU TAKAI, *Nagoya University*

Recently water repellency has been required for many types of substrate (e.g. glass, plastics, fibers, ceramics and metals) in various industrial fields. This paper reports on the preparation of highly water-repellent thin films by plasma CVD (PCVD). We have prepared transparent water-repellent thin films at low substrate temperatures by two types of PCVD, rf PCVD and microwave PCVD, using fluoro-alkyl silanes (FASs) as source gases. Silicon oxide thin films contained fluoro-alkyl functions were deposited onto glass and plastics, and realized the excellent water repellency like polytetrafluoroetylene (PTFE) and the high transparency like glass. Increasing the deposition pressure we have formed ultra water-repellent (contact angle for a water drop of over about 150 degrees) thin films by microwave PCVD using a

multiple gas mixture of tetramethylsilane (TMS), (heptadecafluoro-1,1,2,2-tetrahydro-decyl)-1-trimethoxysilane (FAS-17) and argon. Ultra water-repellency appears at higher total pressures over 40 Pa because the surface becomes rough due to the growth of large particles. The color of these ultra water-repellent films is slightly white because of the scattering of light by the large particles. Recently we have also deposited transparent ultra water-repellent thin films at low substrate temperatures by microwave PCVD using organosilicon compounds without fluorine as source gases. We evaluated water repellency, optical transmittance, surface morphology and chemical composition of the deposited films. At the suitable substrate position the deposited film gave the contact angle of about 150 degrees and the transmittance of over 80 visible region for a coated glass (thickness was about 1 micron). The control of the surface morphology of the deposited films is most important to obtain the transparent ultra water-repellent films.

Contributed Papers

8:00

QR2 2 Gas Phase Diagnosis of Disilane/H_2 RF Glow-Discharge Plasma And Its Application to High Rate Growth of High Quality a-Si:H W. FUTAKO, *Tokyo Institute of Technology* T. TAKAGI, T. NISHIMOTO, M. KONDO, A. MATSUDA, *Electrotechnical Laboratory* Disilane is known to be a suitable source gas for high rate growth of hydrogenated amorphous silicon (a-Si:H) compared to conventional mono-silane source since it is decomposed more easily in RF glow-discharge plasma. But it has been reported that high rate growth from pure disilane source results in films with poor stability against light induced degradation which is fatal for solar cell application. It is also known that hydrogen dilution technique could improve film quality and stability, however the detailed mechanism of such phenomena is still unclear. In this study we investigated the relationship between chemical species in plasma and structural, opt-electronic properties of resulting films in order to control quality and stability of the films. For this purpose, mass spectrometry was used to identify chemical species contributing to the film growth. Stability against light soaking was studied with fill factor of Schottky devices which is sensitive characterization method for stability. It was found that the increase in the signal from mono-silane molecules in the mass spectrum during plasma excitation is comparable to the absolute signal from disilane molecules. We succeeded to improve stability of a-Si:H with proper choice of hydrogen dilution ratio. The detailed data will be presented.

8:15

QR2 3 PECVD of Silicon thin films A. REMSCHEID, *Venture Business Laboratory, Kyoto University, Japan* T. ASAKAWA, P. COURT, F. FUJII, M. KUBO, K. TACHIBANA, *Dept. Electronic Science & Engineering, Kyoto University, Japan* ECR-generated plasma operating in SiH4/H2 gas mixture was used to deposit silicon films on amorphous substrates. By changing plasma conditions and gas composition it is possible to control the phase of the deposited films. The phase is either amorphous or polycrystalline. From TXRD investigation we found most of the crystalline films to be oriented in Si-(111) crystal orientation. In addition to X-ray analysis we analyzed the films with spectroscopic ellipsometry in order to measure the contents of crystal phase as well as the orientation of the grains. The content of hydrogen has been measured with infrared absorption spectroscopy, which is sensitive to Si-H, Si-H2 and Si-H3 bonds in the spectral range 1800-2200cm-1. Evaluation of the plasma has been done by means of electrical Langmuir-probes and plasma monitor in order to measure the plasma parameters and the ion energies as well as the ion/radical composition in the plasma. The results of our investigation will be presented with respect to the influence of plasma parameters on the film quality.

8:30

QR2 4 Deposition of SiNx Thin Film Using μ-SLAN Surface Wave Plasma Source XU YING-YU, *Shizuoka University, Japan* OGISHIMA TAKUYA, *Shizuoka University, Japan* KORZEC DARIUSZ, *Wuppertal University, Germany* NAKANISHI YOICHIRO, *Shizuoka University, Japan* HATANAKA YOSHINORI, *Shizuoka University* Remote plasma CVD method has been used in fabrication of high quality thin films. It is a useful method in decreasing damage from ion bombardment and in analysis of film formation mechanism. In our research, as the film deposition rate depends on neutral radical density, hence high-density plasma is needed for high-speed deposition. In this research, a μ-SLAN (Slot ANtenna) microwave surface wave plasma source was adapted for thin film deposition. The μ-SLAN is an efficient plasma generator in which microwave power is coupled from a ring cavity with several slots around quartz discharge tube. We measured parameters of argon plasma along the discharge tube by a double Langmuir probe. The electron density was measured as about 10^{11} cm^{-3} at an axial position of 43 cm from ring cavity, a microwave power of 500 W and a pressure of 0.5 torr. Using μ-SLAN, SiN_x thin film was deposited and high deposition rate was obtained. The highest deposition rate of 280 nm/min was obtained for plasma gas containing 15% of hydrogen in nitrogen with the pressure and power of 1.5 torr and 500 W respectively.

8:45

QR2 5 Relationship between Plasma Parameters and Sputtering Efficiency in a Hollow Cathode Discharge Sputtering System N. FUKUHARA, *McMaster University (On leave from Toppan Printing Co., Ltd.)* A. A. BEREZIN, *McMaster University* K. UEYAMA, *Toppan Printing Co., Ltd.* S. TAKEUCHI, *Toppan Printing Co., Ltd.* J. S. CHANG, *McMaster University* In order to optimize of metal thin film production based on dc hollow cathode discharge technique, the relationship between plasma parameters and sputtering efficiency was experimentally investigated. Plasma parameters in hollow cathode sputtering system consisted of pin-cavity electrode arrangements were measured by optical emission spectroscopy and electrostatic probe method. Experiments were conducted for gas pressure (P) from 0.25 to 2.0 Torr and applied voltage (V) from 1.0 to 2.0 kV at gap distance between anode and cathode (d_p) 3.0 cm and gap distance between cathode and floating electrode (d_f) 2.0 mm. The experimental results show that : (1) Electron temperature nonmonotonically decreases with increasing gas pressure and monotonically decreases with increasing applied voltage where minimum is observed near 0.7 Torr. (2) Electron density increases with increasing applied voltage and nonmonotonically depends on gas pressure, where electron density maximum at 0.7 Torr. (3) Titanium sputtering yield is proportioned to plasma density and inversely proportioned to electron temperature.

9:00

QR2 6 High Deposition Rate of Poly-Silicon at Low Temperature Using UHF Plasma System. B. MEBARKI, *Department of Quantum Engineering, Nagoya University, Japan* R. YOSHIDA, S. SUMIYA, M. ITO, M. HORI, T. GOTO, *Department of Quantum Engineering, Nagoya University, Japan* S. SAMUKAWA, *NEC Co., Japan* T. TSUKADA, *ANELVA Co., Japan* The ultra-high-frequency (UHF) system attracts the scientific attention for its high-density and low-electron temperatures plasma in large working area. The low-ion energies, du to the low-electron temperatures, favor the crystallinity of plasma materials. Using this UHF system, Poly-silicon (p-Si:H) is expected to be produced at low substrate temperature with high deposition rate. The poly-silicon network quality is monitored from the complex (n and k) refractive index, using in-situ ellipsometry spectroscopy (ES). The films deposited at low silane / hydrogen ratios show contributions coming from the sharp peaks of crystalline silicon at about 3.30 eV and 4.25 eV regarding n and k respectively. According to Raman analysis, the crystallinity increases with substrate temperature. The deposition rate such as the crystallinity depends strongly on the silane / hydrogen ration as well as on UHF power and plasma total pressure. A p-Si:H with a deposition rate of 6.7 / s is successfully obtained for a silane / hydrogen ratio of 30 sccm over 100 sccm, total pressure of 13 Pa, and an UHF power of 600 W. According to in-situ ellipsometry (spectroscopic and kinetic mode) and Raman analysis, p-Si:H can be produced at a substrate surface temperature as low as 180 C.

9:15

QR2 7 Development and Application of a High Power Density, Large Area, Rectangular, Inductive Reactor For CVD* V.A. SHAMAMIAN, J.L. GIULIANI, J.E. BUTLER, *Naval Research Laboratory* R.A. RUDDER, R.E. THOMAS, R.C. HENDRY, *Research Triangle Institute* A.E. ROBSON, *Berkeley Scholars, Inc.* A novel plasma reactor for materials processing has been developed to form a large area ($\sim$ 4000 cm^2) uniform plasma in the 0.5 to 5 Torr range. The reactor containing the plasma is a slotted metal, rectangular chamber which inductively couples RF power up to 200 kW at 5 MHz from a single turn coil. The chamber provides structural integrity, Faraday screening, cooling channels, and the accessibility for process-integrated substrates. The reactor has been applied to chemical vapor deposition of diamond films where high surface power densities (20-50 W/cm^2) are required and can produce $\sim$ 100 g over 60 hrs. Characteristics of the plasma and deposition chemistry, including electron and gas temperatures, H_2 dissociation, field distribution, and residual gas analysis, will be presented. This reactor represents a new tool for plasma processing with potential applications to gas and materials synthesis as well as surface coatings. Finally, new non-diamond material deposition applications will be discussed.

*Supported by BMDO and ARPA.

Invited Paper

9:30

QR2 8 PECVD of low-dielectric constant films for ULSI .

YUKIHIRO SHIMOGAKI, *Department of Metallurgy, University of Tokyo*

We studied the reduction mechanism of the dielectric constant of F-doped silicon oxide films prepared by PECVD from $SiH_4/N_2O/CF_4$ mixture. From the estimation of the dielectric constant at various frequencies, ranging from 1MHz to 100THz, using CV measurement, Kramers-Kronig relation and the square of the refractive index, we suggest that the dielectric constant due to ionic and electronic polarization is not the dominant factor in decreasing the dielectric constant. It is important to remove -OH in films to obtain very low dielectric constant F-doped silicon oxide films, because Si-OH is the main factor of the orientational polarization in silicon oxide films made by PECVD. To investigate the reaction mechanism which controls the film structure, we changed the residence time of gas in chamber by varying the flow rate. When the residence time in chamber decreases, the film deposition rate increases. We tried to explain flow rate dependency of the deposition rate using a simple CSTR (continuous stirred tank reactor) model. It can be concluded that there are two paths to deposit the films. One route is a deposition by the precursors with poor step coverage profile, and the other route is deposition through intermediates formed by gas phase reactions that contribute to have better step coverage. The overall gas phase reaction rate constant was estimated from these kinetic studies. Same approach was also carried out on the PECVD of C:F film deposition.

SESSION QR3: MAGNETIZED PLASMAS
Thursday morning, 22 October 1998
South Pacific Ballroom, Aston Wailea at 7:30
S. Miyake, Osaka University, presiding

7:30

QR3 1 Simulation of ECR Discharges in Cl and Ar with Kinetic Treatment of Resonant Absorption* M. LAMPE, W. M. MANHEIMER, G. JOYCE, R. F. FERNSLER, S. P. SLINKER, *Naval Research Laboratory, Washington, DC 20375-5346* We have formulated the ECR absorption process as a quasilinear response of the plasma electrons, together with a self-consistent wave kinetic equation.[1] The formulation correctly represents the distribution of deposited energy with respect to the electron velocities, but permits numerical time steps that are orders of magnitude longer than the microwave period. This absorption model is used within our 2-D quasineutral PIC/MC code QUASI-rz,[2] which provides a full kinetic description of the plasma without having to resolve short time scales such as the plasma frequency and gyrofrequency, and which includes Coulomb collisions between charged particles,[3] as well as elastic and inelastic encounters between charged and neutral particles. We present spatially resolved calculations of the electron and ion velocity distributions in argon and chlorine plasmas, and discuss the possibility of tailoring the

electron distribution function by adjusting the magnetic field profile in the absorption region.

*Supported by Office of Naval Research
[1]W. M. Manheimer, NRL Memo Report 6707-98-8122 (1998)
[2]M. Lampe, et al, NRL Memo Report 6709-97-7960 (1997)
[3]W. M. Manheimer, et al, J. Comput. Phys. 138, 563 (1997)

7:45

QR3 2 Source effects in a magnetized, rf, SF6 discharge T.E. SHERIDAN, M. BERGUIGA, R.W. BOSWELL, *Plasma Research Lab, Australian National University* Magnetized, rf discharges are widely used in plasma processing. In these systems, electrons can gain energy from rf E- and B-fields in several ways. At low plasma densities, electrons are energized by the oscillating E-field (capacitive, or E-mode). At higher densities, electrons gain energy from induced fields (inductive, or H-mode). At higher densities still, electrons can be energized by Landau damping of helicon waves (W-mode). We have characterized an SF6 discharge [P. Chabert, et al., J. Vac. Sci. Technol. A 16, 78 (1998)] as a function of neutral pressure (0.3 to 5 mtorr), rf power (up to 1000 W), and magnetic field (B 50 G). We find clear evidence for E- and H-modes. In the E-mode, the density profile in the diffusion chamber is relatively flat, indicating plasma is created throughout the chamber. As the rf power is increased, a clear mode jump is observed. In this mode, plasma is created mainly in the source chamber and then diffuses to the wafer. It appears that the nonuniformity of the dc B-field prevents most of the energetic electrons from entering the diffusion chamber (the BD-mode). If the magnetic field coils on the source are turned off, then dc B-field lines intersect the source chamber only once. In this case, density increases linearly with power. However, an E-H transition is still clearly seen in the floating potential profile.

8:00

QR3 3 Plasma uniformity of a 450mm diameter helicon plasma source* JOHN D. EVANS, *UCLA* FRANCIS F. CHEN, *UCLA*† A proof-of-principle experiment has been performed to show that arbitrarily large substrates can be uniformly covered with high-density plasma by using an array of individual sources operating in the helicon mode. Each source is driven by either an m = 0 loop antenna or an m = +1 helical antenna, and a DC magnetic field is applied to the entire array with a large diameter coil. The plasma is injected into a "magnetic bucket" with permanent-magnet surface confinement. A rotatable ion collector array ("lazy susan" probe) measures the azimuthal variations of ion current to the substrate at various radii. This diagnostic shows that the discrete structure of the sources is unmeasurable 20 cm downstream. With 3kW of 13.56MHz power, plasma densities of order 2 x 10^12 cm-3 have been produced over a 40-cm diam area. The device is shown to operate at the "low-field peak" of the helicon discharge, where high densities can be produced for B < 50G by coupling to Trivelpiece-Gould waves.

*Supported by the SRC
†With help and support from George Tynan of Trikon, Inc.

8:15

QR3 4 Broadband Helicon Experiments and 2-D Plasma Profile Simulations* J. SCHARER, X. GUO, L. LOUIS, Y. MOUZOURIS, H. GUI, *Electrical and Computer Engineering Department, University of Wisconsin, Madison, WI 53706* We present results from a new helicon plasma facility and a new 2-D plasma profile simulation of helicon modes including fast and slow electromagnetic and electrostatic field components. We examine the dependence of frequency (2-200 MHz), power (1-3 kW) neutral pressure, magnetic field configuration, and antenna configuration on helicon mode coupling, wave and plasma characteristics. We find that the wave frequency, magnetic field configuration including a stuffed cusp and plasma pressure has a substantial impact on these sources. We present wave magnetic field, Langmuir probe and plasma impedance results for the plasma source for different antenna configurations. Collisional and collisionless processes for wave absorption as well as nonlinear wave-particle effects will be addressed for these sources. In addition, the 2-D finite difference MAXEB code which incorporates both collisional and collisionless wave damping processes and axial density and magnetic field gradient effects is used to compare with experimental results.

*This research is supported in part by ASOFR Grant 49620-97-1-0262, in part by NSF Grant ECS-9632377 and in part by the University of Wisconsin

8:30

QR3 5 Down Stream Control in a Plasma Exited by m=0 Mode Helical Antenna MAHMOOD NASSER, HIROHARU FUJITA, *Department of Electrical and Electronic Engineering, Saga University, Honjo 1, Saga 840-8502, Japan* Recently, attention has been focused on inductively coupled plasma (ICP) and helicon discharge because they fulfil most of the plasma processing requirements. The plasma characteristics such as potential formation and ion energy distribution functions in these discharges have not yet been investigated on great extent. It is important to clarify the ion energy distribution functions from a comparable point of view between the electropositive and the electronegative gas discharges. In this work, down stream control in plasma exited by m=0 mode helical antenna had been investigated. The radio frequency (13.56 MHz) power was supplied to the helical antenna (3 turn) with an azimuthal mode number m = 0 under a uniform static magnetic field. The working pressure was kept at 1 mTorr. The apparatus consisted of discharge and diffused region separated by a negatively biased grid. The stainless steel vacuum vessel was 15 cm in diameter and 116 in length. The quartz discharge tube was 36 mm in internal diameter and 200 mm in length. The results revealed that, when the grid was biased more negatively, a single peak in the ion energy distribution functions appeared instead of two and the oscillating amplitude decreased to zero volt in the diffused region.

8:45

QR3 6 A comparison of two antenna types in a helicon processing device and the subsequent deposition of AlN CHRIS CARTER, JOE KHACHAN, *University of Sydney* A helicon plasma processing source[1] utilising low pressure, high ion density, radial plasma uniformity, low plasma potential, ion energy control at the substrate and simplicity of machine design has been investigated. Experimental comparisons of ion density, radial uniformity and power coupling efficiency, amongst other factors, have been made between two common antenna types in the helicon plasma processing device containing an argon plasma. One antenna dominantly excites the m=0 azimuthal mode of a helicon wave, while the other antenna dominantly couples to the m=1 mode. We identify the antenna better suited to materials processing in our device. Additionally, ion density measurements were obtained from a nitrogen plasma under various conditions. Studies were then performed on depositing the III-V semiconductor aluminium nitride in a nitrogen plasma. AlN has wide application in areas such as, electronic packaging for thermal management, solar energy, and in semiconductor-substrate lattice matching for the semiconductor gallium nitride in blue LEDs. Measurements on deposited films show AlN to be present with some desired prop-

erties, such as high transparency as required in solar tube applications.

[1]D. R. McKenzie, *et al*, Nucl. Inst. and Meth. in Phys. Res. B, 106, 90 (1995).

9:00

QR3 7 Model Investigations of a Helicon Plasma Instability Driven by Neutral Depletion A.W. DEGELING, R.W. BOSWELL, T.E. SHERIDAN, *Plasma Research Lab, Australian National University* At GEC '97 experimental results taken on the WOMBAT helicon plasma source were presented, showing measurements of a high density helicon plasma which was unstable on millisecond timescales. While the plasma production mechanism could be identified, the reason for the instability remained unclear. By considering the conservation equations for argon ion and neutral species averaged over the source region in WOMBAT a holistic model of the helicon plasma is proposed, in which the ionization rates from inductive and helicon wave coupling and the ion and neutral fluxes into and out of the source region are specified. In particular, the helicon wave ionization mechanism is modeled by assuming that the electron trapping process causes a small bump on the tail of the electron distribution function centered on the helicon wave phase velocity. The model of the neutral dynamics is dominated by depletion by ionization and momentum transfer with ions travelling out of the source; refilling from the large volume diffusion chamber. The model shows a high degree of qualitative agreement with the experimental results, implying that the physical processes included in the model are indeed present in the experiment. Most importantly, the instability giving rise to the limit cycle behavior in the model can be directly attributed to the electron trapping mechanism.

9:15

QR3 8 Measurements and Modeling of Plasma Pumping Effects on Neutral Uniformity GEORGE R. TYNAN, *University of California, San Diego** Plasma uniformity has been recognized as a significant parameter in large sized high density plasma processing tools. In this talk we show experimental and modeling results which indicate that significant neutral uniformity variations can occur in high density plasma processing tools. These variations are attributed to the "plasma pumping" effect, where electron impact ionization of neutral particles is followed by their rapid removal from the plasma by the presheath electric field. This net loss of neutral particles can be viewed as a volumetric pumping effect, and can result in significant neutral density variation across next-generation wafers. Experimental results from helicon and ICP discharges are presented and compared with a one-dimensional diffusion model with a distributed neutral particle sink. The results are also compared with published results.

*Discussions with F.F. Chen are acknowledged, as is support from Applied Materials, Inc.

SESSION RR1: COLLISIONAL PROCESSES IN PLASMAS

Thursday morning, 22 October 1998; Plumeria/Jade Room, Aston Wailea at 10:00; B. Jelenkovic, JILA, presiding

Invited Papers

10:00

RR1 1 Electron-Polyatomic Molecules Interactions and Their Applications.

HIROSHI TANAKA, MASASHI KITAJIMA, *Department of Physics, Sophia University, Tokyo 102, JAPAN* .
MINEO KIMURA, *School of Medical Sciences, Yamaguchi University, Ube 755, JAPAN*

Low-temperature, non-equilibrium plasmas have been indispensable for the plasma-assisted etching of microelectronic structures and the plasma-enhanced chemical vapor deposition of high-quality thin films. With the diversification of the processing requirements, various polyatomic-molecules have been employed as the feedgases, such as CF_4, CHF_3, C_4F_8, NF_3, BCl_3, SiH_4, Si_2H_6, CH_4, C_2H_6, GeH_4, etc, alone or in a mixture with H_2, O_2, and noble gas. Modeling and interpreting the behavior of those reactive-plasmas require the knowledge of cross sections for pertinent electron collision processes. For electrons colliding with the molecules, the main processes are elastic scattering in which primarily the electron momentum is changed, and inelastic processes, such as vibrational ex-citation, electronic excitation, dissocitation as well as ionization. In some cases, one needs to know cross sections involving not only the ground vibro-electronic state but also the vibrationally and electronically excited states of molecule. After a short review of commonly used experimental methods for determining the cross sections, i.e. transmission, swarm, and beam techniques, the pre-sent status of cross sections is summarized for the major polyatomic-molecules. Emphasis is placed on how the atomic and molecular community can aid the understanding of processing plasmas from a basic point of view.

10:30

RR1 2 Plasma Processing Modeling and Databases.

W.L. MORGAN, *Kinema Research & Software, Monument, CO 80132 USA**

I will review the availability of atomic and molecular data for use in plasma processing chemistry modeling. The emphasis will be on plasma chemistries for low pressure semiconductor processing using gases such as C_2F_6, c-C_4F_8, CHF_3, and BCl_3. I will discuss the sources of cross sections and other data and how one evaluates data, assembles plasma chemistry models, and validates such models. Finally I will discuss the possibilities available now and in the near future for on-line plasma chemistry that may be directly accessible by modeling codes.

*This work has been supported by SEMATECH

Contributed Papers

11:00

RR1 3 Transport of Resonance Radiation with Partial Frequency Redistribution* J.E. LAWLER, J.J. CURRY, *University of Wisconsin* Lighting technologies, including new electrodeless Hg-Ar systems and Hg-free systems under development, are utilizing glow discharge plasmas at sub-Torr gas pressures. Resonance radiation transport at sub-Torr gas pressures is profoundly affected by partial frequency redistribution during the absorption-remission cycle. In systems having a resonance lineshape dominated by Doppler broadening, resonance collision broadening, and natural broadening, it is possible to parameterize the fundamental mode trapped decay rate in terms of 3 dimensionless parameters. These 3 quantities are the Voigt parameter at low pressure, the number of ground state atoms per cubic wavelength, and the ratio of the characteristic dimension (radius for cylindrical geometry) to the resonance wavelength. More than three hundred Monte Carlo simulations, each tracking more than 100,000 photons, have been performed using a highly realistic code with many decades of variation of the dimensionless parameters. An analytic formula for the fundamental mode decay rate with partial frequency redistribution in cylindrical geometry is constructed from the Monte Carlo results.

*Supported by Osram-Sylvania Inc. and by the NSF.

11:15

RR1 4 Ionization and Ion Kinetics in Tetraethylgermanium. C.Q. JIAO, A. GARSCADDEN, C. DEJOSEPH, P.D. HAALAND, *Air Force Research Laboratory, Wright-Patterson AFB, OH* We have measured cross sections for electron impact ionization of tetraethylgermanium ($GeEt_4$) from 10 to 70 eV, using Fourier transfrom mass spectrometry. Rate coefficients of gas-phase ion-molecule reactions in $GeEt_4$ are also determined. The molecular ion and 15 fragment ions are observed from the electron impact ionization with a total cross section of 3.5 $\pm$ 0.4 $\times$ $10^{-15}cm^2$ at 70 eV. Most of the fragment ions contain Ge, with less than 3% yield of hydrocarbon ions. Below 25 eV, $GeC_6H_{15}^+$ is the most abundant ion while above 25 eV $GeC_4H_{11}^+$ has the largest partial ionization cross section. All fragment ions except $GeC_6H_{15}^+$ react readily with $GeEt_4$ to yield $GeC_6H_{15}^+$, with rate coefficients in the range of 2 $-$ 5 $\times$ $10^{-10}cm^3s^{-1}$. $GeC_6H_{15}^+$ undergoes a slow clustering reaction with $GeEt_4$ to produce $Ge_2C_6H_{17}^+$ and $Ge_2C_8H_{21}^+$ at rates less than $10^{-12}cm^3s^{-1}$. Ar^+ reacts with $GeEt_4$ with a rate coefficient of 5.1 $\times$ $10^{-10}cm^3s^{-1}$, producing mainly $GeC_6H_{15}^+$. Taken together, the ionization cross sections and ion-molecule reaction rates suggest that $GeC_6H_{15}^+$ dominates the ion flux reaching substrate surfaces under many plasma conditions.

11:30

RR1 5 Boltzmann Analysis of Electron Swarm Parameters in CF_4 Using Independently Assessed Electron-Collision Cross Sections MARIE-CLAUDE BORDAGE, *Universite Paul Sabatier* PIERRE SEGUR, *Universite Paul Sabatier* LOUCAS CHRISTOPHOROU, *NIST* JAMES OLTHOFF, *NIST* Electron swarm parameters (drift velocity, transverse and longitudinal diffusion coefficients, ionization and attachment coefficients) in CF_4 and CF_4/Ar mixtures have been calculated using the solution of the Boltzmann equation under the hydrodynamic regime.[1] The calculations are based upon an up-dated set of recommended electron-interaction cross sections derived previously[2] from experimental measurements. Agreement between the calculated and previously measured swarm parameters validates both the model and the cross section set. Analysis of the model results especially shows the high degree of sensitivity of the swarm parameters on the magnitude and threshold of the indirect vibrational excitation cross section.

[1]M. C. Bordage, P. Segur, and A. Chouki, J. Appl. Phys. **80**, 1325 (1996)
[2]L. G. Christophorou, J. K. Olthoff, and M. V. V. S. Rao, J. Phys. Chem. Ref. Data **25**, 1341 (1996)

11:45

RR1 6 Collisional-Radiative Recombination of Ar^+ Ions with Electrons in a Flowing Afterglow Plasma.* MIROSLAW P. SKRZYPKOWSKI, MICHAEL F. GOLDE, RAINER JOHNSEN, *University of Pittsburgh, Pittsburgh, PA* Langmuir probe measurements of electron densities, n_e, in an Ar^+/e^- plasma are quantitatively consistent with the semi-empirical rate coefficient for collisional-radiative recombination given by Stevefelt et al.[1] : $\alpha_{cr} = 1.55 \times 10^{-10}T^{-0.63} + 6.0 \times 10^{-9}T^{-2.18}n_e^{0.37} + 3.8 \times 10^{-9}T^{-4.5}n_e$ over the initial electron density range $5 \times 10^9 - 5 \times 10^{10}cm^{-3}$ at $T = 300K$. Optical emission spectroscopy data reveal transitions from highly-excited states of Ar to $Ar(^3P)$. We believe that the collisional-radiative recombination of Ar^+ ions is responsible for the presence of Ar metastable atoms in flowing afterglow plasmas.

*This work was supported by NASA
[1]J. Stevefelt et al., Phys. Rev A 12, 1246 (1975)

SESSION RR2: PLASMA DIAGNOSTICS
Thursday morning, 22 October 1998
Maile Room, Aston Wailea at 10:00
Masaru Hori, Nagoya University, presiding

Contributed Papers

10:00

RR2 1 Spatial distribution measurement of absolute CFx radical densities in Electron Cyclotron Resonance C_4F_8 plasma MASAYUKI NAKAMURA, HIROTAKA NAKAYAMA, MASAFUMI ITO, MASARU HORI, AKIHIRO KONO, TOSHIO GOTO, *Dept. of Quantum Eng., Nagoya Univ., JAPAN* NOBUO ISHII, *Tokyo Elec. Ltd., JAPAN* Recently, fluorocarbon films are expected to be new materials for the intermetal dielectrics with a low dielectric constant in multilevel interconnections of future high speed ULSIs. Moreover, the wafer size becomes larger (12 inch) and the uniformity of low dielectric constant materials is requested throughout the large wafer. Therefore, the spatial distribution measurement of the absolute radical densities is indispensable for controlling the uniformity. In this study, We have measured the absolute radical densities of CFx (x=1-3) radicals in ECR- C_4F_8 plasma using infrared diode laser absorption spectroscopy (IRLAS) without using multiple reflection cell and with selecting the laser beam path parallel to the wafer. The densities were evaluated as functions of microwave power. The CF_2 radical density in the vicinity of the chamber wall was larger than that in plasma at any microwave power. On the other hand, the spatial distribution of CF radical density showed the tendency different from that of CF_2 radical density. It was explained by the difference of the extinction and the generation of CFx (x = 1,2) radicals, in the plasma region and on the chamber wall. The be-

haviors of CF_3 radical and F atom densities in ECR plasma are also discussed.

10:15

RR2 2 Novel Ion Current Sensors for Monitoring and Control of Plasma Processing MARK A. SOBOLEWSKI, *National Institute of Standards and Technology* Recently, a method has been demonstrated for using external radio-frequency (rf) electrical measurements to monitor the ion current at an electrically insulating or conducting wafer during processing by a high-density plasma. The rf signals are generated by the rf bias power which is normally applied to wafers. There is no need for any probe to be inserted into the plasma or for any additional power supplies which might perturb the plasma. At low rf bias frequencies ion currents measured by this technique agree well with dc measurements of the ion current, but they agree less well at higher frequencies. This disagreement has been investigated using a fluid model of the sheath region of high-density plasmas. Simulations show that, as the rf frequency approaches the ion plasma frequency at the edge of the sheath, the ion current at the electrode varies strongly with time during each rf period. Under these conditions, the rf measurement of ion current differs from the time-averaged value of the ion current. The simulations are used to characterize the error in the rf measurement technique and to suggest new rf methods which more accurately determine the time-averaged ion current.

10:30

RR2 3 Optical Computer Aided Tomography of Inductively Coupled Plasmas in the GEC Reference Reactor E. C. BENCK, *NIST* J. R. ROBERTS, *NIST* Optical emission measurements of a plasma do not provide a direct measure of the plasma uniformity, since each measurement is actually equal to the plasma emissivity integrated along the line of sight through the plasma. In order to determine the actual plasma emissivity distribution, without assuming cylindrical symmetry, optical emission measurements are inverted using computer aided tomography (CAT) with Tikhonov regularization. The accuracy of this inversion process has been studied as a function of the viewing geometry and regularization parameter. This technique is applied to an inductively coupled plasma source built in a modified GEC RF Reference Cell. 2D plasma distributions have been measured for a variety of different plasma conditions. Axially asymmetric discharge distributions have been found as a function of the gas flowrate, molecular gas mixtures and proximity to the induction coil.

10:45

RR2 4 Radical Detection in Etching Plasmas by UV Cavity Ring-Down Spectroscopy JEAN-PAUL BOOTH, DANIELE ROMANINI, LUDOVIC BIENNIER, ALEXANDER KACHANOV, *Laboratoire de Spectrometrie Physique, Universite de Grenoble / CNRS, France* Free radicals play an important role in etching processes in determining etch rates and selectivity. A number of techniques have been used to detect these species: Laser induced fluorescence has excellent space and time resolution, but does not directly give absolute concentrations. Broad-band UV absorption spectroscopy is a simple and powerful technique for obtaining absolute concentrations, but has rather low sensitivity, necessitating long integration times (10's of minutes). The recently developed Cavity Ring-Down technique is a sensitive laser method for high-resolution absorption spectroscopy, that allows weaker absorptions to be measured with shorter integration times. We have detected CF_2 radicals by this technique for the first time. The radicals were created in a capacitively-coupled RF plasma in C_2F_6 and detected by the A(0,10,0)-X(0,0,0) transition around 237 nm. A range of other species, including CF, SiF_2 should be detectable using appropriate mirrors.

Invited Paper

11:00

RR2 5 Plasma Diagnostics: Use and Justification in an Industrial Environment.
PETER LOEWENHARDT, *Applied Materials, Inc.*

The usefulness and importance of plasma diagnostics have played a major role in the development of plasma processing tools in the semiconductor industry. As can be seen through marketing materials from semiconductor equipment manufacturers, results from plasma diagnostic equipment can be a powerful tool in selling the technological leadership of tool design. Some diagnostics have long been used for simple process control such as optical emission for endpoint determination, but in recent years more sophisticated and involved diagnostic tools have been utilized in chamber and plasma source development and optimization. It is now common to find an assortment of tools at semiconductor equipment companies such as Langmuir probes, mass spectrometers, spatial optical emission probes, impedance, ion energy and ion flux probes. An outline of how the importance of plasma diagnostics has grown at an equipment manufacturer over the last decade will be given, with examples of significant and useful results obtained. Examples will include the development and optimization of an inductive plasma source, trends and hardware effects on ion energy distributions, mass spectrometry influences on process development and investigations of plasma-wall interactions. Plasma diagnostic focus, in-house development and proliferation in an environment where financial justification requirements are both strong and necessary will be discussed.

Contributed Papers

11:30

RR2 6 The Argon Dilution Effects on Optical Emission Spectra of Fluorocarbon Ultrahigh-Frequency Plasmas T. NAKANO, *National Defense Academy, Japan* S. SAMUKAWA, *NEC Corporation, Japan* The Ar dilution effects on the ultrahigh-frequency (UHF) plasmas through C_4F_8 and CF_4 are studied by optical emission spectroscopy and Langmuir probe measurement. For the C_4F_8 plasma, the Ar dilution extends the electron energy distribution function (eedf) toward the higher energy and increases the electron density, n_e. The n_e-normalized CF_2 emission intensity is decreased proportionally with the partial pressure of the C_4F_8 feedstock gas. Thus, the Ar dilution increases the ratio of the ion density to the CF_2 density, which changes the balance between the etching and the polymer deposition and affects the SiO_2 etching characteristics significantly. For the CF_4 plasma, the Ar dilution does not change the eedf but increases the n_e in the CF_4/Ar

plasma. Since CF_2 radicals are inferred to be the higher order dissociation products of CF_4 molecules, the increased n_e results in the enhanced production of CF_2 radicals. Approximately the same ratio of the ion density to the CF_2 density in the CF_4/Ar plasma as that in the C_4F_8/Ar plasma suggests that in the SiO_2 etching process by high-density, low-pressure plasmas, the CF_4/Ar plasma chemistry may be a substitution for the C_4F_8/Ar plasma chemistry.

11:45

RR2 7 Electrical Control of Spatial Uniformity of Chamber-Cleaning Plasmas Investigated using Planar Laser-Induced Fluorescence KRISTEN L. STEFFENS, *National Institute of Standards and Technology* MARK A. SOBOLEWSKI, *National Institute of Standards and Technology* Fluorocarbon plasmas are widely used by the semiconductor industry for in situ cleaning of PECVD chambers. The spatial characteristics of these plasmas must be optimized to maximize the cleaning rate at appropriate surfaces. Previous studies in the GEC Reference Cell have indicated that the spatial distributions of chemically reactive species are correlated to the rf current at the upper, grounded electrode. In this study, the current at the upper electrode was varied by adjusting the impedance between the upper electrode and ground, for O_2/CF_4 and O_2/C_2F_6 plasmas at 0.1 to 1 Torr. The 2-D density distribution of the reactive radical, CF_2, was measured by planar laser-induced fluorescence (PLIF), and the regions where reactive species were generated were determined using spatially-resolved, broadband optical emission. As the current at the upper electrode was varied, changes were observed in the axial and radial uniformity of the emission and PLIF. These results suggest that electrical control can be used to optimize the spatial distribution of reactive species in chamber-cleaning and other fluorocarbon plasmas.

12:00

RR2 8 2D images of two frequency capacitively coupled plasmas at VHF* T. KITAJIMA, Y. TAKEO, N. NAKANO, T. MAKABE, *Keio University at Yokohama, Japan* 2D(r,z) images of two frequency capacitively coupled plasmas of Ar and Ar/CF_4 in an axisymmetric parallel plate reactor are investigated by time-resolved OES. Electron densities are also obtained by microwave interferometry. We present the 2D profiles of the net excitation rates of $Ar(3p_5)(\epsilon_{ex} = 14.5eV)$ and $Ar^+(4p\,^4D_{7/2})$ ($\epsilon_{ex} = 35.0eV$), used as the probe. Large area uniformity of plasma production at low pressure($\sim$ 25mTorr) driven at VHF(100MHz) is presented in comparison with that at HF(13.56MHz). Judging from the time variation of the net excitation rate, secondary electrons from the LF bias electrode at 700kHz are considerably influential in the production of the plasma at HF, while they are not at VHF. In case of HF, the electron density increases with the increase of the bias amplitude, since high energy electrons produced by secondary emission are confined in the bulk plasma by the higher self bias voltages at both electrodes. The self bias voltage at HF electrode is $-$ 270V and is equivalent to that at bias electrode ($-$ 260V). However, in case of VHF, the self bias voltage ($-$ 25V) at VHF is much lower than that at bias electrode($-$ 250V) under the same power dissipation. Addition of CF_4 to Ar leads plasma to the better uniformity of the radial profile of the excitation due to the appearance of electronegativity.

*Work supported by ASET.

SESSION RR3: MAGNETIZED PLASMAS AND THERMAL PLASMAS

Thursday morning, 22 October 1998
South Pacific Ballroom, Aston Wailea at 10:00
Uwe Kortshagen, University of Minnesota, presiding

Contributed Paper

10:00

RR3 1 Plasma Production and Wave Propagation in a Plasma Source Using Lower Hybrid Waves YASUYOSHI YASAKA, TETSUO KIKUCHI, KEITARO OHNISHI, KUNIHIDE TACHIBANA, *Department of Electronic Science and Engineering, Kyoto University* TOHRU ITOH, *Plasma System Corp.* Control of spatial profile of power deposition in a plasma is one of the key factors in producing a uniform plasma. The lower hybrid wave, which is in the same frequency range as the helicon wave, is resonant at lower hybrid frequency and does not penetrate into higher-density side of the plasma. This provides localized ionization region at outer plasma radii leading to uniform plasma production. The plasma source is a 10-cmϕ glass tube with three or four electrostatic ring couplers spaced by 9 cm driven at a frequency of 10 – 20 MHz with $0 - \pi - 0 - (\pi)$ phasing in a magnetic field of 100 – 900 G. The source region is connected to a diffusion chamber of 35 cm in diameter. Typical plasma densities at the source region are of the order of 10^{11} cm^{-3} for 10-mTorr Ar and 1-kW rf power. The radial density profile can be controlled by changing the location of the lower hybrid resonance by changing the magnetic field. We measure the radial dependence of rf fields to find that the short-wavelength electrostatic wave is present near the resonance with the global long-wavelength electromagnetic field. The measured wave propagation is compared with calculated dispersion relation of the lower hybrid wave.

Invited Paper

10:15

RR3 2 Self-Consistent Particle Simulation of Target Erosion, Sputtered Atom Transport, and Background Gas Flow in a DC Magnetron.
VLADIMIR SERIKOV, *Nippon Sheet Glass Co., Advanced Simulation Crew, Japan*

Recently, there has been developed an effective Monte Carlo model of magnetron sputtering[1]. It is based on particle simulation of the electron trajectories in the uniform equilibrium background gas under the applied electric and magnetic fields. The flux onto the target of the ions produced in ionizing electron-atom collisions is then sampled to give the target erosion distribution. In the present study, we further elaborate and complete the model by allowing for the background gas condition, since the gas can be substantially heated and pushed by the energetic plasma species and/or sputtered material atoms. A new technique has been suggested for self-consistent particle simulation of the main magnetron discharge species, i.e., electrons, ions, sputtered and background gas atoms. These species, characterized by the disparate

time scales, are treated within the framework of a single model based on the collision scheme accounting for the time scale difference. The model is applied to predict the target erosion and film growth coupled with the background argon gas flow in a two-dimensional planar DC magnetron. The effect of sputtering on the background gas is displayed by the simulated "sputtering wind". Meanwhile, the rarefaction of the heated gas in front of the target is shown to lead to the erosion rate reduction and widening of the erosion profile, the flux and average energy of the deposited atoms being also affected. The examples of the model application to a practical sputter deposition system are to be discussed.

[1]T.E. Sheridan, M.J. Goeckner, and J. Goree: J. Vac. Sci. Technol. A, 8 (1990) 30;
[2]K. Nanbu and I. Warabioka: Space Science and Engineering (AIAA, New York, 1992) p. 428.

Contributed Papers

10:45

RR3 3 Modeling of Physical Vapor Deposition Sources: Validation and Multiple Length Scale Issues P.L.G. VENTZEK, *Motorola Inc.* V. ARUNACHALAM, *Motorola Inc.* D. DENNING, *Motorola Inc.* D. CORONELL, *Motorola Inc.* Ionized metal plasma physical vapor deposition is attractive as a metallization process as it provides both good step coverage and high deposition rates. Process development and extendibility issues have prompted the development of numerous numerical models. Nonetheless, coupling multiple length scales (tool, sheath, feature) continues to be a challenge as it is for other plasma processes. This study couples tool (HPEM)#, sheath and feature scale models for a generic metal deposition process. This coupling is crucial at two locations. At the target, the magnetron plasma behavior adjacent to the sheath dominates how one predicts how the target is eroded and to some degree how one predicts the across wafer deposition uniformity. At the wafer, this coupling dominates how one predicts the film is deposited within the feature. The coupling of the feature, sheath and equipment scale models will be demonstrated and discussed in light of validation experiments. # University of Illinois

11:00

RR3 4 The Ion Energy Distribution at a Biased Substrate Immersed in a Low-density DC Arcjet Plasma MARK CAPPELLI, DARREN BERNS, *Thermosciences Division, Stanford University* The characterization of the ion energy distributions in ion-assisted plasma chemical vapor deposition of boron nitride is critical to the understanding of the physical mechanism responsible for stabilizing the cubic phase (cBN) over the thermodynamically favored hexagonal phase (hBN). Inour prior studies of cBN synthesis, we have found that cBN of high purity can be deposited in a low-density direct-current (dc) arcjet plasma impinging on a negatively biased substrate. In order to understand this process, a combined planar Langmuir probe and retarding potential analyzer (RPA) was designed into the substrate, and implemented to measure the ion flux, the electrical sheath thickness at the substrate, and the impinging ion energy distribution. RPA measurements are compared to Monte Carlo simulations of the transport of ions across the dc sheath. The dependence of the ion energy distribution and the properties of the deposited c-BN films on various process parameters are presented and a simple model of the ion-enhanced stabilization is proposed.

11:15

RR3 5 Diagnostic of Arc Dynamics in a Plasma Spray Torch JOCHEN SCHEIN, ZHENG DUAN, JOACHIM HEBERLEIN, *University of Minnesota, Department of Mechanical Engineering, Minneapolis, MN 55455** Arc instabilities can be the cause of significant power fluctuations in plasma torches. The resulting variations in plasma generation can influence plasma processing results if the characteristic processing times are in the same order of magnitude as the time constants of the instabilities. This is the case in plasma spraying. We describe in this paper a variety of high speed diagnostic methods to caracterize the dynamic behaviour of an arc in a plasma spray torch. The diagnostics include a high speed CCD camera with on-line computerized image analysis which allows end-on observation of the arc in the plasma torch and simultaneous side-on observation of the jet, and a unidirectional microphone for determining the pressure fluctuations of the nozzle exit. The signal are correlated with the current and voltage waveforms, and power spectra are generated using LabVIEW software. The effect of changes in the primary parameters, arc current, gas composition and flow rate, as well as the effect of anode condition is clearly distinguishable. A deteriorating anode is characterized by an increasing peak in the power spectra of voltage and sound. The time resolved measurements have contributed to an improved understanding of the plasma-particle interaction during plasma spraying.

*This work was funded by the ERC for Plasma Aided Manufacturing TA3

11:30

RR3 6 Laser Triggering of Compact High-Current Vacuum Switches JOSEPH R. WOODWORTH, *Sandia National Laboratories* GORDON E. BOETTCHER, *Sandia National Laboratories* RANDAL L. SCHMITT, *Sandia National Laboratories* THOMAS W. HAMILTON, *Sandia National Laboratories* Sandia National Laboratories is building compact (0.16 cm3), high-current (1 - 3 kV, 2 kA), vacuum switches called SPRYTRONS for a variety of applications. We report experiments in which these switches are triggered by focusing the beam from a Nd/YAG laser operating at 1.06 microns onto a carbon insert in the cathode. We find the threshold for low-jitter triggering of this switch is a laser focal intensity of about 200 MW/cm2. This threshold holds over a wide range of focal spot sides. Using an 8.6-cm focal-length lens to focus the laser, we have demonstrated low jitter triggering (plus or minus 3 ns one-sigma jitter) using 10 microjoules of laser energy. Details of the switches and the experiments will be presented. This work was suppported by the U. S. Department of Energy under contract ACO4-94-AL8500. Sandia is a multiprogram laboratory operated by the Sandia Corporation, a Lockheed Martin Company, for the United States Department of Energy.

11:45

RR3 7 Advances in physical study of high enthalpy plasma jets of technological interest: emission spectra and plasma characteristics A.A. BELEVTSEV, V.F. CHINNOV, E.KH. ISAKAEV, A.V. MARKIN, T.F. TAZIKOVA, S.A. TERESHKIN, *Science and Engeneering Centre for Energy Efficient Processes and Equipment, Associated Institute for High Temperatures, Russian Academy of Sciences* Offers a comprehensive study of the emission spectra and plasma characteristics of high enthalpy atmospheric pressure argon and nitrogen jets produced by a high- current industrially important arc plasmatron with a vortex stabilized channel-anode (I< =3D500A, G=3D1-4g/s, jet diameter at a minimum-6mm). The spectra are taken at different distances from the cathode in the 200-950nm region with a spectral resolution

=3D0.01nm allowing a fine structure of vibronic bands to be essentially resolved except that due to the dublet (spin) splitting and Λ-doubling. Also derived (through the Abel inversion) are radial distributions of plasma components. The spectra obtained have been used for determining plasma composition, the electron component parameters (by atomic/ionic Stark half-widths and intensities) and the assessment of rotational and vibrational temperatures by simulating molecular bands.

12:00
RR3 8 Realistic Simulation of the Ignition Procedure Based on the Use of a Grafite Rod for Inductively-Coupled Plasma Torches V. COLOMBO, M. LOMBARDINI, D. BERNARDI, F. TADDEI, *Università di Bologna, Dipartimento di Matematica, C.I.R.A.M., Via Saragozza 8, 40123 Bologna, Italy* G.G.M. COPPA, *Politecnico di Torino, Dipartimento di Energetica, Corso Duca degli Abruzzi 24, 10129 Torino, Italy* Numerical simulation of the distributions of gas temperature and velocity and of the electromagnetic field for discharges in inductively-coupled plasma torches working at atmospheric pressure are presented using a 2-D time-dependent fluid-magnetic code, which simulates the plasma behavior during both the initiation transient and in the final self-substained configuration for different operating conditions, including the presence of a carrier gas injected along the torch axis. Reference has been made to the starting technique that makes use of a grafite rod, which is initially inserted in the coil region and then gradually extracted. The rod has been treated as a real obstacle for the fluid and the electronic emission causing the plasma initiation has been suitably simulated. The advantage of a time-dependent simulation to select different plasma operating conditions that lead to stable plasma discharges is pointed out. Acknowledgements. Partial support of A.S.P., Torino, Italy (Plasma Processing/Plasma Torch Project) and of the National Group for Mathematical Physics of the Italian C.N.R. is acknowledged.

SESSION SR1: ADVANCED PLASMA PROCESSING
Thursday afternoon, 22 October 1998; Plumeria/Jade Room, Aston Wailea at 13:45; K. Sasaki, Nagoya University, presiding

Invited Papers

13:45
SR1 1 Challenges in manufacturing of ULSI devices.
HISATSUNE WATANABE, *R&D Group, NEC Corporation, Japan*

Although the technology roadmap was completed as a future schedule, crisis has been often pointed out in several fields of LSI manufacturing. The present paper describes current status and challenges in developments of CMOS/interconnection, advanced lithography and etching, novel circuits and architectures for low power dissipation. Recent trials for zero-fluctuation processes will be also described.

14:15
SR1 2 Properties and Diagnostics of Pulsed ECR and Helicon Plasmas.
MIENO TETSU, *Dept. Phys., Shizuoka Univ.*
SAMUKAWA SEIJI, *Silicon System Lab., NEC Co.*

Development of advanced plasma etching to fabricate G-bit scale memory is urgent subject of study, and pulse-time-modulated plasmas are promising candidates of this purpose, [1] because charge up and notching of substrates are considerably reduced. Here, time dependence of plasma properties of a pulsed ECR plasma, which is produced in a dry-process chamber with coaxial magnet and 30 cm substrate size, is investigated. [2] As a result, pulsed chlorine plasma modulates plasma density, electron temperature, sheath voltage and negative ion density, which reduces time-averaged electron temperature and positive ion flux to the wall. Electron and negative ion injection to the substrate is also enabled using the RF bias. Properties of pulsed helicon plasma is also investigated and oxygen and fluorine negative ions are prominently produced at the afterglow time.

[1]S. Samukawa et al., J. Vac. Sci. Technol. A14 (1996) 3049.
[2]T. Mieno & S. Samukawa, Plasma Sources Sci. Technol. 6 (1997) 398.

Contributed Papers

14:45
SR1 3 A Theoretical Study on the Reactivity of Negative Ions in High Performance Etching by using a Pulse-Time-Modulated Plasma KEN-ICHIRO TSUDA, HIROTO OHTAKE, SEIJI SAMUKAWA, *NEC Corporation* Charge-free and highly reactive etching (Al, Au, and Pt) can be realized using a pulse-time-modulated ECR Cl_2 plasma in the range of a few tens of microseconds with a low frequency RF bias of less than 1MHz. It is considered that this is due to the generation of a large amount of negative ions (Cl-) in the pulsed plasma. In particular, when compared with volatile materials (Al), the etching rates of non-volatile materials, such as Au and Pt, are drastically increased with an increase in the negative ions. The injection of negative ions could thus enhance the reactivity in Au and Pt etchings. To understand the role of negative ions in the surface reaction with Au, the dissociation energies of the radicals and ionic species of $AlCl_3$ and $AuCl_3$ from Al and Au surface models are calculated using ab

initio Molecular Orbital theory when Cl, Cl^+, and Cl- are adsorbed on Al and Au surfaces. We found, compared with a Cl^+ injection, that a Cl- injection on the Au surface causes a drastic decrease in the dissociation energies of $AuCl_3$. It becomes clear that the evaporation rates of $AuCl_3$ are dramatically increased with an increase in the negative ions in the pulsed plasma. The negative ions also play a very important role in enhancing the reactivity on the surface during etching reactions.

Invited Papers

15:00
SR1 4 Role of Negative Ions in High-Performance Etching using Pulse-Time-Modulated Plasma.
SEIJI SAMUKAWA, *Silicon systems research laboratories, NEC corporation, Japan*

Highly selective and highly anisotropic etching with notch-free and free of damage due to charge-buildup can be done by using high-density Cl2 plasma modulated at a pulse timing of a few tens of microseconds. A large quantity of negative ions are produced with maintaining positive ion density, because the cross-section for the dissociative attachment of Cl_2 is increased as the electron temperature plunges in the afterglow of the pulsed plasma. There is a large negative ion to electron ratio (more than 100) and the normal positive sheath has collapse. The negative ions, exiting the plasma during the power-off period of the modulation, contribute to the drastic reduction of positive surface charge, which causes the local side etching (notch) and topography-dependent charging in the narrow space pattern. These negative ions also increase the etching rate at the low ion energy on the substrate. Moreover, we also found that the injection of negative ions into the surface could accomplish the enhancement of reactivity especially in nonvolatile materials, such as Au and Pt. It is considered that this is due to the increase in the evaporation of etching products with the negative ions. In large-scale etching processes, the generation of negative ions also has a role in producing the excellent uniform etching rate on the large-diameter-substrate because of the diffusion of ambipolar ions (negative and positive ions) at the afterglow. The negative ions in the pulse-time-modulated plasma will play a very important role to breakthrough many of the problems associated with future precise etching processes. Our etching method shows excellent potential for large-scale etching applications to Gbit level ULSI.

15:30
SR1 5 Negative Ion Metal Etching by Employing Magnetic Filter in Halogen Plasma.
Y HORIKE, *Toyo University, Department of Electrical and Electronics Engineering*

To neutralize the positively charged-up bottom surfaces of high aspect ratio holes or gaps, generation of negative ions in halogen downstream plasmas and their alternate irradiation by the transformer coupling of the RF field with the electrode have been studied. In the previous work, the Si etching employing negative ions revealed the high etching reactivity which resulted from the fact that dominant negative species were formed by ions of atoms like F^- in SF_6 and Cl^- in Cl_2 plasmas. It is expected that the negative ion etching is more effective for metals because the metal bonding is weakened by supply of negative charge. Indeed, the Al-Si-Cu etch rate of 130 nm/sec was achieved. However, the negative ions are difficult to be introduced to an electrode covered by insulators such as an electrostatic chucking due to generation of the self biasing. To overcome this problem, the trapping of electrons was examined in the downstream choline plasma by employing a magnetic filter, which consisted of a pair of water-cooled high current coils set in the etching chamber. The ratio of positively biasing to negative biasing saturation currents was reduced as low as several. However, at present still remained electrons generate a little self biasing, thus lowering Al etch rates.

SESSION SR2: PLASMA SURFACE INTERACTIONS
Thursday afternoon, 22 October 1998
Maile Room Aston Wailea at 13:45
M. Bowden, Kyushu University, presiding

Contributed Papers

13:45
SR2 1 Incident Angular Dependence of Electron Transmission Probability in Surface Oxides on Metal Electrodes and Effects of Electron Trapping KOZO OBARA, OSAMU NAGANO, KAZUHITO MUROYA, *Kagoshima University* WOLFGANG FUKAREK, *Institute of Ion Beam Physics and Materials Research*
We present the microscopic informations on the surface electronic states of metal electrodes which were slightly oxidized or adsorbed gas molecules (N2, Ar, H2, O2). The surface states were obtained from the wave number vector dependence of electron transmission current into the surface. The wave number vector (k//,kr) was estimated from the electromagnetic conditions. This technique is very useful for evaluating the surface parameters of wall or electrodes under the practical plasma conditions and also for considering the growth process in it. Main results are following; 1) electron transmission probability strongly depended on the electron trap-states in the oxide, 2) electron capture probabilities in the trap states (surface states) depend on the incident wave number vector, 3) from gas pressure dependence of surface states of adsorbed atoms, two sites (one is depend on the pressure, another is not) were observed. From these facts we conclude that the surface electronic states have anisotropic structures and the trapped electrons modify the electron transmission probability.

14:00

SR2 2 Comments on the Bohm criterion and sheath edge for finite λ_D K.-U. RIEMANN, *Theoretische Physik 1, Ruhr-Universität Bochum, D-44780 Bochum* The usual subdivision of the plasma boundary layer problem in a quasineutral presheath and a collision free planar sheath is strictly valid only in the asymptotic limit $\lambda_D/L \rightarrow 0$ (where λ_D is the electron Debye length and L represents the smallest competing ion length scale). Various questionable attempts have been made to extend the plasma-sheath concept and to generalize the Bohm criterion for finite λ_D. For a simple fluid model of collision dominated ions the consistent matching of plasma and sheath was previously discussed in detail.[1] The present investigation extends this analysis to arbitrary presheath mechanisms and to a kinetic description of the ions.

[1]K.-U. Riemann, Phys. Plasmas **4**, 4158 (1997)

14:15

SR2 3 Wall Loss Rates for the 2^3S_1 Helium Metastable from Diode Laser Absorption MICHAEL W. MILLARD, *University of Datyon, Ohio* PERRY P. YANEY, *University of Dayton, Ohio* BISWA N. GANGULY, *Air Force Research Laboratories, Wright-Patterson AFB, Ohio* CHARLES A. DEJOSEPH, JR., *Air Force Research Laboratories, Wright-Patterson AFB, Ohio* Experimental measurements of the wall loss rates for the 2^3S_1 helium metastable state have been performed in a 2 to 5 Torr parallel plate discharge using diode laser absorption on several different wall materials. Measurements give wall loss rates approaching 90% to 100% for common materials such as stainless steel. Also, a numerical model of the metastable density in a d.c., parallel plate discharge has been developed to simulate both the steady state behaviour and temporal response of the metastables in the discharge. The model includes production and loss due to diffusion of the metastable helium atoms to the wall. The model is in good qualitative agreement with experiment over a range of discharge parameters. Finally, using the same diode laser absorption system, we have measured the diffusion coefficient of 2^3S_1 helium metastable in the fundamental diffusion mode. Initial measurements at a pressure of 2 Torr give a diffusion coefficient of 275 cm^2/s.

14:30

SR2 4 Density of Ar Metastable Atoms on the Discharge Tube-Wall Measured by an Evanescent Laser Spectroscopy T. SAKURAI, T. KUBOTA, Y. TAKAHARA, *Yamanashi University* We demonstrate the validity of laser evanescent wave spectroscopy in order to measure the density of metastable atoms at a boundary between discharge plasma and tube wall. When a laser propagates towards the surface through a glass at an incident angle for total reflection, the evanescent wave is produced on the vacuum side of the dielectric surface and is characterized by the thin penetration depth with a magnitude of laser wavelength in the direction normal to the suface. The fluorescence induced by the laser evanescent wave is measured in the experiment with using a discharge tube and its detection shows the existence of metastable atoms on the wall. The absolute value of the density is obtained from the calibration of the evanescent wave optical system with replacing the discharge tube by a rubidium vapor cell, where the density is determined by a temperature. From the value, a reflectance of metastable atoms at the wall is estimated.

14:45

SR2 5 Sheath relaxation in plasma immersion ion implantation K.-U. RIEMANN, TH. DAUBE, *Theoretische Physik 1, Ruhr-Universität Bochum, D-44780 Bochum, Germany* The sheath relaxation in front of an electrode biased to a pulsed high negative potental is investigated on the basis of a simple step model similar to that of Lieberman [1]. We distinguish the matrix extraction phase and the subsequent sheath expansion phase. For the matrix extraction we give an analytical model that is *not* based on artificial assumptions. This model is extended to describe the sheath expansion and is used to construct an explicit approximation for the ion current and energy distribution at the electrode. The results ahow excellent agreement with numerical solutions of the corrensponding hydrodynamic equations.

[1]M. A. Lieberman, J. Appl. Phys. **66**, 2926 (1989)

15:00

SR2 6 Effect of Pulsing the Plasma Source and the Bias Power on the Deposition of Silicon Oxide in a Helicon Assisted Reactive Evaporation System A. DURANDET, B. MONSMA, R.W. BOSWELL, *Plasma Research Lab, Australian National University* We present the results of the deposition of SiO2 under pulsed plasma conditions in a Helicon Assisted Reactive Evaporation (HARE). The helicon plasma source is pulsed at a frequency varying from 1Hz to 1KHz. This frequency range is slow relative to plasma time scales, but has been selected to compare to the typical time scale of the deposition (0.1 to 1nm of SiO2 deposited in 100ms), and to the operating conditions of HARE (pressure variations during the post discharge and during the pulse). Combining a high deposition rate from neutral species in the post discharge, followed by the ion bombardment of the deposited layer during the plasma pulse, which achieve good quality films (as measured with p-etch and FTIR). An independent bias power is applied to the substrate to control the ion bombardment of the surface during the deposition. The bias power is varied, as well as the duration of the bias pulse with respect to the duration of the source pulse. We investigate the effect of applying a short bias pulse at high power.

15:15

SR2 7 Ionisation and Attachment Processes in an RF Plasma in Carbon Tetrafluoride J.A. REES, T.D. WHITMORE, C.L. GREENWOOD, *Hiden Analytical Limited* In view of the importance of carbon tetrafluoride in plasma processing and its comparatively simple chemical composition, an experimental examination of some of the electron impact ionisation and attachment processes which occur in it is described. The measurements were carried for neutral gas sampled from a parallel plate RF reactor both in the absence and presence of a plasma. The data presented here include measurements of the ionisation efficiency curves for the production of both singly and doubly charged ions of CF3, CF2 and CF and electron attachment curves for the formation of F- and CF3- ions. The data may be compared with those summarised in a recent NIST survey. An important feature of the present data is that the attachment efficiency curves have been measured as a function of the energy of the resulting negative ions. The results may help to explain discrepancies in published electron attachment data.

Invited Paper

15:30

SR2 8 Understanding Plasma-Surface Interactions Through In Situ Surface Diagnostics .

ERAY AYDIL, *Chemical Engineering Department, University of California Santa Barbara*

Multiple total internal reflection Fourier transform infrared (MTIR-FTIR) spectroscopy is a valuable surface-sensitive diagnostic tool that can be used in situ during plasma process development to detect adsorbed species on surfaces and to monitor composition of thin films. This talk will demonstrate how MTIR-FTIR can be utilized in conjunction with other surface and plasma diagnostic techniques such as spectroscopic ellipsometry, and optical emission spectroscopy to address problems in plasma deposition. Specifically, we will discuss experimental results from plasma enhanced chemical vapor deposition of hydrogenated amorphous silicon (a-Si:H), nanocrystalline silicon (nc-Si:H), and silicon nitride. We studied the changes in H bonding on surfaces of a-Si:H and nc-Si:H films during plasma deposition from SiH4/H2/Ar containing discharges. Experimental evidence for reactions that are thought to play key roles in plasma deposition of Si films will be presented. MTIR-FTIR was also used to study H concentration distribution and bonding in bulk a-Si:H films. The H distribution in a-Si:H films is surprisingly complex and far from uniform. The a-Si:H film consists of a very thin H rich layer at the surface that is primarily composed of di- and tri-hydrides. This H-rich surface layer is followed by a subsurface region that is depleted in H. The bulk a-Si:H film grows beneath these two layers, which move up and stay at the surface during deposition.

Author Index

A

Abner, Douglas JTP7 3, **JTP7 4**
Abraham, Ion C. **FT2 6**
Abrams, Cameron F. IT3 2, **IT3 3**
Adamovich, I. V. GT1 3
Adamovich, Igor V. **GT1 4**
Adamovich, I.V. GT1 2
Adams, S.F. **JTP1 3**
Affolter, A. GT2 2
Aikyo, H. JTP1 7
Ajello, J.M. OWP6 2
Ajello, Joseph M. OWP6 10
Akahane, Tadashi EMP4 7, OWP1 2
Akashi, Haruaki **OWP2 7**, OWP2 8
Akitsu, Tetsuya **OWP1 4**
Ali, M.A. OWP6 18
Al-Khateeb, H.M. AM1 3
Allain, Monica M.C. IT3 4
Allan, Graham R. NW3 2
Alman, Darren A. **JTP7 14**
Alvarez, Ignacio JTP7 11
Amemiya, H. JTP6 12
Anderson, Harold **AM3 4**, JTP1 11
Anderson, Heidi M. **IT2 5**, IT2 7
Ando, M DM2 2
Andoh, Yasutaka JTP3 1, JTP3 2
Ang, L.K. KW2 4
Angel, G. JTP6 4
Aono, Masaharu OWP2 3
Arai, Hideyuki **EMP3 2**
Arai, Shigeo JTP1 8
Arai, T. **JTP1 7**
Arikata, I. **EMP2 6**
Arunachalam, V. RR3 3
Asakawa, T. QR2 3
Ash, R.L. OWP4 5
Ashkenazy, Joseph QR1 1
Aydil, Eray S. BM3 1, **SR2 8**

B

Babb, J.F. **EMP7 7**
Badakhshan, Ali EMP4 9
Baker, M.B. KW3 3
Bakker, L. GT1 1
Bakshi , Vivek JTP2 4
Balaceanu, Mihai **EMP4 20**
Baldwin, D.P. KW3 5
Balkey, Matthew EMP8 1, EMP8 2
Balsley, Steven OWP3 2
Barnes, Paul **JTP7 3**, JTP7 4
Bartel, Timothy **FT3 8**, IT3 1
Bartel, T.J. EMP6 1
Barton, A.S. OWP3 1
Bartschat, Klaus **AM1 5**, AM1 6, OWP7 4
Basurto, Eduardo **JTP7 11**
Batelaan, H. **DM3 7**
Bawagan, A.D.O. **JTP6 19**
Bechu, Stéphane QR1 2
Beegle, L.W. **OWP6 2**
Behle, St. DM2 1, JTP6 13
Belevtsev, A.A. **DM3 2**, **RR3 7**
Benck, E.C. **RR2 3**
Bengtson , Roger D. JTP2 4
Benhabib, Djemila JTP6 9
Benjamin, Neil BM3 1
Berezin, A.A. QR2 5
Berguiga, M. QR3 2
Bernardi, D. RR3 8
Berns, Darren RR3 4
Beuthe, T.G. **JTP7 12**
Bhandarkar, U. **GT2 4**, **GT2 5**
Bhattacharjee, S. **JTP6 12**
Biennier, Ludovic RR2 4
Bin Hashim, Abdul Manaf **EMP4 7**
Birdsall, C.K. **OWP5 2**
Birdsall, C.K. OWP5 23
Birdsey, B.G. AM1 3
Bletzinger, Peter **JTP6 2**
Block, Rolf **NW1 2**
Boettcher, Gordon E. RR3 6
Bogaerts, Annemie **AM2 1**
Boivin, Robert EMP8 1, EMP8 2
Bollinger, J.J OWP3 1
Booth, Jean-Paul **RR2 4**
Booth, Paul EMP2 4
Bordage, Marie-Claude **RR1 5**
Borysow, Jacek **JTP1 4**
Bose, Deepak **FT3 2**, FT3 3
Boswell, Rod **DM2 7**
Boswell, R.W. AM2 2, BM2 3, DM3 6, QR3 2, QR3 7, SR2 6
Bouchoule, A. GT1 1
Bouchoule, André **QR1 2**
Boulmer-Leborgne, Chantal JTP1 1
Bowden, M.D. **JTP2 6**, OWP5 8
Bowen, T.C. AM1 3
Bowers, Kevin **OWP5 1**
Bowers, K.J. OWP5 2
Brackbill, Jerry EMP1 1
Braithwaite, Nicholas **BM2 4**
Braithwaite, Nick EMP2 4
Bratescu, Maria Antoaneta **OWP2 9**
Brockhaus, A. **DM2 1**, **JTP6 13**
Brooke, G. **EMP6 8**
Brown, D.J.W. JTP6 4, NW2 2, OWP2 5
Browning, James **OWP3 2**
Brunger, M.J. **KW1 1**
Buckman, S.J. AM1 4, AM1 6
Burrow, P.D. AM1 6
Butler, J.E. QR2 7
Bzenić, S. BM1 4

C

Campbell, R.B. EMP6 1
Cappelli, M.A. EMP2 1, EMP2 10, JTP1 15, **JTP1 16**
Cappelli, Mark **QR1 4**, **RR3 4**
Carman, R.J. **NW2 2**
Carter, Chris **QR3 6**
Caughman, J.B.O. **FT3 5**
Cekic, M. **OWP2 10**
Chabert, P. **DM3 6**
Chaker, Mohamed JTP5 10, JTP6 9, JTP6 10
Champion, Roy EMP7 3
Chandhoke, G. **EMP1 6**
Chang, C.H. **FT3 3**
Chang, Hong-Young **EMP4 1**
Chang, J.S. JTP7 12, QR2 5
Chao, Edward H. **JTP7 2**
Charles, C. **AM2 2**, BM2 3
Chen, Francis F. QR3 3
Chen, T.S. EMP6 12
Cheng, J.H. EMP6 12
Chernukho, Andrey GT1 4
Chiang, Whe-Yi EMP6 7
Chiang, W.Y. EMP6 12
Childs, M.A. **EMP1 7**, EMP1 8
Chinnov, V.F. DM3 2, RR3 7
Cho, Suwon **EMP8 7**
Choi, Chi-Kyu EMP4 1
Choi, S.J. **EMP6 1**, **JTP5 8**
Choi, Y.W. **OWP5 8**
Christenson, Peggy J. DM1 7
Christophorou, Loucas **KW1 3**, RR1 5
Chung, H.-K. EMP7 7
Chung, T.H. JTP4 1, JTP6 18, **OWP5 22**
Chwirot, Stanislaw OWP7 3
Cisneros, Carmen JTP7 11
Cluggish, Brian EMP6 9
Coburn, John W. BM3 5, JTP5 4
Collaboration, Lam Research Corporation BM3 1
Collaboration, University of California Santa Barbara BM3 1
Collins, G.J. EMP6 14, OWP5 5, OWP5 6
Colombo, V. **RR3 8**
Compaan, A.D. DM1 6, OWP2 14
Coppa, G.G.M. RR3 8
Corey, P. JTP6 4
Coronell, D. RR3 3
Cosby, P.C. **JTP7 15**
Costa Bricha, E. EMP5 8
Court, P. QR2 3
Crompton, Robert W. **CM1 1**
Crowley, Brendan OWP5 4
Cunge, Gilles **OWP5 4**
Curry, J.J. **IT2 7**, RR1 3
Czarnetzki, U. **FT2 2**, **OWP5 7**, OWP5 10

D

Dahi, H. IT1 4, NW2 5, OWP7 7
Dalal, Vikram L. EMP4 9
Dalgarno, A. EMP7 7
Daniels, Jarad KW3 8
Dariusz, Korzec QR2 4
Darnon, Franck QR1 2
Date, H. EMP4 6, **FT1 3**, FT1 5
Daube, Th. SR2 5
Davidson, Ronald C. JTP7 2
de Urquijo, Jaime JTP7 11
Dedeke, Martin **OWP2 4**
Deegan, Catherine **OWP5 18**
Deering, Glen JTP1 11
Degeling, A.W. **QR3 7**
DeJoseph, C. RR1 4
DeJoseph Jr., C.A. **JTP6 16**

DeJoseph Jr., Charles A. SR2 3
Delprat, Sébastien **JTP5 10**, JTP6 9
Den, S. EMP8 3
Denning, D. RR3 3
Denpoh, K. **AM2 5**
Derra, Guenther **IT2 2**
Deschenaux, Ch. GT2 2
Dhali, Shirshak EMP3 1
Dinh, T. **OWP4 5**
Djuric, Nada **KW1 2**
Döbele, H.F. EMP5 1, FT2 2, JTP2 2, OWP3 3, OWP4 2, OWP5 7
Dobele, H.F. OWP5 10
Donnelly, Vincent M. **BM3 7**
Driscoll, C.F. JTP7 5
Duan, Zheng RR3 5
Dunn, Gordon H. KW1 2
Duran, Michael S. NW3 2
Durandet, A. **SR2 6**
Dyakov, Ilya EMP7 3
Dyl, Dariusz OWP7 3
Dziczek, D. OWP6 2
Dziczek, Dariusz **OWP7 3**

E

Economou, D.J. **BM2 6**, EMP6 2
Edamitsu, Toshiaki EMP5 9
Eddy, C.R. KW2 8
Edelberg, Erik A. **BM3 1**
Eggs, C. EMP1 6
Ekerdt , John G. JTP2 4
El-Habachi, Ahmed **NW2 6**
Enami, T. OWP2 11
Endo, M. KW2 3
Engemann, J. DM2 1, JTP6 13
Esaki, Hirotoshi JTP3 5
Essenhigh, K. **GT1 2**
Evans, John D. **QR3 3**

F

Falkenstein, Zoran **EMP4 5**
Feagin, Jim **IT1 1**
Fernsler, R.F. QR3 1
Fernsler, Richard **BM2 5**, JTP6 14
Field, D. KW1 5, OWP6 8
Field, T.A. KW1 5, OWP6 8
Filippov, G.A. OWP4 1
Fisch, Nathaniel QR1 1
Fischer, Ernst IT2 2
Flannery, M.R. EMP7 2, EMP7 9, EMP7 10, **LW1 1**
Flesch, Peter **OWP2 1**
Frank, J. OWP2 10
Fruchtman, Amnon QR1 1
Fujii, F. QR2 3
Fujino, S. **OWP6 15**
Fujita, H. EMP1 5, OWP5 19
Fujita, Hiroharu EMP2 5, EMP2 9, EMP6 3, QR3 5
Fujita, Kazushi **KW3 7**
Fujiyama, Hiroshi EMP4 12, EMP4 13, EMP4 14, **GT2 6**, JTP4 3, JTP5 1, OWP3 5
Fukarek, Wolfgang SR2 1
Fukuda, H. JTP5 5
Fukuhara, N. **QR2 5**
Fukumasa, Osamu JTP3 4, **JTP3 5**, **OWP1 5**, **OWP1 7**
Fukute, R. BM3 2
Fukuyama, R. AM3 5
Fukuyama, T. **JTP7 6**
Fukuzawa, T. EMP1 2, EMP1 3, EMP1 4, **EMP1 9**, EMP1 10, EMP4 10, JTP1 6
Fulbright, J.P. DM3 8
Furuhashi, Hideo KW2 6
Furukawa, H. JTP1 12
Futako, W. **QR2 2**

G

Gallagher, Alan EMP1 7, **EMP1 8**
Gallis, Michael FT3 8
Gambús, Gloria EMP5 7
Ganguly, Biswa N. SR2 3
Ganguly, B.N. JTP6 2, **NW1 3**
Garscadden, A. RR1 4
Gavrilov, Nikolai EMP4 5
Gay, T.J. **AM1 3**, DM3 7
Georg, A. DM2 1, JTP6 13
Ghanashev, I. BM3 6, DM2 4, **DM2 5**
Gijbels, Renaat AM2 1
Gilgenbach, R.M. KW2 4
Girshick, S.L. GT2 4
Giuliani, J.L. **EMP4 18**, IT3 5, QR2 7
Glembocki, O.J. **KW2 8**
Goedheer, Wim AM2 1
Goehlich, Andreas **EMP5 1**
Golde, Michael F. OWP6 7, RR1 6
Gomez, S. **EMP5 8**, EMP6 10
Goodyear, Alec **EMP2 4**
Goto, M. JTP1 7
Goto, N **BM2 1**, DM2 2
Goto, T. EMP4 16, QR2 6
Goto, Toshio EMP4 21, EMP7 6, JTP1 8, JTP1 13, JTP5 2, KW3 7, RR2 1
Gottschalk, J.R. **DM1 6**, **OWP2 14**
Govindan, T.R. FT3 2, IT3 7
Gozadinos, George **AM2 8**
Gradziel, Marcin OWP7 3
Graf, M.A. QR1 6
Graham, W.G. EMP2 7, EMP5 8, EMP6 10
Graves, David B. BM3 5, IT3 2, IT3 3, JTP5 4, KW3 8
Green, A.S. DM3 7
Greenwood, C.L. OWP3 4, SR2 7
Greer, Frank **JTP5 4**
Gregori, G. JTP2 5
Grigore, Emil EMP4 20
Gui, H. QR3 4
Gulley, R.J. **KW1 5**, **OWP6 8**
Guo, X. QR3 4
Gupta, G.P. **OWP7 5**

H

Haaland, P.D. RR1 4
Haga, K. **EMP4 8**
Hamada, Akira OWP6 6, OWP6 11, OWP6 13
Hamilton, Thomas W. RR3 6
Han, Seung-Hee EMP5 4
Harada, Kieko JTP5 11
Hargus, William QR1 4
Haruo, Uyama EMP5 10
Hatta, Akimitsu EMP4 19
Hayashi, D. EMP8 3, **OWP3 6**, **OWP3 7**
Hayashi, H. AM3 3, GT3 6, KW2 2, KW2 3
Hayashi, M. **JTP7 7**
Hayashi, N. **EMP1 5**, **OWP5 19**
Hayashi, Toshio **GT3 7**
Hayashi, Yasuaki EMP4 2, **EMP4 22**, NW3 3, **NW3 4**
Hayden, Douglas B. IT3 4
Heberlein, J. JTP2 5
Heberlein, Joachim RR3 5
Hebner, G.A. **DM2 8**, JTP1 17, **OWP5 10**
Hebner, Greg A. FT2 6
Heil, B. GT3 4
Hendry, R.C. EMP4 18, QR2 7
Henins, Ivars GT1 5
Hermann, Jorg JTP1 1
Herrold, Jason T. **EMP4 9**
Hewett, K.B. **EMP7 8**
Hiejima, Shinji OWP3 8
Higashizono, Ryo-ichi OWP2 15
Hikosaka, Y. BM3 2, KW2 2, **KW2 3**
Hioki, K. JTP2 1
Hiramatsu, M. JTP1 10
Hirata, H. **JTP2 1**
Hirose, Satoshi EMP7 6
Hiroshi, Fujiyama EMP5 10
Hitt, B.A. DM3 7
Ho, P. JTP5 8
Ho, Pauline IT3 1
Hodyss, Robert P. JTP7 15
Hollenstein, Ch. **GT2 2**
Holm, R.T. KW2 8
Hong, Mun-Pyo EMP5 4
Hopkins, Michael OWP5 18
Hori, M. EMP4 16, QR2 6
Hori, Masaru EMP4 21, JTP1 8, JTP1 13, JTP5 2, KW3 7, RR2 1
Horie, I. **OWP5 20**, OWP5 21
Horiike, Y **SR1 5**
Horio, N. JTP1 10
Horioka, Tatsuji OWP5 14
Hosoe, Keisuke EMP2 3
Hosokawa, M. BM3 2
Hrycay, M EMP6 15
Hsu, Chung-Jen EMP6 7
Hsu, C.R. EMP6 12
Hu, Yuan EMP6 7
Huang, X.-P. OWP3 1
Hudson, M.L. **IT3 6**
Huebschman, Michael L. **JTP2 4**
Huestis, D.L. **DM3 8**
Huo, Winifred M. OWP6 1, **OWP6 3**
Huo, W.M. OWP6 18
Hwang, Helen **IT3 7**

I
Ido, Shunji **JTP4 5**, **JTP4 6**, QR1 5
Ihara, S. OWP4 7
Ikeda, Akihiro **OWP4 4**
Ikegawa, M. **AM3 5**
Ikuta, N. **EMP7 4**, EMP7 5, JTP7 10
Ikuta, Nobuaki **JTP7 16**
Imamura, Nariaki OWP2 15
Inagaki, K. JTP6 5
Ingold, John H. **JTP6 6**
Inoue, Go KW3 4
Inoue, Jun **OWP5 12**
Inoue, M. AM3 3, BM3 3, BM3 4, GT3 6, KW2 2
Isaacs, W.A. KW1 4
Isakaev, E.Kh. DM3 2, **OWP4 1**, RR3 7
Iserov, A.D. DM3 2
Ishigami, T. **IT2 3**
Ishii, Nobuo DM2 2, JTP5 2, OWP3 8, RR2 1
Ishikawa, Masayuki JTP1 13
Ishikawa, T OWP6 12
Itano, W.M. OWP3 1
Itikawa, Yukikazu OWP6 9, OWP6 12
Ito, A. DM2 4
Ito, Haruhiko **JTP1 13**
Ito, K. GT3 6
Ito, M. EMP4 16, QR2 6
Ito, Masafumi EMP4 21, JTP1 8, JTP1 13, JTP5 2, KW3 7, RR2 1
Ito, Toshimichi EMP4 19
Itoh, H. EMP7 5, JTP7 6
Itoh, Hidenori **JTP1 2**, OWP5 17
Itoh, Tohru RR3 1
Itoyama, Kagehiro **OWP4 3**
Ivanov, P.P. OWP4 1
Izawa, Tetsuo EMP4 21
Izumi, Yori **DM3 3**

J
Jacob, Mammen NW3 1
James, Geoffrey K. **OWP6 10**
James, G.K. OWP6 2, OWP7 2
Janssen, G. M. GT1 7
Jelenković, B.M. **EMP5 6**
Jelenković, B.M. JTP7 1
Jelenkovic, B.M. **OWP3 1**
Jeon, B-H. OWP6 16
Jeon, Hyeongmin **EMP4 19**
Jeong, J.Y. GT1 5
Ji, J.S. **EMP2 1**
Jiang, Weihua KW2 5
Jiao, C.Q. **RR1 4**
Jin, H. **EMP4 10**
Jinno, Masafumi **OWP2 3**
Johannes, Justine FT3 8, **IT3 1**
Johnsen, Rainer OWP6 7, RR1 6
Johnston, M.L. AM1 3
Jonhston, Tudor W. JTP6 10
Joyce, G. QR3 1
Juliano, Daniel R. **EMP4 4**, IT3 4
Jung, Won-Ho EMP2 2
Junichi, Yanagi EMP5 10

K
Kachanov, Alexander RR2 4
Kadlec-Philippe, C. GT1 1
Kadota, K. AM3 2, EMP8 3, JTP1 12, JTP7 13, OWP3 6, OWP3 7
Kagaya, Yoichi EMP4 15
Kalinin, V.I. DM3 2
Kamidaira, M. EMP4 8
Kamiya, K. EMP4 16
Kanai, K. EMP5 2
Kando, Masashi DM2 3, DM3 5, JTP6 11
Kaneko, O. OWP3 6, OWP3 7
Kanik, I. OWP7 2
Karasik, Max **JTP3 3**
Kashiwagi, Mieko JTP4 5, JTP4 6, **QR1 5**
Kataoka, N. **OWP2 11**
Kato, Isamu **EMP4 17**
Kato, Terumasa JTP1 13
Katoh, Masaaki **JTP5 6**
Katsch, H.-M. **OWP3 3**
Katzer, D.S. KW2 8
Kawaguchi, Motoichi OWP5 12, OWP5 13
Kawahara, Yoshio EMP4 17
Kawai, Y. BM2 2, OWP1 3
Kawai, Yoshinobu OWP1 6, OWP3 8, OWP5 14
Kawakami, Satoshi OWP3 8
Kawamura, E. **OWP5 23**
Kawamura, K. OWP5 8
Kawamura, Kazutaka EMP5 11, OWP3 10
Kawasaki, H. **EMP1 2**
Kawashima, Masanori JTP4 5
Kawata, H. **JTP5 5**
Keiter, Eric R. **EMP8 8**, GT3 1
Keiter, Paul EMP8 1, EMP8 2
Keller, John H **FT3 6**
Khabibrakhmanov, I EMP6 15
Khachan, Joe QR3 6
Khakoo, M.A. OWP7 2
Kharchenko, V. EMP7 7
Kikuchi, Masaaki OWP1 2
Kikuchi, Tetsuo RR3 1
Kilgore, Michael EMP6 11
Kim, Dai-Gyoung EMP2 2
Kim, Gon-Ho **EMP2 2**, **EMP5 4**
Kim, Gun-Woo EMP5 4
Kim, J.B. OWP5 8
Kim, J.S. EMP2 1, **EMP2 10**, **JTP1 15**, JTP1 16
Kim, K EMP1 3
Kim, W. OWP2 12
Kim, Y.-K. **OWP6 18**
Kim, Yong-Ki OWP6 3
Kimura, Masahide EMP4 7
Kimura, Mineo EMP7 1, OWP6 5, OWP6 6, OWP6 9, OWP6 11, OWP6 12, OWP6 13, RR1 1
Kimura, T. EMP1 5, **JTP6 5**
Kinder, Ron L. **NW1 7**
Kinoshita, K. BM3 2, **BM3 3**, BM3 4
Kinoshita, Takashi **IT3 9**
Kirby, K. EMP7 7
Kitajima, Masashi OWP6 5, OWP6 6, OWP6 11, OWP6 12, OWP6 13, RR1 1
Kitajima, T. OWP5 15, **RR2 8**
Kitamori, K. AM2 3, OWP5 20, OWP5 21
Kline, John EMP8 1, **EMP8 2**
Knijnik, A. OWP4 6
Kobayashi, H. **EMP6 6**
Kobayashi, J. AM3 5
Kobayashi, Shigeto KW3 7
Kobayashi, Shinji **DM1 2**
Kodera, Hidekazu JTP1 14
Koga, K DM2 2
Kojima, Akira DM3 3, JTP5 6
Kokura, H. BM3 6
Kolobov, V.I. **FT3 4**
Koltunski, Laure JTP1 11
Kondo, K. **FT1 5**
Kondo, M. QR2 2
Kondo, Yoshitaka **OWP6 14**
Konishi, E. **EMP6 4**
Konishi, K. EMP2 6
Kono, Akihiro **EMP7 6**, **FT2 5**, JTP1 8, RR2 1
Korobtsev, S. OWP4 6
Korolev, V.K. DM3 2
Kortshagen, U. EMP1 6, GT2 4, GT2 5
Kortshagen, U. **GT3 4**
Kortshagen, U. JTP2 5, NW1 4, **NW1 5**
Koss, Robert OWP3 2
Kota, Gowri JTP5 4
Kouno, Takayuki JTP5 6
Kouznetsov, I.G. JTP6 18
Kovaleski, S.D. **KW2 4**
Kowari, Ken-ichi FT1 6
Krier, Herman **QR1 3**
Kriesel, J.M. **JTP7 5**
Krishnan, A. FT3 4
Kroesen, Garrit **DM1 1**
Kubo, M. QR2 3
Kubota, T. EMP2 6, SR2 4
Kudela, Jozef **DM2 3**, **JTP6 11**
Kudo, H. JTP2 6
Kudryavtsev, A.A. **JTP5 9**
Kumagai, M. EMP4 3, GT3 2
Kurihara, M. AM2 7, **DM1 4**
Kurokawa, Hisayoshi OWP2 3
Kuroki, Yukinori OWP4 4
Kushida, Masahito **JTP5 11**
Kushima, S EMP1 9
Kushner, Mark J. AM2 4, DM1 5, EMP8 8, GT3 1, NW1 7, OWP2 6
Kuwahara, Hajime EMP4 14
Kuwahara, Kiyoshi EMP4 12, EMP4 14, **JTP4 3**, JTP5 1
Kuzumoto, Masaki **DM3 1**

Kyoichi, Yamamoto EMP5 10

L
Lagorceix, Pascal QR1 2
Lampe, M. **QR3 1**
Lampe, Martin BM2 5, JTP6 14
Lapenta, Giovanni **EMP1 1**
Latham, John KW3 3
Lau, Y.Y. KW2 4
Laure, Claude QR1 2
Lawler, J.E. IT2 5, IT2 7, **NW1 4**, NW1 5, **RR1 3**
Lee, H.S. OWP2 12
Lee, J.K. JTP4 1, OWP2 12, OWP5 22
Leonhardt, D. KW2 8
Leonhardt, Darrin JTP6 14
Leou, K.-C. EMP6 7
Leou, K.C. **EMP6 12**
Li, Yan-Ming **OWP2 2**
Lichtenberg, A.J. **JTP6 18**
Lieberman, M.A. GT3 5, JTP6 18, QR1 6
Lin, T.L. EMP6 12
Lin, Tsang-Lang **EMP6 7**
Lloyd, S. **EMP6 14**
Loewenhardt, Peter **RR2 5**
Lombardini, M. RR3 8
Louis, L. QR3 4
Lu, Junqing **GT3 1**
Luches, Armando JTP1 1
Luggenhölscher, D. FT2 2, OWP5 7
Luggenholscher, D. OWP5 10
Lukas, Christoph JTP2 2
Lungu, Ana Mihaela KW3 4
Lungu, Cristian Petrica **KW3 4**
Lungu, Petrica Cristian EMP4 20
Lunt, S.L. KW1 5, OWP6 8
Lyszyk, Michel QR1 2

M
Maeda, M. OWP2 11
Maeda, S. EMP1 2, **EMP1 10**
Magni, D. GT2 2
Mahony, C.M.O. EMP2 7, EMP6 10
Makabe, T. AM2 7, DM1 4, EMP6 6, GT3 3, IT3 8, JTP2 1, JTP4 2, OWP5 15, RR2 8
Mangina, Rao EMP7 3
Manheimer, Wallace BM2 5, JTP6 14
Manheimer, W.M. QR3 1
Manke II, G.C. EMP7 8
Margot, Joëlle **JTP6 9**, JTP6 10
Margot, Jolle JTP5 10
Marinescu, M. EMP7 9
Markin, A.V. DM3 2, RR3 7
Mashima, Hiroshi OWP5 14
Mashino, S. JTP1 7
Mason, N.J. KW1 5, OWP6 8
Matsuda, A. QR2 2
Matsuda, Yoshinobu **OWP3 5**
Matsui, J. **IT3 8**
Matsumori, Masanori OWP1 5, OWP1 7
Matsumoto, Kazunori **JTP4 7**
Matsumoto, Naoki **DM2 6**
Matsumura, S. JTP2 1
Matsumura, Shosaku **EMP2 3**
Matsunaga, T. JTP5 5
Matsuoka, Mamoru OWP5 12, OWP5 13
Matsuoka, Norikazu EMP8 4
Matsuoka, Y **EMP1 3**, EMP1 9
Matsuzaki, H. JTP7 6
McCurdy, C.W. KW1 4
McEachran, R.P. AM1 6
McFarland, J. **EMP2 7**
McGrath, R.T. JTP1 17
McInerney, E. Jack EMP6 11
McKoy, Vincent **KW1 6**, OWP6 4
Mebarki, B. **QR2 6**
Medvedev, D. OWP4 6
Meeks, E. JTP5 8
Meezan, Nathan QR1 4
Meger, Robert BM2 5, **JTP6 14**
Méndez, Bernardo EMP5 7
Meyyappan, M. FT3 2, IT3 7
Michejda, J.A. AM1 6
Midha, V. EMP6 2
Miichi, T. OWP4 7
Mikio, M. **EMP4 11**
Mildren, R.P. **OWP2 5**
Millard, Michael W. **SR2 3**
Miller, G.P. **FT2 3**, **KW3 5**
Miller, T.A. JTP1 3
Minemoto, A. JTP1 6
Mitchell, T.B. OWP3 1
Mitsuyuki, Ohkubo OWP2 9
Miyake, S. **EMP4 3**, EMP6 5, GT3 2
Miyamoto, Masahiro JTP4 7
Miyazaki, Yasuo EMP4 2
Mizoguchi, H. OWP2 11
Mizuki, Norihisa OWP1 7
Mizutani, N. KW2 3
Moench, Holger IT2 2
Momose, Shun **JTP1 5**
Monsma, B. SR2 6
Moon, Y.S. JTP4 1
Morgan, W.L. **RR1 2**
Mori, Keiichi EMP2 9
Morimoto, T. DM2 2, FT3 1, JTP5 7
Morishita, S. AM3 3, GT3 6, **KW2 2**, KW2 3
Morita, S. BM2 2, DM2 4, DM2 5
Morris, Robert A. **BM1 3**
Morrow, R. **KW3 2**
Moss, William C. **QR1 7**
Motoki, Kentaro JTP4 7
Motomura, Hideki **JTP5 3**
Mouzouris, Y. QR3 4
Murakami, Y. JTP7 6
Muraoka, K. EMP6 13, JTP2 6, OWP2 11, OWP5 8
Murata , K. **EMP4 16**
Murata, K. JTP5 5
Murata, M. BM2 2
Murata, Masayoshi **OWP5 14**
Murata, Takaaki DM1 2
Murillo, M.S. NW3 5
Murnick, D.E. IT1 4, NW2 5, OWP7 7
Muroya, Kazuhito SR2 1
Murphy, Donald BM2 5, JTP6 14
Musil, J. GT3 2
Muta, H. OWP1 3
Muta, Hiroshi **OWP1 1**

N
Nagahiro, Masaaki EMP4 22
Nagai, H. **JTP1 10**
Nagamatsu, Hitomi OWP3 5
Nagano, Osamu SR2 1
Nagano, Teppei **EMP4 13**
Nagashima, Atushi EMP4 21
Nagatsu, M. **DM2 4**, DM2 5
Nakagami, Yuko EMP4 2
Nakagawa, H. BM3 4, **GT3 6**, KW2 3
Nakagawa, Yukito **AM3 6**
Nakamoto, M. OWP3 6, OWP3 7
Nakamura, K. **BM3 6**, EMP6 4
Nakamura, Masayuki **RR2 1**
Nakamura, S. OWP5 21
Nakamura, Toshihiro JTP1 5
Nakamura, Y. **BM1 2**, JTP7 7, OWP6 15, OWP6 16
Nakano, N. AM2 7, DM1 4, EMP6 6, IT3 8, JTP2 1, JTP4 2, OWP5 15, RR2 8
Nakano, Nobuhiko **AM2 6**
Nakano, T. JTP6 15, **RR2 6**
Nakao, Yoshitaka JTP1 2
Nakayama, Hirotaka RR2 1
Nanbu, K. AM2 5, FT3 1, **JTP5 7**, **NW2 4**, OWP5 11
Nasser, Mahmood **EMP6 3**, **QR3 5**
Nawata, M. JTP1 10
Neiger, Manfred KW3 6, OWP2 1
Newman, D.S. AM1 6
Niemöller, Norbert EMP5 1
Niessl, Claudia OWP7 7
Nishikawa, M. EMP5 2
Nishimoto, T. QR2 2
Nishimura, Naoki JTP4 4
Nishino, Shigehiro EMP4 2, EMP4 22
Noda, M. GT2 3
Noda, S. BM3 2, BM3 3, **BM3 4**, GT3 6, KW2 2, KW2 3
Noren, C. **OWP7 2**
Nozaki, T DM2 2
Nozawa, R. EMP4 16

O
Obara, Kozo **OWP2 15**, **SR2 1**

Oda, Akinori OWP2 7, **OWP2 8**
Oda, T. JTP1 9
Odrobina, Igor DM2 3, JTP6 11
Ogata, K. EMP4 3
Ogino, Akihisa DM3 5
Oh, Jin-Sung **GT3 3**
Ohe, K. JTP6 5
Ohiwa, T. **KW2 1**
Ohmori, Y. AM2 3
Ohnishi, Keitaro RR3 1
Ohno, Kazuki **OWP5 13**
Ohta, Hiroyuki **EMP4 21**
Ohtake, Hiroto SR1 3
Ohtani, Sugio JTP5 6
Ohte, Takeo DM3 3, JTP5 6
Ohtsu, Yasunori **EMP2 5**, **EMP2 9**
Ohyabu, Nobuyoshi EMP5 11, OWP3 10
Oka, Y. OWP3 6, OWP3 7
Okada, T. OWP2 11
Okamoto, Yukio **JTP6 17**
Okazawa, K. **JTP4 2**
O'Keefe, Anthony **FT2 4**
Okigawa, M. **AM3 3**, BM3 3, BM3 4, GT3 6, KW2 2
Oks, Eugene **JTP2 3**
Okumo, H. OWP6 15
Olthoff, James **BM1 1**, EMP2 11, EMP7 3, KW1 3, RR1 5
Ono, Masataka EMP5 11
Onoe, Ken-ichi JTP3 1, JTP3 2
Osterbrock, D.E. DM3 8

P

Pakhomov, Andrew V. NW3 2
Palm, P. GT1 2, GT1 3
Palm, Peter GT1 4
Panagopoulos, T.L. **EMP6 2**
Pantelica, Dumitru EMP4 20
Paristyi, I.L. OWP4 1
Park, Jaeyoung **GT1 5**
Park, J.S. JTP4 1
Parker, G.J. **DM1 8**, **NW1 6**, **OWP2 13**
Parker, Greg.J. DM1 7
Parkinson, W.H. EMP7 7
Pashaie, Bijan EMP3 1
Patel, Kedar K. **QR1 6**
Patiño, Pedro **EMP5 7**
Paul, Stephen F. JTP7 2
Pauna, Olivier JTP6 9, JTP6 10
Pavelescu, Gabriela EMP4 20
Pechacek, Robert BM2 5, JTP6 14
Pedder, Randall EMP2 8
Peko, Brian **EMP7 3**
Pepin, Henri JTP5 10
Perrin, J. DM3 6
Perrone, Alessio **JTP1 1**
Perry, Andrew BM3 1
Perry, Lee AM3 4, **JTP1 11**
Peterkin Jr., Robert E. **EMP5 3**
Petrović, Z. JTP2 1
Petrović, Z.Lj. BM1 4, JTP6 3, JTP7 1
Pfender, E. JTP2 5
Phelps, A.V. EMP5 6, **EMP7 11**
Philippe, Christelle QR1 2
Piejak, R.B. **IT2 1**
Piper, J.A. NW2 2, OWP2 5
Piper, James **NW2 1**
Piwinski, Mariusz OWP7 3
Ploenjes, Elke GT1 4
Plönjes, E. GT1 2, **GT1 3**
Pogrebnjak, Alexander KW2 5
Popescu, Aurel EMP4 20
Popovic, S. EMP6 8, **JTP6 7**, OWP2 10, OWP4 5
Potapkin, B. **OWP4 6**
Pryor, Wayne R. OWP6 10

Q

Quandt, E. OWP3 3

R

Racolta, Petre Marin EMP4 20
Radovanov, S.B. JTP6 3, **JTP6 4**
Raitses, Yevgeny **QR1 1**
Raju, Govinda **EMP3 3**
Rao, M.V.V.S. EMP2 10, OWP6 17
Raspopović, Z.M. **BM1 4**
Rauf, Shahid **DM1 5**
RaviPrakash, J. **JTP1 17**
Rees, J.A. **OWP3 4**, **SR2 7**
Rej, Donald EMP4 5
Remscheid, A. **QR2 3**
Rescigno, T.N. **KW1 4**
Rich, J. William GT1 4
Rich, J.W. GT1 2, GT1 3
Richardson, L.M. OWP7 6
Richley, Edward A. **GT1 6**, **JTP7 8**
Riemann, K.-U. **SR2 2**, **SR2 5**
Riley, M.E. **IT1 5**, IT3 6, OWP5 10
Ritchie, A.B. IT1 5
Roberts, J.R. RR2 3
Robson, A.E. EMP4 18, QR2 7
Romanini, Daniele RR2 4
Roybal, Amanda J. **NW3 2**
Rudder, R.A. EMP4 18, QR2 7
Russ, Holger **KW3 6**
Ruzic, David N. EMP4 4, **IT3 4**, JTP7 14
Ryazhsky, D.I. DM3 2
Ryoichi, Kawai OWP3 9

S

Sadeghi, N. **GT1 1**
Sadeghi, Nader QR1 2
Saito, Kyoichi JTP5 11
Sakadžić, S. BM1 4
Sakai, K. FT3 1
Sakai, Yosuke BM1 5, FT1 2, KW3 4, **NW2 3**, OWP2 7, OWP2 8, OWP2 9, OWP5 16
Sakamoto, K. EMP1 2, EMP1 10
Sakamoto, Y EMP8 3, OWP6 11, OWP6 13
Sakawa, Y. EMP4 3, EMP6 5
Sakiyama, Satoshi **JTP3 4**, JTP3 5
Sakoda, T. EMP6 13
Sakurai, T. **SR2 4**
Salvermoser, M. IT1 4, NW2 5, OWP7 7
Samukawa, S. JTP6 15, OWP6 11, QR2 6, RR2 6
Samukawa, Seiji AM3 6, **AM3 7**, SR1 3, **SR1 4**
Sankaranarayanan, Ravisankar **EMP3 1**
Sasaki, A. NW2 4
Sasaki, H. **OWP5 11**
Sasaki, K. **AM3 2**, **EMP8 3**, JTP1 12, **JTP7 13**, OWP3 6, OWP3 7
Sasaki, N. **EMP3 5**
Satake, D. OWP5 19
Satake, K. **GT2 3**
Sato, Hiroshi EMP7 1
Sato, M. EMP3 4, EMP3 5
Sato, Masahiro OWP3 10
Sato, N. **OWP5 9**
Satoh, Kohki JTP1 2, **OWP5 17**
Satoh, S. OWP4 7
Sawai, Akito NW3 4
Sawin, Herbert H. **KW3 1**
Scharer, J. **QR3 4**
Schein, J. **JTP2 5**
Schein, Jochen **RR3 5**
Scherer, James **FT2 7**
Schmitt, Randal L. RR3 6
Schoenbach, Karl H. JTP6 8, NW1 1, NW1 2, NW2 6
Schroeder, Vicki **KW3 3**
Schultz, David R. **IT1 3**
Schulz-von der Gathen, Volker **JTP2 2**
Schwendinger, P. JTP2 5
Scime, Earl **EMP8 1**, EMP8 2
Segawa, S. **AM2 7**
Segur, Pierre RR1 5
Seiji, Samukawa SR1 2
Sekine, M. AM3 3, BM3 2, BM3 3, BM3 4, GT3 6, KW2 2, KW2 3
Selwyn, G.S. GT1 5, NW3 5
Serikov, Vladimir **RR3 2**
Setser, D.W. EMP7 8, **FT1 1**
Setsuhara, Y. EMP4 3, **EMP6 5**, **GT3 2**
Seymour, D. OWP3 4
Shamamian, V.A. EMP4 18, **QR2 7**
Sharma, S.P. EMP2 1, EMP2 10, JTP1 15, JTP1 16, **OWP6 17**
Shaw, D.M. EMP6 14, **OWP5 5**, OWP5 6
Shaw, L.H. IT1 4
Sheridan, T.E. **DM3 4**, **QR3 2**, QR3 7
Sherwin, J.A. JTP1 17
Shi, Wenhui JTP6 8
Shibata, K. EMP4 3
Shibata, T. **OWP6 16**

Shibata, Tetsuji **EMP4 15**, EMP5 9, JTP3 1, JTP3 2
Shida, Y. OWP5 9
Shidoji, E. JTP4 2
Shimizu, Koji EMP2 5
Shimogaki, Yukihiro **QR2 8**
Shimozuma, M. **EMP4 6**, FT1 3
Shin, Y.K. JTP4 1, **OWP2 12**
Shindo, Masako **OWP3 8**
Shindow, Haruo OWP3 10
Shinoda, Tsutae **DM1 3**
Shinohara, Shunjiro **EMP8 4**, **EMP8 5**, EMP8 6, OWP1 6
Shirafuji, Tatsuru **EMP4 2**
Shiratani, M. EMP1 2, EMP1 3, EMP1 4, EMP1 9, EMP1 10, EMP4 10, **GT2 1**, **JTP1 6**
Shiryaevsky, V. OWP4 6
Shizgal, Bernie D. **FT1 6**
Shoji, M. **EMP3 4**
Shoji, T. EMP4 3, EMP6 5, EMP8 3
Shon, C.H. **JTP4 1**, OWP2 12
Shon, J.W. DM1 8, OWP2 13
Short, Robert OWP3 2
Shurgalin, M. EMP7 7
Shvydky, O. DM1 6, OWP2 14
Singh, Harmeet **BM3 5**
Singh, Vikram EMP6 11
Sinkevich, O.A. DM3 2
Skizawa, H. EMP7 5
Skrzypkowski, Miroslaw P. **OWP6 7**, **RR1 6**
Slanger, T.G. DM3 8
Slinker, S.P. QR3 1
Smith, H.B. **BM2 3**
Smolyakov, Andrei **EMP6 15**
Smy, Tom JTP5 10
Snyder, H. R. **NW3 5**
Sobolewski, Mark A. **RR2 2**, RR2 7
Soejima, Tsutomu EMP8 5
Soll, Ch. DM2 1, JTP6 13
Sommerer, Timothy J. **IT2 4**
Soteros, C EMP6 15
Spaan, Michael JTP2 2, **OWP4 2**
Stark, Robert H. **JTP6 8**, **NW1 1**
Steen, P.G. EMP2 7, EMP5 8, **EMP6 10**
Steer, W.A. KW1 5, OWP6 8
Stefanović, I. JTP6 3
Steffens, Kristen L. **RR2 7**
Stibbe, Darian **OWP6 1**
Stojanović, V.D. JTP7 1
Sturm, T. OWP3 3
Stutzman, Brooke S. **KW2 7**
Subramaniam, V. GT1 2
Sueoka, Osamu OWP6 6, OWP6 9, OWP6 11, **OWP6 11**, OWP6 13
Suetani, M. JTP5 7
Sugai, H. BM3 2, BM3 6, DM2 4, DM2 5, EMP6 4, OWP5 6
Sugai, Hideo **HT1 1**
Sugawara, Hirotake **BM1 5**, KW3 4, OWP2 8, OWP5 16
Sugimoto, Seiki **EMP4 14**
Sugita, Kazuyuki JTP5 11
Suh, S.-M. GT2 4
Sullivan, J.P. **AM1 6**
Sumiya, S. QR2 6
Sunaka, E. OWP2 11
Sung, Y.M. **EMP6 13**
Sung-Chae, Yang **EMP5 10**
Suzuki, C. AM3 2, **JTP1 12**
Suzuki, Hajime EMP5 11, OWP3 10
Suzuki, K. EMP6 4
Suzuki, Reiko EMP7 1, **EMP7 1**
Suzuki, S. **EMP7 5**
Suzuki, T **OWP5 21**, OWP6 11
Swihart, M.T. GT2 4

T

Tachibana, K. QR2 3
Tachibana, Kunihide **AM3 1**, JTP1 5, JTP5 3, NW3 3, RR3 1
Taddei, F. RR3 8
Tagashira, H. EMP4 6, FT1 3, FT1 5
Tagashira, Hiroaki JTP1 2, OWP5 16, OWP5 17
Tahara, Hirokazu EMP4 15, **EMP5 9**, JTP1 14, **JTP3 1**, **JTP3 2**, OWP1 8
Takaba, Y. EMP5 2
Takagi, T. QR2 2
Takahara, y. SR2 4
Takahashi, Kazuo **NW3 3**
Takahashi, M. OWP5 11
Takahashi, Mikihiko JTP4 6
Takai, Osamu **QR2 1**
Takaira, S. **JTP6 15**
Takaki, Hideki OWP6 9
Takashima, Seigou **JTP1 8**
Takayama, Kazuo EMP5 11, OWP3 10
Takechi, Seiji **EMP8 6**
Takeda, A. EMP7 4, **JTP7 10**
Takekawa, Michiya **OWP6 9**, **OWP6 12**
Takemoto, Hiroki JTP4 4
Takeo, Takashi JTP1 13
Takeo, Y. **OWP5 15**, RR2 8
Takeuchi, S. QR2 5
Takeuchi, Y. GT2 3
Takiyama, K. JTP1 9
Takuya, Ogishima QR2 4
Tan, Liang JTP5 10
Tanaka, Hiroshi **OWP6 5**, **OWP6 6**, **OWP6 13**, **RR1 1**
Tatsumi, T. KW2 2, KW2 3
Tauchi, Yasushi OWP1 7
Tayal, S.S. OWP7 5, **OWP7 6**
Tazikova, T.F. RR3 7
Teich, Timm H. EMP3 2, NW3 1
Teii, Kungen **JTP5 2**
Terai, Kiyohisa DM1 2
Teraoka, Hirohito DM3 3
Tereshkin, S.A. DM3 2, RR3 7
Terry Jr., Fred L. KW2 7
Terry, R.E. **IT3 5**
Tetsu, Mieno **JTP3 6**, **OWP3 9**, **SR1 2**
Teubner, P.J.O. **AM1 1**
Theirich, D. JTP6 13
Theodosiou, C.E. DM1 6, OWP2 14
Thomas, R.E. EMP4 18, QR2 7
Ting, A. JTP5 8
Tochikubo, Fumiyoshi EMP3 2, **NW3 1**
Toedter, Olaf NW1 2
Tomizawa, Hiromitsu OWP7 7
Tonegawa, Akira **EMP5 11**, **OWP3 10**
Tonnis, Eric J. **KW3 8**
Toyoda, H. **BM3 2**
Toyoda, N. DM2 4, DM2 5
Toyota, H. **JTP1 9**
Trantham, K.W. **AM1 4**
Troitsky, A.A. OWP4 1
Truxon, J.M. OWP2 14
Tsai, C.-H. EMP6 7
Tsai, C.H. EMP6 12
Tsuboi, T. KW2 3
Tsuda, Ken-ichiro AM3 7, **SR1 3**
Tsukada, T. QR2 6
Tsukada, Tsutomu AM3 6
Tsukiashi, Masahiko DM3 3
Tsumori, K. OWP3 6, OWP3 7
Turner, Miles AM2 8, OWP5 4
Turner, M.M. **EMP6 16**
Tuszewski, Michel **EMP6 9**
Tynan, George R. **QR3 8**
Tyuftyaev, A.S. DM3 2, OWP4 1

U

Uchida, Satoshi **FT1 2**
Uchida, Y. EMP3 5
Uchida, Yoshihisa **KW2 6**
Uchida, Yoshiyuki KW2 6
Uchino, K. EMP6 13, JTP2 6, OWP2 11
Uchino, Kiichiro **FT2 1**
Ueda, Kengo **EMP4 12**
Ueda, Y. EMP5 2, **OWP1 3**
Ueda, Yoko OWP1 6, OWP3 8
Uetani, Yasuhiro JTP4 7
Ueyama, K. QR2 5
Uhrlandt, D. NW1 6
Ukai, O. GT2 3
Ukegawa, Shin **IT2 6**
Ulrich, A. IT1 4, **NW2 5**, OWP7 7
Usui, K. AM3 2
Uwabachi, Atushi **OWP1 2**

V

Vahedi, V. OWP5 23
Vaidya, N. FT3 4
Van Der Mullen, J. A. M. GT1 7
Van Dijk, J. **GT1 7**

Veerasingam, Ramana **EMP5 5**
Vender, David AM2 8, OWP5 4, OWP5 18
Ventzek, Peter L.G. OWP5 16
Ventzek, P.L.G. AM2 3, FT1 3, OWP5 20, OWP5 21, **RR3 3**
Verboncoeur, John P. **DM1 7**
Verdeyen, J.T JTP6 2
Vidal, Franois **JTP6 10**
Vitello, P.A. DM1 8, JTP2 4, OWP2 13
Vitello, Peter **FT3 7**
Vivien, Celine JTP1 1
Vrhovac, S. **JTP7 1**
Vrinceanu, D. **EMP7 2**, **EMP7 9**, **EMP7 10**
Vuskovic , L. OWP4 5
Vuskovic, L. EMP6 8, JTP6 7
Vuskovic, Leposava **AM1 2**
Vyvoda, Michael A. **IT3 2**
Živanov, S. JTP6 3
Živković, J. **JTP6 3**

W

Wakatsuchi, M. **EMP5 2**
Walther, S. JTP6 4
Wang, Yicheng **EMP2 11**
Watanabae, Tuguhiro OWP3 10
Watanabe, H. EMP4 8
Watanabe, Hisatsune **SR1 1**
Watanabe, M. EMP6 14, OWP5 5, **OWP5 6**
Watanabe, S OWP6 5, OWP6 12
Watanabe, Tsuneo EMP3 2, FT1 2
Watanabe, Tuguhiro EMP5 11
Watanabe, Y. EMP1 2, EMP1 3, **EMP1 4**, EMP1 9, EMP1 10, EMP4 10, JTP1 6
Wei, Jian **EMP2 8**
Wharmby, David O. IT2 4
Whitmore, T.D. SR2 7
Wiese, L.M. **IT1 2**
Wieser, J. **IT1 4**, NW2 5, **OWP7 7**
Wiley , James C. JTP2 4
Williamson Jr., W. DM1 6, OWP2 14
Wineland, D.J. OWP3 1
Winske, D. NW3 5
Winstead, Carl **OWP6 4**
Winstead, C.B. FT2 3
Withford, M.J. NW2 2
Woods, R. Claude FT2 6
Woodworth, Joseph R. **RR3 6**
Wu, Han-Ming **EMP6 11**
Wu, W.C. EMP6 12
Wu, Yaoxi **GT3 5**

X

Xu, Xudong ''Peter'' **OWP2 6**
Xu, Zu-Shun OWP2 15

Y

Yablonsky, A.E. OWP4 1
Yamabe, C. **OWP4 7**
Yamada, Hiroshi **JTP5 1**
Yamada, Jun KW2 6
Yamada, Tadahiko OWP6 14
Yamaguchi, K. BM2 2
Yamaguchi, T. **AM2 3**
Yamakoshi, H. **BM2 2**
Yamamoto, K. EMP7 4
Yamamoto, Kohji JTP7 16
Yamamoto, T DM2 2
Yamane, Tsukasa OWP5 14
Yamashiro, Yasumasa JTP4 4
Yamashita, M. GT3 2
Yaney, Perry P. SR2 3
Yang, Jing **OWP5 16**
Yasaka, Yasuyoshi **DM2 2**, **RR3 1**
Yasuda, M. JTP5 5
Yasui, Kanji EMP4 7, OWP1 2
Yasui, Toshiaki EMP4 15, EMP5 9, **JTP1 14**, JTP3 1, JTP3 2, **OWP1 8**
Yatsenko, Nikolai **OWP5 3**
Yatsui, Kiyoshi **KW2 5**
Ying-Yu, Xu **QR2 4**
Yoichiro, Nakanishi QR2 4
Yoneda, Katsumi JTP1 8
Yonemura, S. **FT3 1**, NW2 4
Yonesu, Akira **JTP4 4**, **OWP1 6**
Yoon, H.J. OWP5 22
Yoshida, R. QR2 6
Yoshikawa, Takao EMP4 15, EMP5 9, JTP1 14, JTP3 1, JTP3 2, OWP1 8
Yoshinaga, Kunihiro EMP2 9
Yoshinaka, Toshiro EMP8 4
Yoshino, K. EMP7 7
Yoshino, M. EMP4 6
Yoshinori, Hatanaka QR2 4
Yoshioka, M. BM2 2

Z

Zeman, Vlado **OWP7 4**
Zhang, Da **AM2 4**
Zheng, Wei **DM3 5**
Zhu, Z. KW3 5
Ziesel, J.P. KW1 5, OWP6 8
Zweben, S.J. JTP3 3

Maui

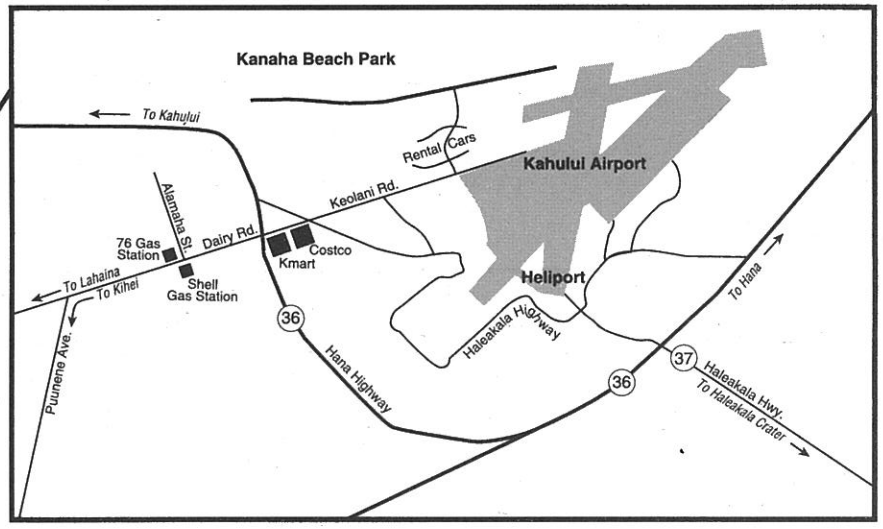

Kahului Airport

KAPALUA
Kahakuloa
Waihee
Waiehu
KAANAPALI
LAHAINA
Front Street
340
Hookipa Beach Park
Paia
Haiku
WAILUKU
32
Dairy Road
Iao Needle
Maui Tropical Plantation
KAHULUI
36
Spreckelsville
Hana Hwy.
Keanae
Kaumahina State Park
Haleakala
37
Hwy.
Halimaile
Makawao
30
Waikapu Golf Course
380
Kuihelani Hwy.
Puunene
Olowalu
Honoapiilani Hwy.
Pukalani
Wailua
Pua'a Ka'a State Park
Makawao Hwy.
350
377
Hana Airport
MAALAEA
S. Kihei Rd.
Piilani Hwy.
37
Kula
378
Crater Road
36
Waianapanapa State Park
HANA
KIHEI
31
HALEAKALA
Visitor Center
Science City
WAILEA
Wailea Golf Course
Oheo Gulch
(Seven Sacred Pools)
MAKENA
Makena Golf Course
Ulupalakua
Tedeschi Winery
Molokini
Kaupo
Kanaio
N

Kihei

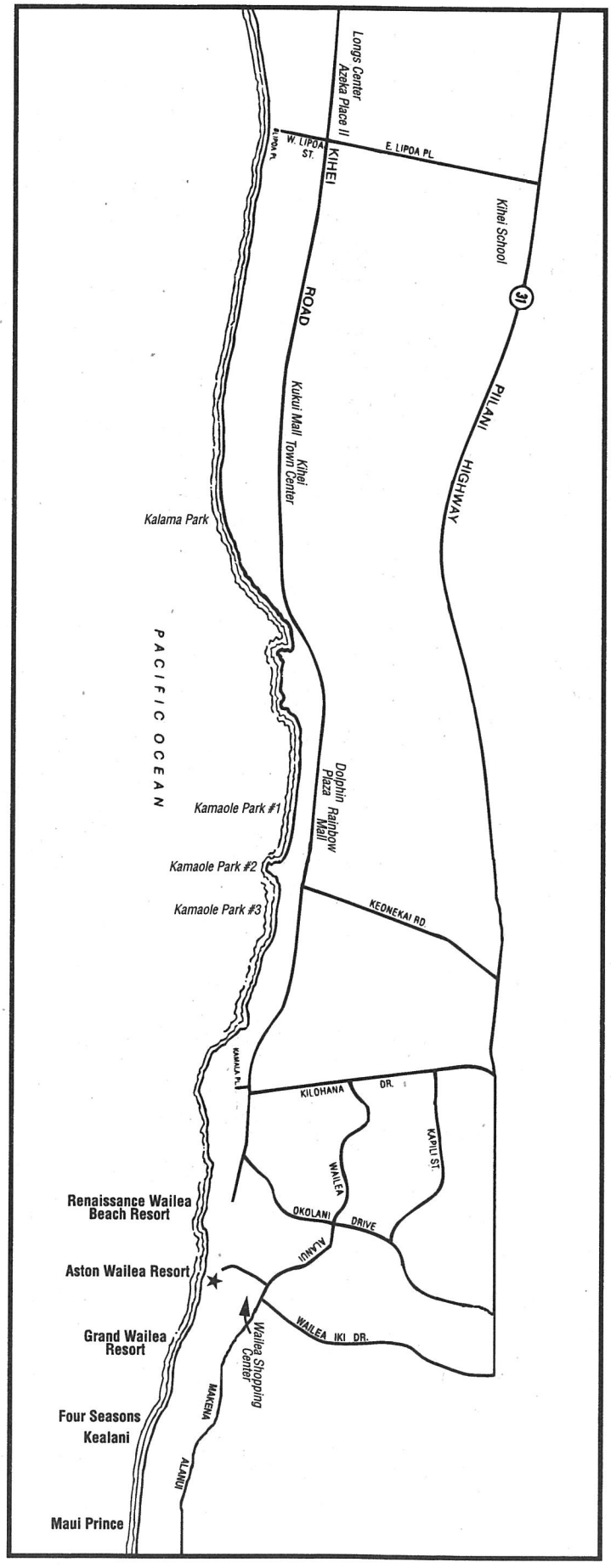
Longs Center
Azeka Place II
W. LIPOA ST.
E. LIPOA PL.
KIHEI ROAD
Kihei School
31
PILI-ANI HIGHWAY
Kukui Mall
Kihei Town Center
Kalama Park
PACIFIC OCEAN
Dolphin Plaza
Rainbow Mall
Kamaole Park #1
Kamaole Park #2
Kamaole Park #3
KEONEKAI RD
KILOHANA DR.
KAPILI ST.
WAILEA OKOLANI DRIVE
ALAMI
WAILEA IKI DR.
Wailea Shopping Center
MAKENA
ALANUI
Renaissance Wailea Beach Resort
Aston Wailea Resort
Grand Wailea Resort
Four Seasons Kealani
Maui Prince

Aston Wailea Resort

Facilities Plan

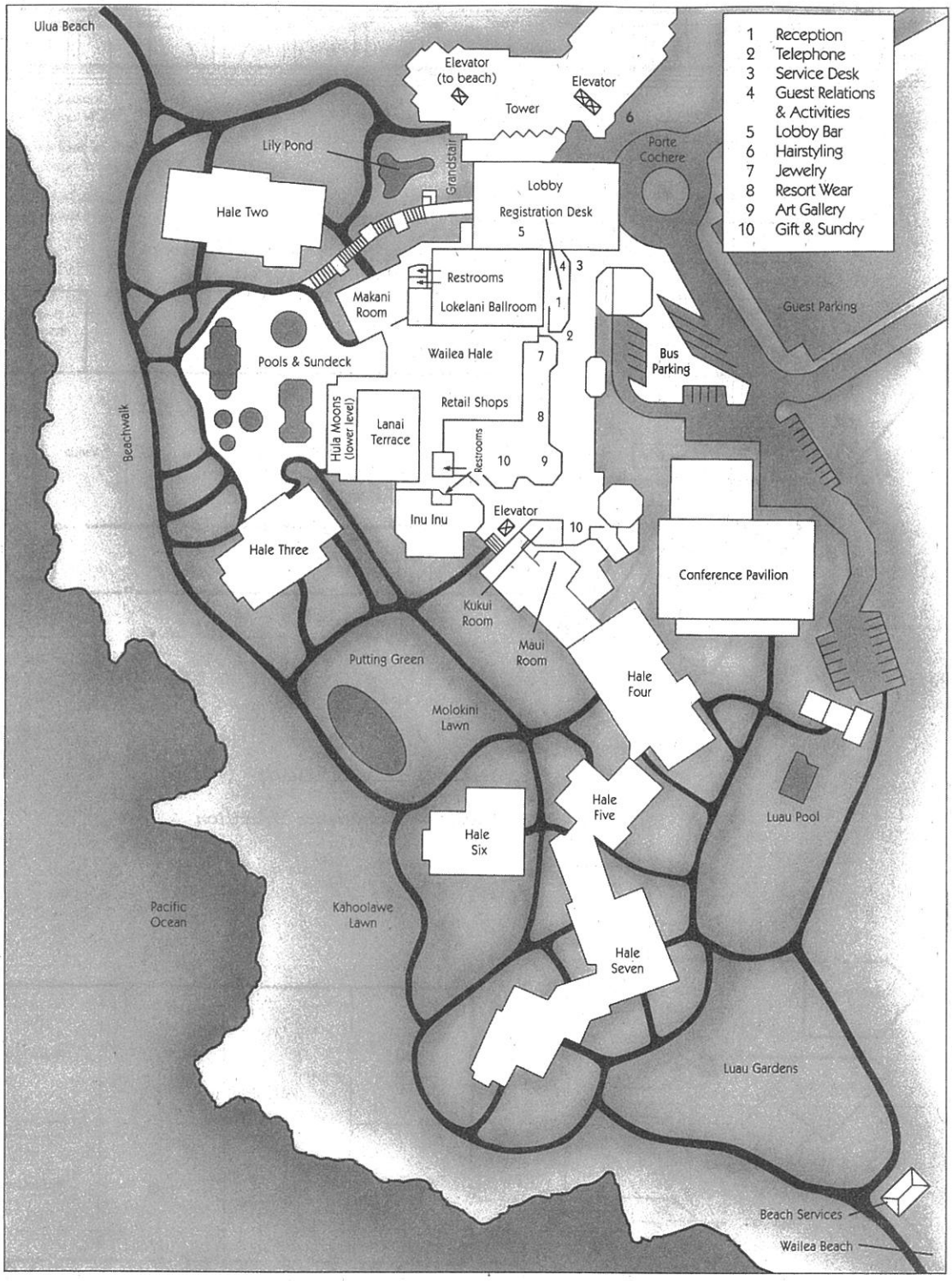

Conference Pavilion

Longitudinal Section

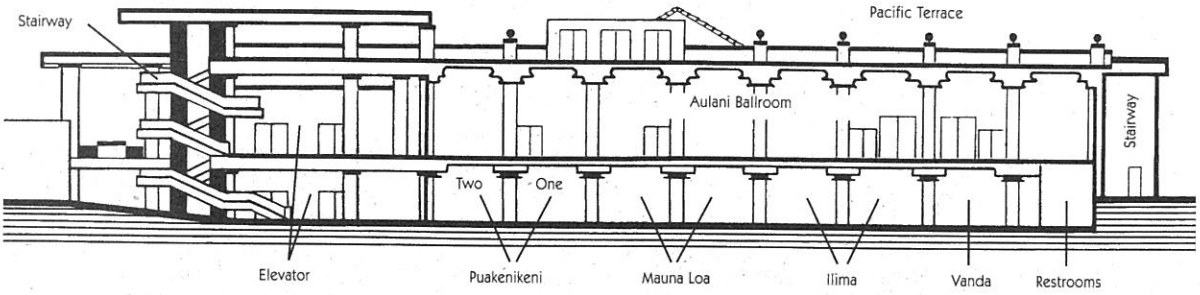

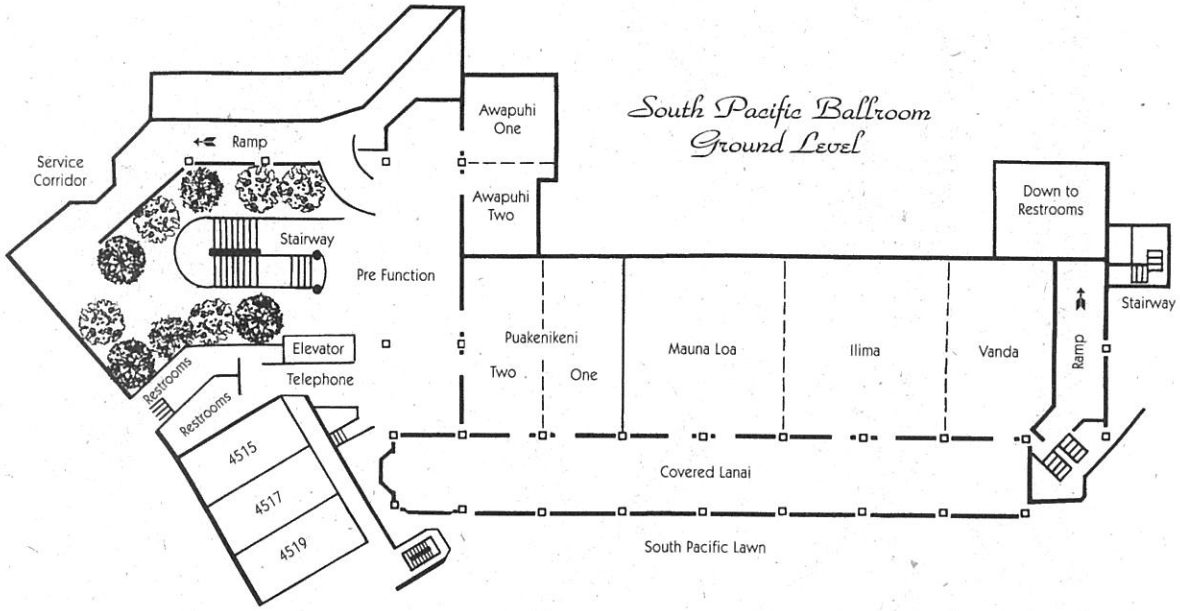

Aulani Ballroom

Second Level — Conference Pavilion

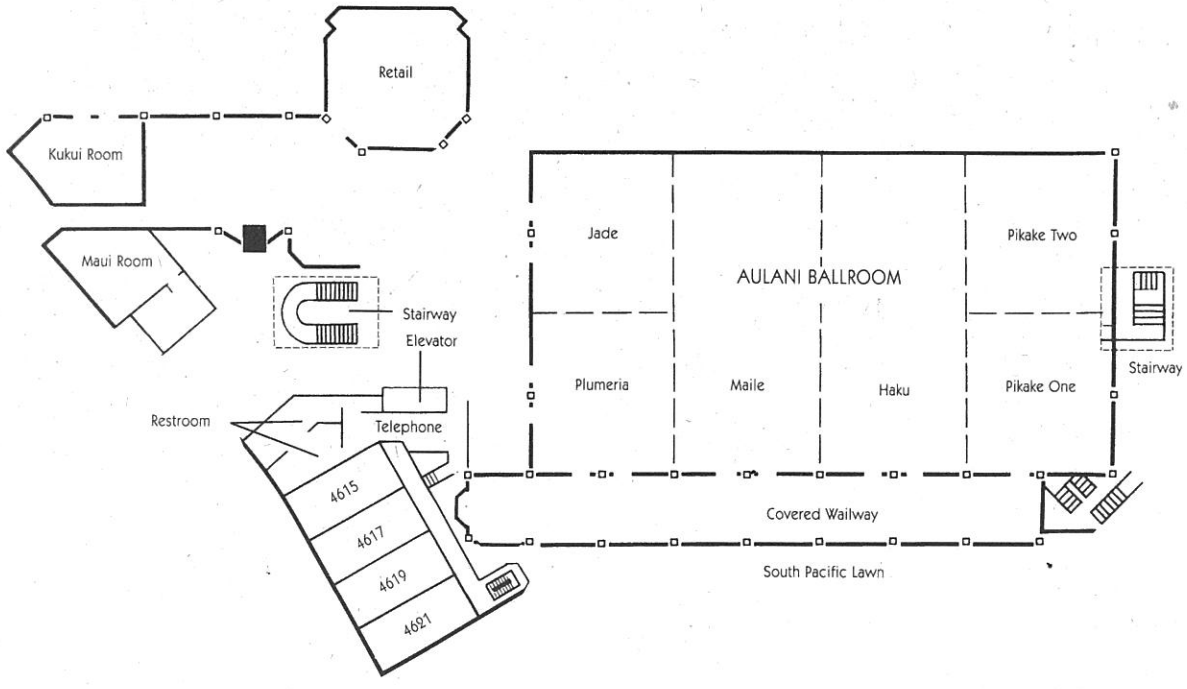

NW2 **Lasers and Excimer Sources**
Piper, Sakai
Maile Room, Aston Wailea

NW3 **Transient Discharges and Collective Effects in Dusty Plasmas**
South Pacific Ballroom,
Aston Wailea

15:15 WEDNESDAY AFTERNOON
21 OCTOBER 1998

OWP1 **ECR Plasmas**
Haku/Pikake Room, Aston Wailea

OWP2 **Displays, Lamps, and Lasers**
Haku/Pikake Room, Aston Wailea

OWP3 **Positive and Negative Ions in Plasmas**
Haku/Pikake Room, Aston Wailea

OWP4 **Innovative Plasma Applications**
Haku/Pikake Room, Aston Wailea

OWP5 **RF Glows**
Haku/Pikake Room, Aston Wailea

OWP6 **Lepton Collisions with Molecules**
Haku/Pikake Room, Aston Wailea

OWP7 **Electron-Atom Collisions**
Haku/Pikake Room, Aston Wailea

18:00 WEDNESDAY AFTERNOON
21 OCTOBER 1998

PW1 **Reception and Banquet**
Aulani Ballroom, Aston Wailea

7:30 THURSDAY MORNING
22 OCTOBER 1998

QR1 **Plasma Jets**
Krier, Moss
Plumeria/Jade Room, Aston Wailea

QR2 **Deposition**
Takai, Shimogaki
Maile Room, Aston Wailea

QR3 **Magnetized Plasmas**
South Pacific Ballroom,
Aston Wailea

10:00 THURSDAY MORNING
22 OCTOBER 1998

RR1 **Collisional Processes in Plasmas**
Tanaka, Morgan
Plumeria/Jade Room, Aston Wailea

RR2 **Plasma Diagnostics**
Loewenhardt
Maile Room, Aston Wailea

RR3 **Magnetized Plasmas and Thermal Plasmas**
Serikov
South Pacific Ballroom,
Aston Wailea

13:45 THURSDAY AFTERNOON
22 OCTOBER 1998

SR1 **Advanced Plasma Processing**
Watanabe, Tetsu, Samukawa, Horiike
Plumeria/Jade Room, Aston Wailea

SR2 **Plasma Surface Interactions**
Aydil
Maile Room, Aston Wailea

Epitome of the 1998 GEC/ICRP Meeting

7:30 MONDAY MORNING
19 OCTOBER 1998

AM1 **Electron-Atom Scattering**
Teubner, Vuskovic
Plumeria/Jade Room, Aston Wailea

AM2 **RF Glows**
Nakano.
Maile Room, Aston Wailea

AM3 **Oxide Etch**
Tachibana, Nakagawa
South Pacific Ballroom, Aston Wailea

10:00 MONDAY MORNING
19 OCTOBER 1998

BM1 **Electron Transport**
Olthoff, Nakamura, Morris
Plumeria/Jade Room, Aston Wailea

BM2 **RF & Pulsed Plasmas**
Braithwaite, Economou
Maile Room, Aston Wailea

BM3 **Energy Distribution Diagnostics**
Donnelly
South Pacific Ballroom, Aston Wailea

13:30 MONDAY AFTERNOON
19 OCTOBER 1998

CM1 **Foundations of Gaseous Electronics**
Crompton
Plumeria/Jade/Maile Room, Aston Wailea

14:45 MONDAY AFTERNOON
19 OCTOBER 1998

DM1 **Lamps and Displays**
Kroesen, Shinoda
Plumeria/Jade Room, Aston Wailea

DM2 **Pulsed & Microwave Glows**
Boswell, Hebner
Maile Room, Aston Wailea

DM3 **Innovative Plasma Sources: Diagnostics and Applications**
Kuzumoto
South Pacific Ballroom, Aston Wailea

17:15 MONDAY AFTERNOON
19 OCTOBER 1998

EMP1 **Dusty Plasmas**
Haku/Pikake Room, Aston Wailea

EMP2 **Charged Particle Diagnostics**
Haku/Pikake Room, Aston Wailea

EMP3 **Coronas/Breakdown**
Haku/Pikake Room, Aston Wailea

EMP4 **Deposition**
Haku/Pikake Room, Aston Wailea

EMP5 **Plasma-Surface Interaction and Sheaths**
Haku/Pikake Room, Aston Wailea

EMP6 **Inductively Coupled Plasma**
Haku/Pikake Room, Aston Wailea

EMP7 **Heavy Particle Collisions**
Haku/Pikake Room, Aston Wailea

EMP8 **Helicon Plasmas**
Haku/Pikake Room, Aston Wailea

7:30 TUESDAY MORNING
20 OCTOBER 1998

FT1 **Electron / Ion Transport**
Setser
Plumeria/Jade Room, Aston Wailea

FT2 **Laser Diagnostics**
Uchino, Kono
Maile Room, Aston Wailea

FT3 **Inductively Coupled Plasmas I**
Caughman
South Pacific Ballroom, Aston Wailea

10:00 TUESDAY MORNING
20 OCTOBER 1998

GT1 **Post-Deadline Session**
Plumeria/Jade Room, Aston Wailea

GT2 **Nucleation and Growth of Dust Particles**
Shiratani, Fujiyama
Maile Room, Aston Wailea

GT3 **Inductively Coupled Plasmas II**
Hayashi
South Pacific Ballroom, Aston Wailea

13:30 TUESDAY AFTERNOON
20 OCTOBER 1998

HT1 **ICRP Distinguished Lecturer**
Sugai
Plumeria/Jade/Maile Room, Aston Wailea

14:45 TUESDAY AFTERNOON
20 OCTOBER 1998

IT1 **Heavy-Particle Interactions**
Feagin, Wiese, Schultz
Plumeria/Jade Room, Aston Wailea

IT2 **Lamps**
Piejak, Ishigami, Ukegawa
Maile Room, Aston Wailea

IT3 **Etching and Deposition Simulation**
Kinoshita
South Pacific Ballroom, Aston Wailea

17:15 TUESDAY AFTERNOON
20 OCTOBER 1998

JTP1 **Optical Diagnostics: Active Species**
Haku/Pikake Room, Aston Wailea

JTP2 **Optical Diagnostics**
Haku/Pikake Room, Aston Wailea

JTP3 **Plasma Jets**
Haku/Pikake Room, Aston Wailea

JTP4 **Magnetron Plasmas**
Haku/Pikake Room, Aston Wailea

JTP5 **Etch**
Haku/Pikake Room, Aston Wailea

JTP6 **Glows**
Haku/Pikake Room, Aston Wailea

JTP7 **Electron / Ion Transport and Chemistry**
Haku/Pikake Room, Aston Wailea

7:30 WEDNESDAY MORNING
21 OCTOBER 1998

KW1 **Electron-Molecule Scattering**
Brunger, McKoy
Plumeria/Jade Room, Aston Wailea

KW2 **Surface Reactions**
Ohiwa, Hikosaka
Maile Room, Aston Wailea

KW3 **Environmental Applications**
Sawin, Morrow
South Pacific Ballroom, Aston Wailea

10:15 WEDNESDAY MORNING
21 OCTOBER 1998

LW1 **Allis Prize Lecture**
Flannery
Plumeria/Jade/Maile Room, Aston Wailea

11:15 WEDNESDAY MORNING
21 OCTOBER 1998

MW1 **GEC Business Meeting**
Plumeria/Jade/Maile Room, Aston Wailea

13:15 WEDNESDAY AFTERNOON
21 OCTOBER 1998

NW1 **DC and Microwave Glows**
Ganguly
Plumeria/Jade Room, Aston Wailea

0003-0503(199810)43:5;1-P